# Self-assembled pentablock copolymers for selective and sustained gene delivery

by

**Bingqi Zhang**

A dissertation submitted to the graduate faculty

in partial fulfillment of the requirements for the degree of

DOCTOR OF PHILOSOPHY

Major: Chemical Engineernig

Program of Study Committee:
Surya K. Mallapragada, Major Professor
Aaron R. Clapp
Monica H. Lamm
Jesse M. Hostetter
Zhiqun Lin

Iowa State University

Ames, Iowa

2011

# TABLE OF CONTENTS

# LIST OF FIGURES

# LIST OF TABLES

# ACKNOWLEDGEMENTS

First and foremost, I wish to express my sincerest and deepest gratitude to my major advisor, Surya Mallapragada. Her inspiration, vision and encouragement have been a great source of strength throughout my graduate studies. I also wish to thank the members of my program of study committee, Aaron Clapp, Monica Lamm, Jesse Hostetter and Zhiqun Lin, for their continued support and helpful suggestions.

I am appreciative of past and present members in Prof. Mallapragada's group, Ankit, Umai, Erin, Carlos, Ying, Xunpei, Feng, Bob and Tanya, for the great research environment and their valuable friendship. I would like to especially thank Dr. Aaron Clapp and Yanjie Zhang in his group for their passion and hard work in our collaboration. I would also like to thank Dr. Ian Schneider for his kind help with cell imaging. A special thank you goes out to my lab & office mate Yue Hou for her willingness to help me at any time.

Last, but not the least, I would like to thank my dearest parents and husband for their unending love, support and encouragement.

# ABSTRACT

The poly(diethylaminoethyl methacrylate) (PDEAEM) - Pluronic F127 - PDEAEM pentablock copolymer (PB) gene delivery vector system has been found to possess an inherent selectivity in transfecting cancer cells over non-cancer cells *in vitro*, without attaching any targeting ligands. In order to understand the mechanism of this selective transfection, three possible intracellular barriers to transfection were investigated in both cancer and non-cancer cells. We concluded that escape from the endocytic pathway served as the primary intracellular barrier for PB-mediated transfection. Most likely, PB vectors were entrapped and rendered non-functional in acidic lysosomes of non-cancer cells, but survived in less acidic lysosomes of cancer cells. The work highlights the importance of identifying intracellular barriers for different gene delivery systems and provides a new paradigm for designing targeting vectors based on intracellular differences between cell types, rather than through the use of targeting ligands.

The PB vector was further developed to simultaneously deliver anticancer drugs and genes, which showed a synergistic effect demonstrated by significantly enhanced gene expression *in vitro*. Due to the thermosensitive gelation behavior, the PB vector packaging both drug and gene was also investigated for its *in vitro* sustained release properties by using polyethylene glycol diacrylate as a barrier gel to mimic the tumor matrix *in vivo.* Overall, this work resulted in the development of a gene delivery vector for sustained and selective gene delivery to tumor cells for cacner therapy.

# CHAPTER 1. GENERAL INTRODUCTION

## 1.1 Introduction

Despite all the effort and work over the last 30 years, cancer is still the second leading cause of death in the US, surpassed only by heart disease. Currently available therapies must be augmented with new strategies that take advantage of innovative technologies. Gene therapy for cancer is one of those emerging strategies, which can be defined as transmission of the genetic material into the target cells to treat inherited and acquired diseases by correcting genetic defects or introducing new therapeutic functions into target cells.

From this concept, gene therapy basically requires a therapeutic gene, a method to induce it into target cells, and its subsequent expression into those cells. The therapeutic gene or the gene of interest is usually encoded in a plasmid, which also contains other signal sequences, such as a promoter and enhancer that could regulate gene expression. The promoter provides recognition sites for RNA polymerase to initiate DNA transcription. Enhancers can enhance the production of desired genes by several hundred times(1). DNA delivery methods mainly fall into two categories: physical techniques and vector-assisted delivery systems. Physical methods are usually adopted in the delivery of naked DNA, which include microinjection(2), bombardment such as gene gun(3), electroporation(4-6), laser beam(7), ultrasonic(8-9) and high pressure(3). Although significant transfection efficiencies have been achieved using these mechanical and electrical strategies, the associated harmful effects and invasive nature greatly inhibit their clinical

application.

Vector-assisted systems include viral and non-viral gene vectors. Viral vectors, such as adenoviruses, adeno-associated viruses and retroviruses, posses an inborn ability to access host cells, thus leading to a highly efficient transfection. That is why more than 70% of current clinical trials for gene therapy have employed viral vectors. However, viral vectors tend to induce an immune response that might trigger severe inflammatory reaction and cause insertion mutagenesis(10), In addition, they have a limited DNA packaging capability and are difficult to manufacture(11). Especially after the death of Jesse Gelsinger in a clinical trial in 1999(12-13) and the leukemia-like disease developed in a French patient in 2002(14), considerable attention has been turned to finding safer alternatives. Non-viral vectors are promising candidates with attractive advantages in flexible design, low cost and easy scale-up production except for bearing low safety risks. Improving the transfection efficiency to the level of their viral counterparts is believed to be the main task. Non-viral vectors mainly include naked DNA, liposomes and polymeric carriers. Naked DNA requires physical methods to achieve transfection as stated above. Liposomes have a unique bilayer structure that can encapsulate DNA in the aqueous core while fusing with the hydrophobic cell membrane. Currently they account for the largest fraction of non-viral vectors that are under clinical trials. The main problem with liposomes is clearance from the blood stream, which has been shown to be decreased by the modification of targeting ligands(15-16), but disadvantages in preparation and storage still limit their development. Polymeric vectors provide researchers numerous possibilities to design the desired multifunctional structures.

Cationic polymers are a family of polymer-based non-viral vectors that are most widely studied. Electrostatic interactions make it possible to form a DNA-polycation complex, which is termed a polyplex. Polymers frequently used for DNA encapsulation and delivery include polyethyleneimine (PEI)(17-19), poly-L-lysine (PLL)(20) and dendritic PLL(21-23), arginine or guanidine-rich proteins(24-25), synthetic peptides(26), polyamidoamine (PAMAM) dendrimers(27), chitosan(28-30) and their various derivatives. These amine-carrying cationic polymers are all able to condense DNA efficiently and protect it from enzyme degradation, which is a prerequisite but does not necessarily guarantee successful gene delivery. This is because gene delivery is a process involving multiple steps that could individually or cooperatively limit the ultimate transfection efficiency depending on different cell types and vector systems. In general, polyplexes need to undergo extracellular delivery, attach to the surface of target cell, be internalized and entrapped in endosomes, escape from endosomes, move through the cytoplasm toward the nucleus and get across the nuclear membrane for possible gene expression. Based on increasingly understanding the mechanism of gene delivery, multifunctional vectors could be designed to overcome rate-limiting barriers and achieve desired transfection with high selectivity and low toxicity.

We synthesized a family of self-assembling pentablock copolymers via atom transfer radical polymerication (ATRP) reaction(31), which exhibit temperature- and pH- induced micellization and gelation. The central triblock is commercially available Pluronic F127 whose amphiphilic nature make it form micelles in aqueous solution above critical micelle concentration (CMC)(32). This micellar structure has been

shown to promote cellular entry(33). The cationic end-blocks poly(diethylaminoethyl methacrylate) (PDEAEM) are the essential functioning segments to condense DNA and provide pH buffering in the endosome with their protonable tertiary amine groups(34). The pentablock copolymers retain the thermo-sensitivity of Pluronic and the pH sensitivity of PDEAEM, meanwhile obtaining enhanced mechanical properties(35). The stronger gel is favorable for in vivo sustained release because it can resist the current in tissue fluid or blood stream and keep a steady release profile. These self-assembled injectable hydrogels have clinical advantages over other chemically cross-linked hydrogels(36) that involve harsh crosslinking environments, or scaffolds(37) that need to be surgically implanted. Moreover, in order to improve the stability and reduce the cytotoxicity caused by excess positive charges on the surface of polyplexes, free Pluronic was added to shield these charges by hydrophobic interaction between polypropylene oxide (PPO) blocks(38). Taken together, this novel vector can be injected into tumors or tissues as sol and transform to gel under body temperature and release DNA drug in a sustained way. The previous work has proved the biocompatibility and effectiveness of this pentablock copolymer for *in vitro* gene delivery. Preliminary results were also obtained for sustained release and *in vivo* transfection.

## 1.2 Objectives

The overall objective of this research was to explore the mechanism of the pentablock copolymer mediated gene delivery and develop a multifunctional vector system that can not only selectively transfect cancer cells, but also provide a long

term gene expression by sustained release.

### 1.3 Dissertation Organization

In Chapter 3, the pentablock copolymer vector was investigated for its transfection efficacy in different cell types. A selective transfection in cancerous cells over non-cancerous cells was found. Intracellular trafficking was undertaken to understand this selective transfection, which implied that different barriers to transfection in specific cells might be a possible reason.

Chapter 4 and Chapter 5 continued investigation into the mechanism of the selectivity observed with pentablock copolymer vectors by examining each possible barrier to transfection in cancer and non-cancer cell types. Epidermal growth factor (EGF), nuclear localization signals (NLS) and chloroquine (CLQ) were either conjugated to or mixed with the vector to examine their influence on transfection through overcoming the corresponding barrier.

Chapter 6 focused on investigating the effect of CLQ on polyplex dissociation by using water soluble quantum dots. Because CLQ was found to have restored the difference in gene expression between cancer and non-cancer cells, study on its role in gene delivery is of great importance. This part of research was a collaboration with Dr. Aaron Clapp in the department of chemical and biological engineering at ISU.

Chapter 7 presented a new application of the vector in co-delivery of gene and drug. Sustained release *in vitro* was also investigated with an improved experimental set-up to mimic the situation *in vivo*.

## References


1. W. Waltherand U. Stein. Cell type specific and inducible promoters for vectors in gene therapy as an approach for cell targeting. J Mol Med. 74:379-392 (1996).
2. D.V. McAllister, M.G. Allen, and M.R. Prausnitz. Microfabricated microneedles for gene and drug delivery. Annu Rev Biomed Eng. 2:289-313 (2000).
3. J. Dileo, T.E. Miller, S. Chesnoy, and L. Huang. Gene Transfer to Subdermal Tissues via a New Gene Gun Design. Human Gene Therapy. 14:79-87 (2003).
4. M.F. Bureau, J. Gehl, V. Deleuze, L.M. Mir, and D. Scherman. Importance of association between permeabilization and electrophoretic forces for intramuscular DNA electrotransfer. Biochimica et Biophysica Acta (BBA) - General Subjects. 1474:353-359 (2000).
5. M.F. Bureau, S. Naimi, R. Torero Ibad, J. Seguin, C. Georger, E. Arnould, L. Maton, F. Blanche, P. Delaere, and D. Scherman. Intramuscular plasmid DNA electrotransfer: Biodistribution and degradation. Biochimica et Biophysica Acta (BBA) - Gene Structure and Expression. 1676:138-148 (2004).
6. F. Liuand L. Huang. A Syringe Electrode Device for Simultaneous Injection of DNA and Electrotransfer. Mol Ther. 5:323-328 (2002).
7. E. Zeira, A. Manevitch, A. Khatchatouriants, O. Pappo, E. Hyam, M. Darash-Yahana, E. Tavor, A. Honigman, A. Lewis, and E. Galun. Femtosecond infrared laser[mdash]an efficient and safe in vivo gene delivery system for prolonged expression. Mol Ther. 8:342-350 (2003).
8. D.J. Wells. Gene Therapy Progress and Prospects: Electroporation and other physical methods. Gene Ther. 11:1363-1369 (2004).
9. D.M. Hallow, A.D. Mahajan, and M.R. Prausnitz. Ultrasonically targeted delivery into endothelial and smooth muscle cells in ex vivo arteries. Journal of Controlled Release. 118:285-293 (2007).
10. T. Reschel, Č. Koňák, D. Oupický, L.W. Seymour, and K. Ulbrich. Physical properties and in vitro transfection efficiency of gene delivery vectors based on complexes of DNA with synthetic polycations. Journal of Controlled Release. 81:201-217 (2002).
11. I.M. Vermaand N. Somia. Gene therapy - promises, problems and prospects. Nature. 389:239-242 (1997).
12. S. Lehrman. Virus treatment questioned after gene therapy death. Nature. 401:517-518 (1999).
13. E. Marshall. CLINICAL TRIALS:Gene Therapy Death Prompts Review of Adenovirus Vector. Science. 286:2244-2245 (1999).
14. E. Marshall. Clinical research - Gene therapy a suspect in leukemia-like disease. Science. 298:34-35 (2002).

15. S. Suzuki, S. Watanabe, T. Masuko, and Y. Hashimoto. Preparation of long-circulating immunoliposomes containing adriamycin by a novel method to coat immunoliposomes with poly(ethylene glycol). Biochimica et Biophysica Acta (BBA) - General Subjects. 1245:9-16 (1995).

16. K. Maruyama, N. Takahashi, T. Tagawa, K. Nagaike, and M. Iwatsuru. Immunoliposomes bearing polyethyleneglycol-coupled Fab' fragment show prolonged circulation time and high extravasation into targeted solid tumors in vivo. FEBS Letters. 413:177-180 (1997).

17. O. Boussif, F. Lezoualc'h, M.A. Zanta, M.D. Mergny, D. Scherman, B. Demeneix, and J. Behr. A Versatile Vector for Gene and Oligonucleotide Transfer into Cells in Culture and in vivo: Polyethylenimine. Proceedings of the National Academy of Sciences. 92:7297-7301 (1995).

18. W.T. Godbey, K.K. Wu, and A.G. Mikos. Poly(ethylenimine) and its role in gene delivery. Journal of Controlled Release. 60:149-160 (1999).

19. M.R. Park, K.O. Han, I.K. Han, M.H. Cho, J.W. Nah, Y.J. Choi, and C.S. Cho. Degradable polyethylenimine-alt-poly(ethylene glycol) copolymers as novel gene carriers. Journal of Controlled Release. 105:367-380 (2005).

20. L.-L. Farrell, J. Pepin, C. Kucharski, X. Lin, Z. Xu, and H. Uludag. A comparison of the effectiveness of cationic polymers poly-l-lysine (PLL) and polyethylenimine (PEI) for non-viral delivery of plasmid DNA to bone marrow stromal cells (BMSC). European Journal of Pharmaceutics and Biopharmaceutics. 65:388-397 (2007).

21. T. Kawano, T. Okuda, H. Aoyagi, and T. Niidome. Long circulation of intravenously administered plasmid DNA delivered with dendritic poly(L-lysine) in the blood flow. Journal of Controlled Release. 99:329-337 (2004).

22. T. Okuda, A. Sugiyama, T. Niidome, and H. Aoyagi. Characters of dendritic poly(-lysine) analogues with the terminal lysines replaced with arginines and histidines as gene carriers in vitro. Biomaterials. 25:537-544 (2004).

23. M. Yamagata, T. Kawano, K. Shiba, T. Mori, Y. Katayama, and T. Niidome. Structural advantage of dendritic poly(l-lysine) for gene delivery into cells. Bioorganic & Medicinal Chemistry. 15:526-532 (2007).

24. N. Cheng, W. Liu, Z. Cao, W. Ji, D. Liang, G. Guo, and J. Zhang. A study of thermoresponsive poly(N-isopropylacrylamide)/polyarginine bioconjugate non-viral transgene vectors. Biomaterials. 27:4984-4992 (2006).

25. B. Zhang, W. Ji, W. Liu, and K. Yao. Guanidinylated allylamine-N-isopropylacrylamide copolymer nonviral transgene vectors. International Journal of Pharmaceutics. 331:116-122 (2007).

26. M.E. Martinand K.G. Rice. Peptide-guided gene delivery. AAPS Journal. 9:E18-29 (2007).

27. J.H. Lee, Y.b. Lim, J.S. Choi, Y. Lee, T.i. Kim, H.J. Kim, J.K. Yoon, K. Kim, and J.s. Park. Polyplexes Assembled with Internally Quaternized PAMAM-OH Dendrimer and Plasmid DNA Have a Neutral Surface and Gene Delivery Potency. Bioconjugate Chem. 14:1214-1221 (2003).

28. W.G. Liu, X. Zhang, S.J. Sun, G.J. Sun, K.D. Yao, D.C. Liang, G. Guo, and J.Y. Zhang. N-Alkylated Chitosan as a Potential Nonviral Vector for Gene Transfection. Bioconjugate Chem. 14:782-789 (2003).

29. S. Mansouri, P. Lavigne, and K. Corsi, et al. Chitosan-DNA nanoparticles as non-viral vectors in gene therapy: strategies to improve transfection efficacy. European Journal of Pharmaceutics and Biopharmaceutics. 57:1-8 (2004).

30. S. Sun, W. Liu, N. Cheng, B. Zhang, Z. Cao, K. Yao, D. Liang, A. Zuo, G. Guo, and J. Zhang. A Thermoresponsive Chitosan-NIPAAm/Vinyl Laurate Copolymer Vector for Gene Transfection. Bioconjugate Chem. 16:972-980 (2005).

31. M.D. Determan, J.P. Cox, S. Seifert, P. Thiyagarajan, and S.K. Mallapragada. Synthesis and characterization of temperature and pH-responsive pentablock copolymers. Polymer. 46:6933-6946 (2005).

32. A.V. Kabanov, P. Lemieux, S. Vinogradov, and V. Alakhov. Pluronic(R) block copolymers: novel functional molecules for gene therapy. Advanced Drug Delivery Reviews. 54:223-233 (2002).

33. A.V. Kabanov, E.V. Batrakova, and V.Y. Alakhov. Pluronic(R) block copolymers as novel polymer therapeutics for drug and gene delivery. Journal of Controlled Release. 82:189-212 (2002).

34. A. Agarwal, R. Unfer, and S.K. Mallapragada. Novel cationic pentablock copolymers as non-viral vectors for gene therapy. Journal of Controlled Release. 103:245-258 (2005).

35. A. Agarwal, R.C. Unfer, and S.K. Mallapragada. Dual-role self-assembling nanoplexes for efficient gene transfection and sustained gene delivery. Biomaterials. 29:607-617 (2008).

36. D. Lee, W. Zhang, S. Shirley, X. Kong, G. Hellermann, R. Lockey, and S. Mohapatra. Thiolated Chitosan/DNA Nanocomplexes Exhibit Enhanced and Sustained Gene Delivery. Pharmaceutical Research. 24:157-167 (2007).

37. H. Cohen-Sacks, V. Elazar, J. Gao, A. Golomb, H. Adwan, N. Korchov, R.J. Levy, M.R. Berger, and G. Golomb. Delivery and expression of pDNA embedded in collagen matrices. Journal of Controlled Release. 95:309-320 (2004).

38. A. Agarwal, R.C. Unfer, and S.K. Mallapragada. Investigation of in vitro compatibility of novel pentablock copolymers for gene delivery. Journal of Biomedical Materials Research 81A:24-39 (2007).

# CHAPTER 2. LITERATURE REVIEW

Remarkable progress has been achieved in polymeric gene delivery within the last fifty years. Aiming at the transfection efficiency of viral vectors while maintaining non-toxicity, researchers have come up with a large number of systems either derived from the “classical” cationic polymers, such as polyethyleneimine (PEI), poly(L-lysine) (PLL), polyamidoamine (PAMAM), poly (2-(dimethylamino)ethyl methacrylate) (PDMAEMA) and chitosan, or developed out of novel architectures such as the synthetic peptides. Multifunctionality becomes an increasingly recognized requirement for current polymeric vectors owning to the complicated nature of the gene delivery mechanism. In fact, it is pertinent to first understand the biological barriers encountered by transgene vectors before considering various carriers in detail. In this chapter, principle barriers (extracellular and intracellular) to polymeric gene delivery will be reviewed and possible strategies to overcome these obstacles will be discussed thereafter.

## 2.1 Principal Barriers to Polymeric Gene Delivery Systems

Upon complexation of DNA and cationic polymers (polycation) via electrostatic interactions, the formulated polyplexes are administrated to the tissues or cells of interest. Unless administrated locally, polyplexes need to traverse the whole extracellular route and reach the target cells (Fig. 2.1). Once the attached polyplexes get internalized via endocytosis, they are first sequestered in an acidic vesicle termed endosome, which begins the intracellular delivery. Endosomes tend to fuse

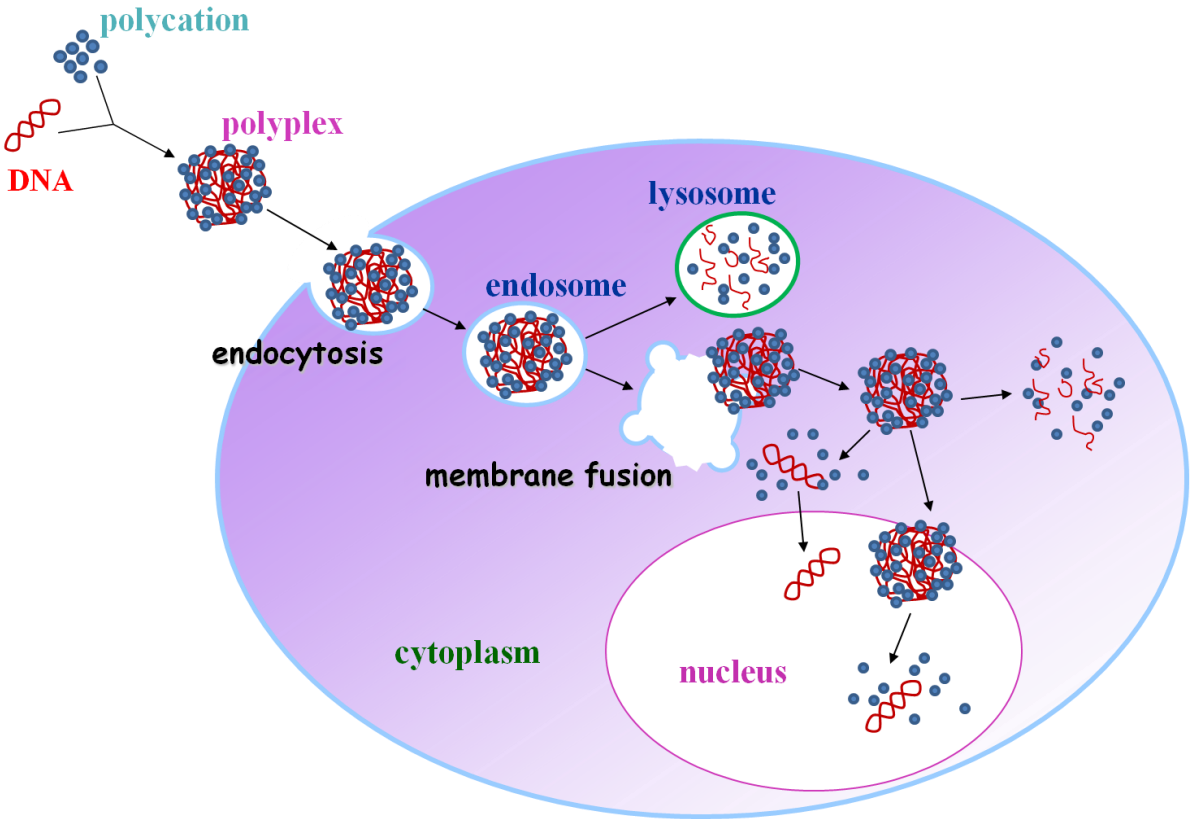


Fig. 2.1. Schematic illustration of polymeric gene delivery *in vitro*

with lysosomes where various enzymes could degrade the DNA payload and bring an end to the delivery. Thus, it is required for polyplexes to escape endosomal compartments to continue the route towards nucleus. Although several challenges exist in the crowded cytoplasm, the surviving DNA or/and well maintained polyplexes can enter the nucleus for gene expression. Detailed discussion about each barrier will be stated below with an emphasis on intracellular ones.

### 2.1.1 Extracellular Barriers

Polycations condense DNA into tight polyplexes under salt-free or very low salt

conditions to completely or partially block the access of nucleolytic enzymes(2). However, the electrostatic interactions between DNA and polycations will become weaker as the surrounding salt concentration increases and might consequently result in the unpacking of DNA from its carrier. When polyplexes travel to distant target sites of action, blood components such as serum proteins and blood cells could absorb on their surface either by ionic binding or hydrophobic interaction, which leads to increase in particle size and formation of large aggregates(3-6). Rapid clearance will then occur by phagocytic cells and reticulo-endothelial system (RES)(7). In particular, when polyplexes were intramuscularly injected, they were most likely be trapped in the negatively charged extracellular matrix and unable to transfer further to tissues of interest(8).

The biological environment is far more complicated than *in vitro* conditions. Many properties of vectors, such as size, zeta potential, colloidal stability and protection for DNA depend on the local environment. The optimization of vectors in serum-free conditions may not be as effective as expected, because certain biophysical characteristics of vectors exhibited in buffers probably tend to alter *in vivo*. For example, the positive charges are necessary for condensing DNA, associating cells and hence efficient transfection *in vitro*; however, these charges can cause a number of side effects with blood constituents and specialized organs during *in vivo* application(9-10), leading to quick clearance and short half-lives. Therefore, it is highly necessary to consider or mimic the practical situation when designing vectors and making *in vitro* transfection protocols.

### 2.1.2 Cellular Uptake

Even if the polyplexes can manage to evade the degradation by nuclease in plasma and the clearance by RES, they still face significant challenges from the cell. The first challenge is to associate with cell membrane and get entry in the cell.

Cell membrane carries negative charges due to the presence of negatively charged glycoproteins, proteoglycans and glycerophosphate(11-12). This enables polyplexes carrying positive charges to bind to the cell surface and then be internalized by endocytosis (refers to cellular uptake of macromolecules into membrane-bound vesicles derived by invagination and pinching-off of pieces of plasma membrane(13)). Endocytosis can be classified into two broad categories, phagocytosis or cell eating which is typically restricted to specialized mammalian cells, and pinocytosis or cell drinking which occurs in all cells(14). Depending on the membrane coat, the size of particle generated and intracellular fate of the internalized particle, pinocytosis mainly has three endocytic pathways: clathrin-mediated endocytosis, caveolae-mediated endocytosis and macropinocytosis. Kinetically, endocytosis can also be divided into three modes: fluid-phase, adsorptive, and receptor-mediated endocytosis(15).

The predominant entry pathway for polymeric gene delivery systems is clathrin-mediated endocytosis (CME), which is also the most extensively studied form of endocytosis. Briefly, transmembrane receptors and their bound ligands are assembled by cytosolic coat proteins (e.g. clathrin) into clathrin coated membrane pits. These pits invaginate and pinch-off from the membrane to form clathrin-coated vesicles that carry the encapsulated receptor-ligands into cells(16). The efficiency of

receptor-mediated endocytosis correlates with both the affinity of the ligand-receptor interaction and the concentration of these complexes in clathrin-coated pits. Following internalization, the clathrin coat is rapidly depolymerized, which allows endocytic vesicles to fuse with each other to form early endosomes(17). From there, endosomal contents are sorted to appropriate intracellular destinations. Fusing with lysosomes is the fate for most polyplexes failing to escape endosomes, which leads to enzymatic degradation of DNA payloads and no more access to their target sites. By contrast, the internalization through caveolae-mediated endocytosis is believed to use the non-digestive route(18-19). Caveolae-mediated endocytosis, also termed potocytosis, is a mechanism by which both small and large molecules can be transported into cells(20-21). Caveolae are hydrophobic, caveolin-coated membrane microdomains, usually appearing as flask-shaped invaginations of the plasma membrane. They are now known to be present on most cells(22), but especially abundant in skeletal muscle cells, adipocytes and endothelial cells in which they were first described(23). Caveolae are suggested to mediate the extracellular shuttling of serum proteins from the bloodstream into tissues(14). Besides, it has been reported that caveolae play a role in the uptake of PLL/DNA complexes(19). Actually, the endocytic pathways for entry of polyplexes are cell type(24)and intruding particle dependent (25-26). For example, in one study, small particles (<200 nm) were found to be internalized via clathrin-mediated endocytosis, whereas large particles (>500 nm) gain cellular entry via caveolae-mediated endocytosis(27). But it was recently discovered that small polymeric particles (< 25 nm) but not larger particles (> 42 nm) enter live cells via a novel mechanism that results in trafficking

outside of the endo/lysosomal pathway(28). Since polyplexes becoming ineffective with DNA degradation in lysosomes is a crucial obstacle for inefficient transfection, caveolar uptake that avoids lysosomal degradation holds the promise for entry of polymeric gene-delivery vectors (13, 19), especially in endothelial cells in which caveolae constitute 10 to 20% of the cell surface(14).

Macropinocytosis is another pathway allowing avoidance of lysosomal degradation. It also has the potential to mediate the uptake of cationic carriers because of its ability to engulf large molecules such as bacteria (29). The vesicle formed is called macropinosome whose membrane components are recycled back to plasma membrane(30). The dynamic structure and leaky nature of macropinosomes enables encapsulated particles to escape readily, which together with the advantage in non-digestive route make macropinocytosis gain increasing attention as a potential mode of cellular uptake for gene vectors. It has been demonstrated that the uptake of large TAT-fusion proteins occurs via macropinocytosis(31).

No matter what kind of endocytic pathway is employed, polyplexes need to be efficiently and specifically internalized into tissues or cells of interest. To improve the internalization efficiency, especially to endow the vector system with impactful targeting ability seems to be the major task concerning cellular uptake, which, however, should be based on further understanding of the mechanism and influencing factors involved in this process. Recently, the uptake process of PEI-based polyplexes has been reported to contain three phases according to their movement characteristics(32). Phase I was characterized by very slow cytoskeleton-

mediated movement, phase II showed polyplexes of increased velocity with normal and confined diffusion in the cytoplasm, phase III was characterized by fast active transport within the endocytic vesicles along the microtubules with motor proteins.

### 2.1.3 Endosomal Escape

Unless polyplexes take the non-digestive route to enter cells(12), they will be completely or partially entrapped in the first endocytic vesicle, early endosome. The early endosomes are formed with close proximity to the plasma membrane and then depending on the physiochemical properties of internalized materials(33-34), either fuse with sorting endosomes to recycle the encapsulated content back to cell membrane and out of the cell by exocytosis, or develop into late endosomes which are located further away from cell membrane. The late endosomes primarily function to transport internalized materials to the lysosomes probably along microtubules(32, 35). Although endosomes show some cell dependent characteristics(36-39), the typical pH of early endosome ranges between 5.5-7.0 and late endosomal pH drops to 5.0-5.5, while lysosomal pH further goes down to 4.0-5.0. Polyplexes that have been sequestered in lysosomes usually suffer a loss in DNA activity due to the richness of various acidic hydrolases. This enzymatic degradation of DNA is considered to be a major intracellular barrier that dramatically compromises the transfection efficiency(40). Even though a portion of DNA can fortunately be kept away from vesicular degradation, this only results in accumulation of transgenes in the vesicles and limits their further transport to the nucleus. Thus degradation and entrapment in endo/lysosomes can be regarded as two separate barriers(13). When

DNA was directly delivered into the cytosol by microinjection or osmotic shock (41), gene expression was found to be much higher than obtained using the co-culture method probably due to successfully overcoming the barriers associated with endo/lysosomes.

### 2.1.4 Cytoplasmic Delivery

Polyplexes that have managed to escaped from endo/lysosomes need to undergo cytoplamic trafficking towards the nucleus. The cytoplasm is composed of cytoskeletal elements, a variety of subcellular organelles, large molecules, and small organic and inorganic solutes. The cytoskeleton, constructed by three classes of filaments, actin filaments, microtubules and intermediate filaments, not only gives the cell its shape, but also regulated the cytoplasmic transport of organelles and large complexes. Although the solvent viscosity of cytoplasm is comparable to that of water(42-43), cytoplasmic vesicles or microinjected beads diffuse in the cytoplasm 500 to 1000 times slower than in aqueous solutions(44-45). The cytoplasmic movement becomes even more limited for proteins, because of potential interactions with intracellular components(46). Therefore, the cytoplasm constitute a major diffusional barrier for polyplexes or plasmid DNA to accomplish nuclear localization(47).

The endocytic route can transport polyplexes along microtubules for a little while before releasing them into the cytoplasm(32, 35). This indeed provides some help. However, polyplexes still need travel through the rest of route in the cytoplasm and gain their entry into the nucleus. Because of the large of number of available salts

and proteins including enzymes in the cytoplasm, polyplexes get involved again in threats of dissociation and attacks from nucleases (48) as they met during the transport in biological fluids. But the polyplexes may become more susceptible at this moment after experiencing several hostile situations. Thus, polyplex unpacking could occur due to the interaction with other competing particles, such as spermine and spermidine at concentrations in the millimolar range (49). In that case, the DNA payload loses the protection of polymeric carriers and is subjected to degradation by nucleases. It has been reported that the plasmid DNA microinjected into the cytoplasm undergoes rapid degradation with half-life of less than 90min(48). In another study, more than three orders of magnitude higher plasmid DNA needed to be injected into the cytoplasm to give the same level of expression as when it was microinjected in the nucleus(50). But the reasons for this finding may also involve the barrier associated with nuclear entry and not the cytoplasmic entrapment. Dowty et al. reported that microinjection of plasmid DNA into the proximity of the nucleus resulted in significant enhancement of the transfection efficiency compared to the microinjection far (60-90 μm) from the nucleus(51). This indicates the trafficking of plasmid DNA toward the nucleus is indeed hindered in cytoplasm and affects the overall gene transfer. The metabolic instability(48) and negligible mobility (for sequences larger than 2000 bp(52))(51) of plasmid DNA mainly account for its loss or sequestration in the cytoplasm. Thus, the diffusion of DNA in cytoplasm might be an important rate-limiting barrier in non-viral gene delivery(52).

For the polyplexes not experiencing dissociation to release DNA payload into cytoplasm, they will continue transport to the nucleus. In this case, DNA can be

effectively protected against degradation and saved for later gene expression. But the diffusion difficulty still applies to cytoplasmic trafficking of polyplexes. In general, the larger the polyplexes are, the slower the mobility. However, there may exist other mechanisms for the transport of polyplexes in the cytoplasm in addition to passive diffusion. It has been reported by Suh and co-workers that PEI/DNA nanocomplexes displayed efficient perinuclear accumulation within minutes, which was proposed to be mediated by motor protein-driven transport on microtubules(53). But they did not examine whether the polyplexes were localized in endosomes or cytoplasm. Further research must be done to understand the machinery underlying this proposed active transport.

### 2.1.5 Nuclear Localization

Unlike drug delivery in which the cytoplasm is the desired destination for therapeutic drugs, gene delivery requires the gene of interest to be delivered into the nucleus, transcribed into mRNA, and subsequently translated into the desired proteins. Nuclear import, the final barrier known to limit gene expression(51, 54-55), includes two basic mechanisms: through nuclear pores or by sequestration on nuclear membrane breakdown during mitosis(56). The transport of polyplexes or DNA from the cytoplasm into the nucleus is limited by the presence of the nucleus envelope, which consists of two lipid layers, the outer membrane is continuous with the endoplasmic reticulum, and the inner membrane is the main residence of integral membrane proteins. Nuclear pore complex (NPC) span the nuclear envelope, which allow passive diffusion of small molecules (up to 9nm in diameter, or 50kDa) or

active transport of larger molecules (up to 26-28nm or 1MDa)(57-58). Active transport is mediated by the nuclear localization signal (NLS) in an energy dependent manner. Classical NLS sequences are characterized by a stretch of basic amino acids. SV40 NLS, the monopartite NLS derived from simian virus (SV) 40 large T-antigen, is the most extensively studied NLS with one cluster of basic amino acids(59-62). Bipartite NLS, found within the Xenopus protein known as nucleoplasmin, contains two clusters of basic amino acid regions separated by a 10-12 residues(63). The cargo containing the classical NLS binds to importin-α adapter, which in turn binds to importin-β to form a complex. The complex then mediates the interaction with NPC for an active nuclear import(22).The nonclassical NLS lacks the stretch of amino acid and binds to transportin instead of importin-β(64). Due to the dynamic nature of NPC, its conformation could undergo considerable changes in response to specific signals. For example, during passive transport, the NPC channel has a cross section of 9 nm, while this channel increases up to 25 nm during active translocation(46); in some cases the channel can be further dilated (e.g. up to 60nm) by some specific interaction(65). This conformational change of the NPC make it possible to permit active translocation of molecules as large as 25-50MDa(46).

The molecular weight cut-off for passive diffusion of linear double stranded DNA was reported to be between 200-310bp(66), or around 600bp, as observed elsewhere(67). The plasmid DNA usually has several kilobase pairs, which make it extremely difficult to enter the nucleus by passive diffusion(46). However, the plasmid DNA can make its way to the nucleus by active translocation after binding to

NLS containing proteins present in the cytoplasm, for example, the plasmid DNA was found to enter the nucleus by a process mediated by the nuclear targeting signal included in karyophilic proteins(51). It has been suggested that the molecular diameter is important for the entry to the nucleus through NPC, but there is no limitation on the length of the molecule(68). The plasmid DNA is very flexible in shape with a diameter ranging from 3.5 to 14nm(69), and is thus capable of being transported though the NPC. The polyplexes, however, usually have a spherical shape with the diameter up to several hundreds of nanometers, and are unlikely to undergo the nuclear uptake though NPC, though the fairly small polyplexes could still achieve access to nucleus in this manner(70).

The primary mechanism for nuclear transport of polyplexes lies in the disruption of nuclear envelope during mitotic phase in dividing cells. Once the only barrier separating the cytoplasm and nucleus disappears, polyplexes in the proximity of the nucleus can go straight inside by diffusion. As a result, the proliferation rate plays a significant role in gene transfer due to the high dependence of nuclear uptake on mitosis(71-73). Rapidly dividing cells with frequent nuclear envelope breakdown are much more likely to be transfected than non-dividing cells. There may also exist other mechanisms for nuclear uptake of polyplexes or DNA. Godbey and coworkers reported that PEI/DNA polyplexes could enter the nucleus via fusion with the nuclear envelope(74). They suggested the polyplexes could come into contact with phospholipids during endosomal disruption or cytoplasmic trafficking, and the phospholipids might remain adhered to the polyplexes by ionic interactions and facilitate the nuclear import. But a later study showed that the nuclear entry of

PEI/DNA polyplexes into L929 cells did not involve phospholipid fusion, since no signal of endosomal membrane was observed in the nucleus; instead, membrane disruption seemed necessary for nuclear entry which was suggested to depend on the cell type(72). Contrasting studies proposed that cell division is not required for some PEI-based polyplexes for they could transfect non-dividing cells(50, 75). More efforts are still needed to fully understand the mechanism of nuclear transport of polyplexes. As the final obstacle for gene delivery, the nuclear envelope can prevent a large portion of cytoplasmic polyplexes and/or plasmid DNA from entering the nucleus for carrying out gene expression(50).

### 2.1.6 Vector Unpacking

For DNA transcription to occur, the polymer/DNA polyplexes must dissociate and release the intact DNA somewhere along the route. The order of nuclear import and vector unpacking is still unclear. It has been reported that PEI/DNA polyplexes were found in the nucleus as associated condensates(74). In another study, the cytoplasmic release of pDNA from polyplexes composing different polycations was analyzed by fluorescence resonance energy transfer (FRET) with confocal microscopy. Linear (L) PEI/DNA polyplexes underwent a rapid unpacking after escaping from endosomes, while branched (B) PEI/DNA polyplexes retained in a condensed state. These intracellular characteristics showed a clear correlation to the transfection efficiency with LPEI/DNA polyplexes revealing considerably higher and faster gene expression compared to BPEI/DNA polyplexes. In the pDNA/PLL polyplexes, neither endosomal escape nor pDNA disassembly was observed(76).

The degree of polymerization was suggested to play an important role in the dissociation of polyplexes by examining the transfection efficacy of PLL with various lengths. Above an optimal length, overall transfection decreases as PLL length increases, indicating shorter polycations have a higher probability of dissociating from DNA(77). Following the same line, 25 kDa PEI is known to lead to higher transfection efficacy than that obtained with higher molecular weight of PEI(78). However, the polycations should have enough protonable moieties to effectively condense DNA and provide desired protection. Thus there is certain lower limit for the molecular weight of each type of polycation in gene delivery. For example, PEI and poly(β-amino esters) with molecular weights below 10 kDa exhibited poor performance as compared to higher molecular weight versions(79). Early disassembly and release of DNA from the vector into the cytoplasm may suffer severe loss of DNA by cytoplasmic sequestration or degradation. The disassembly occurring in perinuclear region, or inside of the nucleus would be desirable for efficient gene delivery and expression(50).

## 2.2 Strategies to Improve Extracellular and Intracellular Trafficking

Once polymer-DNA polyplexes form, they need to reach the site of action safely by overcoming many extracellular barriers, and eventually need to enter the nuclei of interested cells for desired gene expression by addressing all intracellular obstacles along the route. Strategies that have been developed for fighting against the limitations in polymeric gene delivery will be reviewed.

### 2.2.1 Hydrophilic Modification by PEG

Positive charges are necessary for polymers to condense DNA and associate with cell membrane. However, these charges may lead to unwanted interactions with blood components, fast clearance and cytotoxicity(80). Improving the stability of polyplexes in biological environment and prolonging their circulation time represent the main challenges for extracellular delivery. PEG is a linear polymer that can be fully hydrated in aqueous solution. Once conjugated to cationic polymers, the highly mobile and hydrated PEG chains can form a protective layer to inhibit the interaction from approaching particles. PEG is nontoxic and poorly immunogenic and has been approved by the food and drug administration (FDA) for topical and internal use in human. Gene delivery vesicles with PEG blocks on their surfaces can circumvent the adsorption of serum proteins, thus lowering the recognition by RES and keeping them active in blood circulation for longer period of time(81). The prolonged circulation time enables them to diffuse into malignant tissues by enhanced permeability and retention (EPR) effect(82-83). PEGylation or pegnology originated in the 1960s and has been extensively applied to cationic polymer-based transgene systems, such as PEI(84-85), PLL(86-89), PAMAM(90), Chitosan(91), PDMAEM(92-94), primarily to enhance the stability and biocompatibility of polyplexes by shielding the excess positive charges. Most of this PEGylation is achieved by covalent coupling (grafting or blocking) to the target polymers (prePEGylation), which could in turn change the biophysical properties of that polymer or the corresponding polyplex. For example, it has been reported that PEG interfered with DNA condensation process and resulted in more linear structured DNA condensates with PEGylated

PAMAM relative to the case of PAMAM(95). Furthermore, as the degree of PEGylation increases, the overall gene delivery efficiency tends to decrease as observed in PEI-based vectors, which might be due to the change in PEI ability of condensing DNA and buffering in endosomes(96-97). Similar results were reported for PEO modified polymeric systems(88, 98). The molecular weight of PEG might also cast some influence on the transfection efficiency(99). In order to minimize the negative influences of PEG on the conjugated polymers especially in term of DNA condensation, PEG has been be alternatively introduced to the vector after polyplex formation, that is postPEGylation or PEGylated polyplexes(3, 100-102). This strategy has been shown to provide higher shielding effect and longer circulation time relative to prePEGylation in two subcutaneous tumor models(103). The major drawback of postPEGylation lies in the additional sequential step of synthesis and purification which is inconvenient and time-consuming; furthermore, the degree of surface PEGylation is not well defined(96).

Aside from PEG (or PEO), Pluronics (triblock copolymer of PEO-PPO-PEO) are another attractive and safe alternative to improve the stability of polyplexes in biological conditions(104). Pluronics could be included in the gene carrier system via chemical reactions as those used for PEGylation; moreover, because of its hydrophobic PPO moiety, Pluronic forms micellar structures in aqueous solution which can then be bound to other hydrophobic segments by self-assembly(105). Also, Pluronics have been reported to be able to improve gene expression in different delivery routes(106-107). For example, Pluronic P123 has been shown to perform better than PEO with addition of free Pluronic 123 on PEI based gene

delivery(98). In addition to shielding the positively charged surfaces of polycation based vectors, nano-particles with overall neutral or even negative charge may also be desirable to prevent unwanted serum interactions due to charge-charge repulsion(10, 108-109).

### 2.2.2 Receptor Mediated Endocytosis

After successful extracellular delivery out of the blood into several organs, polyplexes mainly accumulate in the liver or lung(110). Selective association with and entrance into the desired tissues or cells are required and considered to be essential for later intracellular delivery and final gene expression. This process is usually achieved by modification of transgene vectors with specific targeting ligands that can recognize the corresponding receptors expressed on cell surfaces and promote cellular uptake via receptor-mediated endocytosis through the clathrin-coated pits. For targeted gene delivery, both transfection efficiency and selectivity are expected to improve due to the increased internalization of polyplexes. Construction of a targeting gene vector begins with selection of appropriate ligands for specific cell types. First of all, the ligand should bind with high affinity to the receptors expressed on the target cells; second of all, the ligand should be able to be coupled to the vector conveniently; Finally, modification with the ligand should not negatively affect the original properties of the vector, such as the particle size, interaction between polymer and DNA, stability of polyplexes in serum, and other special functionalities induced by different polymers.

Ligands that have been identified to be effective for targeted gene delivery

include: asialoglycoproteins(111-113), lactose(5) and galactose(114), which specifically bind to hepatocytes; transferrin (Tf)(96, 115-116), epidermal growth factor (EGF)(32, 117) and folate(102, 118), which are usually used for targeting tumor cells, mannose specifically associating with macrophages(119); RGD peptides for integrin-mediated targeted delivery, and so forth. Large ligands, such as Tf and EGF, could bring certain changes (e.g. the steric hindrance) to the vector system and need to be characterized carefully, whereas smaller ligands, such as lactose, galactose, mannose, folate, and short RGD sequences, would be relatively less complicated in use. Some ligands are very specific to certain cell types, such as asialoglycoproteins, whereas others are not, such as Tf and EGF, because of the universal expression of these kinds of receptors on cell surface, yet tumors over-express them compared to normal cells. Ligands also differ in the internalization rate and other biophysical properties that should be considered when choosing them for targeted gene delivery.

In general, the targeting ligands only provide targeting or enhanced uptake by receptor-mediated endocytosis, but they do not help in DNA packaging or particle stabilization. Thus, they need to be incorporated to a gene transfer system that has already been tested for the required properties to delivery gene and optimized for transfection conditions. Regarding the approach of ligand conjugation, there are different strategies in terms of the binding sites. The targeting ligands can be directly conjugated to the polymer that is responsible for condensing DNA. Galactosylated PEI (5% galactose) has been reported to efficiently neutralize DNA and selectively transfect the hepatocytes compared to fibroblasts(120), but the large

size of these polyplexes limited their use *in vivo*, so the length of the saccharide was tuned to produce relatively small and stable particles(121). However, the tendency of cationic polyplexes to form aggregates in physiological conditions does not change by adjusting the size of attaching ligands. As it has been mentioned above, PEGylation can effectively stabilize polyplexes in serum containing environment. Using PEG as a spacer between targeting ligands and DNA binding domains can not only improve the aqueous solubility and serum stability, but also increase the accessibility of the targeting ligands on the surface of polyplexes for the ligands could be protruded outwards with PEG chains(97, 122-123). By using PEG as a tether, a multifunctional transgene carrier could be constituted as a ligand-PEG-polycation, in which cell specificity, steric stabilization and DNA affinity are integrated(124). For short ligands, highly mobile PEG chains may also shield the ligands and inhibit their functions as has been found in a study of conjugation of a tetrapeptide of RGDC to PEI with or without PEG spacer(125). Whereas a longer RGD peptide, ACDCRGDCFC, indeed rendered great specificity when incorporated to PEI gene delivery system with a PEG spacer(97). To further fulfill the accessibility and the efficiency of targeting ligands, conjugation of ligands could be carried out after the formation of polyplexes. Blessing and coworkers compared the different strategies of including EGF into PEI-based transgene vectors shielded by PEG, and found EGF binding at the distal end of the PEG showed one order of magnitude more efficient than direct attachment of EGF to PEI with post PEG shielding(126).

Besides the position of ligand binding, the number of ligands in polyplexes also matters. Moreover, the properties of the polymers, the buffers used to make

polyplexes and other transfection facilitators may work cooperatively with the targeting ligands and should be considered when designing vectors for targeted gene delivery(77, 100, 117, 126-129).

### 2.2.3 Endosomal Buffering

Several strategies have been developed to ensure the protection and release of polyplexes from endocytic vesicles, which include co-administrating lysosomotropic agents to trigger membrane disruption, and incorporating polymeric components possessing great buffer capability or fusogenic peptides in vector constructs.

#### 2.2.3.1 Lysosomotropic Agents

Lysosomotropic agents are weak bases, such as chloroquine, ammonium chloride and methylamine, that can accumulate in acidic compartments (e.g. endosomes and lysosomes), raise the lumen pH, lead to osmotic swelling and inhibit the biological functions of corresponding organelles(130), for example, inhibit the maturation of endosomes thus retards degradation of DNA by lysosomal enzymes. Chloroquine is the most frequently used enhancer for achieving better endosomal release and high level of gene expression. In the earlier days of polymeric gene delivery, chloroquine was routinely added to cells along with the transgene vectors to facilitate endosomal escape and achieve high level of gene expression(131-133). However, ammonium chloride, another compound known to inhibit the acidification of endocytotic vesicles, has been found to produce a lower increase in transfection efficiency compared to chloroquine(131, 134), though it has also been shown to lead to complete escape of nanoparticles from endo/lysosomes(135). Similar results were

reported for the contributing effects to transfection between CLQ and sucrose(136). It seems that chloroquine possesses some other feature that can affect transfection in a positive way. Cheng and coworkers synthesized a family of chloroquine analogues and concluded though a series of comparative studies that chloroquine has at least three mechanistic features to induce enhancement in gene expression: pH buffering, polyplex unpacking, and alteration of the biophysical properties of the released DNA(137). Moreover, they suggested that the essential part of chloroquine is the aliphatic amino moiety, but the aromatic ring also plays an important role. These findings are very helpful in the development of the ideal substitutes for chloroquine, because the use, especially in term of clinical application, of chloroquine is limited due to its toxic properties. In *in vitro* studies, chloroquine could still be used as a tool to investigate the mechanism of gene delivery for specific systems. What is worth mentioning is the effectiveness of chloroquine in enhancing gene transfer is also cell type specific(138-139).

#### 2.2.3.2 Buffering Polymers and Fusogenic Peptides

An alternative approach to achieving endosomal release is osmotic endosomal disruption. Polymeric carriers that have protonable groups, such as secondary and tertiary amines, can buffer in acidic compartments and induce corresponding rupture under osmotic pressure, which is usually considered as the proton sponge effect. The “proton sponge hypothesis” was first proposed by Boussif et al. in testing PEI for its gene transfer potential in 1995(140). When PEI buffers the inner acidic endosome, a number of protons will be pumped into compartment via ATPase, and

counter-ions such as chloride will flow inside passively to neutralize the membrane potential, which together lead to an increase in the internal osmotic pressure and eventually the breakage of endosome (Fig. 2.2). This hypothesis has been evidenced by Sonawane et al. who reported that internalization of vectors containing strongly buffering polyamines PEI or polyamidoamine (PAMAM), compared to the vectors containing non-buffering PLL, further increased the endosomal $Cl^-$ concentration,

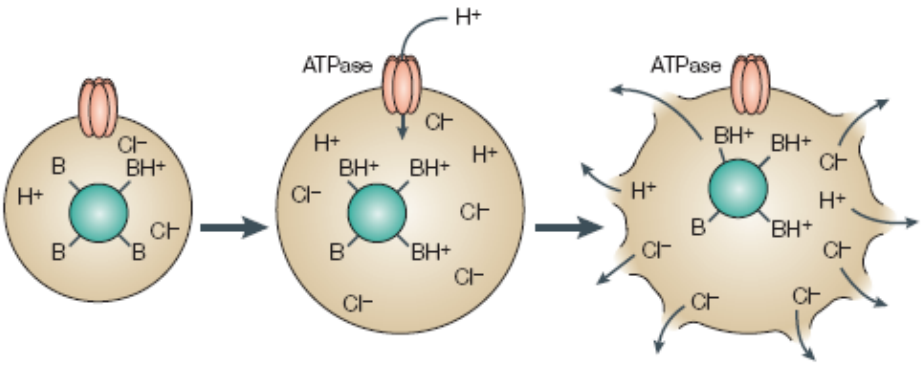


Fig. 2.2. Schematic of the pronton-sponge mechanism. Protonation of the proton-sponge polymer (green) causes increased influx of protons (and counter-ions) into endocytic vesicels. Increasing osmotic pressure causes the vesicle to swell and rupture (1)

lowered the acidification rate, swelled the endosome in size, and lead to the lysis of endosome(141). Fluorescence imaging also showed the far better endosomal escape ability of PEI-containing polyplexes than PLL-containing ones(142). These studies highlighted the importance of biologically titratable amine groups in the vector constructs. PEI has a very high density of amines, but only 15-25% of which are protonated at physiological pH(143), making it an extraordinary proton sponge. Likewise, with large numbers of second and tertiary amines, PAMAM dendrimers are

thought be another proton sponge type of polymers. In particular, the surface charge and buffering capability could be controlled by varying the number of generations in synthesis(144). This tunability makes it possible to design most effective vectors for specific applications(145). Poly (2-(dimethylamino)ethyl methacrylate) (PDMAEMA) also shows good endosomal escape indicating its potential as a proton sponge(92). Imidazole-containing polymers represent a new class of polymers that exhibit both required buffering capacity and great biocompability since imidazole is a component of histidine(146-147). But the pKa of imidazole ring is around 6(147), which indicates that histidines could only be protonated in an acidic environment. However, at biological pH, histidines or polyhistidines cannot be positively charged and are unable to form polyplexes with DNA, thereby requiring their grafting onto other cationic polymers.

The high transfection efficiency among proton sponge polymers is believed to be due in large part to the efficient endosomal release from digestive endocytic pathways. However, for those polymers lacking the ability to escape endosomes, structure modification is applicable. It has been reported that PLL has minimal buffering capacity in the range of pH 5 to 7 relative to PEI and PAMAM dentrimers (148). Thereby, PLL-based vectors usually work with certain membrane disrupting agents(149) or consist of other polymers that have great buffering capacity to achieve better endosomal release. Histidine has been incorporated into PLL in various strategies to provide an endosomal/lysosomal escape route without the addition of endosomolytic agents; histidylated polylysines (HpK) have been shown to be significantly more efficient and less toxic than unmodified PLL (89, 150-152).

Depending on the cell type, the optimal histidine conjugation was found to be 33-50% of the amino groups in PLL(153). In another study, the transfection efficiency of HpK polymers was found to have a strong correlation with the pH of endocytic vesicles(154). PLL was also modified with PAMAM to form a head-tail type polycation and resulted in around 100-fold higher transfection efficiency relative to that for PLL polyplexes(155). Imidazole modified β-cyclodextrin(156) or chitosan(157-158), and PEI modified chitosan(159-160) are some other representative examples of polymeric carriers that are constructed with endosomal escaping functionality.

Apart from including proton sponge polymers in the vector structures, fusogenic peptides, synthesized to mimic the process of membrane destabilization by viruses, were also used to enhance endosomal escape. These peptides destabilize membranes by increasing the negative curvature strain of the lipid bilayer or undergo change in formation to trigger endosomal membrane rupture (161). There are a good number of peptides that have been identified as fusogenic peptides(161-163). For instance, HA2 (sequences from influenza virus hemagglutinin)(164-166), amphipathic peptide GALA(167-168) and a truncated HIV-1 Tat protein(169) function via conformational change following membrane fusion, whereas peptides HRVs derived from rhinovirus VP-1 (170) induce membrane destabilization by increasing the curvature of membrane. These functional peptides can be conjugated to polymers to increase the efficacy of gene transfer by facilitating endosomal release. Moore and coworkers incorporated fusogenic peptides, INF7 and H5WYG which function at different pHs, into PEG-peptide based carrier system, respectively. The

transfection efficiency was shown to gain great enhancements by coupling these peptides, but INF7 performed better than H5WYG in that study(171-172). Lee et al. also reported the effectiveness of attaching fusogenic peptide KALA to PEG-g-PLL vectors to improve gene transfer(87).

### 2.2.4 Cytoplasmic Trafficking

The loss of DNA and slow mobility are two main obstacles for the cytoplasmic transport of gene delivery vesicles. The naked DNA that is released into the cytoplasm after polyplex disassociation becomes far more susceptible to the attack from endogenous nucleases, but complexing with polymeric carriers can reduce this damage to DNA payload(48). Thus, the approaches to improve the stability of polyplexes can also help to decrease the loss and DNA in cytoplasm. Moreover, the cytoplasmic mobility of polyplexes is superior to that of DNA alone owning to the advantage of smaller size and probably the potential active transport mechanism via cytoskeletal networks. Although the applicability of this active transport of polyplexes was hyphothesized, it provides a new perspective to explore and address the barrier associated with cytoplasm, and needs to be paid attention to(173).

### 2.2.5 Active Nuclear Localization

Although the exogenous material can definitely achieve the nuclear import through the nuclear membrane embedded nuclear pore complex (NPC)(174), the hourglass-like NPC cannot allow large cargo to transit though passively(175). It was suggested that plasmid DNA does not have the ability to actively go across the nuclear envelope(22, 58), unless assisted by the particular nuclear localization

signal (NLS). Both the size limit and the intensity of DNA nuclear transport could be increased by the attachment of strong nuclear localization signals(66). Therefore, including an NLS in the plasmid DNA is considered as an applicable approach to improve nuclear transport, especially in non-dividing cells(176).

One approach involves non-covalent association of NLS sequences to DNA via electrostatic interactions. Microinjection of SV40-derived NLS bound DNA into the cytosol of sebrafish embryo resulted in rapid nuclear uptake and enhanced gene expression(177-178). Through ionic interactions, the NLS peptide is bound to DNA to facilitate nuclear localization, and meanwhile it also packages DNA into small particles similar to what DNA condensing agents do. Nevertheless, only peptide sequences with more than eight positively charged amino acids could efficiently condense DNA(133), and longer peptides provides better condensation. Ritter et al. developed a tetrametric NLS peptide consisting of four copies of the SV40 NLS with glycine residues as the spacers(179). This NLS construct was able to condense DNA into small polyplexes and improve both nuclear uptake and gene expression on several cell lines. The non-specific ionic interactions do not allow control of the DNA-peptide binding sites, and thus might interfere with the transcription activity of the DNA. Sequence specific binding of NLS to DNA could be achieved by the specific interaction between DNA and peptide nucleic acid (PNA) consisting of certain NLS. In this manner, the NLS could be designed to bind the DNA in a region not involved in gene expression (180-181). Alternatively, DNA and NLS could be associated specifically though biotin-streptavidin interactions. The NLS-conjugated streptavidin was coupled to biotinylated linear DNA, resulting in enhanced nuclear transport in a

size dependent manner in permeabilized cells. Increased gene expression was observed after microinjection of this DNA-NLS conjugates into the cytoplasm of HeLa cells(182-183).

In a construct of DNA-NLS associated by non-covalent binding, the NLS could be lost during the intracellular trafficking. To prevent this dissociation, various methods have been used to covalently attach NLS peptides to plasmid DNA. Covalent coupling of SV40 NLS peptides to plasmid DNA by photoactivation has been shown to significantly increase the binding to importin-α, but no nuclear uptake was observed after cytoplasmic microinjection(184). Similar results were reported for NLS-plasmid DNA conjugates covalently bonded by diazo-coupling through PEG(185). These trials of non-specific association of NLS peptides to plasmid DNA bring about increase of binding to importins, but not of gene expression, which probably due to the inhibition of the reporter gene expression. Several approaches of sequence specific binding have been developed to address this problem. A single NLS peptide was coupled to a specific site on plasmid DNA by triple helix formation and photoactivated psoralen binding(186). By this technique, multiple NLSs could be introduced in a site-specific manner. Nevertheless, in spite of the defined structure of DNA-NLS conjugate, there was no significant increase in gene expression over the non-modified plasmid(58). In another study, one SV40 derived NLS was coupled to linear DNA at the 3' end capped with hairpin. 10- to 1000-fold increase in gene expression was observed relative to unmodified DNA(187). However, with the same method or just coupling NLS to the 5' end rather than 3' end of the linear DNA, no increase in gene expression was observed in the cell lines studied(188-189). The

discrepancy between these results indicates that the effectiveness of NLS incorporation in gene delivery depends on different experimental setups and cell types(190). The number of NLS coupled to DNA might also be an influencing factor, yet the results are controversial regarding how the number of NLS affects the gene expression. As shown above, one single NLS linked to a linear DNA lead to significant enhancement in the gene expression(187), while others reported an active transport with around 100 NLS per plasmid DNA(183). Contrasting results suggested large number of NLS could inhibit the gene expression(184). Currently, no definitive conclusion could be drawn in regard to the optimal number of NLS for efficient gene expression.

Besides adding NLS peptides to plasmid DNA, the NLS can also be attached to the DNA condensing components. In one study, the polyplexes containing NLS coupled PLL showed about 50-60% increase in the transfection efficiency compared to PLL without NLS, which could be attributed to the enhanced binding to importins, because PLL itself cannot do(191-192). Melittin, a component of bee sting venom, has been covalently attached to PEI to enhance the nuclear transport. Microinjection of melittin-PEI/DNA into the cytoplasm in HeLa cells resulted in 4-fold increase in gene expression over PEI/DNA polyplexes alone. This activity was abolished after co-injection with wheat germ agglutinin (WGA), indicating the involvement of NPC in the nuclear important of melittin containing polyplexes(193-194). Although inclusion of NLS in the vector could facilitate its nuclear transit though the NPC whose size limit which can be dilated up to 60nm, the polyplexes sized around 150nm are still excluded (195). Thus even with NLS, most of polyplexes are still too large to be

imported into the nucleus(55). Furthermore, the current literature is unclear on the efficacy of adding NLS to gene delivery vesicles with some researchers demonstrating enhanced gene expression and others showing little to no improvement. Further study is required to ascertain which type and extent of NLS signal incorporation is the most effective.

### 2.2.6 Improve Vector Unpacking

The vector packing and unpacking seems to be a dilemma in gene delivery. For the earlier route towards the target cells, DNA needs to be effectively condensed and remain undamaged; following the internalization and endocytic transport, DNA still needs the protection of polymeric carriers in an enzyme rich environment; even during the later cytoplasmic transport towards nucleus, DNA can hardly avoid the fate of being inactivated by nucleases unless it stays complexed with its carrier. But upon getting into the nucleus, DNA must be unpacked from the carrier to enable transcription. Efficient disassociation of polyplexes could be facilitated using degradable polymers. Low molecular weight polymers or oligomers can be crosslinked via disulfide bonds to develop thiol-triggered degradable polymers which can condense DNA in the extracellular environment and release DNA upon the intracellular balance of thiols and disulfide bonds(149, 196-199). With the characteristics of degradability, poly(Cys-$Lys_{10}$-Cys) showed better transfection efficiency than PLL alone(149, 198). Although the degradable carriers could release DNA intracellularly more readily, it is impossible to control the degradation site. Too much DNA released into the cytoplasm can result in considerable DNA loss. To

better control the intracellular unpacking of polymer/DNA polyplexes, thermo-responsive polymeric carriers have been developed to condense and release DNA in response to the temperature change(200-203). At higher temperatures such as 37ºC, the thermo-responsive polymeric carriers can compact DNA tightly and deliver it into the target cells safely; whereas as the temperature decreases below the transition temperature, the polyplex will become loosely bound and even dissociated. Thus, by applying appropriate stimuli, the DNA could be released site- and timing-specifically. Significant increase in the transfection efficiency was observed by introducing a short cooling period during the process of post-transfection as compared to the process with constant temperature at 37ºC. Furthermore, cooling the cells in 20h of transfection resulted in much higher level of gene expression than cooling them immediately after transfection, indicating it is more favorable to release DNA in the later intracellular stage which is probably closer to the nucleus(200, 202).

## 2.3 Concluding Remarks

The use of functional polymeric carriers is the strategy to overcome the extracellular and intracellular barriers in gene delivery. However, mono- or bifunctional polyplexes are not enough to address the multiple barriers present for most gene delivery systems. The ideal polymeric carriers should incorporate multifunctional components to address the rate limiting barriers with minimal interference between one functionality and another. For different vectors and cell

types, the rate limiting steps may vary and thus need to be examined before incorporating any additional functional component.

## References


1. D.W. Pack, A.S. Hoffman, S. Pun, and P.S. Stayton. Design and development of polymers for gene delivery. - 4:- 593 (2005).
2. H.C. Chiou, M.V. Tangco, S.M. Levine, D. Robertson, K. Kormis, C.H. Wu, and G.Y. Wu. Enhanced resistance to nuclease degradation of nucleic-acids complexed to asialoglycoprotein-polylysine carriers. Nucleic Acids Research. 22:5439-5446 (1994).
3. M. Ogris, S. Brunner, S. Schüller, R. Kircheis, and E. Wagner. PEGylated DNA/transferrin-PEI complexes: reduced interaction with blood components, extended circulation in blood and potential for systemic gene delivery. Gene Therapy. 6:595-605 (1999).
4. A. Agarwal, R. Vilensky, A. Stockdale, Y. Talmon, R.C. Unfer, and S.K. Mallapragada. Colloidally stable novel copolymeric system for gene delivery in complete growth media. Journal of Controlled Release. 121:28-37 (2007).
5. M. Hashimoto, M. Morimoto, H. Saimoto, Y. Shigemasa, and T. Sato. Lactosylated Chitosan for DNA Delivery into Hepatocytes: The Effect of Lactosylation on the Physicochemical Properties and Intracellular Trafficking of pDNA/Chitosan Complexes. Bioconjugate Chem. 17:309-316 (2006).
6. H. Ai, J.J. Pink, X.T. Shuai, D.A. Boothman, and J.M. Gao. Interactions between self-assembled polyelectrolyte shells and tumor cells. Journal of Biomedical Materials Research Part A. 73A:303-312 (2005).
7. P.R. Dash, M.L. Read, L.B. Barrett, M. Wolfert, and L.W. Seymour. Factors affecting blood clearance and in vivo distribution of polyelectrolyte complexes for gene delivery. Gene Therapy. 6:643-650 (1999).
8. M. Ruponen, P. Honkakoski, S. Ronkko, J. Pelkonen, M. Tammi, and A. Urtti. Extracellular and intracellular barriers in non-viral gene delivery. Journal of Controlled Release. 93:213-217 (2003).
9. T. Merdan, J. Kopecek, and T. Kissel. Prospects for cationic polymers in gene and oligonucleotide therapy against cancer. Advanced Drug Delivery Reviews. 54:715-758 (2002).
10. V.S. Trubetskoy, S.C. Wong, V. Subbotin, V.G. Budker, A. Loomis, J.E. Hagstrom, and J.A. Wolff. Recharging cationic DNA complexes with highly charged polyanions for in vitro and in vivo gene delivery. Gene Therapy. 10:261-271 (2003).

11. A.K. Singh, B.S. Kasinath, and E.J. Lewis. Interaction of polycations with cell-surface negative charges of epithelial-cells. Biochimica et Biophysica Acta. 1120:337-342 (1992).
12. K.A. Mislickand J.D. Baldeschwieler. Evidence for the role of proteoglycans in cation-mediated gene transfer. Proceedings of the National Academy of Sciences of the United States of America. 93:12349-12354 (1996).
13. I.A. Khalil, K. Kogure, H. Akita, and H. Harashima. Uptake Pathways and Subsequent Intracellular Trafficking in Nonviral Gene Delivery. Pharmacol Rev. 58:32-45 (2006).
14. S.D. Connerand S.L. Schmid. Regulated portals of entry into the cell. Nature. 422:37-44 (2003).
15. M. Amyere, M. Mettlen, P. Van der Smissen, A. Platek, B. Payrastre, A. Veithen, and P.J. Courtoy. Origin, originality, functions, subversions and molecular signalling of macropinocytosis, *10th European Workshop Conference on Bacterial Protein Toxins (ETOX 10)*, Urban & Fischer Verlag, Bhon, Belgium, 2001, pp. 487-494.
16. F.M. Brodsky, C.Y. Chen, C. Knuehl, M.C. Towler, and D.E. Wakeham. Biological basket weaving: Formation and function of clathrin-coated vesicles. Annu Rev Cell Dev Biol. 17:517-568 (2001).
17. P. Midoux, G. Breuzard, J.P. Gomez, and C. Pichon. Polymer-Based Gene Delivery: A Current Review on the Uptake and Intracellular Trafficking of Polyplexes. Curr Gene Ther. 8:335-352 (2008).
18. A. Ferrari, V. Pellegrini, C. Arcangeli, A. Fittipaldi, M. Giacca, and F. Beltram. Caveolae-mediated internalization of extracellular HIV-1 tat fusion proteins visualized in real time. Molecular Therapy. 8:284-294 (2003).
19. J. Rejman, A. Bragonzi, and M. Conese. Role of clathrin- and caveolae-mediated endocytosis in gene transfer mediated by lipo- and polyplexes. Molecular Therapy. 12:468-474 (2005).
20. R.G.W. Anderson, B.A. Kamen, K.G. Rothberg, and S.W. Lacey. Potocytosis - sequestration and transport of small molecules by caveolae. Science. 255:410-411 (1992).
21. K.M. Wagstaffand D.A. Jans. Nucleocytoplasmic transport of DNA: enhancing non-viral gene transfer. Biochem J. 406:185-202 (2007).
22. M. Belting, S. Sandgren, and A. Wittrup. Nuclear delivery of macromolecules: barriers and carriers. Advanced Drug Delivery Reviews. 57:505-527 (2005).
23. G.E. Palade. Fine structure of blood capillaries. J Appl Phys. 24:1424-1424 (1953).
24. K.L. Douglas, C.A. Piccirillo, and M. Tabrizian. Cell line-dependent internalization pathways and intracellular trafficking determine transfection efficiency of nanoparticle vectors. European Journal of Pharmaceutics and Biopharmaceutics. 68:676-687 (2008).

25. G. Sahay, E.V. Batrakova, and A.V. Kabanov. Different Internalization Pathways of Polymeric Micelles and Unimers and Their Effects on Vesicular Transport. Bioconjugate Chemistry. 19:2023-2029 (2008).
26. S.K. Lai, K. Hida, C. Chen, and J. Hanes. Characterization of the intracellular dynamics of a non-degradative pathway accessed by polymer nanoparticles. Journal of Controlled Release. 125:107-111 (2008).
27. J. Rejman, V. Oberle, I.S. Zuhorn, and D. Hoekstra. Size-dependent internalization of particles via the pathways of clathrin-and caveolae-mediated endocytosis. Biochem J. 377:159-169 (2004).
28. S.K. Lai, K. Hida, S.T. Man, C. Chen, C. Machamer, T.A. Schroer, and J. Hanes. Privileged delivery of polymer nanoparticles to the perinuclear region of live cells via a non-clathrin, non-degradative pathway. Biomaterials. 28:2876-2884 (2007).
29. C.L. Francis, T.A. Ryan, B.D. Jones, S.J. Smith, and S. Falkow. Ruffles induced by salmonella and other stimuli direct macropinocytosis of bacteria. Nature. 364:639-642 (1993).
30. J.A. Swansonand C. Watts. MACROPINOCYTOSIS. Trends Cell Biol. 5:424-428 (1995).
31. I.M. Kaplan, J.S. Wadia, and S.F. Dowdy. Cationic TAT peptide transduction domain enters cells by macropinocytosis. Journal of Controlled Release. 102:247-253 (2005).
32. K. de Bruin, N. Ruthardt, K. von Gersdorff, R. Bausinger, E. Wagner, M. Ogris, and C. Brauchle. Cellular dynamics of EGF receptor-targeted synthetic viruses. Molecular Therapy. 15:1297-1305 (2007).
33. A.R. Frenchand D.A. Lauffenburger. Intracellular receptor/ligand sorting based on endosomal retention components. Biotechnology and Bioengineering. 51:281-297 (1996).
34. A.R. French, D.K. Tadaki, S.K. Niyogi, and D.A. Lauffenburger. Intracellular trafficking of epidermal growth-factor family ligands is directly influenced by the ph sensitivity of the receptor-ligand interaction. Journal of Biological Chemistry. 270:4334-4340 (1995).
35. R. Bausinger, K. von Gersdorff, K. Braeckmans, M. Ogris, E. Wagner, C. Brauchle, and A. Zumbusch. The transport of nanosized gene carriers unraveled by live-cell imaging. Angew Chem-Int Edit. 45:1568-1572 (2006).
36. S.L. Rybakand R.F. Murphy. Primary cell cultures from murine kidney and heart differ in endosomal pH. J Cell Physiol. 176:216-222 (1998).
37. N.R.G.S.K.Z.M.B. Robert J. Gillies. MRI of the tumor microenvironment. Journal of Magnetic Resonance Imaging. 16:430-450 (2002).
38. O.A. Weisz. Organelle acidification and disease. Traffic. 4:57-64 (2003).
39. S.M. Simon. Role of organelle pH in tumor cell biology and drug resistance. Drug Discovery Today. 4:32-38 (1999).

40. A. Akincand R. Langer. Measuring the pH environment of DNA delivered using nonviral vectors: Implications for lysosomal trafficking. Biotechnology and Bioengineering. 78:503-508 (2002).

41. T. Takaiand H. Ohmori. DNA transfection of mouse lymphoid-cells by the combination of deae-dextran-mediated DNA uptake and osmotic shock procedure. Biochimica et Biophysica Acta. 1048:105-109 (1990).

42. K. Fushimiand A.S. Verkman. Low viscosity in the aqueous domain of cell cytoplasm measured by picosecond polarization microfluorimetry. Journal of Cell Biology. 112:719-725 (1991).

43. K. Lubyphelps, S. Mujumdar, R.B. Mujumdar, L.A. Ernst, W. Galbraith, and A.S. Waggoner. A novel fluorescence ratiometric method confirms the low solvent viscosity of the cytoplasm. Biophysical Journal. 65:236-242 (1993).

44. K. Luby-Phelps. Cytoarchitecture and physical properties of cytoplasm: Volume, viscosity. diffusion, intracellular surface area. International Review of Cytology - a Survey of Cell Biology, Vol 192, Vol. 192, Academic Press Inc, San Diego, 2000, pp. 189-221.

45. J.A. Steyer, H. Horstmann, and W. Almers. Transport, docking and exocytosis of single secretory granules in live chromaffin cells. Nature. 388:474-478 (1997).

46. D. Lechardeur, A.S. Verkman, and G.L. Lukacs. Intracellular routing of plasmid DNA during non-viral gene transfer. Advanced Drug Delivery Reviews. 57:755-767 (2005).

47. M. Arrio-Dupont, G. Foucault, M. Vacher, P.F. Devaux, and S. Cribier. Translational diffusion of globular proteins in the cytoplasm of cultured muscle cells. Biophysical Journal. 78:901-907 (2000).

48. D. Lechardeur, K.J. Sohn, M. Haardt, P.B. Joshi, M. Monck, R.W. Graham, B. Beatty, J. Squire, H. O'Brodovich, and G.L. Lukacs. Metabolic instability of plasmid DNA in the cytosol: a potential barrier to gene transfer. Gene Therapy. 6:482-497 (1999).

49. C.W. Taborand H. Tabor. Polyamines. Annual Review of Biochemistry. 53:749-790 (1984).

50. H. Pollard, J.-S. Remy, G. Loussouarn, S. Demolombe, J.-P. Behr, and D. Escande. Polyethylenimine but Not Cationic Lipids Promotes Transgene Delivery to the Nucleus in Mammalian Cells. J Biol Chem. 273:7507-7511 (1998).

51. M.E. Dowty, P. Williams, G.F. Zhang, J.E. Hagstrom, and J.A. Wolff. Plasmid DNA entry into postmitotic nuclei of primary rat myotubes. Proceedings of the National Academy of Sciences of the United States of America. 92:4572-4576 (1995).

52. G.L. Lukacs, P. Haggie, O. Seksek, D. Lechardeur, N. Freedman, and A.S. Verkman. Size-dependent DNA mobility in cytoplasm and nucleus. Journal of Biological Chemistry. 275:1625-1629 (2000).

53. J. Suh, D. Wirtz, and J. Hanes. Efficient active transport of gene nanocarriers to the cell nucleus. Proceedings of the National Academy of Sciences of the United States of America. 100:3878-3882 (2003).

54. Zabner J, Fasbender A J, Moninger T, et al. Cellular and molecular barriers to gene transfer by a cationic lipid. Journal of Biological Chemistry. 270:18997-19007 (1995).

55. C.W. Pouton, K.M. Wagstaff, D.M. Roth, G.W. Moseley, and D.A. Jans. Targeted delivery to the nucleus. Advanced Drug Delivery Reviews. 59:698-717 (2007).

56. D. Putnam. Polymers for gene delivery across length scales. Nat Mater. 5:439-451 (2006).

57. B. Talcottand M.S. Moore. Getting across the nuclear pore complex. Trends Cell Biol. 9:312-318 (1999).

58. V. Escriou, M. Carriere, D. Scherman, and P. Wils. NLS bioconjugates for targeting therapeutic genes to the nucleus. Advanced Drug Delivery Reviews. 55:295-306 (2003).

59. D. Kalderon, B.L. Roberts, W.D. Richardson, and A.E. Smith. A short amino-acid sequence able to specify nuclear location Cell. 39:499-509 (1984).

60. D.A. Dean. Import of plasmid DNA into the nucleus is sequence specific. Exp Cell Res. 230:293-302 (1997).

61. G.L. Wilson, B.S. Dean, G. Wang, and D.A. Dean. Nuclear import of plasmid DNA in digitonin-permeabilized cells requires both cytoplasmic factors and specific DNA sequences. Journal of Biological Chemistry. 274:22025-22032 (1999).

62. A.M. Millerand D.A. Dean. Cell-specific nuclear import of plasmid DNA in smooth muscle requires tissue-specific transcription factors and DNA sequences. Gene Therapy. 15:1107-1115 (2008).

63. J. Robbins, S.M. Dilworth, R.A. Laskey, and C. Dingwall. 2 interdependent basic domains in nucleoplasmin nuclear targeting sequence - identification of a class of bipartite nuclear targeting sequence. Cell. 64:615-623 (1991).

64. V.W. Pollard, W.M. Michael, S. Nakielny, M.C. Siomi, F. Wang, and G. Dreyfuss. A novel receptor-mediated nuclear protein import pathway. Cell. 86:985-994 (1996).

65. V. Shahin, L. Albermann, H. Schillers, L. Kastrup, C. Schafer, Y. Ludwig, C. Stock, and H. Oberleithner. Steroids dilate nuclear pores imaged with atomic force microscopy. J Cell Physiol. 202:591-601 (2005).

66. J.J. Ludtke, G.F. Zhang, M.G. Sebestyen, and J.A. Wolff. A nuclear localization signal can enhance both the nuclear transport and expression of 1 kb DNA. J Cell Sci. 112:2033-2041 (1999).

67. H. Salman, D. Zbaida, Y. Rabin, D. Chatenay, and M. Elbaum. Kinetics and mechanism of DNA uptake into the cell nucleus. Proceedings of the National Academy of Sciences of the United States of America. 98:7247-7252 (2001).

68. H. Eliyahu, Y. Barenholz, and A.J. Domb. Polymers for DNA delivery. Molecules. 10:34-64 (2005).

69. H.G. Abdelhady, S. Allen, S.J. Ebbens, C. Madden, N. Patel, C.J. Roberts, and J.X. Zhang. Towards nanoscale metrology for biomolecular imaging by atomic force microscopy. Nanotechnology. 16:966-973 (2005).

70. T.L. Fink, P.J. Klepcyk, S. Oette, C.R. Gedeon, S.L. Hyatt, T.H. Kowalczyk, R.C. Moen, and M.J. Cooper. Plasmid size up to 20 kbp does not limit effective in vivo lung gene transfer using compacted DNA nanoparticles. Gene Therapy. 13:1048-1051 (2006).

71. I. Mortimer, P. Tam, I. MacLachlan, R.W. Graham, E.G. Saravolac, and P.B. Joshi. Cationic lipid-mediated transfection of cells in culture requires mitotic activity. Gene Therapy. 6:403-411 (1999).

72. A. Remy-Kristensen, J.-P. Clamme, C. Vuilleumier, J.-G. Kuhry, and Y. Mely. Role of endocytosis in the transfection of L929 fibroblasts by polyethylenimine/DNA complexes. Biochimica et Biophysica Acta (BBA) - Biomembranes. 1514:21-32 (2001).

73. S. Brunner, T. Sauer, S. Carotta, M. Cotten, M. Saltik, and E. Wagner. Cell cycle dependence of gene transfer by lipoplex, polyplex and recombinant adenovirus. Gene Therapy. 7:401-407 (2000).

74. W.T. Godbey, K.K. Wu, and A.G. Mikos. Tracking the intracellular path of poly(ethylenimine)/DNA complexes for gene delivery. Proceedings of the National Academy of Sciences. 96:5177-5181 (1999).

75. S. Brunner, E. Furtbauer, T. Sauer, M. Kursa, and E. Wagner. Overcoming the nuclear barrier: Cell cycle independent nonviral gene transfer with linear polyethylenimine or electroporation. Molecular Therapy. 5:80-86 (2002).

76. K. Itaka, A. Harada, Y. Yamasaki, K. Nakamura, H. Kawaguchi, and K. Kataoka. In situ single cell observation by fluorescence resonance energy transfer reveals fast intra-cytoplasmic delivery and easy release of plasmid DNA complexed with linear polyethylenimine. Journal of Gene Medicine. 6:76-84 (2004).

77. D.V. Schaffer, N.A. Fidelman, N. Dan, and D.A. Lauffenburger. Vector unpacking as a potential barrier for receptor-mediated polyplex gene delivery. Biotechnology and Bioengineering. 67:598-606 (2000).

78. M. Thomasand A.M. Klibanov. Non-viral gene therapy: polycation-mediated DNA delivery. Applied Microbiology and Biotechnology. 62:27-34 (2003).

79. D.G. Anderson, A. Akinc, N. Hossain, and R. Langer. Structure/property studies of polymeric gene delivery using a library of poly(beta-amino esters). Molecular Therapy. 11:426-434 (2005).

80. S. Boeckle, K. von Gersdorff, S. van der Piepen, C. Culmsee, E. Wagner, and M. Ogris. Purification of polyethylenimine polyplexes highlights the role of free polycations in gene transfer. Journal of Gene Medicine. 6:1102-1111 (2004).

81. S.M. Moghimi, A.C. Hunter, and J.C. Murray. Long-Circulating and Target-Specific Nanoparticles: Theory to Practice. Pharmacol Rev. 53:283-318 (2001).

82. J. Fang, T. Sawa, and H. Maeda. Factors and mechanism of "EPR" effect and the enhanced antitumor effects of macromolecular drugs including SMANCS. Polymer Drugs in the Clinical Stage: Advantages and Prospects. 519:29-49 (2003).

83. K. Greish, J. Fang, T. Inutsuka, A. Nagamitsu, and H. Maeda. Macromolecular therapeutics - Advantages and prospects with special emphasis on solid tumour targeting. Clinical Pharmacokinetics. 42:1089-1105 (2003).

84. A. Kichler, M. Chillon, C. Leborgne, O. Danos, and B. Frisch. Intranasal gene delivery with a polyethylenimine-PEG conjugate. Journal of Controlled Release. 81:379-388 (2002).

85. J.W. Hong, J.H. Park, K.M. Huh, H. Chung, I.C. Kwon, and S.Y. Jeong. PEGylated polyethylenimine for in vivo local gene delivery based on lipiodolized emulsion system. Journal of Controlled Release. 99:167-176 (2004).

86. J.-W. Nah, L. Yu, S.-o. Han, C.-H. Ahn, and S.W. Kim. Artery wall binding peptide-poly(ethylene glycol)-grafted-poly(-lysine)-based gene delivery to artery wall cells. Journal of Controlled Release. 78:273-284 (2002).

87. H. Lee, J.H. Jeong, and T.G. Park. PEG grafted polylysine with fusogenic peptide for gene delivery: high transfection efficiency with low cytotoxicity. Journal of Controlled Release. 79:283-291 (2002).

88. Y.H. Choi, F. Liu, J.S. Kim, Y.K. Choi, J.S. Park, and S.W. Kim. Polyethylene glycol-grafted poly-L-lysine as polymeric gene carrier. Journal of Controlled Release. 54:39-48 (1998).

89. M. Bikram, C.H. Ahn, S.Y. Chae, M. Lee, J.W. Yockman, and S.W. Kim. Biodegradable Poly(ethylene glycol)-co-poly(L-lysine)-g-histidine Multiblock Copolymers for Nonviral Gene Delivery. Macromolecules. 37:1903-1916 (2004).

90. T.i. Kim, H.J. Seo, J.S. Choi, H.S. Jang, J.u. Baek, K. Kim, and J.S. Park. PAMAM-PEG-PAMAM: Novel Triblock Copolymer as a Biocompatible and Efficient Gene Delivery Carrier. Biomacromolecules. 5:2487-2492 (2004).

91. H.-Q. Mao, K. Roy, V.L. Troung-Le, K.A. Janes, K.Y. Lin, Y. Wang, J.T. August, and K.W. Leong. Chitosan-DNA nanoparticles as gene carriers: synthesis, characterization and transfection efficiency. Journal of Controlled Release. 70:399-421 (2001).

92. N.J. Zuidam, G. Posthuma, E.T.J. de Vries, D.J.A. Crommelin, W.E. Hennink, and G. Storm. Effects of physicochemical characteristics of poly(2-(dimethylamino)ethyl methacrylate)-based polyplexes on cellular association and internalization. J Drug Target. 8:51-66 (2000).

93. M. Oishi, K. Kataoka, and Y. Nagasaki. pH-Responsive Three-Layered PEGylated Polyplex Micelle Based on a Lactosylated ABC Triblock Copolymer as a Targetable and Endosome-Disruptive Nonviral Gene Vector. Bioconjugate Chem. 17:677-688 (2006).

94. A. Bonsted, B.O. Engesaeter, A. Hogset, G.M. Maelandsmo, L. Prasmickaite, C. D'Oliveira, W.E. Hennink, J.H. Steenis, and K. Berg. Photochemically enhanced transduction of polymer-complexed adenovirus targeted to the epidermal growth factor receptor. Journal of Gene Medicine. 8:286-297 (2006).

95. B.J. Rackstraw, A.L. Martin, S. Stolnik, C.J. Roberts, M.C. Garnett, M.C. Davies, and S.J.B. Tendler. Microscopic investigations into PEG-cationic polymer-induced DNA condensation. Langmuir. 17:3185-3193 (2001).

96. M. Kursa, G.F. Walker, V. Roessler, M. Ogris, W. Roedl, R. Kircheis, and E. Wagner. Novel Shielded Transferrin-Polyethylene Glycol-Polyethylenimine/DNA Complexes for Systemic Tumor-Targeted Gene Transfer. Bioconjugate Chem. 14:222-231 (2003).

97. W. Suh, S.O. Han, L. Yu, and S.W. Kim. An angiogenic, endothelial-cell-targeted polymeric gene carrier. Molecular Therapy. 6:664-672 (2002).

98. H.K. Nguyen, P. Lemieux, S.V. Vinogradov, C.L. Gebhart, N. Guerin, G. Paradis, T.K. Bronich, V.Y. Alakhov, and A.V. Kabanov. Evaluation of polyether-polyethyleneimine graft copolymers as gene transfer agents. Gene Therapy. 7:126-138 (2000).

99. M.R. Park, K.O. Han, I.K. Han, M.H. Cho, J.W. Nah, Y.J. Choi, and C.S. Cho. Degradable polyethylenimine-alt-poly(ethylene glycol) copolymers as novel gene carriers. Journal of Controlled Release. 105:367-380 (2005).

100. M. Ogris, G. Walker, T. Blessing, R. Kircheis, M. Wolschek, and E. Wagner. Tumor-targeted gene therapy: strategies for the preparation of ligand-polyethylene glycol-polyethylenimine/DNA complexes. Journal of Controlled Release. 91:173-181 (2003).

101. S. Mishra, P. Webster, and M.E. Davis. PEGylation significantly affects cellular uptake and intracellular trafficking of non-viral gene delivery particles. European Journal of Cell Biology. 83:97-111 (2004).

102. J.H. van Steenis, E.M. van Maarseveen, F.J. Verbaan, R. Verrijk, D.J.A. Crommelin, G. Storm, and W.E. Hennink. Preparation and characterization of folate-targeted pEG-coated pDMAEMA-based polyplexes. Journal of Controlled Release. 87:167-176 (2003).

103. F.J. Verbaan, C. Oussoren, C.J. Snel, D.J.A. Crommelin, W.E. Hennink, and G. Storm. Steric stabilization of poly(2-(dimethylamino)ethyl methacrylate)-based polyplexes mediates prolonged circulation and tumor targeting in mice. The Journal of Gene Medicine. 6:64-75 (2004).

104. K.C. Cho, S.H. Choi, and T.G. Park. Low molecular weight PEI conjugated pluronic copolymer: Useful additive for enhancing gene Transfection efficiency. Macromol Res. 14:348-353 (2006).

105. A. Agarwal, R.C. Unfer, and S.K. Mallapragada. Dual-role self-assembling nanoplexes for efficient gene transfection and sustained gene delivery. Biomaterials. 29:607-617 (2008).

106. A.V. Kabanov, E.V. Batrakova, and V.Y. Alakhov. Pluronic(R) block copolymers as novel polymer therapeutics for drug and gene delivery. Journal of Controlled Release. 82:189-212 (2002).

107. A. Kabanov, J. Zhu, V. Alakhov, and M.-C.H.a.E.W. Leaf Huang. Pluronic Block Copolymers for Gene Delivery. Advances in Genetics, Vol. Volume 53, Academic Press, 2005, pp. 231-261.

108. H.W. Zhang, A. Mitin, and S.V. Vinogradov. Efficient Transfection of Blood-Brain Barrier Endothelial Cells by Lipoplexes and Polyplexes in the Presence of Nuclear Targeting NLS-PEG-Acridine Conjugates. Bioconjugate Chemistry. 20:120-128 (2009).

109. C.-W. Chang, D. Choi, W.J. Kim, J.W. Yockman, L.V. Christensen, Y.-H. Kim, and S.W. Kim. Non-ionic amphiphilic biodegradable PEG-PLGA-PEG copolymer enhances gene delivery efficiency in rat skeletal muscle. Journal of Controlled Release. 118:245-253 (2007).

110. A.G. Schatzlein. Targeting of synthetic gene delivery systems. J Biomed Biotechnol. 2003:149-158 (2003).

111. K. Koike, T. Hara, Y. Aramaki, S. Takada, and S. Tsuchiya. Receptor-Mediated Gene Transfer into Hepatic Cells Using Asialoglycoprotein-Labeled Liposomes. Annals of the New York Academy of Sciences. 716:331-333 (1994).

112. E.-M. Kim, H.-J. Jeong, I.-K. Park, C.-S. Cho, H.-B. Moon, D.-Y. Yu, H.-S. Bom, M.-H. Sohn, and I.-J. Oh. Asialoglycoprotein receptor targeted gene delivery using galactosylated polyethylenimine-graft-poly(ethylene glycol): In vitro and in vivo studies. Journal of Controlled Release. 108:557-567 (2005).

113. S. Diez, G. Navarro, and C.T. de Ilarduya. In vivo targeted gene delivery by cationic nanoparticles for treatment of hepatocellular carcinoma. Journal of Gene Medicine. 11:38-45 (2009).

114. S. Kawakami, S. Fumoto, M. Nishikawa, F. Yamashita, and M. Hashida. In Vivo Gene Delivery to the Liver Using Novel Galactosylated Cationic Liposomes. Pharmaceutical Research. 17:306-313 (2000).

115. S. Kakimoto, T. Moriyama, T. Tanabe, S. Shinkai, and T. Nagasaki. Dual-ligand effect of transferrin and transforming growth factor alpha on polyethyleneimine-mediated gene delivery. Journal of Controlled Release. 120:242-249 (2007).

116. R. Kircheis, L. Wightman, A. Schreiber, B. Robitza, V. Rossler, M. Kursa, and E. Wagner. Polyethylenimine/DNA complexes shielded by transferrin target gene expression to tumors after systemic application. Gene Therapy. 8:28-40 (2001).

117. K. von Gersdorff, M. Ogris, and E. Wagner. Cryoconserved shielded and EGF receptor targeted DNA polyplexes: cellular mechanisms. European Journal of Pharmaceutics and Biopharmaceutics. 60:279-285 (2005).

118. S.H. Kim, H. Mok, J.H. Jeong, S.W. Kim, and T.G. Park. Comparative evaluation of target-specific GFP gene silencing efficiencies for antisense ODN, synthetic siRNA, and siRNA plasmid complexed with PEI-PEG-FOL conjugate. Bioconjugate Chemistry. 17:241-244 (2006).

119. W. Wijagkanalan, S. Kawakami, M. Takenaga, R. Igarashi, F. Yamashita, and M. Hashida. Efficient targeting to alveolar macrophages by intratracheal administration of mannosylated liposomes in rats. Journal of Controlled Release. 125:121-130 (2008).

120. M.A. Zanta, O. Boussif, A. Adib, and J.P. Behr. In vitro gene delivery to hepatocytes with galactosylated polyethylenimine. Bioconjugate Chemistry. 8:839-844 (1997).

121. T. Bettinger, J.S. Remy, and P. Erbacher. Size reduction of galactosylated PEI/DNA complexes improves lectin-mediated gene transfer into hepatocytes. Bioconjugate Chemistry. 10:558-561 (1999).

122. K. Sagaraand S.W. Kim. A new synthesis of galactose-poly(ethylene glycol)-polyethylenimine for gene delivery to hepatocytes. Journal of Controlled Release. 79:271-281 (2002).

123. M. Leeand S.W. Kim. Polyethylene glycol-conjugated copolymers for plasmid DNA delivery. Pharmaceutical Research. 22:1-10 (2005).

124. K. Chul Cho, J. Hoon Jeong, H. Jung Chung, C. O Joe, S. Wan Kim, and T. Gwan Park. Folate receptor-mediated intracellular delivery of recombinant caspase-3 for inducing apoptosis. Journal of Controlled Release. 108:121-131 (2005).

125. K. Kunath, T. Merdan, O. Hegener, H. Haberlein, and T. Kissel. Integrin targeting using RGD-PEI conjugates for in vitro gene transfer. Journal of Gene Medicine. 5:588-599 (2003).

126. T. Blessing, M. Kursa, R. Holzhauser, R. Kircheis, and E. Wagner. Different Strategies for Formation of PEGylated EGF-Conjugated PEI/DNA Complexes for Targeted Gene Delivery. Bioconjugate Chem. 12:529-537 (2001).

127. H. Lee, T.H. Kim, and T.G. Park. A receptor-mediated gene delivery system using streptavidin and biotin-derivatized, pegylated epidermal growth factor. Journal of Controlled Release. 83:109-119 (2002).

128. M.F. Wolschek, C. Thallinger, M. Kursa, V. Rössler, M. Allen, C. Lichtenberger, R. Kircheis, T. Lucas, M. Willheim, W. Reinisch, A. Gangl, E. Wagner, and B. Jansen. Specific systemic

nonviral gene delivery to human hepatocellular carcinoma xenografts in SCID mice. Hepatology. 36:1106-1114 (2002).

129. T.K.W. Lee, J.S. Han, S.T. Fan, Z.D. Liang, P.K. Tian, J.R. Gu, and I.O.L. Ng. Gene delivery using a receptor-mediated gene transfer system targeted to hepatocellular carcinoma cells. International Journal of Cancer. 93:393-400 (2001).
130. D.D. Plessand R.B. Wellner. In vitro fusion of endocytic vesicles: Effects of reagents that alter endosomal pH. J Cell Biochem. 62:27-39 (1996).
131. P. Erbacher, A.C. Roche, M. Monsigny, and P. Midoux. Putative role of chloroquine in gene transfer into a human hepatoma cell line by DNA lactosylated polylysine complexes. Exp Cell Res. 225:186-194 (1996).
132. J.D. Fritz, H. Herweijer, G.F. Zhang, and J.A. Wolff. Gene transfer into mammalian cells using histone-condensed plasmid DNA. Human Gene Therapy. 7:1395-1404 (1996).
133. C. Plank, M.X. Tang, A.R. Wolfe, and F.C. Szoka. Branched cationic peptides for gene delivery: Role of type and number of cationic residues in formation and in vitro activity of DNA polyplexes. Human Gene Therapy. 10:319-332 (1999).
134. G. Misinzo, P.L. Delputte, and H.J. Nauwynck. Inhibition of endosome-lysosome system acidification enhances porcine circovirus 2 infection of porcine epithelial cells. J Virol. 82:1128-1135 (2008).
135. J. Panyam, W.Z. Zhou, S. Prabha, S.K. Sahoo, and V. Labhasetwar. Rapid endo-lysosomal escape of poly(DL-lactide-co-glycolide) nanoparticles: implications for drug and gene delivery. Faseb J. 16:10 (2002).
136. T. Katav, L. Liu, T. Traitel, R. Goldbart, M. Wolfson, and J. Kost. Modified pectin-based carrier for gene delivery: Cellular barriers in gene delivery course. Journal of Controlled Release. 130:183-191 (2008).
137. J.J. Cheng, R. Zeidan, S. Mishra, A. Liu, S.H. Pun, R.P. Kulkarni, G.S. Jensen, N.C. Bellocq, and M.E. Davis. Structure - Function correlation of chloroquine and analogues as transgene expression enhancers in nonviral gene delivery. J Med Chem. 49:6522-6531 (2006).
138. D.M. Sipe, A. Jesurum, and R.F. Murphy. Absence of Na+,K+-ATPase regulation of endosomal acidification in K562 erythroleukemia-cells - analysis via inhibition of transferrin recycling by low-temperatures. Journal of Biological Chemistry. 266:3469-3474 (1991).
139. K. Ciftciand R.J. Levy. Enhanced plasmid DNA transfection with lysosomotropic agents in cultured fibroblasts. International Journal of Pharmaceutics. 218:81-92 (2001).
140. O. Boussif, F. Lezoualc'h, M.A. Zanta, M.D. Mergny, D. Scherman, B. Demeneix, and J. Behr. A Versatile Vector for Gene and Oligonucleotide Transfer into Cells in Culture and in vivo: Polyethylenimine. Proceedings of the National Academy of Sciences. 92:7297-7301 (1995).

141. N.D. Sonawane, F.C. Szoka, Jr., and A.S. Verkman. Chloride Accumulation and Swelling in Endosomes Enhances DNA Transfer by Polyamine-DNA Polyplexes. J Biol Chem. 278:44826-44831 (2003).

142. W.T. Godbey, M.A. Barry, P. Saggau, K.K. Wu, and A.G. Mikos. Poly(ethylenimine)-mediated transfection: A new paradigm for gene delivery. Journal of Biomedical Materials Research. 51:321-328 (2000).

143. J. Suh, H.J. Paik, and B.K. Hwang. Ionization of Poly(ethylenimine) and Poly(allylamine) at Various pHs. Bioorganic Chem. 22:318-327 (1994).

144. D.A. Tomalia, A.M. Naylor, and W.A. Goddard. Starburst dendrimers - molecular-level control of size, shape, surface-chemistry, topology, and flexibility from atoms to macroscopic matter. Angew Chem-Int Edit Engl. 29:138-175 (1990).

145. J. Haenslerand F.C. Szoka. Polyamidoamine cascade polymers mediate efficient transfection of cells in culture. Bioconjugate Chemistry. 4:372-379 (1993).

146. S. Asayama, H. Kato, H. Kawakami, and S. Nagaoka. Carboxymethyl poly(L-histidine) as a new pH-sensitive polypeptide at endosomal/lysosomal pH. Polymers for Advanced Technologies. 18:329-333 (2007).

147. S. Asayama, T. Sekine, H. Kawakami, and S. Nagaoka. Design of aminated poly(1-vinylimidazole) for a new pH-Sensitive polycation to enhance cell-specific gene delivery. Bioconjugate Chemistry. 18:1662-1667 (2007).

148. M.X. Tangand F.C. Szoka. The influence of polymer structure on the interactions of cationic polymers with DNA and morphology of the resulting complexes. Gene Therapy. 4:823-832 (1997).

149. M.L. Read, S. Singh, Z. Ahmed, M. Stevenson, S.S. Briggs, D. Oupicky, L.B. Barrett, R. Spice, M. Kendall, M. Berry, J.A. Preece, A. Logan, and L.W. Seymour. A versatile reducible polycation-based system for efficient delivery of a broad range of nucleic acids. Nucleic Acids Research. 33:16 (2005).

150. P. Midouxand M. Monsigny. Efficient gene transfer by histidylated polylysine pDNA complexes. Bioconjugate Chemistry. 10:406-411 (1999).

151. J.M. Benns, J.S. Choi, R.I. Mahato, J.S. Park, and S.W. Kim. pH-Sensitive Cationic Polymer Gene Delivery Vehicle: N-Ac-poly(L-HISTIDINE)-GRAFT-POLY(L-lysine) Comb Shaped Polymer. Bioconjugate Chem. 11:637-645 (2000).

152. D. Putnam, C.A. Gentry, D.W. Pack, and R. Langer. Polymer-based gene delivery with low cytotoxicity by a unique balance of side-chain termini. Proceedings of the National Academy of Sciences of the United States of America. 98:1200-1205 (2001).

153. P. Midoux, C. Pichon, J.J. Yaouanc, and P.A. Jaffres. Chemical vectors for gene delivery: a current review on polymers, peptides and lipids containing histidine or imidazole as nucleic acids carriers. Br J Pharmacol. 157:166-178 (2009).

154. Q.R. Chen, L. Zhang, P.W. Luther, and A.J. Mixson. Optimal transfection with the HK polymer depends on its degree of branching and the pH of endocytic vesicles. Nucleic Acids Research. 30:1338-1345 (2002).

155. A. Harada, M. Kawamura, T. Matsuo, T. Takahashi, and K. Kono. Synthesis and Characterization of a Head-Tail Type Polycation Block Copolymer as a Nonviral Gene Vector. Bioconjugate Chem. 17:3-5 (2006).

156. S. Mishra, J.D. Heidel, P. Webster, and M.E. Davis. Imidazole groups on a linear, cyclodextrin-containing polycation produce enhanced gene delivery via multiple processes, *9th European Symposium on Controlled Drug Delivery*, Elsevier Science Bv, Noordwijk, NETHERLANDS, 2006, pp. 179-191.

157. T.H. Kim, J.E. Ihm, Y.J. Choi, J.W. Nah, and C.S. Cho. Efficient gene delivery by urocanic acid-modified chitosan. Journal of Controlled Release. 93:389-402 (2003).

158. H. Jin, T.H. Kim, S.K. Hwang, S.H. Chang, H.W. Kim, H.K. Anderson, H.W. Lee, K.H. Lee, N.H. Colburn, H.S. Yang, M.H. Cho, and C.S. Cho. Aerosol delivery of urocanic acid-modified chitosan/programmed cell death 4 complex regulated apoptosis, cell cycle, and angiogenesis in lungs of K-ras null mice. Mol Cancer Ther. 5:1041-1049 (2006).

159. H.-L. Jiang, Y.-K. Kim, R. Arote, J.-W. Nah, M.-H. Cho, Y.-J. Choi, T. Akaike, and C.-S. Cho. Chitosan-graft-polyethylenimine as a gene carrier. Journal of Controlled Release. 117:273-280 (2007).

160. K. Wong, G. Sun, X.Q. Zhang, H. Dai, Y. Liu, C.B. He, and K.W. Leong. PEI-g-chitosan, a Novel Gene Delivery System with Transfection Efficiency Comparable to Polyethylenimine in Vitro and after Liver Administration in Vivo. Bioconjugate Chem. 17:152-158 (2006).

161. C. Plank, W. Zauner, and E. Wagner. Application of membrane-active peptides for drug and gene delivery across cellular membranes. Advanced Drug Delivery Reviews. 34:21-35 (1998).

162. A. El-Sayed, S. Futaki, and H. Harashima. Delivery of Macromolecules Using Arginine-Rich Cell-Penetrating Peptides: Ways to Overcome Endosomal Entrapment. AAPS Journal. 11:13-22 (2009).

163. A. El-Sayed, T. Masuda, I. Khalil, H. Akita, and H. Harashima. Enhanced gene expression by a novel stearylated INF7 peptide derivative through fusion independent endosomal escape. Journal of Controlled Release. 138:160-167 (2009).

164. R.W. Doms, A. Helenius, and J. White. Membrane-fusion activity of the influenza-virus hemagglutinin - the low pH-induced conformational change. Journal of Biological Chemistry. 260:2973-2981 (1985).

165. E. Wagner, C. Plank, K. Zatloukal, M. Cotten, and M.L. Birnstiel. Influenza-virus hemagglutinin-HA-2 N-terminal fusogenic peptides augment gene-transfer by transferrin polylysine DNA complexes - toward a synthetic virus-like gene-transfer vehicle. Proceedings of the National Academy of Sciences of the United States of America. 89:7934-7938 (1992).

166. M. Rafalski, A. Ortiz, A. Rockwell, L.C. Vanginkel, J.D. Lear, W.F. Degrado, and J. Wilschut. Membrane-fusion activity of the influenza-virus hemagglutinin - interaction of HA2 N-terminal peptides with phospholipid-vesicles. Biochemistry. 30:10211-10220 (1991).

167. R.A. Parente, S. Nir, and F.C. Szoka. Mechanism of leakage of phospholipid vesicle contents induced by the peptide GALA. Biochemistry. 29:8720-8728 (1990).

168. W.J. Li, F. Nicol, and F.C. Szoka. GALA: a designed synthetic pH-responsive amphipathic peptide with applications in drug and gene delivery. Advanced Drug Delivery Reviews. 56:967-985 (2004).

169. E. Vives, P. Brodin, and B. Lebleu. A truncated HIV-1 Tat protein basic domain rapidly translocates through the plasma membrane and accumulates in the cell nucleus. Journal of Biological Chemistry. 272:16010-16017 (1997).

170. W. Zauner, D. Blaas, E. Kuechler, and E. Wagner. RHINOVIRUS-MEDIATED ENDOSOMAL RELEASE OF TRANSFECTION COMPLEXES. J Virol. 69:1085-1092 (1995).

171. N.M. Moore, C.L. Sheppard, T.R. Barbour, and S.E. Sakiyama-Elbert. The effect of endosomal escape peptides on in vitro gene delivery of polyethylene glycol-based vehicles. Journal of Gene Medicine. 10:1134-1149 (2008).

172. N.M. Moore, C.L. Sheppard, and S.E. Sakiyama-Elbert. Characterization of a multifunctional PEG-based gene delivery system containing nuclear localization signals and endosomal escape peptides. Acta Biomater. 5:854-864 (2009).

173. E. Wagner. Strategies to improve DNA polyplexes for in vivo gene transfer: Will "artificial viruses" be the answer? Pharmaceutical Research. 21:8-14 (2004).

174. G. Liu, D. Li, M.K. Pasumarthy, T.H. Kowalczyk, C.R. Gedeon, S.L. Hyatt, J.M. Payne, T.J. Miller, P. Brunovskis, T.L. Fink, O. Muhammad, R.C. Moen, R.W. Hanson, and M.J. Cooper. Nanoparticles of Compacted DNA Transfect Postmitotic Cells. J Biol Chem. 278:32578-32586 (2003).

175. N. Panteand M. Kann. Nuclear Pore Complex Is Able to Transport Macromolecules with Diameters of ~39 nm. Mol Biol Cell. 13:425-434 (2002).

176. D.A. Dean, B.S. Dean, S. Muller, and L.C. Smith. Sequence requirements for plasmid nuclear import. Exp Cell Res. 253:713-722 (1999).

177. P. Collas, H. Husebye, and P. Aleström. The nuclear localization sequence of the SV40 T antigen promotes transgene uptake and expression in zebrafish embryo nuclei. Transgenic Research. 5:451-458 (1996).

178. P. Collasand P. Alestrom. Rapid targeting of plasmid DNA to zebrafish embryo nuclei by the nuclear localization signal of SV40 T antigen. Molecular Marine Biology and Biotechnology. 6:48-58 (1997).

179. W. Ritter, C. Plank, J. Lausier, C. Rudolph, D. Zink, D. Reinhardt, and J. Rosenecker. A novel transfecting peptide comprising a tetrameric nuclear localization sequence. J Mol Med. 81:708-717 (2003).

180. L.J. Branden, A.J. Mohamed, and C.I.E. Smith. A peptide nucleic acid-nuclear localization signal fusion that mediates nuclear transport of DNA. Nat Biotechnol. 17:784-787 (1999).

181. L.J. Branden, B. Christensson, and C.I.E. Smith. In vivo nuclear delivery of oligonucleotides via hybridizing bifunctional peptides. Gene Therapy. 8:84-87 (2001).

182. J.J. Ludtke, G. Zhang, M.G. Sebestyen, and J.A. Wolff. A nuclear localization signal can enhance both the nuclear transport and expression of 1 kb DNA. J Cell Sci. 112:2033-2041 (1999).

183. M.G. Sebestyen, J.J. Ludtke, M.C. Bassik, G.F. Zhang, V. Budker, E.A. Lukhtanov, J.E. Hagstrom, and J.A. Wolff. DNA vector chemistry: The covalent attachment of signal peptides to plasmid DNA. Nat Biotechnol. 16:80-85 (1998).

184. C. Ciolina, G. Byk, F. Blanche, V. Thuillier, D. Scherman, and P. Wils. Coupling of Nuclear Localization Signals to Plasmid DNA and Specific Interaction of the Conjugates with Importin &#x03B1. Bioconjugate Chemistry. 10:49-55 (1999).

185. T. Nagasaki, T. Myohoji, T. Tachibana, S. Futaki, and S. Tamagaki. Can nuclear localization signals enhance nuclear localization of plasmid DNA? Bioconjugate Chemistry. 14:282-286 (2003).

186. C. Neves, G. Byk, D. Scherman, and P. Wils. Coupling of a targeting peptide to plasmid DNA by covalent triple helix formation. Febs Letters. 453:41-45 (1999).

187. M.A. Zanta, P. Belguise-Valladier, and J.-P. Behr. Gene delivery: A single nuclear localization signal peptide is sufficient to carry DNA to the cell nucleus. Proceedings of the National Academy of Sciences. 96:91-96 (1999).

188. M. Tanimoto, H. Kamiya, N. Minakawa, A. Matsuda, and H. Harashima. No enhancement of nuclear entry by direct conjugation of a nuclear localization signal peptide to linearized DNA. Bioconjugate Chemistry. 14:1197-1202 (2003).

189. M. van der Aa, G.A. Koning, C. d'Oliveira, R.S. Oosting, K.J. Wilschut, W.E. Hennink, and D.J.A. Crommelin. An NLS peptide covalently linked to linear DNA does not enhance transfection efficiency of cationic polymer based gene delivery systems. Journal of Gene Medicine. 7:208-217 (2005).

190. M. van der Aa, E. Mastrobattista, R.S. Oosting, W.E. Hennink, G.A. Koning, and D.J.A. Crommelin. The nuclear pore complex: The gateway to successful nonviral gene delivery. Pharmaceutical Research. 23:447-459 (2006).

191. C.K. Chanand D.A. Jans. Enhancement of polylysine-mediated transferrinfection by nuclear localization sequences: Polylysine does not function as a nuclear localization sequence. Human Gene Therapy. 10:1695-1702 (1999).

192. C.K. Chan, T. Senden, and D.A. Jans. Supramolecular structure and nuclear targeting efficiency determine the enhancement of transfection by modified polylysines. Gene Therapy. 7:1690-1697 (2000).

193. R.C. Carlisle, T. Bettinger, M. Ogris, S. Hale, V. Mautner, and L.W. Seymour. Adenovirus hexon protein enhances nuclear delivery and increases transgene expression of polyethylenimine/plasmid DNA vectors. Molecular Therapy. 4:473-483 (2001).

194. M. Ogris, R.C. Carlisle, T. Bettinger, and L.W. Seymour. Melittin enables efficient vesicular escape and enhanced nuclear access of nonviral gene delivery vectors. Journal of Biological Chemistry. 276:47550-47555 (2001).

195. C.-K. Chanand D.A. Jans. Using nuclear targeting signals to enhance non-viral gene transfer. Immunol Cell Biol. 80:119-130 (2002).

196. D.L. McKenzie, E. Smiley, K.Y. Kwok, and K.G. Rice. Low molecular weight disulfide cross-linking peptides as nonviral gene delivery carriers. Bioconjugate Chemistry. 11:901-909 (2000).

197. E. Dauty, J.S. Remy, T. Blessing, and J.P. Behr. Dimerizable cationic detergents with a low cmc condense plasmid DNA into nanometric particles and transfect cells in culture. Journal of the American Chemical Society. 123:9227-9234 (2001).

198. D. Oupicky, R.C. Carlisle, and L.W. Seymour. Triggered intracellular activation of disulfide crosslinked polyelectrolyte gene delivery complexes with extended systemic circulation in vivo. Gene Therapy. 8:713-724 (2001).

199. K.Y. Kwok, Y. Park, Y.S. Yang, D.L. McKenzie, Y.H. Liu, and K.G. Rice. In vivo gene transfer using sulfhydryl cross-linked PEG-peptide/glycopeptide DNA co-condensates. Journal of Pharmaceutical Sciences. 92:1174-1185 (2003).

200. M. Yokoyama. Gene delivery using temperature-responsive polymeric carriers. Drug Discovery Today. 7:426-432 (2002).

201. S. Sun, W. Liu, N. Cheng, B. Zhang, Z. Cao, K. Yao, D. Liang, A. Zuo, G. Guo, and J. Zhang. A Thermoresponsive Chitosan-NIPAAm/Vinyl Laurate Copolymer Vector for Gene Transfection. Bioconjugate Chem. 16:972-980 (2005).

202. M. Kurisawa, M. Yokoyama, and T. Okano. Gene expression control by temperature with thermo-responsive polymeric gene carriers. Journal of Controlled Release. 69:127-137 (2000).

203. N. Cheng, W. Liu, Z. Cao, W. Ji, D. Liang, G. Guo, and J. Zhang. A study of thermoresponsive poly(N-isopropylacrylamide)/polyarginine bioconjugate non-viral transgene vectors. Biomaterials. 27:4984-4992 (2006).

# CHAPTER 3. NOVEL PENTABLOCK COPOLYMERS FOR SELECTIVE GENE DELIVERY TO CANCER CELLS

Modified from a paper published in Pharmaceutical Research, 2009, 26: 700-713

Bingqi Zhang, Mathumai Kanapathipillai and Surya Mallapragada

## Abstract

The ideal transgene vectors for cancer therapy are expected to show no or low transfection efficiencies in normal cells but high transfection efficiency in carcinoma cells. In this study, the novel poly(diethylamino ethylmethacrylate)(PDEAEM) /Pluronic F127 pentablock copolymers were found to be able to mediate high-efficiency transfection of human cancerous SKOV3 and HT1080 cell lines while showing significantly lower efficacy in non-cancerous ARPE-19 and 3T3 cell lines. This is in contrast to the uniformly high transfection seen in all the cell lines using ExGen, a commonly used polymeric vector. The intracellular routes of polyplexes were investigated by confocal microscopy in SKOV3 and ARPE-19 cell lines after appropriately labeling the polymer and DNA. It was found that many polyplexes translocated into nuclei within 3h of transfection in SKOV3 cells, yet only few polyplexes were observed in the nuclei of APRE-19 cells. This difference in the number of polyplexes in the nuclei was also observed in the cells at 10h and 24h post-transfection, indicating that lesser nuclear entry in the ARPE-19 cells may result

in the lower efficiency of transfection. Since the SKOV3 proliferation rate was found to be much higher than that of the ARPE-19 cells, the nuclear entry of polyplexes was assumed to be correlated with the proliferation rate, and it was hypothesized that the novel pentablock copolymers could mediate gene delivery selectively in fast growing cells. Furthermore, in APRE-19 cells, free DNA showed a weak signal or was localized around the cell membrane area, which implied that the uncomplexed DNA may have been degraded or exported out of the cell via exocytosis. Thus the different intracellular barriers to gene transfer may also account for the observed difference of transfection efficacy. In co-cultures of HT1080 and ARPE-19 cell lines, the selectivity of GFP transfection in HT1080 versus the ARPE-19 cells was around 21 and 1 for the transfection mediated by pentablock copolymers and ExGen, respectively. Although the validity of the hypothesis that our pentablock copolymer could selectively transfect hyperproliferative cells needs further examination, this present work provides a new perspective to design targeting vectors for cancer therapies based on different characteristics among specific cell types.

## 3.1 Introduction

One of the features of the ideal non-viral transgene vector is cell specificity, which is so far usually achieved via receptor-mediated endocytosis by integrating cell specific ligands in the gene transfer system(*1-3*). With a receptor on the target cell surface and a matching ligand that can be attached to the synthetic vector, a

targeting gene delivery system could be established and expected to enhance the gene expression by increasing cellular uptake in the specific cell types. Through this receptor-mediated uptake, only the cells having some recognized over-expressed receptors could be “designed” as the target with the prerequisite that the ligand is also available and attachable to the vector of interest without compromising its DNA condensing ability, serum resistance and/or other particular properties. Commonly investigated ligands include asialoglycoprotein specific for hepatocytes(*4-6*), mannose for macrophages(*7-9*), and transferrin(10-11)and folate(*12-13*) for certain tumor cells. These have been reported to improve the transfection efficacy selectively in the target cells. Although the polymeric vectors have great flexibility to be tailored for particular applications like ligand modification, there are several limitations of this approach. In many cases, the receptors are over-expressed on the specific cell types, but they are also expressed by other cells, thereby decreasing the targeting efficiency. Moreover, interactions with serum proteins in the bloodstream and aggregation could further reduce the specificity of cellular uptake(*14-15*). A well known fact is that the same gene delivery system may exhibit quite different transfection efficiencies in different cell types(*16-18*), indicating there are particular cellular characteristics that affect the gene expression and could potentially be used to build up a cellular screen to selectively express foreign genes by specific cells. As an important cellular characteristic, the cell cycle has been reported to play a significant role in gene

transfer due to high dependence of gene expression on the mitotic phase, especially with the use of non-viral vectors(*19-21*). This suggests that the entry of complexes into the nucleus may require or benefit from the disruption of nuclear membrane; thus, the greater the number of cells entering mitosis, the higher the gene expression(*19*). But in some cases, mitotic activity would not act as a limiting factor if the vectors possess an excellent nuclear localization ability and turn out to be versatile like poly(ethyleneimine) (PEI)(*22*). However, if the vectors only have access to nucleus during mitosis, their transfection efficiency would be extremely dependent on how fast the cells proliferate. In other words, targeting could be achieved among cell types with significantly different proliferation rates, such as most tumor cells and normal cells, even without the use of targeting ligands.

In this present work, we report a novel pentablock copolymer with the potential selectivity to selectively transfect fast growing cells. The novel amphiphilic pentablock copolymer developed in our laboratory exhibits temperature- and pH-induced micellization and gelation(*23*). The central triblock Pluronic F127 contributes to the temperature responsiveness and has been reported to be able to promote cellular entry(*24*). The end-blocks of poly(diethylaminoethyl methacrylate) (PDEAEM) are the essential functional cationic segments to complex with DNA and to provide pH buffering in the endosome with their protonatable tertiary amine groups(*25*). In order to improve the stability and reduce the cytotoxicity caused by the excess positive

charges on the surface of copolymer/DNA polyplexes, free Pluronic F127 was added to the polymer-DNA complexes to shield these excess charges(*26*). Previous work has proved the high transfection efficiency of the pentablock copolymer and the stabilization effect induced by Pluronic F127 in serum supplemented medium in cancer cell lines. Furthermore, this transgene system is also injectable and can form thermoreversible gels *in vivo* for sustained release. Therefore, combining its potential selectivity for transfecting fast-growing cells, and its ability to be injected intra-tumorally to form gels for sustained gene delivery makes it promising as an ideal sustained and targeted transgene vector for cancer therapies.

## 3.2 Materials and Methods

### 3.2.1 Materials

The SKOV3 human ovarian carcinoma and ARPE-19 human retinal cell lines were obtained from ATCC™(Manassas, VA). The 3T3 Swiss mouse fibroblast cell line was kindly donated by Dr. Nilsen-Hamilton's Laboratory (ISU, Ames). Living Colors™ HT-1080 Retro DsRed-Express cell line, a clonal human fibrocarcinoma derived cell line that stably expresses DsRed-Express, was obtained from BD Biosciences-Clontech. Cell culture reagents including Dulbecco's Modified Eagle Medium (DMEM), heat inactivated fetal bovine serum (FBS), 0.25% trypsin-EDTA and Hank's buffered salt saline (HBSS) were purchased from Invitrogen (Carlsbad,

CA) and the Dulbecco's MEM : Ham's Nutrient Mixture F-12, 1:1 Mix (DMEM/F-12) from ATCC (Manassas, VA). Luciferase assay system and passive lysis buffer were purchased from Promega (Madison, WI). HEPES salt used to make Hepes buffer saline (HBS), Lactate dehydrogenase (LDH) kit, paraformaldehyde and Bromodeoxyuridine (Brdu) were obtained from Sigma (St Louis, MO). Alexa Fluor®647 carboxylic acid, succinimidyl ester (written as Alexa 647 henceforth), ethidium monoazide (EMA), 4',6-diamidino-2-phenylindole (DAPI) dilactate and ProLong® Gold antifade reagent were also purchased from Invitrogen (Carlsbad, CA). ExGen 500® (written as ExGen henceforth) was purchased from Fermentas Life Sciences (Hanover, MD). DNase I was purchased from Ambion (Austin, TX). HiSpeed Plasmid Maxi Kit was obtained from Qiagen (Valencia, CA). Pluronic F127 [$(PEO)_{100}$-b-$(PPO)_{65}$-b-$(PEO)_{100}$], (where PEO represents poly(ethylene oxide) and PPO represents poly(propylene oxide)) micro pastille surfactant was donated by BASF (Florham Park, NJ) and used without further modification.

### 3.2.2 Pentablock Copolymer Synthesis and Attachment of Alexa Fluor 647

The pentablock copolymer $PDEAEM_{13}$-b-$PEO_{100}$-b-$PPO_{65}$-b-$PEO_{100}$-b-$PDEAEM_{13}$ used in the present work (Scheme 3.1) was synthesized via atom transfer radical polymerization (ATRP) as previously reported(*23*), with $M_n$=17,533

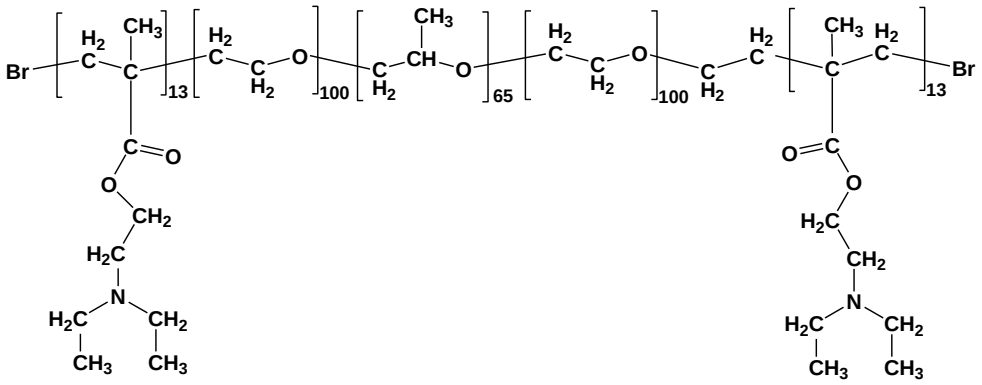

Scheme 3.1. Chemical structure of pentablock copolymers

and $M_w/M_n$=1.14, as judged by $^1$H NMR (in deuterated chloroform) and Gel Permeation Chromatography (GPC) (tetrahydrofuran mobile phase, poly(methylmethacrylate) calibration standards) respectively. In order to attach the fluorescent dye Alexa Fluo 647 for intracellular trafficking studies, this pentablock copolymer was amine functionalized by transforming the bromine group into azide and then further into triphenylphosphine and finally into the amine group after hydroxylation (Scheme 3.2). The transformation was confirmed by the presence and subsequent absence of a peak at about 31 ppm in the $^{31}$P NMR spectrum. Alexa 647 was reacted with amine modified pentablock similar to a procedure reported previously(*27*). Briefly, for a 20mg/ml polymer solution in 0.1 M sodium bicarbonate buffer, around 100 µg of the dye was added. The mixture was stirred in the dark at room temperature for 1 hour. The unattached dye was removed by extensive dialysis for 2 days. The polymer with conjugated dye was then freeze dried.

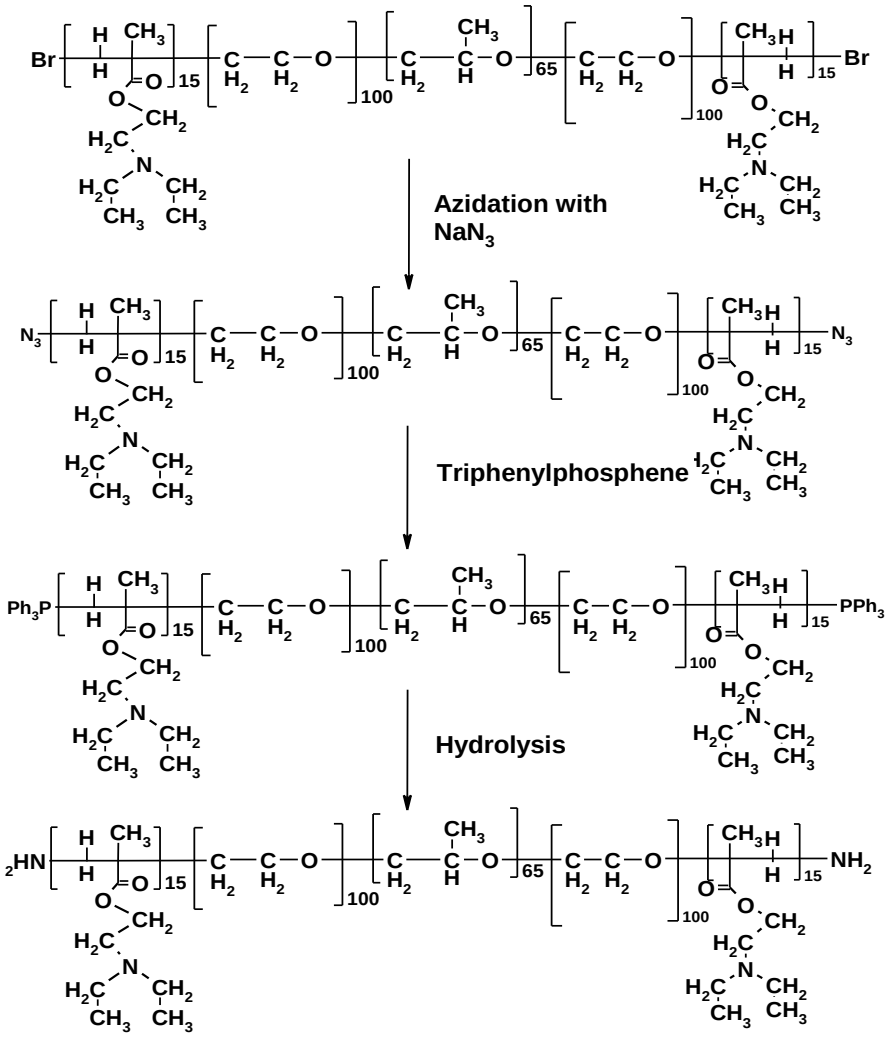


Scheme 3.2. Amine functionalization of pentablock copolymers

### 3.2.3 Plasmid DNA Purification and EMA Attachment

Bacteria containing the 6.7 kb pGWIZ-luc plasmid (GeneTherapy Systems Inc, CA) encoding the luciferase reporter gene or the 4.7 kb pEGFP-N1 plasmid (ClonTech, CA) encoding for green fluorescence protein (GFP) were grown in selective Luria-Bertani (LB) medium and then purified using the Qiagen HiSpeed

Maxi Kit. The concentration of DNA was tested using a NanoDrop spectrophotometer. A260/A280 was at least 1.8 for all DNA used. DNA was labeled with the fluorescent probe ethidium monoazide (EMA, 8-azido-3-amino-6-phenyl-5-ethylphenanthradinium chloride) according to the procedures reported elsewhere(*28-29*) with minor modifications. Briefly, appropriate amounts of plasmid and EMA were mixed giving a 50:1 molar ratio of nucleotide to probe. The solution was incubated on ice for 30min before being exposed to UV light of principal wavelength 312nm. After 20 min photolysis, most of the DNA had been covalently bound with EMA, and the excess EMA and intercalated EMA were removed by performing ethanol precipitation three times.

### 3.2.4 Polyplex Formation

Polymer/DNA polyplexes at various N/P ratios were formulated by adding appropriate quantities of unlabeled or labeled pentablock copolymer (2mg/ml) solution in 0.5× HBS, pH 7.0 to plasmid DNA solutions which were properly prediluted with the same HBS buffer to get the equal mixing volume. The mixture was briefly vortexed and allowed to incubate at room temperature for 20 min to ensure complexation. If required, Pluronic F127 solution (10 mg/ml) in 0.5× HBS, pH 7.0 was added to the formulation to get the F127/pentablock copolymer wt. ratio of 5 with gentle vortexing followed by another 10 min incubation. We will be referring throughout this work to four abbreviations for the different vectors used to form

polyplexes: PB refers to the pentablock copolymer alone, PBD refers to the pentablock copolymer with the fluorescent dye attached, PL refers to Pluronic F127, and correspondingly, PB-PL refers to the pentablock copolymer with subsequent added Pluronic F127 for shielding the excess positive charges.

### 3.2.5 Cell Culture

The SKOV3, 3T3 and HT1080 cells were grown in Dulbecco's Modified Eagles Medium (DMEM, Invitrogen) supplemented with 10% (v/v) fetal bovine serum (FBS, heat inactivated, GIBCO) at 37°C under a humidified atmosphere containing 5% $CO_2$. ARPE-19 cells were grown in DMEM/F-12 (ATCC) containing 10% FBS under the same conditions. Cells were passaged approximately every 2-3 days for SKOV3 and HT1080, 4-5 days for APRE-19 and 7-8 days for 3T3 cells.

### 3.2.6 In vitro Transfection

For the transfection based on luciferase activity, cells of interest were seeded into a 96-well plate at an initial density of $1.2\times10^4$ to $3\times10^4$ cells per well in 200μl growth medium and allowed to incubate for 24~48h depending on the cell type, to reach 70% confluence when transfection could be performed. Polyplexes prepared at given N/P ratios were added to the newly changed FBS-supplemented medium with 0.6ug of DNA per well. After 3h transfection at 37°C, the medium containing polyplexes was replaced with fresh growth medium and cells were allowed to grow

for another 45h post-transfection until the luciferase assay was performed. The total duration of transfection and post-transfection was kept at 48h. ExGen 500, a sterile solution of linear 22 kDa polyethylenimine (PEI), was used as positive control at N/P ratio of 6 according to the manufacturer's protocol. The luminescence from lysed cells in 20μL passive lysis buffer per well was measured in arbitrary Relative Luminescence Units (RLU) on an automated Veritas™ Microplate Luminometer using the Renilla Luciferase Assay System from Promega. Each transfection was done in triplicate.

To compare the transfection efficacy between different cell types, luciferase activity in each well was normalized by the total amount of proteins determined by Bicinchoninic Acid (BCA) protein assay kit and expressed as mean RLU per milligram of cell protein. As for the comparison between different conditions of the same type of cells, RLU per well was utilized to obtain values since transfection was performed with the same initial number of cells per well. In the trafficking experiments, cells of interest were seeded onto poly-L-lysine coated coverslips in 6 well-plates at a density of $1\times10^5$ cells per well and subsequently transfected with polyplexes at 3μg DNA per well following the same procedures used in the case of 96-well plate. At specific time points during transfection or post-transfection, cells were fixed with 4% paraformaldehyde and mounted on the glass slide that held a drop of mounting medium to keep cells from drying out.

Specifically for the transfection of HT1080/ARPE-19 co-cultured cells, separately cultured HT1080 and ARPE-19 cells were seeded together onto 6-well plates at varied ratios of cell number and incubated in co-culture media, 50/50 (v/v) until being transfected with polyplexes at 2μg EGFP-N1 plasmid per well. EGFP expression was examined qualitatively by fluorescence microscopy and quantitatively by flow cytometry.

### 3.2.7 Flow Cytometry

After transfection, the cells were harvested from 6-well plates and cells from each well were suspended in 3ml HBSS. Then cell suspensions were transferred to 15ml centrifuge tubes and centrifuged for 12min at 1200rpm. Supernatants were removed and cells pellets were resuspended in 3ml fresh HBSS. After another centrifugation, cells were finally suspended in 0.5ml of 2% paraformaldehyde in PBS and stored at 4°C for later analysis with a Becton-Dickinson FACSCanto flow cytometer.

### 3.2.8 Cytotoxicity

The cytotoxicity of polyplexes was measured with LDH assay, as the amount of LDH in the cell culture medium is representative of the cell death following the membrane rupture. To get a better knowledge of the stage at which most cell death occurs, the LDH activity was assayed twice, at the end of 3h transfection and after

the additional 45h post-transfection. Triton-X was used as a negative control to provide 100% cytotoxicity.

### 3.2.9 Confocal Microscopy

EMA and Alexa Fluor 647 were selected to label DNA and the pentablock copolymer respectively in this study, because their non-overlapping spectra minimized the potential interference that could occur between the two dyes. Confocal images were collected with a Prairie Technologies Confocal Microscope (Prairie Technologies, Madison, WI) and analyzed with MetaView software (Universal Imaging Corporation). An argon/krypton mixed gas laser with 488 and 633nm excitation lines was used to induce fluorescence. Excitation of EMA bound to DNA was achieved by using the 488 nm laser, with the emitted fluorescent wavelengths observed using a 600/40 nm notch filter. Alexa Fluor 647 attached to pentablock copolymer was excited by the 633nm laser with the emitted fluorescent wavelengths observed using a 700/75 nm notch filter. The thickness of the cells was estimated by varying the scanning plane from the bottom to the top of the cells and images were collected at the central plane with optical sections of 0.5~0.7μm.

### 3.2.10 Proliferation Measurement

Proliferation rate was expressed as the ratio of the number of daughter cells to the number of total cells and measured by counting cells stained with Brdu and DAPI.

Brdu labeling was performed immediately following transfection by replacing the medium containing polyplexes with fresh growth medium containing 5μM Brdu. After 18h incubation, cells were fixed with 4% paraformaldehyde and stored in 1% paraformaldehyde at 4°C until performing immunocytochemistry.

### 3.2.11 Statistical Analysis

The data is presented as mean and standard deviation, which are calculated over at least three independent experiments. Significant differences between two groups were evaluated by Students' t-test with $p <= 0.05$ or $p<0.1$, as specified.

## 3.3 Results and Discussion

### 3.3.1 Transfection and Cytotoxicity among Different Cell Types

In order to use the pentablock copolymers for cancer therapy, we tested the ability of the pentablock copolymer vectors to selectively transfect cancer cells (SKOV3) versus ARPE-19 cells using reporter genes (Fig. 3.1). Relative to the blank cells and naked DNA, polyplexes of PB and PB-PL under different N/P ratio conditions exhibited up to three orders of magnitude higher efficiency in SKOV3 cells contrasting with the slight difference in ARPE-19 cells. ExGen, a linear polyethyleneimine vector, was used as a positive control, and did not exhibit a significant difference in transfection efficiency between the two different cell types,

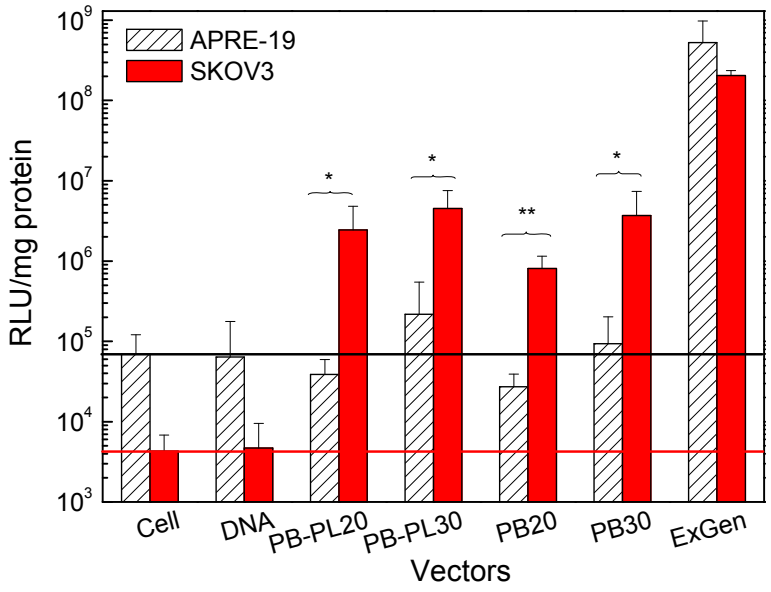


Fig. 3.1. Transfection of ARPE-19 and SKOV3 cells by PB/DNA and PB-PL/DNA at N/P ratios of 20 and 30 as denoted by the numbers following abbreviations. Blank cells and naked DNA were used as negative controls and ExGen at N/P ratio of 6 was used as the positive control according to the provided protocol. Luciferase activity was expressed as the relative light units (RLU) per mg of protein (n= 4, mean±S.D.* =$p<0.05$, ** = $p<0.01$).

and the transfection efficiencies in both cell types were over three orders of magnitude higher than those of the negative controls. This demonstrates a potential selective transfection ability of the pentablock copolymer vectors compared to established vectors such as ExGen.

Although it is a commonly known fact that transfection efficiency could be largely dependent on cells due to the complex cellular structure and consequently varied gene delivery mechanisms, the big differences in transfection efficiencies of SKOV3 and ARPE-19 cells, which we may refer to as a cancer cell line and “normal” cell line respectively, provides a challenging possibility that this pentablock copolymer might

possess a natural selectivity to transfect cancer cells or in general, the type of cells bearing some specific features of SKOV3 cells. Therefore, 3T3 cells were used to further test the transfection of normal cell lines mediated by pentablock copolymers. As shown in Fig. 3.2, similar to the case of APRE-19 cells, the pentablock copolymers lead to very low transfection efficiencies, almost comparable to those of blank cells, and ExGen still appeared to be a highly effective vector independent of the cell-line type. Therefore, the hypothesis that pentablock copolymers might specifically transfect the cancer cells sharing some key feature with SKOV3 cells was investigated further to determine if differences in proliferation rates of the different cell types were responsible for the differences in transfection efficiencies using the pentablock copolymers.

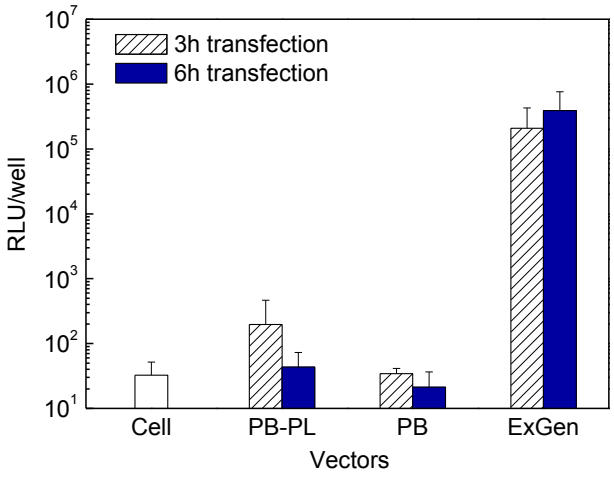


Fig. 3.2. Transfection of 3T3 cells by PB/DNA and PB-PL/DNA at N/P ratios of 20 and by ExGen at N/P ratio of 6 for different transfection periods. Luciferase activity was expressed as relative light units (RLU) per well (n= 4, mean±S.D.).

### 3.3.2 Proliferation Measurement

The cell cycle mitotic phase has been reported to be a favorable period for nuclear transport using non-viral vectors(*20*). Although there are a number of intracellular barriers that work synergistically to cause a low level of gene expression relative to the DNA taken up by cells, usually less than 1%(*30*), the nuclear transport of polyplexes has been recognized as the rate-limiting step in DNA delivery(*31*), and has been found to be an important factor in the transfection of cell lines versus slow-dividing primary cells such as neurons. Hence, theoretically, the faster the cell proliferates, the greater the chances for DNA to enter nuclei, thus the higher the gene expression would be. It was reported that gene expression was enhanced by enhancing cell proliferation with growth factor(*32*). To test the proliferation rates of the different cell types, Brdu was employed to stain the newly created cells with all nuclei labeled with DAPI. With the concern of minimizing the influence of host species on transfection characteristics, SKOV3 and ARPE-19 cells, which are both of human origin, were used for this study as opposed to the 3T3 cells which are mouse-derived. The test was conducted on transfected cells, in case the polyplexes have an effect on the proliferation. (Representative images shown in Fig.3.3). The proliferation rate was expressed as the number of daughter cells (pink) divided by the number of total cells (blue). The SKOV3 cells were found to proliferate significantly faster ($p<0.1$) than the

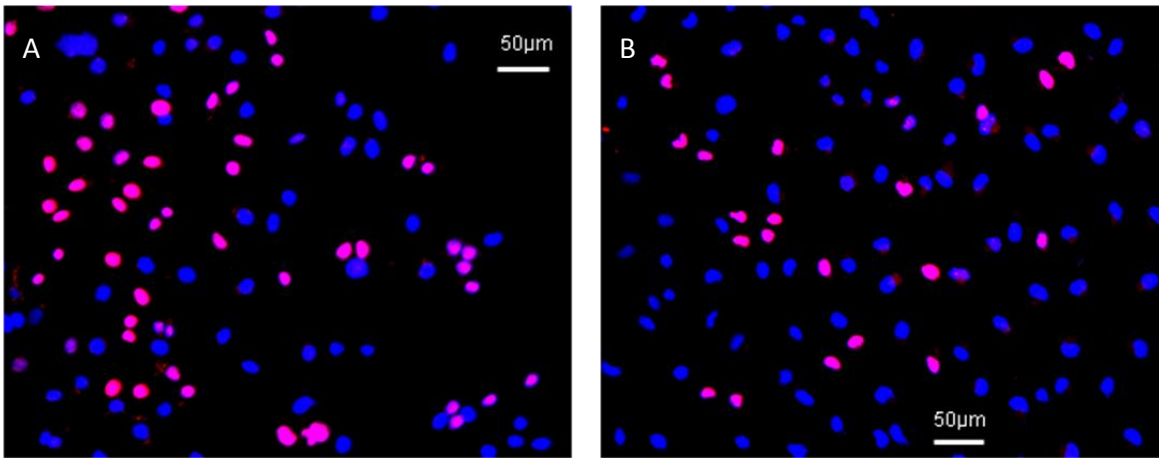


Fig. 3.3. Proliferation measurement of SKOV3 cells (A) and ARPE-19 cells (B) with nuclei labeled by DAPI (blue) and newly formed cells labeled by Brdu (pink)

ARPE-19 cells, with the rate of 54%±15% vs. 25%±12%. This potentially supports our hypothesis that the slower dividing rate of ARPE-19 cells probably resulted in less DNA importation to the nuclei of ARPE-19 cells and consequently to lower levels of gene expression.

To investigate this further, intercellular trafficking studies of pentablock copolymer/DNA polyplexes in SKOV3 and ARPE-19 cells were performed during transfection and post-transfection, by labeling the pentablock copolymer with a fluorescent dye. Since any modification to the polymer can potentially change its physiochemical properties, the transfection efficiency and cytotoxicity of the dye labeled pentablock copolymer PBD was investigated. Fig. 3.4 indicates that there are indeed differences between PBD and the pentablock copolymer alone. Higher N/P ratios are required for PBD to obtain a similar level of gene expression as PB does,

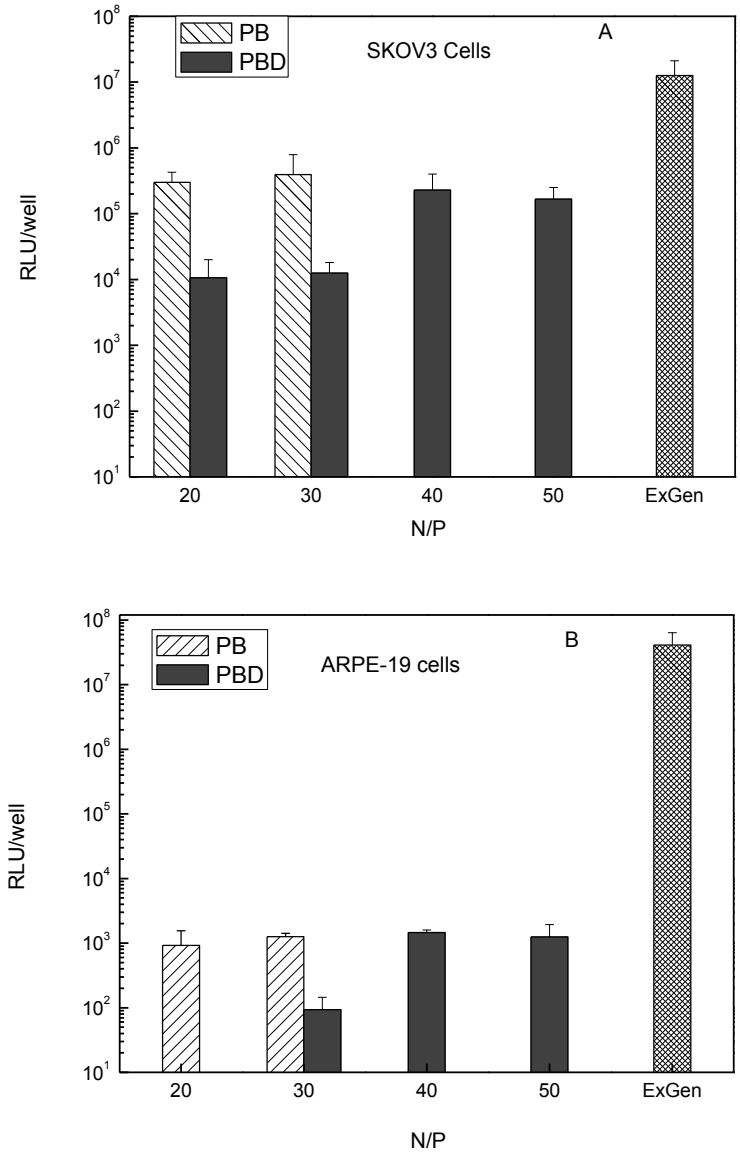


Fig. 3.4. Transfection of SKOV3 cells (A) and ARPE-19 cells (B) with the vector of PB and PBD at various N/P ratios. (n= 4, mean±S.D.)

which might be most likely due to the compromised DNA affinity by the dye attachment. There have been previous reports that oversubstitution of the molecular conjugates could interfere with the interaction of the polymers with DNA(*33*). In this

case, the dye Alexa 647 attached to the end of polymer main chain could affect the polymer complexation with DNA in an unfavorable way, either by steric hindrance or by positive charge shielding. The Alexa 647 molecule (MW=1250) accounts for ~50wt. % of a PDEAEM block (MW=2405 with 13 units), and together with the proximity between the dye and the tertiary nitrogen, it is reasonable to see a negative influence of Alexa 647 on transfection. However, it is interesting to point out that such a significant difference was brought about by only five percent of dye with respect to the pentablock copolymer. In addition to the DNA binding capability reduction by the conjugation of Alexa 647, the resulting reduced charge density might also contribute to a lower cytotoxicity at a given N/P ratio.

### 3.3.3 Cytotoxicity Analysis Using LDH Assay

Cationic vectors can be cytotoxic, though the cytotoxicity of the pentablock copolymers can be tailored by adjusting the ratio of the cationic and non-cationic blocks in the copolymer (*25*). To evaluate the cell viability during the total transfection, an LDH assay was used. As shown in Fig. 3.5, the cytotoxicity of all the polyplexes is fairly acceptable for both SKOV3 and APRE-19 cells, expect for the P30 vector with the very high N/P ratio, and these two cell types seem to have a similar susceptibility to the vector. The vector of PB-PL with the Pluronic shielding the excess positive charges showed less damage to cells than the pentablock copolymer alone, suggesting that the shielding effect from PL improved the biocompatibility of

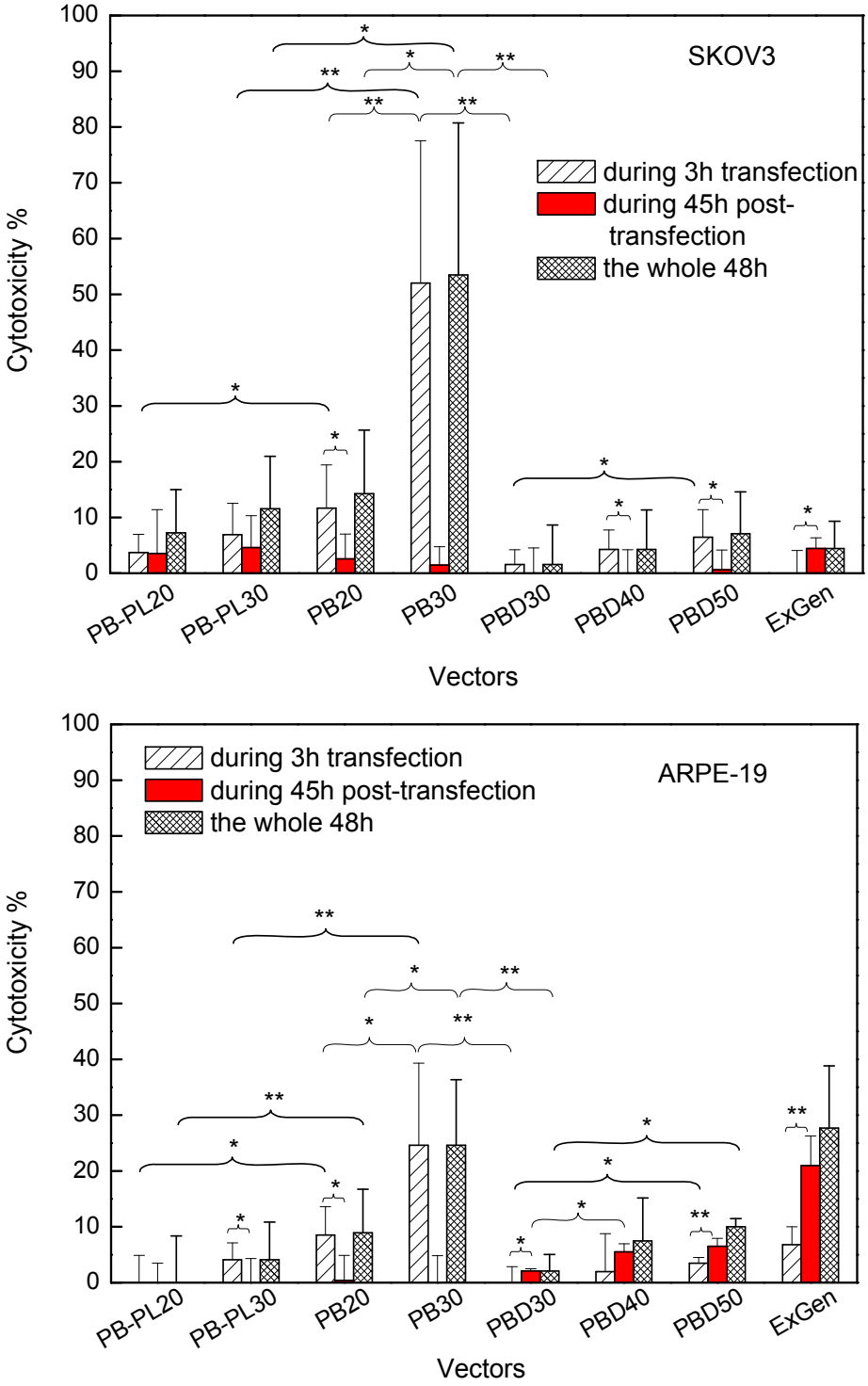


Fig. 3.5. Cytotoxicity of polyplexes on SKOV3 (top) and ARPE-19 cells (bottom) with LDH assay at various N/P ratio as denoted by the numbers following abbreviations. n= 4, mean±S.D. * =p<0.05, ** =p<0.01

pentablock/DNA polyplexes. Cytotoxicity of PBD/DNA was indeed much lower than that of PB/DNA counterparts for both cell types, which further proved the great influence of dye conjugation on the charge density. It was also found that interestingly, for both cell types, ExGen led to an even higher toxicity in the later 45h of post-transfection relative to the first 3h, while most of pentablock copolymer polyplexes seemed to act differently. It is worth noting that for the polyplexes such as P30/DNA that exhibited a high toxicity in the first 3h transfection, there was not much additional cytotoxicity in the next 45h.

ExGen carries plenty of primary and secondary amines and is known to be much more cytotoxic than complexed ExGen where most charges of amines have been neutralized by DNA; moreover, the membrane destabilization effect(*34*) of free PEI and its interference with transcriptional and translational processes(*35*) might also account for its toxicity. On the other hand, the intense charge density of PEI would not allow the release of the DNA cargo readily, so the ExGen/DNA polyplexes showed a slower toxicity rather than a quick one, which is in good agreement with the report by Godbey and co-workers(*35*). However, transgene vectors with tertiary amines as the functional moieties like pentablock copolymers, have been reported to be less toxic than those with primary residues like PEI(*26, 36*). Therefore, even after uncomplexing from DNA they did not show as much long-term toxicity as ExGen, instead showing an initial cytotoxicity during the first 3h probably due to relatively

larger percentage of uncomplexed polymer at a given higher N/P ratio or the relatively faster release of DNA. However, the cytotoxicity of PBD/DNA was found to show a different trend during the whole transfection process compared to PB/DNA in the ARPE-19 cells, with higher cytotoxicity in the post-transfection stage than that in the transfection period. If the uncomplexed PBD is presumed to be a major source of cytotoxicity, apart from the membrane damage during cellular entry, there should be more uncomplexed PBD in the later 45h post-transfection in ARPE-19 cells relative to SKOV3 cells where nearly no cytotoxicity was observed. This implies that some intracellular differences between the two cell types may affect the relatively weak complexation of PBD and DNA, which was investigated in the intracellular trafficking studies of the polyplexes. Taking the transfection efficacy and cytotoxicity into account, PBD at an N/P ratio of 40 was used for the intracellular trafficking study.

### 3.3.4 Intracellular Trafficking of PBD/DNA Polyplexes

Based on the proliferation results that showed that SKOV3 cells proliferate faster than ARPE-19 cells, our initial hypothesis was that the significant differences in transfection efficacy between the two cell lines were largely due to the positive effect of proliferation rate on nuclear transport. To check if nuclear uptake actually occurs more in SKOV3 cells than in ARPE-19 cells, pentablock copolymer/DNA polyplexes were tracked at 3h, 10h and 24h after the start of transfection. Fig. 3.6 shows a representative image of the APRE-19 cells at 3h, where colocalization of pentablock

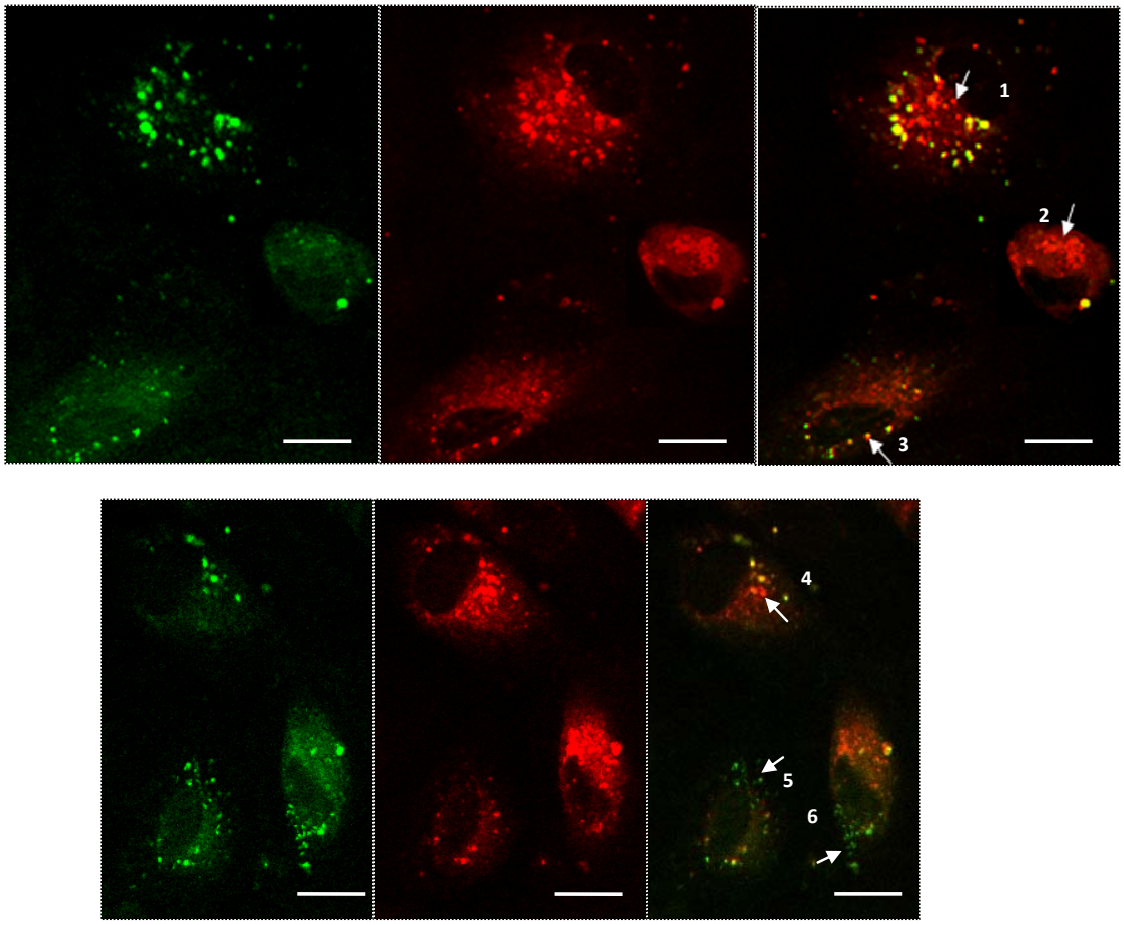


Fig. 3.6. Confocal images from labeled pentablock copolymers and DNA in ARPE-19 cells 3h after transfection. Images on the left colored green represent DNA, the center ones colored red represent the pentablock copolymers and the images on the right are the alignment of the other two images. Panel A and Panel B are from different observation spots. Scale bar is 20 μm.

copolymer and DNA was clearly observed with yellow dots, suggesting that polyplexes remained in their original form, and in particular some polyplexes had localized to the perinucleus as seen in cells 1, 3, and 4. However, the most impressive feature of the 3h sample resides in the dissociated polyplexes which could be easily detected by the abundant red, and relatively fewer green dots.

Moreover, except for cells 3 and 4, the red free pentablock copolymer appeared to be dominant and the green DNA was just absent, especially in cells 1 and 2. We have postulated two possible reasons for the absence of the free DNA. One possibility is that DNA was degraded by the nuclease in the cytosol, and the other is that the DNA was exported out of the cell. The appearance of strong red and weak green signals has been found to be typical among all the images), which may imply that the DNA is subjected to degradation during or after release from the polyplexes. This was proved by testing the intensity of fluorescence of DNA-EMA and degraded DNA-EMA (as shown in Fig. 3.7), and by integrating within the range of the filter from 580nm to 620nm. It was found that the untreated DNA-EMA was as twice fluorescent as the degraded one. It was once reported that the digestion of EMA labeled RNA induced a 14-fold decrease in the fluorescence intensity (*37*). Therefore, the free DNA was not

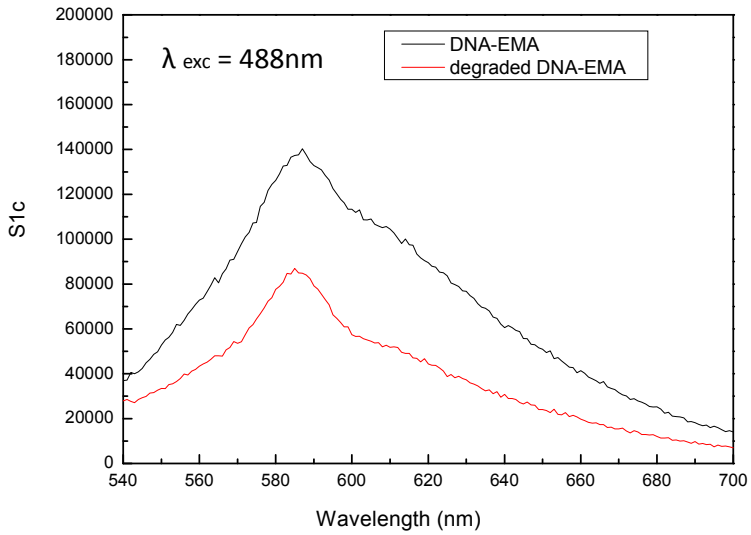


Fig. 3.7. Fluorescence spectra of DNA-EMA and degraded DNA-EMA treated with nuclease I

totally absent as it appeared to be in the aligned images, but had probably been degraded by the nucleases to some extent and showed less intense fluorescence compared to the bright red fluorescence from pentablock copolymer. When focusing on cells 5 and 6, free DNA was found localized around the cell membrane or close to the membrane, potentially awaiting transportation out of the cell. This feature was also found commonly in the 10h samples as it was shown in the representative cell 3 of Fig. 3.8, where free DNA accumulated along the outer membrane or may be sequestrated by the cell membrane. The nearly doubled nucleus and the incompletely separated nuclear envelope of cell 3, as indicated by the lower arrow, demonstrates an obvious late mitosis phase – telophase. Moreover, DNA and pentablock polymer have been observed in the dividing nucleus with non-perfect colocalization, suggesting that they both either entered into the nucleus in an

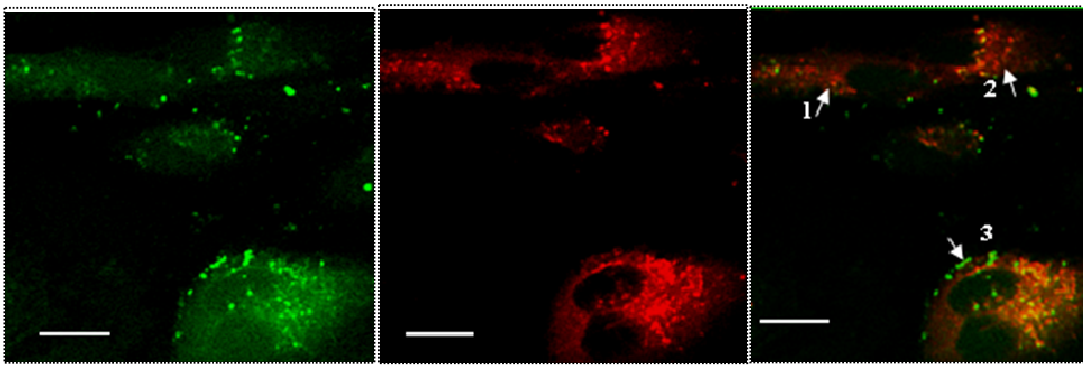


Fig. 3.8. Confocal images from labeled pentablock copolymer and DNA in ARPE-19 cells 10h after transfection. Image on the left colored green represents DNA, the center one colored red represents the pentablock copolymers and the image on the right is the alignment of the other two images. Scale bar is 20 μm.

uncomplexed form or dissociated from each other after nuclear entry as polyplexes. But the large number of polyplexes accumulating right outside the nucleus, as well as the small amount of free DNA observed, point to the second possibility. The intranuclear DNA and pentablock copolymer are close to the dividing area, indicating that the nuclear entry possibly took place during the nuclear division and may have been facilitated by nuclear membrane breakdown (*21*). In addition, the feature of strong red and weak green was also found in this 10h sample as shown by arrows in cells 1 and 2. Therefore, by comparing the cells after 3h transfection, and those after another 7h posttransfection, the latter showed an enhanced nuclear uptake probably due to the mitotic activity, but maintained the appearance of dominant red fluorescence. This implies that the DNA might be degraded after uncomplexation, and the accumulation of DNA close to or even at the cell membrane suggests a possible export mechanism from the cell. When post-transfection time was extended to 21h as seen in Fig. 3.9, the transfected cells exhibited an increased amount of DNA in the nuclei either complexed or uncomplexed as shown in cells 3, 4 and 5. The other features were consistent with the previous two time points concerning varied intensity of green fluorescence from DNA and membrane concentrated distribution of DNA, as especially indicated with the arrow in cell 2.

The polyplexes, however, had a totally different intracellular route in SKOV3 cells as shown in Fig. 3.10. A large quantity of fairly good colocalization of green and red dots

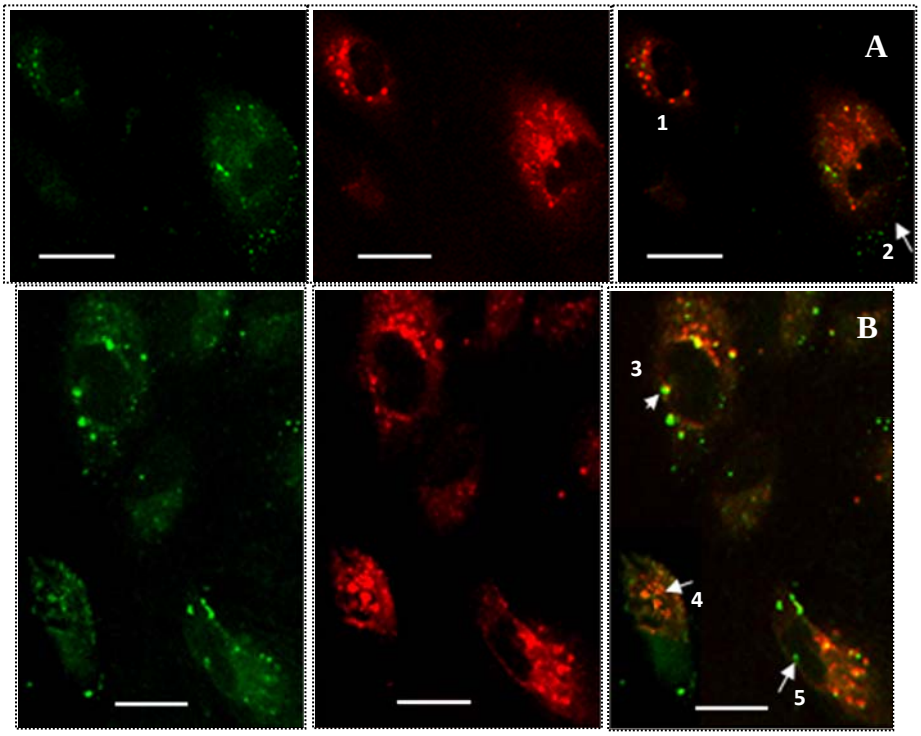


Fig. 3.9. Confocal images from labeled pentablock copolymer and DNA in ARPE-19 cells 24h after transfection. Images on the left colored green represent DNA, the center ones colored red represent the pentablock copolymers and the images on the right are the alignment of the other two images. Panel A and Panel B are from different observation spots. Scale bar is 20 μm.

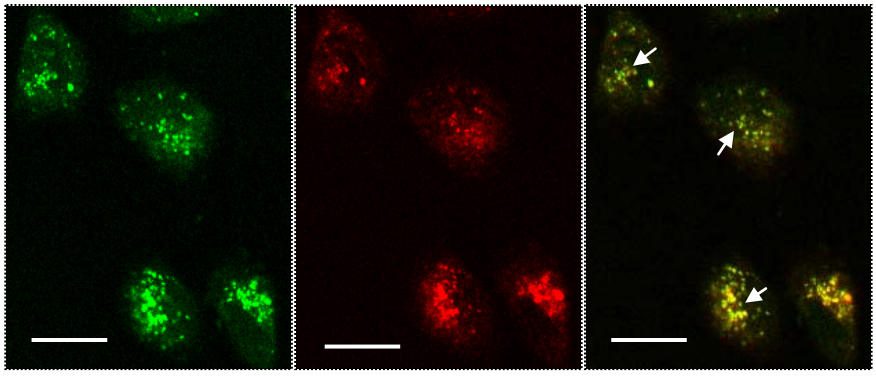

Fig. 3.10. Confocal images from labeled pentablock copolymer and DNA in SKOV3 cells 3h after transfection. Images on the left colored green represent DNA, the center ones colored red represent the pentablock copolymers and the images on the right are the alignment of other two images. Scale bar is 20 μm.

suggests that DNA was still effectively protected from degradation in the well maintained polyplexes. More importantly, polyplexes had localized into nuclei in considerable numbers at 3h after transfection which is dramatically higher than the cases of all APRE-19 cell samples in test, and which might be contribute to the differences in the transfection efficacy of the pentablock copolymers between the two cell types. Besides, all of the DNA and pentablock copolymers have been shown to be perfectly overlaid; therefore the polyplexes in the nuclei are the ones originally present in the cytoplasm rather than being reformed by the DNA and pentablock copolymers that entered into the nuclei separately. Therefore, at least a portion of DNA is transported into nuclei complexed with the pentablock copolymer. There is a possibility of uncomplexed DNA entering the nucleus as well, since plasmid DNA has been well known to be able to enter into the nuclei(*30*). But considering the degradation by nucleases(*38*) and the low diffusion rate caused by the hindrance of cytoskeleton and binding with other cytoplasmic elements(*39*), the free DNA would have a small chance to successfully locate into the nuclei.

As SKOV3 cells proliferate faster than the ARPE-19 cells, the higher transfection efficiency of SKOV3 cell line was hypothesized to result from its consequently facilitated nuclear uptake. The nuclear uptake of polyplexes appeared to be common in SKOV3 cells samples, even as early as 3h after transfection. Panels A to C in Fig. 3.11 might represent three different stages in mitosis according to the varied

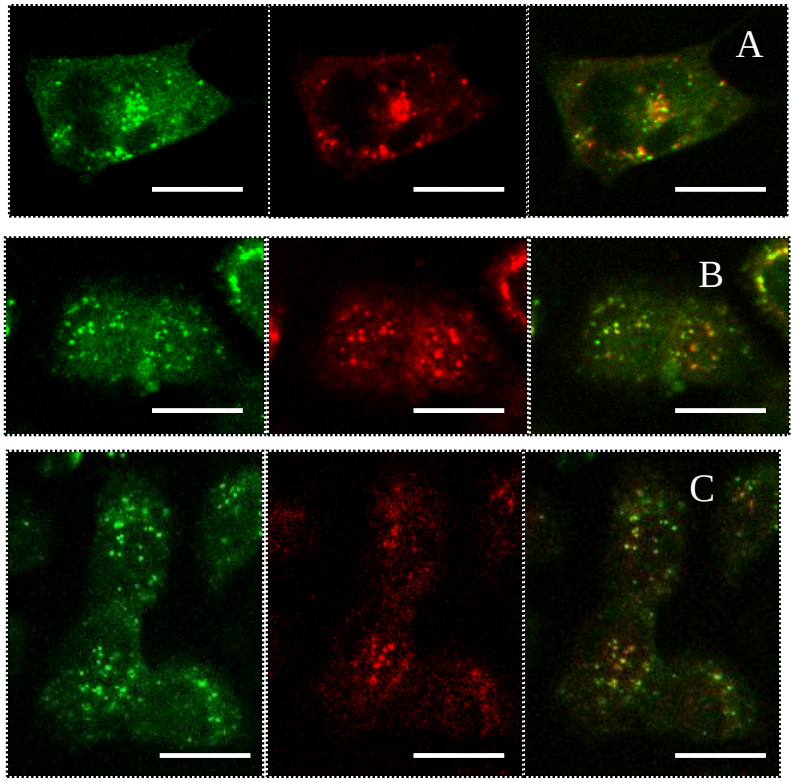


Fig. 3.11. Nuclear transport of polyplexes during mitosis from SKOV3 cells after 3h transfection. Images on the left colored green represent DNA, the center ones colored red represent pentablock copolymers and the images on the right are the alignment of other two images. Panels A, B and C are from different observation spots. Scale bar is 20 μm.

appearance of nuclei. Although it is hard to say at which exact stage each set of cells is in, they all seem to be after prometaphase, during which the disintegration of the nuclear membrane occurs. That is probably the reason why each nucleus undergoing division shows polyplexes inside. Since similar phenomena were just observed less frequently in the ARPE-19 cells 10h after transfection, the slower dividing rate could largely account for the lower transfection efficiency.

The SKOV3 samples for 10h and 24 after transfection look similar to those of 3h

(Fig. 3.12), except for the less perfect colocalization and more free DNA in the nuclei, which is reasonable as the dissociation can be expected to develop over time. However, relative to the rare colocalization at the same time points in ARPE-19 cells, the tight binding in SKOV3 cells implied a long-term protection provided by the

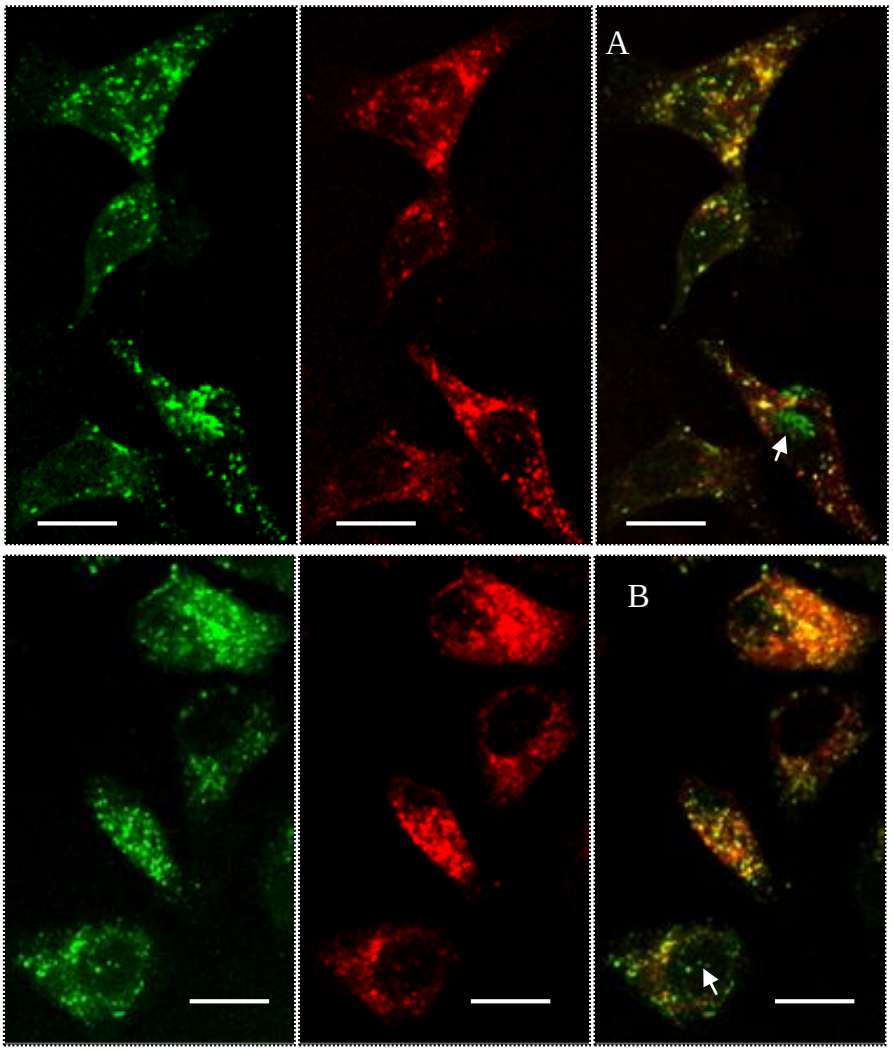


Fig. 3.12. Confocal images from labeled pentablock copolymer and DNA in SKOV3 cells 10h (panel A) and 24h (panel B) after transfection. Images on the left colored green represent DNA, center ones colored red represent the pentablock copolymers and the images on the right are the alignment of the other two images. Panel A and Panel B are from different observation spots. Scale bar is 20 μm.

pentablock copolymer. This agrees well with LDH results regarding the cytotoxicity of PBD/DNA in post-transfection, which appears to be proportional to the amount of uncomplexed PBD. Although long-term protection might reduce the cytotoxicity as well as the loss of DNA, the relatively few DNA released for further transcription and translation might present a potential bottleneck to gain higher gene expression. Therefore, the differences in transfection efficiency between ARPE-19 and SKOV3 cell lines might be due to the lower proliferation rate of the ARPE-19 cells, thereby lowering nuclear uptake. Although the exogenous material can definitely achieve the nuclear import in the interphase cells through the nuclear membrane embedded nuclear pore complex (NPC)(*40*), the hourglass-like NPC cannot allow large cargo to transit though passively(*41*)with the midplane as narrow as 40 nm(*42*). The inclusion of nuclear localization signal (NLS) in the vector could facilitate the transit and to some extent enhance the size limit up to 60nm, but the polyplexes sized around 150nm are still excluded(*43*). Thus even with a NLS, the polyplexes are still too large to be imported into the nucleus(*31*). Since our pentablock copolymer/DNA polyplexes formed at N/P ratios of 20 have a size distribution ranging from 100nm to 500nm in serum supplemented growth media (data not shown), and do not possess any NLS moieties, it would be difficult for them to traverse the nuclear membrane through NPC even though opportunities exist to bind with the intracellular NLS. In this case, the more realistic strategy of nuclear localization should be the entry after nuclear

breakdown in mitosis. The more often cells experience a mitotic phase, the more DNA could be transported into the nuclei to get more genes expressed. Based on the fact that much more DNA either complexed or uncomplexed has been found in the nuclei of faster dividing SKOV3 cells, the higher level of gene expression in SKOV3 with respect to ARPE-19 cell line is related to the faster proliferation rate of the SKOV3 cells.

To test this assumption further, we extended the duration of transfection of ARPE-19 cells to 6h (Fig. 3.13) and found that the gene expression mediated by

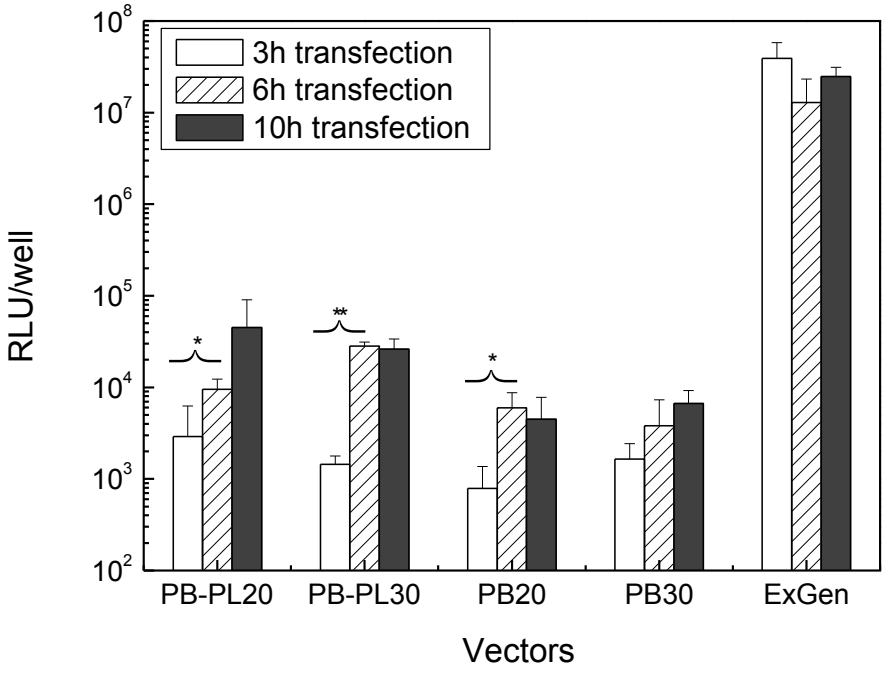


Fig. 3.13. Transfection of ARPE-19 cell line by PB/DNA and PB-PL/DNA polyplexes with different transfection period at N/P ratio of 20 and 30 as denoted by the numbers following abbreviations. ExGen was used as a positive control at N/P ratio of 6 according to the provided protocol. Luciferase activity was expressed as the relative light unit (RLU) per well (n= 4, mean±S.D.* =$p<0.05$, ** = $p<0.01$).

most of the pentablock copolymer vectors was enhanced to a significantly higher level relative to the case of 3h transfection, suggesting more DNA has been available for the cells in mitosis. The exception of P30 and ExGen might be due to the negative effect of the accompanying increased cytotoxicity especially at higher N/P ratios. In addition to this cause, the excellent nuclear delivery ability of ExGen could make it benefit little from lengthened transfection. Further extending transfection to 10h, resulted in no significant differences. Apart from causing increased cytotoxicity, cells might have been too confluent to proliferate any further to aid in nuclear uptake. Secondarily the intracellular DNA in ARPE-19 cells was found to be much lesser than that in SKOV3 cells, which may be directly caused by the less effective cellular uptake, or probably due to the degradation of DNA by the nuclease in lysosome or cytoplasm, or due to the exocytosis of DNA. Consequently, the limited amount of DNA available in cytoplasm further inhibited the nuclear transport. In the SKOV3 images, the polyplexes were dominant in the cytoplasm especially at 3h indicating that almost all the intracellular pentablock copolymers were complexed with DNA when entering into cells. Since the amount of pentablock copolymer in SKOV3 and ARPE-19 cells have not been found to be very different, the less powerful cellular uptake may just partially explain the small quantity of DNA in ARPE-19 cells. The degradation and exocytosis of DNA are also possibilities. After being internalized via endocytosis which is known as the major, if not the sole mode of cellular entry(*20*),

the polyplexes are trapped in the early endosomes. These early endosomes either fuse with each other to form late endosomes and subsequently endo-lysosomes by fusing with lysosomes or recycle their contents back to the cell surface(*44*). The endocytosed polyplexes are accordingly subjected to three fates, being recycled to plasma membrane and subsequent exocytosis, released into cytoplasm, or delivered to endo-lysosomes via late endosomes(*39*). Although the degradation most likely takes place in endolysosomes(*45*), the escape might also be facilitated by the lower pH (~5.0) of endolysosomes(*46*). Polyplexes released into cytoplasm still encounter diffusional barriers to traverse the highly crowded cytoplasm(*47*), and metabolic barriers to maintain DNA intact before eventually localizing into the nucleus. It has also been reported that the intracellular barriers to DNA transfer vary with cell type(*20, 22*). Therefore, under the intracellular environment of APRE-19 cells, the binding affinity of the internalized polyplexes might be reduced, which in turn caused more DNA to be degraded or released. The released DNA again could be degraded during the long journey to the nucleus. As a result, lesser DNA was observed in ARPE-19 cells than in SKOV3 cells.

### 3.3.5 Transfection of Co-cultured HT1080/ARPE-19 cells

The selectivity that potentially between cancer and normal cells transfected with pentablock copolymer polyplexes was further studied on another carcinoma cell line HT1080 by co-culturing it with ARPE-19. In this manner both qualitative and

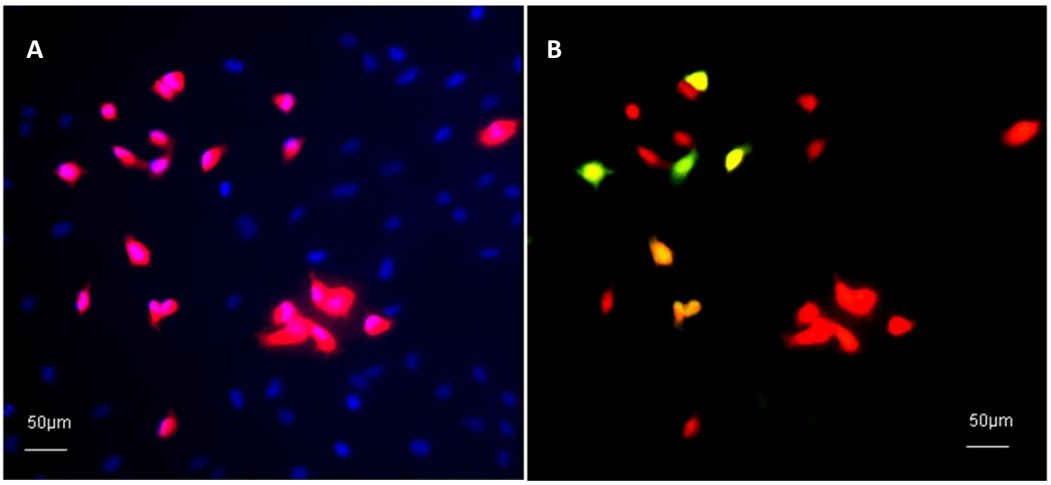


Fig. 3.14. Transfection of HT1080/ARPE-19 cells with PB/DNA (EGFP-N1) polyplexes at N/P ratio of 20. After being labeled with DAPI, HT1080 cells are shown in purple (overlap of red and blue) and ARPE-19 cells are shown in blue (A); EGFP expression in HT1080 cells are indicated in yellow (B).

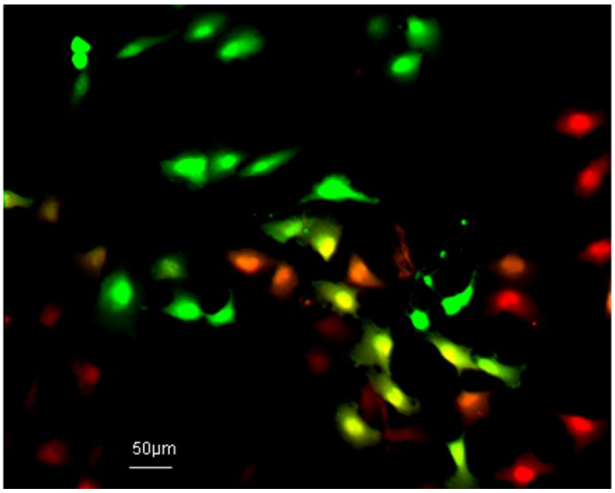


Fig. 3.15. EGFP expression in HT1080/ARPE-19 co-cultures transfected with ExGen/DNA (EGFP-N1) polyplexes at N/P ratio of 6.

quantitative data can be obtained in an environment closer to the *in vivo* situation. Consistent with the earlier results obtained using separate cultures of different cell lines, the pentablock copolymers showed selectivity of transfection of cancer cells

even in co-culture with non-cancerous cells. EGFP expression was seen only in the HT1080 cells even though they were fewer in number relative to the ARPE-19 cells (see Fig. 3.14). For the transfection mediated by ExGen, however, EGFP was evenly expressed in both of these two cell types (see Fig. 3.15), indicating that the transfection efficacy of ExGen is indeed independent of cell type. This finding was further confirmed and quantified with flow cytometry (Fig. 3.16) where the selectivity of transfection of cancer cells using the pentablock copolymer vectors was around 21 whereas no selectivity was exhibited in the transfection mediated by ExGen. Since HT1080 cells were found toproliferate even faster than SKOV3 cells (data not shown here), this selectivity obtained using the pentablock copolymer mediated transfection

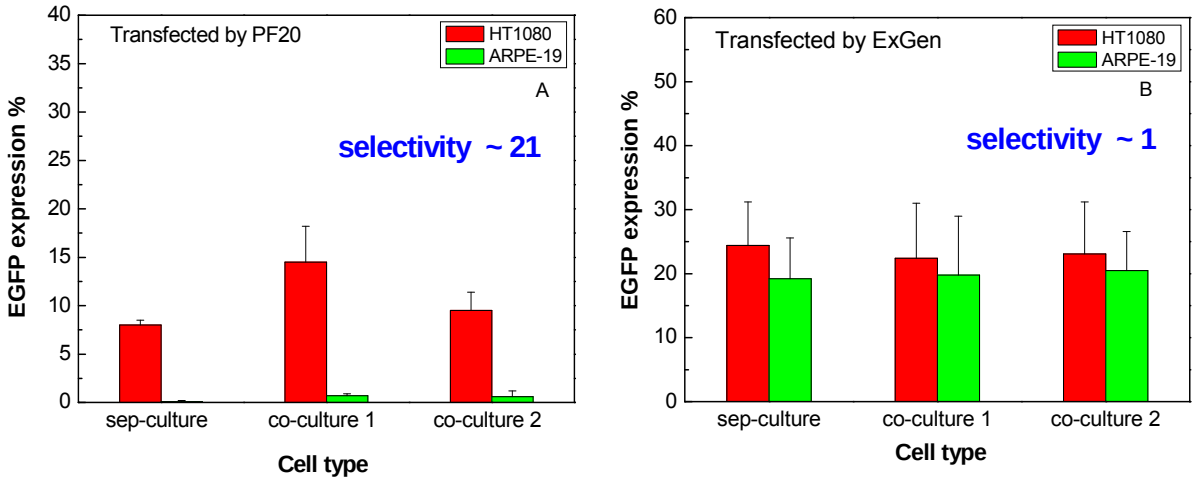


Fig. 3.16. EGFP expression in co-cultured HT1080/ARPE-19 cells mediated by PB-PL at N/P ratio of 20 (A) and ExGen at N/P ratio of 6 (B). Selectivity was expressed as the ratio of percentage of cells with EGFP expression in cancerous HT1080 cells over the percentage in ARPE-19 cells. Co-culture 1 and co-culture 2 indicate two co-culture conditions in which HT1080 and ARPE-19 cells were initially seeded at ratios of 1:2 and 1:3, respectively. Sep-culture represents the transfection performed on individually cultured cells as opposed to co-cultures.

could be related to the proliferation rate.

### 3.4 Conclusions

In summary, we have reported an interesting finding that the pentablock copolymer-mediated transfection was significantly higher in the cancerous SKOV3 and HT1080 cell lines as compared to the non-cancerous APRE-19 and 3T3 cell lines, which implies that they may possess natural transfection selectivity for specific cell types. Through proliferation measurements and confocal microscopy-based trafficking studies, the faster proliferation rate of SKOV3 cells and the more formidable intracellular barriers of APRE-19 cells were found to contribute to this result. The selectivity was found to be about 21 for the transfection of HT1080 over that of APRE-19 cells using pentablock copolymers. However, the well-known and commonly used vector ExGen induced an almost evenly high transfection in all cell types in this study and did not show any selectivity. Since primary cells typically have even slower proliferation rates than most cell lines, the pentablock copolymers are expected to have a better selectivity between carcinoma and primary normal cells, thereby providing an excellent vector to deliver genes for cancer therapies.

### Acknowledgments

We would like to acknowledge financial support from the Bailey Career Development grant. We would also like to thank Marit Nilsen-Hamilton for providing

3T3 cells. Mallapragada would like to dedicate this manuscript to Prof. Nicholas Peppas for his exceptional guidance, mentoring and friendship.

## References


1. J.C. Perales, T. Ferkol, M. Molas, and R.W. Hanson. An Evaluation of Receptor-Mediated Gene Transfer Using Synthetic DNA-Ligand Complexes. European Journal of Biochemistry. 226:255-266 (1994).
2. H. Lee, T.H. Kim, and T.G. Park. A receptor-mediated gene delivery system using streptavidin and biotin-derivatized, pegylated epidermal growth factor. Journal of Controlled Release. 83:109-119 (2002).
3. L. Jabr-Milane, L. van Vlerken, H. Devalapally, D. Shenoy, S. Komareddy, M. Bhavsar, and M. Amiji. Multi-functional nanocarriers for targeted delivery of drugs and genes. Journal of Controlled Release. In Press, Corrected Proof.
4. K. Koike, T. Hara, Y. Aramaki, S. Takada, and S. Tsuchiya. Receptor-Mediated Gene Transfer into Hepatic Cells Using Asialoglycoprotein-Labeled Liposomes. Annals of the New York Academy of Sciences. 716:331-333 (1994).
5. C. Plank, K. Zatloukal, M. Cotten, K. Mechtler, and E. Wagner. Gene transfer into hepatocytes using asialoglycoprotein receptor mediated endocytosis of DNA complexed with an artificial tetra-antennary galactose ligand. Bioconjugate Chem. 3:533-539 (1992).
6. K. Chul Cho, J. Hoon Jeong, H. Jung Chung, C. O Joe, S. Wan Kim, and T. Gwan Park. Folate receptor-mediated intracellular delivery of recombinant caspase-3 for inducing apoptosis. Journal of Controlled Release. 108:121-131 (2005).
7. W. Wijagkanalan, S. Kawakami, M. Takenaga, R. Igarashi, F. Yamashita, and M. Hashida. Efficient targeting to alveolar macrophages by intratracheal administration of mannosylated liposomes in rats. Journal of Controlled Release. 125:121-130 (2008).
8. I.Y. Park, I.Y. Kim, M.K. Yoo, Y.J. Choi, M.-H. Cho, and C.S. Cho. Mannosylated polyethylenimine coupled mesoporous silica nanoparticles for receptor-mediated gene delivery. International Journal of Pharmaceutics. 359:280-287 (2008).
9. J.H. Wong, H.Y.E. Chan, and T.B. Ng. A mannose/glucose-specific lectin from Chinese evergreen chinkapin (Castanopsis chinensis). Biochimica et Biophysica Acta (BBA) - General Subjects. In Press, Corrected Proof.
10. Y. Li, M. Ogris, E. Wagner, J. Pelisek, and M. Ruffer. Nanoparticles bearing polyethyleneglycol-coupled transferrin as gene carriers: preparation and in vitro evaluation.

International Journal of Pharmaceutics. 259:93-101 (2003).

11. C.R. Dassand P.F.M. Choong. Selective gene delivery for cancer therapy using cationic liposomes: In vivo proof of applicability. Journal of Controlled Release. 113:155-163 (2006).
12. X.B. Zhaoand R.J. Lee. Tumor-selective targeted delivery of genes and antisense oligodeoxyribonucleotides via the folate receptor. Advanced Drug Delivery Reviews. 56:1193-1204 (2004).
13. B. Liang, M.-L. He, Z.-P. Xiao, Y. Li, C.-y. Chan, H.-F. Kung, X.-T. Shuai, and Y. Peng. Synthesis and characterization of folate-PEG-grafted-hyperbranched-PEI for tumor-targeted gene delivery. Biochemical and Biophysical Research Communications. 367:874-880 (2008).
14. S. Kawakami, S. Fumoto, M. Nishikawa, F. Yamashita, and M. Hashida. In Vivo Gene Delivery to the Liver Using Novel Galactosylated Cationic Liposomes. Pharmaceutical Research. 17:306-313 (2000).
15. S. Fumoto, F. Nakadori, S. Kawakami, M. Nishikawa, F. Yamashita, and M. Hashida. Analysis of Hepatic Disposition of Galactosylated Cationic Liposome/Plasmid DNA Complexes in Perfused Rat Liver. Pharmaceutical Research. 20:1452-1459 (2003).
16. K. Corsi, F. Chellat, L. Yahia, and J.C. Fernandes. Mesenchymal stem cells, MG63 and HEK293 transfection using chitosan-DNA nanoparticles. Biomaterials. 24:1255-1264 (2003).
17. S.-W. Kim, T. Ogawa, Y. Tabata, and I. Nishimura. Efficacy and cytotoxicity of cationic-agent-mediated nonviral gene transfer into osteoblasts. Journal of Biomedical Materials Research Part A. 71A:308-315 (2004).
18. H. Shen, J. Tan, and W.M. Saltzman. Surface-mediated gene transfer from nanocomposites of controlled texture. Nat Mater. 3:569-574 (2004).
19. I. Mortimer, P. Tam, I. MacLachlan, R.W. Graham, E.G. Saravolac, and P.B. Joshi. Cationic lipid-mediated transfection of cells in culture requires mitotic activity. Gene Therapy. 6:403-411 (1999).
20. A. Remy-Kristensen, J.-P. Clamme, C. Vuilleumier, J.-G. Kuhry, and Y. Mely. Role of endocytosis in the transfection of L929 fibroblasts by polyethylenimine/DNA complexes. Biochimica et Biophysica Acta (BBA) - Biomembranes. 1514:21-32 (2001).
21. S. Brunner, T. Sauer, S. Carotta, M. Cotten, M. Saltik, and E. Wagner. Cell cycle dependence of gene transfer by lipoplex, polyplex and recombinant adenovirus. Gene Therapy. 7:401-407 (2000).
22. H. Pollard, J.-S. Remy, G. Loussouarn, S. Demolombe, J.-P. Behr, and D. Escande. Polyethylenimine but Not Cationic Lipids Promotes Transgene Delivery to the Nucleus in Mammalian Cells. J Biol Chem. 273:7507-7511 (1998).
23. M.D. Determan, J.P. Cox, S. Seifert, P. Thiyagarajan, and S.K. Mallapragada. Synthesis and characterization of temperature and pH-responsive pentablock copolymers. Polymer.

46:6933-6946 (2005).

24. A.V. Kabanov, E.V. Batrakova, and V.Y. Alakhov. Pluronic(R) block copolymers as novel polymer therapeutics for drug and gene delivery. Journal of Controlled Release. 82:189-212 (2002).
25. A. Agarwal, R. Unfer, and S.K. Mallapragada. Novel cationic pentablock copolymers as non-viral vectors for gene therapy. Journal of Controlled Release. 103:245-258 (2005).
26. A. Agarwal, R.C. Unfer, and S.K. Mallapragada. Investigation of in vitro compatibility of novel pentablock copolymers for gene delivery. Journal of Biomedical Materials Research 81A:24-39 (2007).
27. W.T. Godbey, K.K. Wu, and A.G. Mikos. Tracking the intracellular path of poly(ethylenimine)/DNA complexes for gene delivery. Proceedings of the National Academy of Sciences. 96:5177-5181 (1999).
28. T. Serikawa, N. Suzuki, H. Kikuchi, K. Tanaka, and T. Kitagawa. A new cationic liposome for efficient gene delivery with serum into cultured human cells: a quantitative analysis using two independent fluorescent probes. Biochimica et Biophysica Acta (BBA) - Biomembranes. 1467:419-430 (2000).
29. M. Ruponen, S. Ronkko, P. Honkakoski, J. Pelkonen, M. Tammi, and A. Urtti. Extracellular Glycosaminoglycans Modify Cellular Trafficking of Lipoplexes and Polyplexes. J Biol Chem. 276:33875-33880 (2001).
30. M.E. Dowty, P. Williams, G. Zhang, J.E. Hagstrom, and A.W. Jon. Plasmid DNA Entry Into Postmitotic Nuclei of Primary Rat Myotubes. Proceedings of the National Academy of Sciences of the United States of America. 92:4572-4576 (1995).
31. C.W. Pouton, K.M. Wagstaff, D.M. Roth, G.W. Moseley, and D.A. Jans. Targeted delivery to the nucleus. Advanced Drug Delivery Reviews. 59:698-717 (2007).
32. K.W. Riddle, H.-J. Kong, J.K. Leach, C. Fischbach, C. Cheung, K.S. Anseth, and D.J. Mooney. Modifying the Proliferative State of Target Cells to Control DNA Expression and Identifying Cell Types Transfected In Vivo. Mol Ther. 15:361-368.
33. A.-G. Ziady, T. Ferkol, T. Gerken, D.V. Dawson, D.H. Perlmutter, and P.B. Davis. Ligand substitution of receptor targeted DNA complexes affects gene transfer into hepatoma cells. Gene Ther. 5:1685-1697 (1998).
34. I.M. Helander, H.-L. Alakomi, K. Latva-Kala, and P. Koski. Polyethyleneimine is an effective permeabilizer of Gram-negative bacteria. Microbiology. 143:3193-3199 (1997).
35. W.T. Godbey, K.K. Wu, and A.G. Mikos. Poly(ethylenimine)-mediated gene delivery affects endothelial cell function and viability. Biomaterials. 22:471-480 (2001).
36. D. Fischer, Y. Li, B. Ahlemeyer, J. Krieglstein, and T. Kissel. In vitro cytotoxicity testing of polycations: influence of polymer structure on cell viability and hemolysis. Biomaterials.

24:1121-1131 (2003).

37. P.H. Boltontand D.R. Kearns. Spectroscopic properties of ethidium monoazide: a fluorescent photoaffmity label for nucleic acids. Nucleic Acids Research. 5:4891-4903 (1978).
38. M.F. Bureau, S. Naimi, R. Torero Ibad, J. Seguin, C. Georger, E. Arnould, L. Maton, F. Blanche, P. Delaere, and D. Scherman. Intramuscular plasmid DNA electrotransfer: Biodistribution and degradation. Biochimica et Biophysica Acta (BBA) - Gene Structure and Expression. 1676:138-148 (2004).
39. D. Lechardeur, A.S. Verkman, and G.L. Lukacs. Intracellular routing of plasmid DNA during non-viral gene transfer. Advanced Drug Delivery Reviews. 57:755-767 (2005).
40. G. Liu, D. Li, M.K. Pasumarthy, T.H. Kowalczyk, C.R. Gedeon, S.L. Hyatt, J.M. Payne, T.J. Miller, P. Brunovskis, T.L. Fink, O. Muhammad, R.C. Moen, R.W. Hanson, and M.J. Cooper. Nanoparticles of Compacted DNA Transfect Postmitotic Cells. J Biol Chem. 278:32578-32586 (2003).
41. N. Panteand M. Kann. Nuclear Pore Complex Is Able to Transport Macromolecules with Diameters of ~39 nm. Mol Biol Cell. 13:425-434 (2002).
42. R.Y.H. Limand B. Fahrenkrog. The nuclear pore complex up close. Current Opinion in Cell Biology. 18:342-347 (2006).
43. C.-K. Chanand D.A. Jans. Using nuclear targeting signals to enhance non-viral gene transfer. Immunol Cell Biol. 80:119-130 (2002).
44. I.A. Khalil, K. Kogure, H. Akita, and H. Harashima. Uptake Pathways and Subsequent Intracellular Trafficking in Nonviral Gene Delivery. Pharmacol Rev. 58:32-45 (2006).
45. H. Kamiya, H. Tsuchiya, J. Yamazaki, and H. Harashima. Intracellular trafficking and transgene expression of viral and non-viral gene vectors. Advanced Drug Delivery Reviews. 52:153-164 (2001).
46. M. Colin, G. Maurice, G. Trugnan, M. Kornprobst, R.P. Harbottle, A. Knight, R.G. Cooper, A.D. Miller, J. Capeau, C. Coutelle, and M.C. Brahimi-Horn. Cell delivery, intracellular trafficking and expression of an integrin-mediated gene transfer vector in tracheal epithelial cells. Gene Ther. 7:139-152 (2000).
47. J. Suh, D. Wirtz, and J. Hanes. Efficient active transport of gene nanocarriers to the cell nucleus. Proceedings of the National Academy of Sciences. 100:3878-3882 (2003).

# CHAPTER 4. THE MECHANISM OF SELECTIVE TRANSFECTION MEDIATED BY PENTABLOCK COPOLYMERS; PART I: INVESTIGATION OF CELLULAR UPTAKE

Modified from a paper published in Acta Biomaterialia, 2011, 7:1570-1579

Bingqi Zhang and Surya Mallapragada

**Abstract**

We have developed poly(diethylaminoethylmethacrylate) (PDEAEM) and Pluronic F127 based pentablock copolymer vectors with the ability to selectively transfect cancer cells over normal cells in *in vitro* cultures, as described in a previous report. Understanding the mechanism of this selectivity will enable us to better design polymeric vectors with *inherent selectivity for specific cell types based on intracellular differences* and not on the use of targeting ligands that have shown variable success, depending on the system. We assume that the selectivity was due to different intracellular barriers to transfection in the different cell types. Part I (this manuscript) focuses on investigating if cellular entry is one of the barriers to transfection, through conjugation of epidermal growth factor (EGF) to the pentablock copolymer vector. Results indicate that EGF conjugation increased transfection efficiency the most when conjugated to the outer surface of polyplexes, with minimal disruption to DNA

packaging and maximal accessibility to receptors. The overall resulting enhancement in transfection, however, was a moderate three to five fold increase as compared to the condition with no EGF involved, implying that the addition of EGF fails to overcome the intracellular barrier to transfection that probably involves some step other than cellular uptake in pentablock copolymer system. Therefore the differences observed in the selectivity of transfection between cancer and normal cell lines is probably not controlled by differences in cellular entry, and the intracellular barriers to transfection in this system are likely to be endosomal escape or nuclear entry, as investigated in Part II, the companion manuscript to this work.

## 4.1 Introduction

Successful gene delivery systems exhibit good transfection efficiencies, specifically in cells of interest, while minimizing toxicity to untargeted cells. For clinical applications, safe, efficient and convenient methods are required. While viral gene carriers exhibit significantly higher transfection efficiencies than non-viral vectors, they show increased potential for immune responses that can hinder gene delivery, trigger severe inflammatory reactions, and cause nonspecific gene integration into host genome. Therefore, there has been significant interest in recent years to develop non-viral polymeric vectors because of their low immunogenicity, great DNA packaging capability and flexible tunability of structures. Through rational design, multifunctional vectors are desired that exhibit not only good transfection efficiencies,

but also good biocompatibility, and cell selectivity. Previously, we reported a novel self-assembling pentablock copolymer/Pluronic F127 transgene system(1). The cationic poly(diethylaminoethyl methacrylate) (PDEAEM) blocks bind to DNA and provide pH buffering capability. The central Pluronic F127 blocks contribute to temperature responsiveness and have been reported to be able to promote cellular entry(2). Besides the attractive properties above, recent work has shown that pentablock-based vectors might have intrinsic selectivity in transfecting cancer cell lines as opposed to normal cell lines, presumably due to different intracellular barriers to transfection in the different cell types(3). Understanding the mechanism of selectivity will potentially help in designing polymeric vectors with inherent selectivity for different cell types, and we aim to do this by identifying the intracellular barriers to transfection using the pentablock copolymer vectors, and then investigating differences in intracellular barriers to transfection between cancer cell lines and normal cell lines.

The three commonly investigated intracellular barriers include cellular uptake, endosomal escape and nuclear entry. In Part I of this study, we investigate whether cellular entry is one of the main intracellular barriers to transfection in the pentablock copolymer vector systems by incorporating epidermal growth factor (EGF), a 53-residue peptide that binds to the EGF receptor with high affinity(4), into the polyplex constructs in different ways, with the aim of enhancing transfection in cancer

cell lines through receptor-mediated cellular uptake. A number of studies have shown the efficacy of EGF incorporation in enhancing transfection efficiency of some polymeric vectors in tumor cells that overexpress the EGF-receptor(5-11). However, most of these published results are based on polyethyleneimine (PEI) or poly-L-lysine (PLL) type vectors and the results might not be broadly applicable to all polymeric vectors. Different gene delivery systems could be limited by different intracellular barriers; for instance, in a system where cellular uptake significantly limit transfection efficiency, addition of EGF may lead to significant enhancement of transfection efficiency, whereas it may make no difference for a system where the vector can enter cells easily. Thus, influence of EGF attachment to the vector on transfection efficiency in tumor cells could demonstrate whether or not cellular uptake is a major transfection barrier in that system.

To achieve prolonged circulation of the vector in the blood stream and accumulation in target sites, free Pluronic F127 was further added to form a shield around the polyplex by self-assembly and block undesired interactions with serum proteins(12). Compared to various PEGylation strategies (prePEGylation or postPEGylation) that have been most frequently and extensively employed to reduce surface charges(13-17), Pluronic shielding in our system can be achieved conveniently, and provides the additional feature of thermosensitive gelation, allowing for the development of an injectable gel for clinically feasible sustained gene delivery.

To fulfill the potential of EGF as a cellular uptake facilitator for tumor cells while minimizing its interference in the resulting vectors, we employed various incorporation strategies such as attaching the EGF to the pentablock copolymers, or to the Pluronic shields. All of these studies were accompanied by detailed characterization of vector properties, with an aim to understand how the cellular uptake and transfection of pentablock copolymer vectors are affected by EGF.

## 4.2 Experimental

### 4.2.1 Materials

N,N-(diethyl amino)ethyl methacrylate (DEAEM) were purchased from Sigma (St Louis, MO) and Pluronic F127 was kindly donated by BASF (Florham Park, NJ). Recombinant human epidermal growth factor (EGF), Alexa Fluor 647 carboxylic acid, succinimidyl ester, (written as AF647 hereafter), 4',6-diamidino-2- phenylindole (DAPI) dilactate and ProLong Gold antifade reagent were purchased from Invitrogen (Carlsbad, CA). Luciferase assay system and passive lysis buffer were purchased from Promega (Madison, WI). Lactate dehydrogenase (LDH) assay kit and HEPES used to make Hepes buffered saline (HBS) was obtained from Sigma-Aldrich (St Louis, MO). ExGen 500 was purchased from Fermentas Life Sciences (Hanover, MD). Cell culture reagents: Dulbecco's Modified Eagle Medium (DMEM), heat inactivated fetal bovine serum (FBS), 0.25% trypsin-EDTA and Hank's buffered salt saline (HBSS) were purchased from Invitrogen (Carlsbad, CA). HiSpeed Plasmid Maxi Kit was

obtained from Qiagen (Valencia, CA). pGWIZ-luc (GeneTherapy Systems Inc, CA) plasmid encoding the luciferase reporter gene and EGFP-N1 (ClonTech, CA) plasmid encoding GFP reporter gene were purified with Qiagen HiSpeed Maxi Kit. Chemicals for synthesis, copper bromide, succinic anhydride, N-hydroxysuccinimide, sodium azide, 1-propylamine, 2-pyridinecarbaldehyde were obtained from Sigma-Aldrich (St Louis, MO). Pyridine, dimethylformamide (DMF), tetrahydrofuran (THF) and all other chemicals were purchased from Fisher Scientific and used without further purification. N-Propyl-pyridynyl methanimine (Nppm) was prepared by reacting 1-propylamine with 2-pyridinecarbaldehyde(18). All chemicals were used without further purification.

### 4.2.2 Cell Culture

The human ovarian carcinoma SKOV3 and human epidermoid carcinoma A431 cell lines were obtained from ATCC™(Manassas, VA). Cells were grown in DMEM supplemented with 10% (v/v) heat-inactivated FBS at 37°C under a humidified atmosphere containing 5% $CO_2$. Subculture was carried out every 2~3 days. A431 cells are known to overexpress EGF receptors(19). They are thus expected to show higher rates of transfection when using EGF containing vectors, as compared to SKOV3 cells that just express moderate level of EGF receptors(20).

### 4.2.3 EGF Attachment to The Pentablock Copolymers

The pentablock copolymers (Fig. 4.1a) used in this study were synthesized by

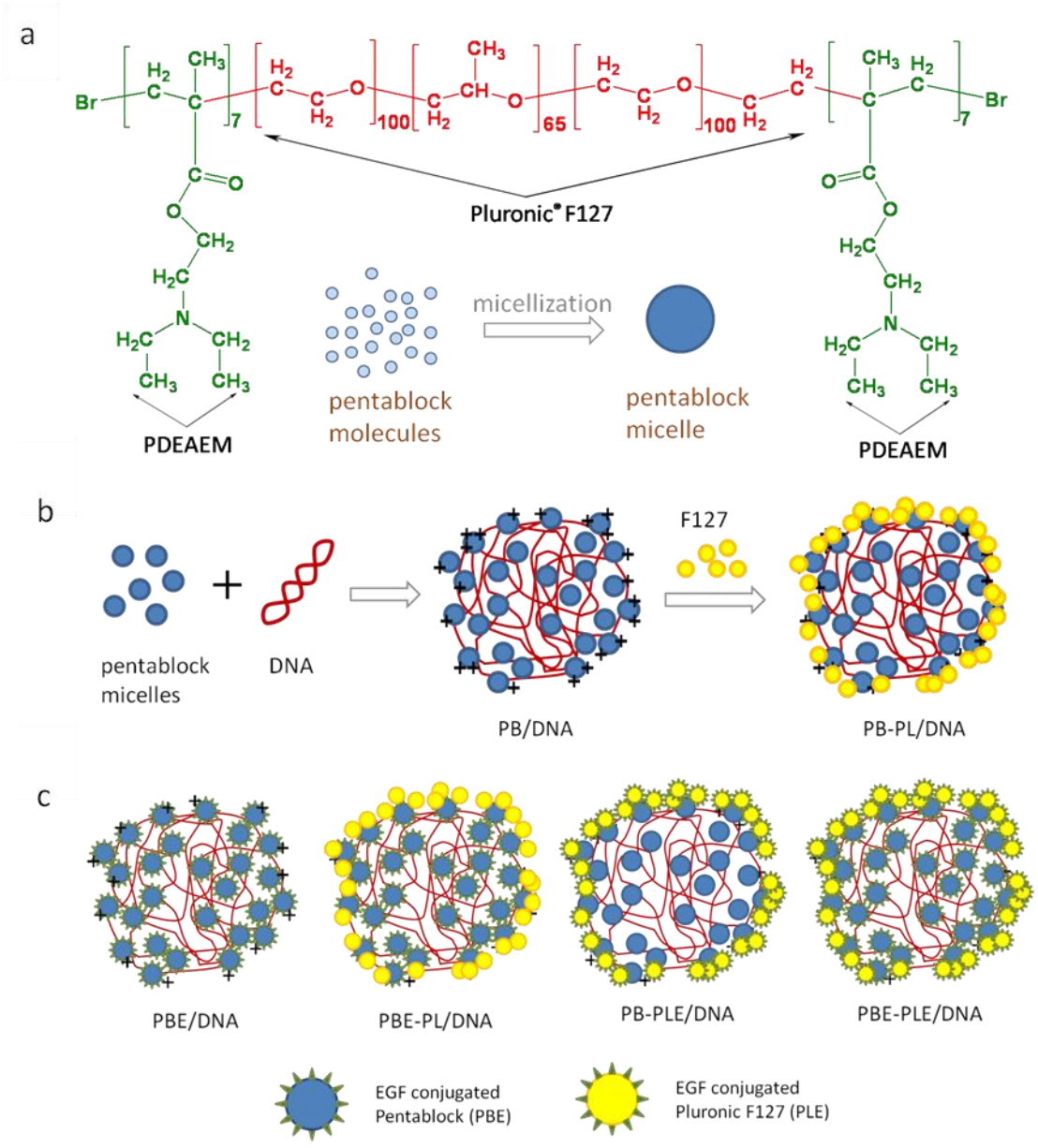


Fig. 4.1. Schematic illustration of formation of various polyplexes with pentablock copolymer (PB) and Pluronic F127 (PL). (a) The pentablock copolymer molecules form micelles in aqueous solution via self-assembly in the same way as Pluronic F127; The pentablock micelles condense plasmid DNA into polyplexes of PB/DNA via ionic interactions. (b) Excess positive charges on the surface of PB/DNA were shielded by further addition of free F127 micellar solution via self-assembly; (c) By using EGF conjugated pentablock copolymer and Pluronic F127, four other types of polyplexes, PBE/DNA, PBE-PL/DNA, PB-PLE/DNA and PBE-PLE/DNA, were produced and investigated for use in transfection.

atom transfer radical polymerization and have been characterized in detail and tested for cytotoxicity, as described earlier(1, 18). Four abbreviations are used: PB - the pentablock copolymer alone; PBE - the pentablock copolymer attached to EGF; PL - Pluronic F127; PLE - Pluronic F127 attached to EGF; and correspondingly, PB-PL, PB-PLE, PBE-PL and PBE-PLE refer to the vectors with DNA complexed and shielded with varied physical mixture combinations of PB, PBE, PL and PLE. Formation of various polyplexes investigated in this study are shown schematically in Fig. 4.1.

To achieve EGF conjugation, the chain ends of the pentablock copolymer were first converted to an amine reactive N-Hydroxysuccinimide (NHS) ester through azidation, carboxylation and NHS activation. The azidation reaction was adopted from a procedure reported by Lutz and co-workers(21). In short, the pentablock copolymer with bromide end groups (18 000 g. $mol^{-1}$, 5.4 g, 0.3 mmole), sodium azide (195 mg, 3 mmole) and DMF (8 ml) were added to a flask. The mixture was reacted for 24 hours at 50°C. After that, the pentablock copolymer was precipitated in n-hexane, filtered and dried under reduced pressure. Carboxylation was achieved by click chemistry. Briefly, the azide functionalized pentablock (2.1 g, 0.11 moles), copper bromide (47 mg, 0.33 mole) and Nppm ligand (99 mg, 0.66mole) were added into a round-bottom flask, followed by purging with argon for a couple of minutes. Degassed THF (4 ml) and pentyonic acid (64.8 mg, 0.66 mmole) were added into the mixture that was then stirred overnight at room temperature. The carboxyl-functionalized pentablock was

precipitated in n-hexane and filtered and dried under vacuum.

The carboxyl terminated pentablock was then activated by reacting with NHS as reported in literature(22). Briefly, to a round bottom flask connected with an argon line and bubbler, 2.3 g of carboxy-pentablock (0.128 mmole), 0.0792 g of N,N'-dicyclohexylcarbodiimide (DCC) (3× excess, 0.384 mole), 0.0442 g of N-hydroxysuccinimide (NHS) (3× excess, 0.384 mole), and 8 ml of dichloromethane were added. After reaction for 24 hours at room temperature, the mixture was filtered and precipitated in cold diethyl ether. Next, the NHS functionalized pentablock copolymer was conjugated with EGF. 30 mg of NHS activated pentablock copolymer was mixed with 200μg of EGF in 1 ml of PBS (pH 7.4). After 4h reaction, an additional 30 mg of NHS-pentablock was added. The reaction was maintained at room temperature for 24 hours. The reaction mixture was dialyzed against 0.2× PBS using cellulose ester membrane (MWCO, 10000, Spectrum Labs) for 48 h in order to remove the uncoupled EGF. Finally, lyophilized products were collected.

### 4.2.4 EGF Attachment to Pluronic F127

The strategy for attaching EGF to Pluronic F127 was similar to that employed with pentablock copolymer. Firstly, the hydroxyl end groups of Pluronic were converted to carboxyl groups by treating it with succinic anhydride in pyridine as reported in the literature(23). In short, Pluronic (32g, 2.5 mmole) and succinic anhydride (1g, 10 mmole) were dissolved in pyridine (100 ml). The reaction was carried out at 40° C for

24 hours. The mixture was precipitated in diethyl ether, dissolved in toluene and reprecipitated in diethyl ether. Dried product was then achieved under vacuum. Next, the carboxyl terminated Pluronic was converted to an amine reactive NHS ester following the procedure described above. Finally, EGF was conjugated to Pluronic via reaction between amine and NHS groups. The amount of EGF in modified Pluronic or pentablock copolymer was found to be about half of the amount initially added in the reaction based on EGF ELISA kit, indicating either a moderate conjugation efficiency or some change in EGF activity after being conjugated to Pluronic.

### 4.2.5 Polyplex Formation

All polymer solutions used in forming polyplexes were prepared in 0.5× HBS buffer, pH 7.0 unless stated otherwise. Briefly, various quantities of EGF- or EGF-free pentablock copolymer solution (2mg/ml) were added to the fixed volume of plasmid DNA solution (in water) to get desired N/P (nitrogen/phosphate) ratios. The mixture was gently vortexed and allowed to incubate at room temperature for 20 min to ensure complexation. An appropriate amount of EGF-containing or EGF-free Pluronic F127 solution (10 mg/ml) was added to the mixture to form a shield layer around the newly formed polyplexes by self-assembly.

### 4.2.6 Gel Retardation Assay

A gel retardation assay was used to assess complexation between the DNA and

the polymer(s) under various conditions. Polymer/DNA complexes were formed as described above. 40µl of each complex solution was loaded in a well for electrophoresis assay on a 1% agarose gel with Tris-acetate (TAE) buffer at 50V for 120 min. DNA bands were visualized under UV light with ethidium bromide staining.

### 4.2.7 Particle Size

Test polyplex solutions were transferred to Malvern disposable cuvettes and measured by a Malvern Zetasizer Nano-ZS90 dynamic light scattering system (Malvern Instruments, Southborough, MA). The size distribution profile was graphed as the mean of three independent experiments.

### 4.2.8 Atomic Force Microscopy (AFM)

Samples were prepared according to the procedure used for formation of polyplexes, but using water instead of HBS buffer. Each sample contains 3ug DNA in a 300µl volume. The polyplexes were imaged on a Dimension3000 AFM with a version IV controller (Digital Instruments, Santa Barbara, CA) in tapping mode. Topographical images were obtained with 512×512 pixel resolution at a scan size of 5µm and scan speed of 1 Hz, and analyzed with nanoscope software (version 5.30r3).

### 4.2.9 Cytotoxicity

The cytotoxicity of polyplexes was examined based on the amount of cytoplasmic lactate dehydrogenase (LDH) released into the medium following membrane rupture.

For a better understanding of how cytotoxicity develops with transfection, medium was collected twice for LDH assay, at the end of 3h transfection and additional 45h post-transfection. Blank cells were used as a negative control to provide 0% cytotoxicity and Triton-X was used as a negative control to provide 100% cytotoxicity. Cytotoxicity was determined as follows:

$$\text{Cytotoxicity \%} = \frac{\text{Abs (sample)} - \text{Abs (blank cells)}}{\text{Abs (Triton-x)} - \text{Abs (blank cells)}} \times 100$$

Here, Abs refers to the absorbance at 490nm characterizing LDH.

### 4.2.10 In vitro Transfection

Cells of interest were seeded into a 96-well plate or 6-well plate with an initial density of $1.2\times10^4$ or $1.5\times10^5$ cells per well one or two days before transfection. Polyplexes prepared at given N/P ratios were added to each well with 0.6μg of DNA per well for 96-well plates and 3μg DNA per well for 6-well plates in serum-containing media. Cells were allowed to incubate for 3h when polyplexes were removed by replacing the old medium with fresh growth medium (at t=3h).Cells in the 6-well plate were sampled at different time points within the 3h transfection for flow cytometry. After additional 45h post-transfection (at t=48h), cells in 96-well plate were lysed and tested for luciferase activity. The luminescence was measured in arbitrary Relative Luminescence Units (RLU) on an automated Veritas™ Microplate Luminometer. Each transfection was done in triplicate. ExGen 500, a sterile solution of linear 22kDa

polyethylenimine (PEI), was used as positive control at an N/P ratio of 6 according to the manufacturer's protocol.

### 4.2.11 Flow Cytometry

The pentablock copolymer was labeled with AF647 according to a procedure reported elsewhere, named PBD for short(3). Cells grown in the 6-well plate were transfected with PBD contained polyplexes following the procedures described above. At specific time points during transfection, cells in the well of interest were trypsinized and resuspended in 2% paraformaldehyde after centrifuging twice in HBSS buffer. Samples were stored at 4°C for later analysis with a Becton-Dickinson FACSCanto flow cytometer.

### 4.2.12 Confocal Microscopy

Cells of interest were seeded onto poly-L-lysine coated coverslips and subsequently transfected with PBD containing polyplexes. Following 3h transfection, cells were fixed with fresh 4% paraformaldehyde and then treated with 300nM DAPI in PBS for 5min. The coverslip was washed thoroughly with PBS and mounted on a glass slide. Confocal images were collected with the objective of 63-er Oil / N.A. 1.4 on a Leica TCS SP5 X Supercontinuum Confocal Microscope.

### 4.2.13 Statistics

The data are presented as mean and standard deviations calculated over at least

three independent experiments. Significant differences between two groups were evaluated by Student's t-test with p≤ 0.05.

## 4.3 Results and Discussion

### 4.3.1 Effect of EGF Conjugation on the Polyplex Properties

The particle size of polyplexes in HBS buffer (Fig. 4.2) and serum-containing media (Fig. 4.3) were measured by the Malvern Zetasizer Nano-ZS90 system. All polyplexes in HBS buffer appeared to be of a fairly stable size around 150nm with a narrow distribution. There were no aggregates even when the time was extended to 5h. However, in the media containing serum, both size and distribution increased with time, indicating that polyplexes were interacting with serum proteins (data were summarized in Table 4.1). The addition of free PL or PLE did stabilize the polyplexes to a mean size of 200-250nm as compared to unshielded counterparts, which

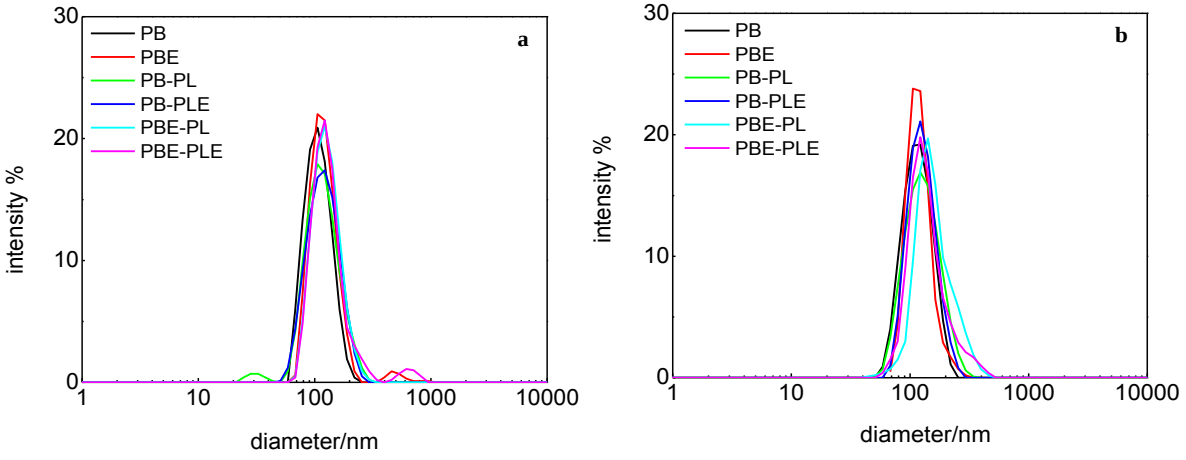


Fig. 4.2. Size distribution of polyplexes at N:P ratio of 20 in 0.5× HBS buffer pH=7.0 measured (a) immediately; and (b) 5h after polyplex formation.

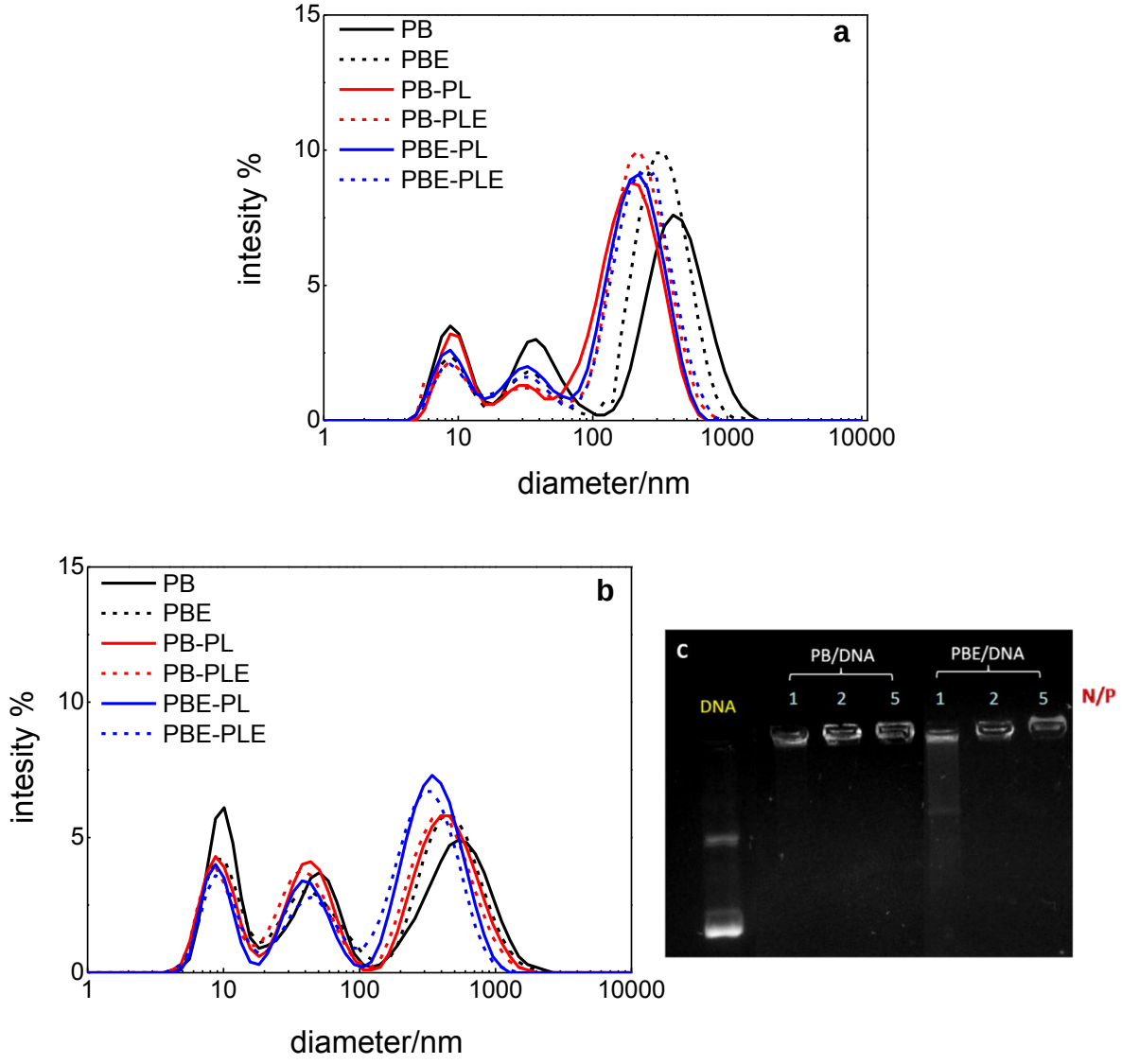


Fig. 4.3. Size distribution of polyplexes at N:P ratio of 20 in media with 10% serum measured (a) immediately; and (b) 5h after polyplex formation. (c) The ability of PB and PBE to condense DNA was examined using agarose gel electrophoresis.

indicates that the presence of EGF did not affect the charge shielding by Pluronic. The size of PBE-based polyplexes was found to be much smaller than PB-based polyplexes at both time 0h and 5h. Similarly, the other two pairs of vectors

distinguished only by the DNA condensing agent, PB-PL and PBE-PL, and PB-PLE and PBE-PLE, exhibited a similar trend after 5h of incubation in serum-containing media, implying that the EGF conjugated to PB might help reduce the formation of large aggregates with serum proteins by charge shielding, similar to that reported for other targeting ligands(24-25). However, that also implies that the DNA binding affinity of the conjugated polymer could be reduced at the same time. In our study, this negative effect of EGF conjugation on DNA interactions was shown using a gel retardation assay (Fig. 4.3c). PBE exhibited a slightly weaker inhibition of DNA

Table. 4.1 Mean size of polyplexes in buffer and media containing serum.

Values indicate means ± standard deviations (n = 3); 0 or 5h means the incubation time after polyplex formation; *, ^ and # indicate p≤0.05; ** indicates p≤0.01.

| | Mean diameter in buffer Time=0 | | Mean diameter in buffer Time=5h | | Mean diameter in serum containing media/nm | |
|---|---|---|---|---|---|---|
| | Diameter/nm | PDI[a] | Diameter/nm | PDI[a] | Time=0 | Time=5h |
| PB | 110±5 | 0.26±0.04 | 113±5 | 0.31±0.00 | 425±17 ** | 564±73 * |
| PBE | 114±10 | 0.38±0.04 | 114±3 | 0.59±0.07 | 323±24 ** | 444±18 * |
| PB-PL | 123±16 | 0.28±0.02 | 133±13 | 0.29±0.04 | 200±35 | 420±34 ^ |
| PB-PLE | 123±14 | 0.43±0.05 | 129±10 | 0.42±0.01 | 215±40 | 389±47 # |
| PBE-PL | 130±13 | 0.43±0.04 | 144±25 | 0.40±0.08 | 212±16 | 344±27 ^ |
| PBE-PLE | 131±20 | 0.54±0.06 | 130±19 | 0.52±0.09 | 243±30 | 309±37 # |

[a] polydispersity index by DLS. Samples in serum containing media showed high PDI ≈ 1 due to the variety of particles in serum.

migration relative to PB as shown with the gel pattern at N/P =1. At higher N/P ratios, DNA was completely retarded in the wells for both polyplexes. The non-neutralized charges have been considered a major cause for cytotoxicity by destabilizing the cell membrane in cationic polymer-based gene delivery systems(26-27). Thus EGF conjugation might also lead to a change in cytotoxicity. As shown in Fig. 4.4, PBE indeed showed a significantly lower toxicity compared to PB at the end of 3h transfection, further confirming the occurrence of charge shielding from EGF, though it was still inferior to the charge shielding from PL or PLE. However, EGF scarcely affected the toxicity of polyplexes when it was conjugated to Pluronic, which was

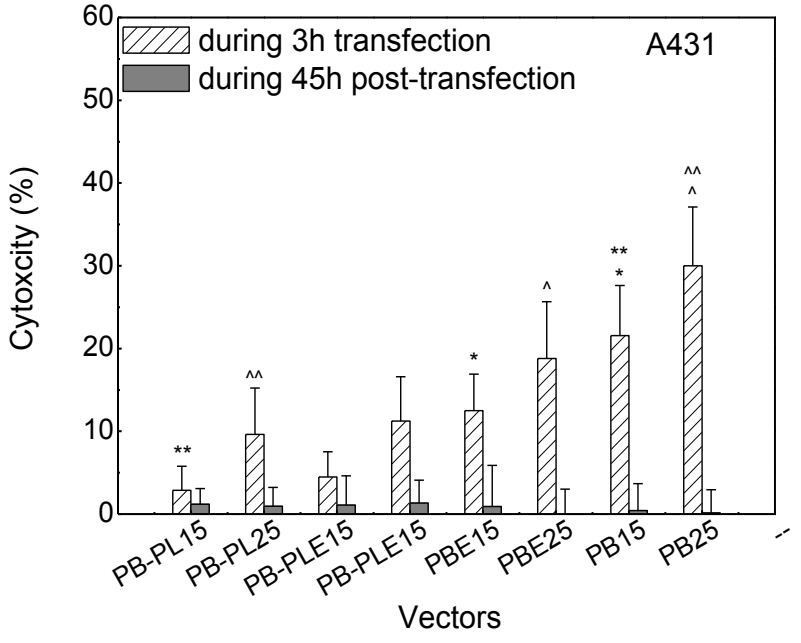


Fig. 4.4. Cytotoxicity of various polyplexes on A431 cells measured by LDH assay during and after transfection. The number following each abbreviation denotes the N/P ratio. Values indicate means ± standard deviations (n = 3)

consistent with the size measurement results. After removing the medium containing polyplexes, the toxicity post-transfection would be caused by the internalized polyplexes, which was found to be very low for all types of polyplexes.

AFM was employed to further investigate the influence of EGF on the morphology of polyplexes (Fig. 4.5) The main structures of both kinds of polyplexes appeared to be rods, toroids, spheres and some intermediates, which are the typical structures for DNA condensates(28-29). Herein, the EGF conjugated to Pluronic did not cause any obvious change in the morphology of polyplexes.

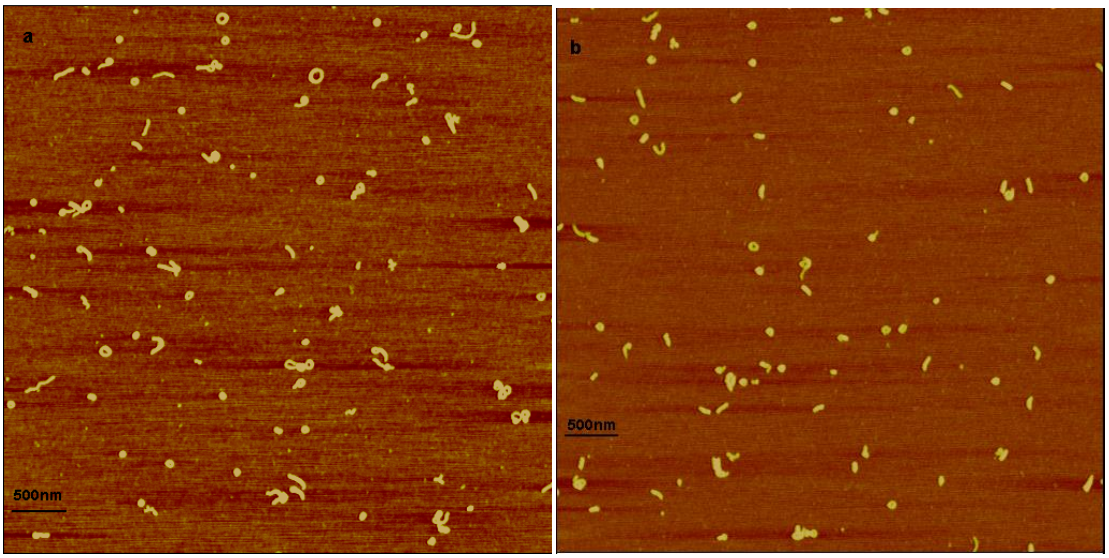


Fig. 4.5. AFM images of polyplexes of (a) PB-PL and (b) PBE-PLE at N:P ratio of 25 on the surface of mica

### 4.3.2 Effect of EGF Conjugation on Transfection

Higher N/P ratios lead to tighter DNA binding and thus better DNA protection, but

they also result in higher cytotoxicity and less DNA release. The balance between these two makes the transfection efficiency change with N/P ratio nonlinearly, which is as shown for most of our polyplexes (Fig. 4.6). For SKOV3 cells, PB-PLE mediated the highest level of transfection at N/P of 30 among all competitive counterparts. There may be two reasons: PB-PLE has better accessibility of EGF to EGF receptors on the cell surface; EGF will not affect the complexation between PB and DNA, since the PLE was added after the formation of DNA condensates. This greatest effectiveness of incorporating a ligand on the most accessible position has been reported by attaching a peptide or EGF to PEGylated PEI polyplexes(5-6, 30). Thus, it is not surprising that PBE-PL showed the most inefficient transfection due to the less chance of EGF being exposed to the cell surface receptors and the potential interference with DNA condensation by conjugating EGF to the pentablock copolymer. But even with the potential beneficial effects of EGF attachment, such as facilitating internalization, reducing aggregation and decreasing toxicity, PBE did not induce any improvement of gene expression, and instead performed even worse than PB, which emphasized the negative influence of EGF on transfection when conjugated to DNA condensing agents. This effect was consistently seen in PB-PL vs. PBE-PL and PB-PLE vs. PBE-PLE. Although the EGF-caused decrease in DNA binding affinity was found to be not dramatic in the gel retardation assay, it truly made a big difference on the overall transfection efficiency.

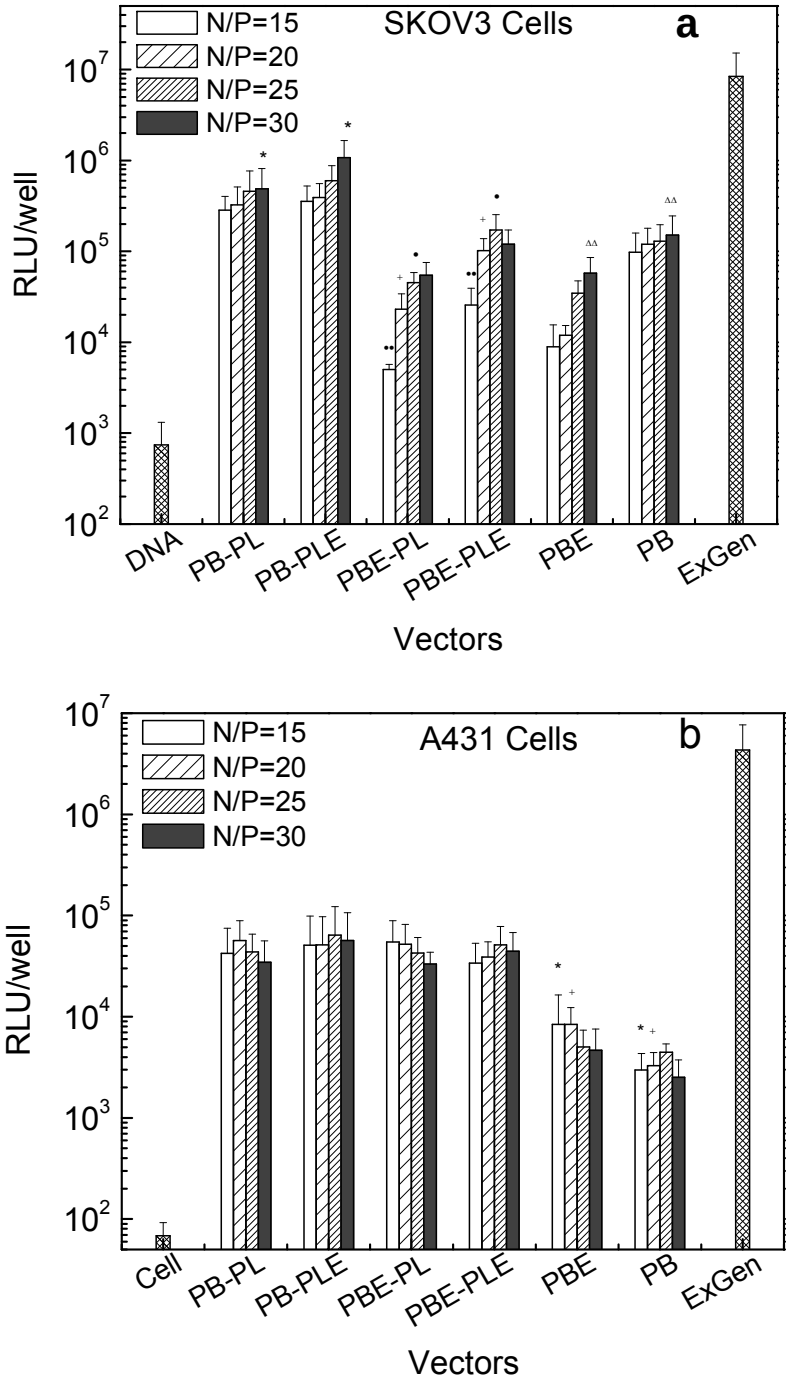


Fig. 4.6. Influence of EGF conjugation on luciferase transfection efficiency of various polymeric vectors in (a) SKOV3 and (b) A431 cells at different N/P ratios. PB-PL represents the polyplexes composed of pentablock/DNA condensate and free Pluronic F127 shield. PBE and PLE represent the EGF conjugated pentablock copolymer and Pluronic F127, respectively. Values indicate means ± standard deviations; n≥5; and symbols indicate the significant differences with p≤0.05 (single symbol) or ≤ 0.01(double symbols)

The A431 cell line is known to over-express EGF receptors (EGFR) and the incorporation of EGF in the polyplexes is expected to produce a greater effect in these cells. PB-PLE, however, did not perform the best in A431 cells as in SKOV3 cells; instead PB-PL, PB-PLE, PBE-PL, PBE-PLE lead to similar levels of gene expression. PBE performed better than PB at lower N/P ratios as opposed to the trends seen in SKOV3 Cells. Interference of EGF conjugation with DNA affinity did not seem to reduce the transfection efficiency as much as it did in SKOV3 cells. Presumably, the benefit due to the presence of EGF outweighs the loss of DNA binding affinity in the microenvironment of A431 cells, as indicated by the slight influence of N/P ratio on overall gene expression level. However, the EGF conjugated to the Pluronic shield was not able to introduce any enhancement of transfection, even with the large number of available EGFRs on the cells. There might be two reasons for this. Firstly, the PB-PL type of vectors might have a good ability to get across cell membrane by themselves, and the presence of EGF thereby did not cause any significant changes in overcoming this barrier, compared to PB type vectors. Apart from the benefits associated with charge shielding, Pluronic has been found to promote cellular uptake(31). Secondly, the amount of EGF might be not sufficient to show a significant effect. The number of EGF molecules per polyplex has been found to be crucial for efficient gene delivery(7, 32). When EGF concentration was doubled in the reaction with NHS activated Pluronic F127, the PB-PLE vector led to 3~5 fold enhancement in

transfection efficiency as compared to PB-PL in both cell types (Fig. 4.7a,b). Free EGF was added along with transfection to test whether the enhancement was due to EGF receptor mediated endocytosis. As shown in Fig. 4.7c, transfection by PB-PL was not

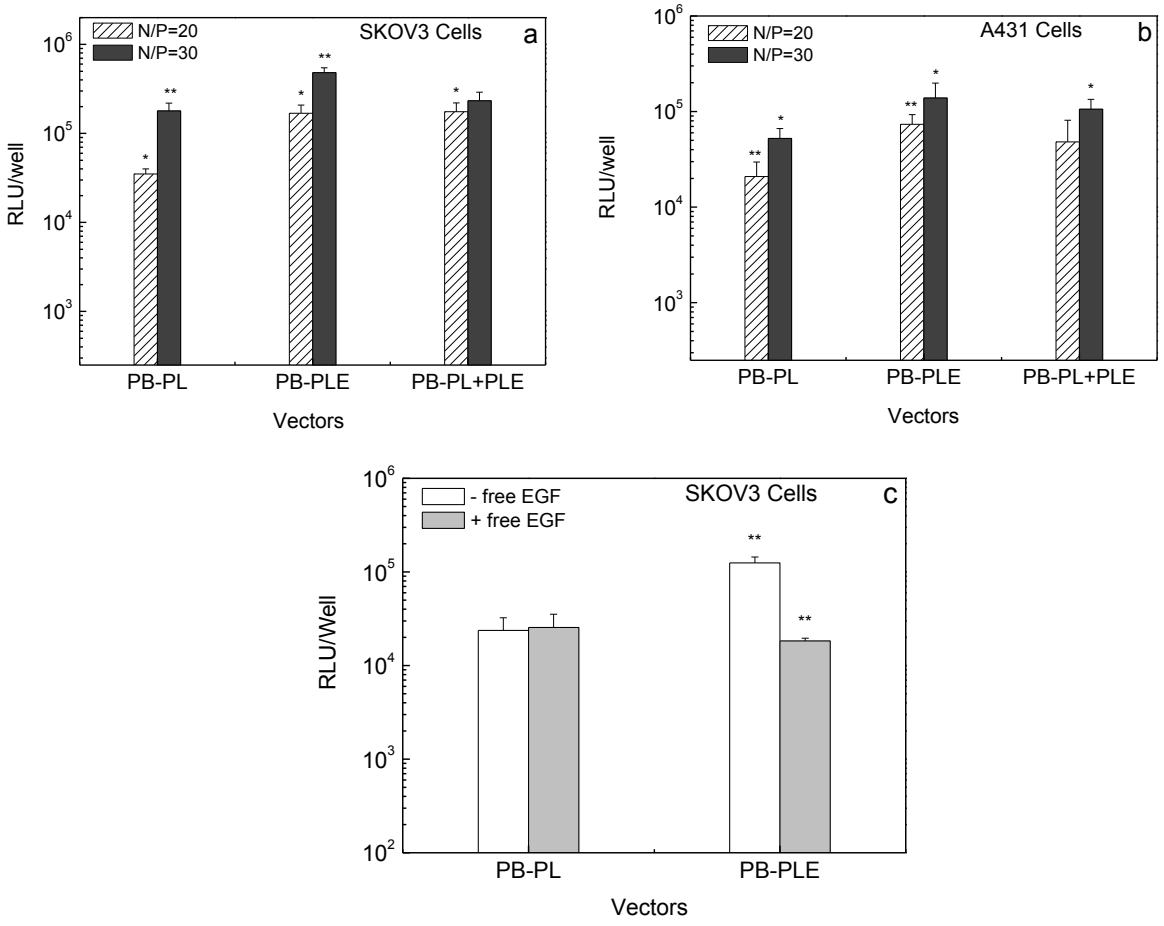


Fig. 4.7. Transfection of (a,c) SKOV3 and (b) A431 cells mediated with PB-PL type polyplexes containing high concentration of EGF. Free EGF (2μg/well) was added along with polyplexes (N/P=20) in transfection (c) as competitor to polymer-conjugated EGF. PB-PL presents the polyplexes composed of pentablock/DNA condensate and free Pluronic F127 shield. PLE represents the EGF conjugated Pluronic F127. In regard to PB-PL+PLE, the polyplex was first formulated with PB-PL as usual but using 80% of the required amount of PL, the additional 20% was made up by PLE following 10min incubation. In this manner, PLE might have a greater chance to locate on the outer surface of Pluronic shield. Values indicate means ± standard deviations (n=3), * and ** indicate the significant difference compared to PB-PL with $p \leq 0.05$ and $p \leq 0.01$, respectively.

affected by addition of exogenous EGF, whereas PB-PLE performed far less efficiently in the presence of EGF as compared to the condition without EGF competition. This confirms the involvement of EGF-EGF receptor interaction in PB-PLE mediated transfection.

Expression levels of EGFR are high in A431 (~$3\times10^6$ receptors/cell)(33) and intermediate in SKOV3 (~$1\times10^5$ receptors/cell)(20), but SKOV3 achieved 2-fold increment in transfection efficiency by vector PB-PLE at lower EGF concentration while A431 was not enhanced at all; at higher EGF concentration, SKOV3 and A431 showed similar degree of transfection improvement by PB-PLE. There seem to be other factors that could limit EGF-EGFR interaction. It has been suggested by Swell et al. that the level of EGFR was not simply associated with magnitude of ligand response(34). Frederiksen et al. also reported that overexpression of EGFR might not be a prerequisite for efficient gene delivery through receptor-mediated internalization, because of nonlinear relationship between transfection and the amount of EGFR(35). Since only 0.1~0.2% of the EGFRs in A431 are high-affinity receptors with a $K_d$ of 7 $\times10^{-11}$M(35), the affinity of EGFR might also relate to transfection efficiency and account for the present finding for A431 cells compared to SKOV3 cells. On the other hand, doubling of EGF just brought slight increase to the transfection by PB-PLE in SKOV3 cells, indicating that the level of EGF in polyplexes might have been sufficient in facilitating transfection. In particular, the position of EGF in the polyplexes played an

important role for accomplishing improvement on transfection. When PLE was added after the formation of PB-PL/DNA and formed a vector referred to as PB-PL+PLE, the resultant improvement in transfection efficiency was comparable to that achieved with PB-PLE, but the amount of PLE used in PB-PL+PLE was only 20% of that in PB-PLE. The PLE added later probably helped transfection much more than the PLE directly used as a shield agent. Since the outer surface of the polyplex potentially interacts the most with cell membrane receptors, ligands such as EGF only need to occupy this most advantageous surface to show effect on transfection efficiencies. However, the improvement in transfection efficiency was only modest at best, suggesting that cellular uptake might not be the main intracellular barrier that the pentablock copolymer vectors need to overcome.

### 4.3.3 Cellular Uptake

Flow cytometry measurements revealed that more than 95% of cells had been internalized by both PB-PL and PB-PLE type of polyplexes within 30 minute of incubation (Fig. 4.8a). After just 10 minutes of transfection, nearly all cells showed fluorescence from PB-PL type of polyplexes (data not shown). This internalization rate was much faster than linear PEI and PEGylated PEI that was reported to ferry DNA into only 10% of cells after 30 minutes of incubation, and even faster than EGF conjugated PEGylated PEI which showed an internalization in more than 80% of cells in the same time period(36). Conjugation of EGF may have increased the cellular

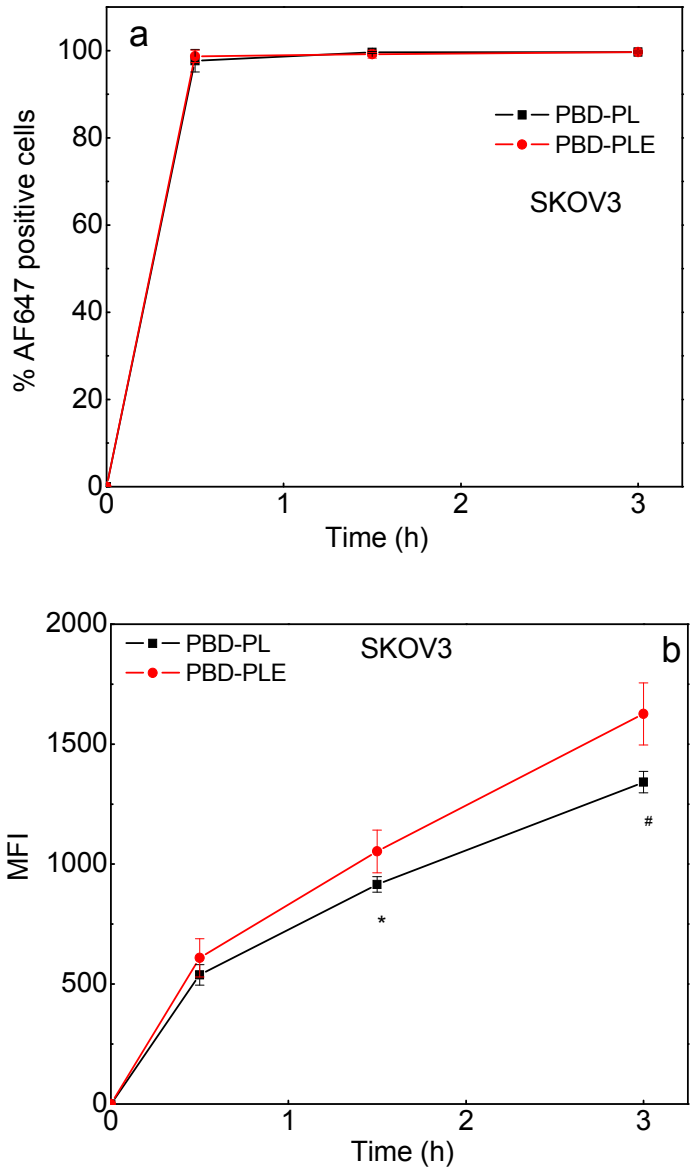


Fig. 4.8. Cellular uptake of polyplexes with and without EGF conjugation in SKOV3 cells, reflected by percentage of cells that are positive for (a) AF647 and (b) the median fluorescence intensity (MFI) per cell. Values indicate means ± standard deviations (n=3), * or # indicate significant difference between PBD-PL and PBD-PLE with $p \leq 0.05$, where PBD denotes the pentablock copolymer labeled with AF647.

internalization rate as reported in PEI systems(9, 36). However, in the pentablock copolymer vector system, polyplexes with and without EGF showed an equally fast

internalization. This result further confirmed our previous assumption that the PB-PL type of polyplexes might be inherently very efficient at passing through cell membranes. Even though functionalization with EGF made no difference to the internalization rate, it did lead to an increased internalization in the time course of transfection as shown in Fig. 4.8b. The increase in the amount of internalized polyplexes as characterized by the fluorescence intensity developed with time smoothly and ended up with a 1.2-fold enhancement at 3h transfection. Compared to other reports of 3 to 4-fold increase in internalization and up to 100-fold enhancement in transfection efficiency in EGF modified PEI systems(5, 36), the improvement in the pentablock copolymer vector system is small; however, it is in good agreement with the moderately enhanced transfection efficiency. Intracellular trafficking showed similar results for internalization of polyplexes formed with PB-PL and PB-PLE (Fig. 4.9). After quantification of over 400 cells at various regions of each sample, the count of red dots representing pentablock copolymers was found to be 91±15 per cell with EGF containing constructs as compared to 63±5 per cell with the EGF-free counterparts ($p=0.06$). In both cases, we observed no particles clearly attached to the cell membrane, which indicates that flow cytometry only measuring internalized polyplexes.

### 4.3.4 Effect of EGF in Different Systems

Considering the multiple barriers for highly efficient gene delivery, there might be

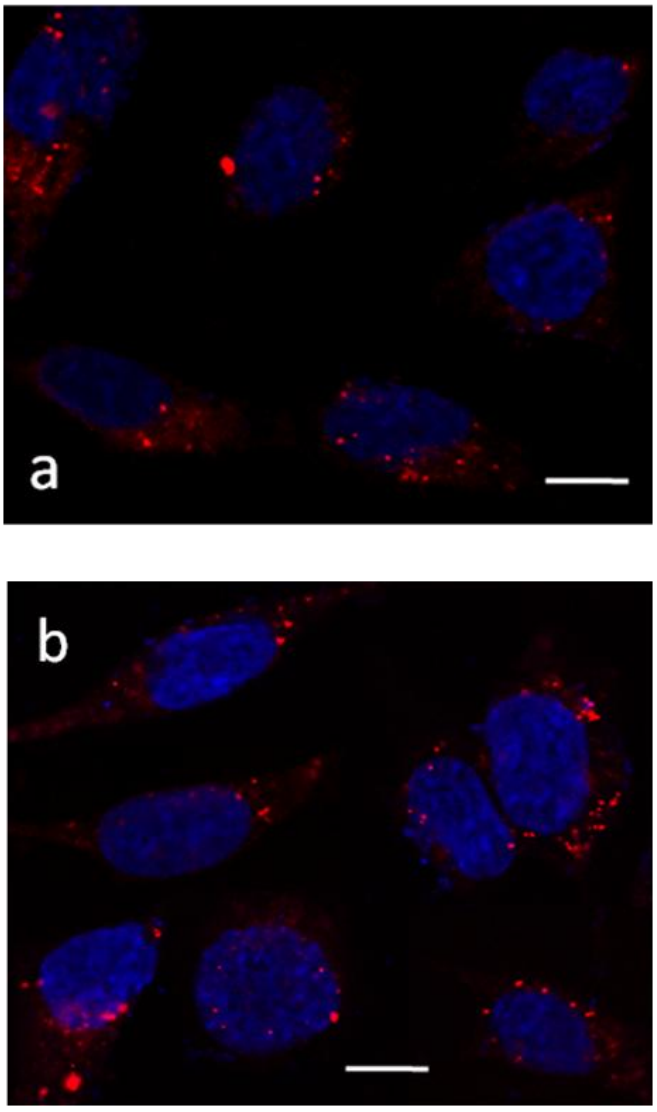


Fig. 4.9. Representative confocal images of SKOV3 cells after 3h incubation with PBD-PL/DNA (a) and PBD-PLE/DNA (b). Pentablock copolymers were labeled with AF647 (pseudo-red) and nuclei were stained with DAPI (pseudo-blue). Scale bar = 10μm.

other rate limiting steps other than cellular uptake, such as endosomal escape, DNA unpacking and nuclear localization. Overcoming a single barrier cannot necessarily guarantee the success of transfection. As it has been reported for Poly(L-lysine) (PLL) based vectors, gene delivery through EGF receptor-mediated internalization was

inefficient without the aid of endosome-releasing agents(10, 35, 37), implying that the ligand and endosomolytic agents together play an essential role in PLL mediated gene delivery. However, for vectors composed of PEI with great advantage in escaping the endosome, the incorporated EGF could make an independent contribution on increasing transfection efficiency(5-6). Thus, rate-limiting steps are specific for vectors and cell types and need to be investigated individually for each system. In our pentablock copolymer/Pluronic based vectors, the cellular uptake does not seem to be the major barrier, since the intrinsic internalization of non-EGF polyplexes was found to be very fast and the enhancement in transfection efficiency triggered by EGF was not dramatic. These results provide some insights into the intracellular barriers for transfection, and the fact that cellular entry might be more of a barrier for vectors such as PEI but not for the pentablock copolymers. This could potentially be related to the micellar structure of the copolymers, which has been shown in drug delivery studies to improve cellular entry(2). Further investigation of other potential intracellular barriers that may markedly increase the transfection efficiency by overcoming them is described in Part 2 of this manuscript.

### 4.4 Conclusions

EGF receptor mediated gene delivery was investigated with various EGF containing polyplexes on SKOV3 and A431 cells. PB-PLE exhibited the best transfection efficiency on two different tumor cell lines due to increased internalization.

However, the observed overall 3~5 fold enhancement by EGF was relatively low compared to other reports involving PEI and different polymeric vectors. This discrepancy should result from different intracellular barriers among transgene systems. Our PB-PL type of polyplexes showed an extraordinarily fast internalization, implying that cellular uptake might not be the real barrier step for this specific system, thus compromising the beneficial effect from EGF. This work provides valuable insights into the design of gene delivery vectors by changing the polymer architecture to facilitate cellular entry. Furthermore, in order to design multifunctional vectors, the corresponding barrier steps, which are usually vector and cell specific should be extensively examined and evaluated.

## Acknowledgments

We thank Dr. Mathumai Kanapathipillai for help with polymer synthesis, Paul Bisso for help with transfection and Kyle Anderson for taking AFM images. Support from the Bailey Career Development award is greatly appreciated. We would like to also acknowledge the US Department of Energy's Ames Laboratory and the US Army (W81XWH-09-1-0386) for financial support.

## References

1. A. Agarwal, R.C. Unfer, and S.K. Mallapragada. Investigation of in vitro compatibility of novel pentablock copolymers for gene delivery. Journal of Biomedical Materials Research 81A:24-39 (2007).

2. A.V. Kabanov, E.V. Batrakova, and V.Y. Alakhov. Pluronic(R) block copolymers as novel polymer therapeutics for drug and gene delivery. Journal of Controlled Release. 82:189-212 (2002).
3. B. Zhang, M. Kanapathipillai, P. Bisso, and S. Mallapragada. Novel Pentablock Copolymers for Selective Gene Delivery to Cancer Cells. Pharmaceutical Research. 26:700-713 (2009).
4. C.R. Savage, Jr., T. Inagami, and S. Cohen. The Primary Structure of Epidermal Growth Factor. J Biol Chem. 247:7612-7621 (1972).
5. T. Blessing, M. Kursa, R. Holzhauser, R. Kircheis, and E. Wagner. Different Strategies for Formation of PEGylated EGF-Conjugated PEI/DNA Complexes for Targeted Gene Delivery. Bioconjugate Chem. 12:529-537 (2001).
6. M. Ogris, G. Walker, T. Blessing, R. Kircheis, M. Wolschek, and E. Wagner. Tumor-targeted gene therapy: strategies for the preparation of ligand-polyethylene glycol-polyethylenimine/DNA complexes. Journal of Controlled Release. 91:173-181 (2003).
7. H. Lee, T.H. Kim, and T.G. Park. A receptor-mediated gene delivery system using streptavidin and biotin-derivatized, pegylated epidermal growth factor. Journal of Controlled Release. 83:109-119 (2002).
8. M.F. Wolschek, C. Thallinger, M. Kursa, V. Rössler, M. Allen, C. Lichtenberger, R. Kircheis, T. Lucas, M. Willheim, W. Reinisch, A. Gangl, E. Wagner, and B. Jansen. Specific systemic nonviral gene delivery to human hepatocellular carcinoma xenografts in SCID mice. Hepatology. 36:1106-1114 (2002).
9. K. von Gersdorff, M. Ogris, and E. Wagner. Cryoconserved shielded and EGF receptor targeted DNA polyplexes: cellular mechanisms. European Journal of Pharmaceutics and Biopharmaceutics. 60:279-285 (2005).
10. T.K.W. Lee, J.S. Han, S.T. Fan, Z.D. Liang, P.K. Tian, J.R. Gu, and I.O.L. Ng. Gene delivery using a receptor-mediated gene transfer system targeted to hepatocellular carcinoma cells. International Journal of Cancer. 93:393-400 (2001).
11. D.V. Schaffer, N.A. Fidelman, N. Dan, and D.A. Lauffenburger. Vector unpacking as a potential barrier for receptor-mediated polyplex gene delivery. Biotechnology and Bioengineering. 67:598-606 (2000).
12. A. Agarwal, R. Vilensky, A. Stockdale, Y. Talmon, R.C. Unfer, and S.K. Mallapragada. Colloidally stable novel copolymeric system for gene delivery in complete growth media. Journal of Controlled Release. 121:28-37 (2007).
13. J.W. Hong, J.H. Park, K.M. Huh, H. Chung, I.C. Kwon, and S.Y. Jeong. PEGylated polyethylenimine for in vivo local gene delivery based on lipiodolized emulsion system. Journal of Controlled Release. 99:167-176 (2004).
14. N.M. Moore, C.L. Sheppard, and S.E. Sakiyama-Elbert. Characterization of a multifunctional PEG-based gene delivery system containing nuclear localization signals and endosomal escape peptides. Acta Biomater. 5:854-864 (2009).
15. C.p. Chen, J.s. Kim, D. Liu, G.R. Rettig, M.A. McAnuff, M.E. Martin, and K.G. Rice. Synthetic PEGylated Glycoproteins and Their Utility in Gene Delivery. Bioconjugate Chem (2007).

16. F.J. Verbaan, C. Oussoren, C.J. Snel, D.J.A. Crommelin, W.E. Hennink, and G. Storm. Steric stabilization of poly(2-(dimethylamino)ethyl methacrylate)-based polyplexes mediates prolonged circulation and tumor targeting in mice. The Journal of Gene Medicine. 6:64-75 (2004).
17. S. Fukushima, K. Miyata, N. Nishiyama, N. Kanayama, Y. Yamasaki, and K. Kataoka. PEGylated Polyplex Micelles from Triblock Catiomers with Spatially Ordered Layering of Condensed pDNA and Buffering Units for Enhanced Intracellular Gene Delivery. J Am Chem Soc. 127:2810-2811 (2005).
18. M.D. Determan, J.P. Cox, S. Seifert, P. Thiyagarajan, and S.K. Mallapragada. Synthesis and characterization of temperature and pH-responsive pentablock copolymers. Polymer. 46:6933-6946 (2005).
19. J.W. Park, H. Mok, and T.G. Park. Epidermal growth factor (EGF) receptor targeted delivery of PEGylated adenovirus. Biochemical and Biophysical Research Communications. 366:769-774 (2008).
20. J.-H. Choi, K.-C. Choi, N. Auersperg, and P.C.K. Leung. Gonadotropins Activate Proteolysis and Increase Invasion through Protein Kinase A and Phosphatidylinositol 3-Kinase Pathways in Human Epithelial Ovarian Cancer Cells. Cancer Res. 66:3912-3920 (2006).
21. J.F. Lutz, H.G. Borner, and K. Weichenhan. Combining atom transfer radical polymerization and click chemistry: A versatile method for the preparation of end-functional polymers. Macromolecular Rapid Communications. 26:514-518 (2005).
22. F.Q. Zeng, H. Lee, and C. Allen. Epidermal growth factor-conjugated poly(ethylene glycol)-block-poly(delta-valerolactone) copolymer micelles for targeted delivery of chemotherapeutics. Bioconjugate Chemistry. 17:399-409 (2006).
23. D. Bali, L. King, and S. Kim. Syntheses of new gramicidin A derivatives. Aust J Chem. 56:293-300 (2003).
24. R. Kircheis, L. Wightman, A. Schreiber, B. Robitza, V. Rossler, M. Kursa, and E. Wagner. Polyethylenimine/DNA complexes shielded by transferrin target gene expression to tumors after systemic application. Gene Therapy. 8:28-40 (2001).
25. M. Kursa, G.F. Walker, V. Roessler, M. Ogris, W. Roedl, R. Kircheis, and E. Wagner. Novel Shielded Transferrin-Polyethylene Glycol-Polyethylenimine/DNA Complexes for Systemic Tumor-Targeted Gene Transfer. Bioconjugate Chem. 14:222-231 (2003).
26. H.J.P. Ryser. A membrane effect of basic polymers dependent on molecular size. Nature. 215:934-& (1967).
27. S. Boeckle, K. von Gersdorff, S. van der Piepen, C. Culmsee, E. Wagner, and M. Ogris. Purification of polyethylenimine polyplexes highlights the role of free polycations in gene transfer. Journal of Gene Medicine. 6:1102-1111 (2004).
28. S. Danielsen, K.M. Varum, and B.T. Stokke. Structural Analysis of Chitosan Mediated DNA Condensation by AFM: Influence of Chitosan Molecular Parameters. Biomacromolecules. 5:928-936 (2004).
29. Y.T.A. Chim, J.K.W. Lam, Y. Ma, S.P. Armes, A.L. Lewis, C.J. Roberts, S. Stolnik, S.J.B.

Tendler, and M.C. Davies. Structural Study of DNA Condensation Induced by Novel Phosphorylcholine-Based Copolymers for Gene Delivery and Relevance to DNA Protection. Langmuir. 21:3591-3598 (2005).

30. G.A. Rao, R. Tsai, D. Roura, and J.A. Hughes. Evaluation of the transfection property of a peptide ligand for the fibroblast growth factor receptor as part of PEGylated polyethylenimine polyplex. J Drug Target. 16:79-89 (2008).
31. Z. Yang, G. Sahay, S. Sriadibhatla, and A.V. Kabanov. Amphiphilic Block Copolymers Enhance Cellular Uptake and Nuclear Entry of Polyplex-Delivered DNA. Bioconjugate Chemistry. 19:1987-1994 (2008).
32. B. Xu, S. Wiehle, J.A. Roth, and R.J. Cristiano. The contribution of poly-L-lysine, epidermal growth factor and streptavidin to EGF/PLL/DNA polyplex formation. Gene Therapy. 5:1235-1243 (1998).
33. H. Haigler, J.F. Ash, S.J. Singer, and S. Cohen. Visualization by fluorescence of binding and internalization of epidermal growth-factor in human carcinoma cells A-431. Proceedings of the National Academy of Sciences of the United States of America. 75:3317-3321 (1978).
34. J.M. Sewell, K.G. Macleod, A. Ritchie, J.F. Smyth, and S.P. Langdon. Targeting the EGF receptor in ovarian cancer with the tyrosine kinase inhibitor ZD 1839 (/`Iressa/'). Br J Cancer. 86:456-462 (2002).
35. K.S. Frederiksen, N. Abrahamsen, R.J. Cristiano, L. Damstrup, and H.S. Poulsen. Gene delivery by an epidermal growth factor/DNA polyplex to small cell lung cancer cell lines expressing low levels of epidermal growth factor receptor. Cancer Gene Ther. 7:262-268 (2000).
36. K. de Bruin, N. Ruthardt, K. von Gersdorff, R. Bausinger, E. Wagner, M. Ogris, and C. Brauchle. Cellular dynamics of EGF receptor-targeted synthetic viruses. Molecular Therapy. 15:1297-1305 (2007).
37. D. Deshpande, D. ToledoVelasquez, D. Thakkar, W.W. Liang, and Y. Rojanasakul. Enhanced cellular uptake of oligonucleotides by EGF receptor-mediated endocytosis in A549 cells. Pharmaceutical Research. 13:57-61 (1996).

# CHAPTER 5. THE MECHANISM OF SELECTIVE TRANSFECTION MEDIATED BY PENTABLOCK COPOLYMERS; PART II: NUCLEAR ENTRY AND ENDOSOMAL ESCAPE

Modified from a paper submitted to Acta Biomaterialia, 2011, 7:1580-1587

Bingqi Zhang and Surya Mallapragada

## Abstract

Transfection efficiencies of non-viral gene delivery vectors commonly vary with cell type, due to differences in proliferation rates and intracellular characteristics. Our previous work has demonstrated that the poly(diethylaminoethylmethacrylate) (PDEAEM)/Pluronic F127 pentablock copolymers exhibit transfection *in vitro* selectively in cancer cell lines as opposed to non-cancerous cell lines. This study continues the investigation of intracellular barriers to transfection using this vector in "normal" and cancer cell lines to understand the underlying mechanisms of the selectivity. Results from part I of this investigation showed, using conjugated epidermal growth factor (EGF), that cellular uptake of these polyplexes is not a major barrier in these systems. In part II of this work, we continue investigation into the other potential intracellular barriers, endosomal escape and nuclear entry, using a lysosomotropic agent chloroquine (CLQ), and a nuclear localization signal (NLS)

SV40 respectively. Lack of effectiveness of NLS peptide in improving the transfection efficiency suggests that nuclear uptake might not be the major intracellular barrier using the pentablock copolymer vectors, or that the nuclear transport might not be primarily achieved through nuclear pores. However, inclusion of CLQ led to a dramatic enhancement in the level of gene expression, with almost two orders of magnitude increase in expression seen in normal cell lines, compared to that the increase observed in cancer cell lines. The different lysosomal pH values in normal versus cancer cells was believed to cause the pentablock copolymer vectors to behave distinctly during transport through endocytic pathways, with greater loss of functional DNA occurring in normal cells containing more acidic endocytic vesicles in contrast to cancer cells with less acidic vesicles. Interestingly, CLQ introduced almost no enhancement in the transfection with the control vector ExGen that lacked selectivity of transfection. Exploiting intracellular differences between normal and cancer cells for gene delivery vector design offers a new paradigm to achieve transfection selectivity based on intracellular differences rather than conventional approaches involving vector modification using specific ligands for targeted delivery.

## 5.1 Introduction

Cell physiology may affect the intracellular trafficking of non-viral vectors, leading to cell type specific transfection efficiency(1-2). However, there might be similarities in

transfection profiles of cells that can be grouped into the same category based on shared specific characteristics that could be involved in the process of gene delivery; for example, polarized cells vs. non-polarized cells, and endothelial vs. epithelial cells(3). Therefore the differences in these influencing characteristics among cell categories could be utilized to design cellular and/or subcellular targeting transgene vectors. The most frequently used “difference” comes from cell membranes containing various receptors, such as the epidermal growth factor (EGF) receptors and folate receptors, which make it possible to achieve selectivity between specific receptor over-expressing cells and non-overexpressing counterparts via receptor-mediated endocytosis. However, the goal of achieving desired selectivity implies selective gene expression in cells of interest, rather than the selective gene uptake by those cells. Although many researchers have reported selective transfection based on ligand-receptor aided cellular entry, this works only if the cellular entry is the barrier to transfection. However, gene delivery is a complex process and following the cellular entry, there are several potential barriers to overcome, such as endosomal escape(4-7), efficient protection for DNA(8), trafficking in the cytoplasm(9), nuclear uptake and vector unpacking (10-11). Efforts to improve transfection efficiency and selectivity need to be based on a detailed identification of rate limiting barriers to the specific gene delivery system(10).

We have shown earlier that the poly(diethylaminoethylmethacrylate) (PDEAEM)

/Pluronic F127 pentablock copolymers developed in our group possesses natural selectivity for transfecting cancerous cell lines versus non-cancerous cell lines, and this selectivity was assumed to be correlated with cell proliferation rate and other cellular characteristics that may affect the gene delivery(12). Identifying the rate limiting step(s) and intracellular barriers in gene delivery is important for understanding the mechanism and perfecting the vector design. For the pentablock copolymer and Pluronic system, we have observed a positive effect of increasing cellular uptake on the overall gene expression by incorporating EGF, but the small 3~5 fold enhancement in transfection and lack of differences in cellular uptake rates suggest that cellular entry might not be the rate limiting step(13). The micellar structure of the polymer probably makes it already very accessible to the cell membrane(14), thus minimizing the role of a cellular uptake facilitator such as EGF. In this work, we investigated two other possible barriers for the gene delivery mediated by this pentablock copolymer, namely nuclear uptake and endosomal escape. By comparing the effects of these other potential intracellular barriers in cancer and normal cell lines, we hope to elucidate the mechanism behind the selectivity of transfection.

Nuclear uptake has been considered a common barrier for gene expression, especially for slowly dividing or quiescent cells(15-17). Plasmid DNA can enter the nucleus in two ways, through nuclear pores or by sequestration on nuclear

reformation during mitosis(18). However, it was suggested that plasmid DNA does not have the ability to actively go across the nuclear envelope(19-20), unless assisted by the particular nuclear localization signals (NLS) such as SV40 NLS, the most commonly used NLS that is derived from the SV40 large T-antigen(21-23). DNA-NLS conjugates can bind to importin-α and subsequently importin-β to form a complex that mediates the interaction with the nuclear pore complex for an active nuclear import(19). Here we aim to determine the influence of incorporating SV40 NLS in the transgene vector on the transfection efficiency.

To accomplish nuclear entry, the DNA payload must first be available in the cytoplasm by escaping from the endosome before it transforms to a lysosome. Otherwise the DNA would be degraded within the lysosome or recycled back to the cell surface(6). That is why endosomal escape has been recognized as another key step in non-viral gene delivery(5-6). In the present work, we used chloroquine, a diprotic weak base known to facilitate endosomal escape(24), to examine the effect of endo/lysosomal trapping on transfection efficiency with the pentablock copolymers in cancer versus non-cancerous cell lines. The identification of the intracellular barrier(s) to transfection can allow for examination of differences in cancer and non-cancerous cell lines to understand the mechanism of selective gene expression in specific cell types.

## 5.2 Experimental

### 5.2.1 Materials

The human ovarian carcinoma SKOV3, human epidermoid carcinoma A431 and human retinal cell lines ARPE-19 were obtained from ATCC™(Manassas, VA). The human skin keratinocyte cell line HaCaT was kindly donated by Dr. Ian Schneider's Laboratory (ISU, Ames). Dulbecco's Modified Eagle Medium (DMEM), heat inactivated fetal bovine serum (FBS), 0.25% trypsin-EDTA and Hank's buffered salt saline (HBSS) were purchased from Invitrogen (Carlsbad, CA). ARPE-19 growth media Dulbecco's MEM: Ham's Nutrient Mixture F-12, 1:1 Mix (DMEM/F-12) was purchased from ATCC (Manassas, VA). Luciferase assay system and passive lysis buffer were purchased from Promega (Madison, WI). HEPES salt used to make Hepes buffered saline (HBS), chloroquine diphosphate salt, heparin, Deoxyribonuclease II (DNase II) from bovine spleen and paraformaldehyde were obtained from Sigma (St Louis, MO). SV40 NLS (PKKKRKVG) was obtained from AnaSpec (Fremont, CA). Recombinant human epidermal growth factor (EGF), Alexa Fluor®647 carboxylic acid, succinimidyl ester (written as AF647 hereafter), LysoTracker® Red DND-99, 4',6-diamidino-2-phenylindole (DAPI) dilactate and ProLong® Gold antifade reagent were purchased from Invitrogen (Carlsbad, CA). ExGen 500 was purchased from Fermentas Life Sciences (Hanover, MD). HiSpeed Plasmid Maxi Kit was obtained from Qiagen (Valencia, CA). Pluronic F127

[$(PEO)_{100}$-b-$(PPO)_{65}$-b-$(PEO)_{100}$], (where PEO represents poly(ethylene oxide) and PPO represents poly(propylene oxide)) was donated by BASF (Florham Park, NJ) and used without further modification. 6.7kb pGWIZ-luc (GeneTherapy Systems Inc, CA) plasmid encoding the luciferase reporter gene was purified with Qiagen HiSpeed Maxi Kit.

### 5.2.2 Polyplex Formation

The pentablock copolymer used in this study was synthesized by atom transfer radical polymerization and has been characterized in detail and tested for cytotoxicity as described earlier (25-26). For intracellular trafficking studies, the pentablock copolymers were labeled with AF647 according to the procedure reported elsewhere and named PBD for short(12). During the polyplex formation, all polymer solutions were prepared in 0.5× HBS buffer, pH 7.0 unless stated otherwise. Briefly, various quantities of unlabeled or labeled pentablock copolymer solution (2mg/ml) was added to plasmid DNA solution (in water) which was either pre-complexed with SV40 NLS or not, to obtain desired N/P (nitrogen/phosphate) ratios. The mixture was gently vortexed and allowed to stand at room temperature for 20 min to ensure complexation. Appropriate amount of Pluronic F127 solution (10 mg/ml) was further added to form a shield layer around the newly formed polyplexes by self-assembly. In some cases, EGF attached Pluronic F127 was used to endow the polyplexes with cell surface targeting ability. The procedure for EGF attachment is described in Part I of

this investigation(13). Four abbreviations are used: PB the pentablock copolymer alone, PBD the AF67 labeled pentablock copolymer, PBE the pentablock copolymer attached by EGF, PL Pluronic F127, PLE Pluronic F127 attached to EGF and correspondingly, PB-PL and PB-PLE refers to the pentablock copolymer with subsequently added PL and PLE, respectively.

### 5.2.3 NLS Attachment to Pluronic F127

Pluronic F127 was functionalized to be amine active through N-hydroxysuccinimide (NHS) activation following the procedure described previously(13). Due to the fact that SV40 NLS possesses multiple primary amines on a single molecule, the amount of SV40 NLS in the feed was maintained in excess in such a way that each peptide could only be reacting with a single NHS. Briefly, 10mg of NHS-activated Pluronic was added to a solution of 2mg of SV40 NLS in 1ml of PBS (pH 7.4). The mixture was stirred at room temperature for 4 hours when an additional 10 mg of NHS-Pluronic was added. After reacting for another 20h, the resultant solution was dialyzed against 0.2× PBS using Dialysis Cassette (Thermo Scientific, MW cut off 10000) for 48 h and lyophilized product was finally obtained.

### 5.2.4 Gel Retardation Assay

Polymer/DNA polyplexes with or without NLS were formed as described above. 40μl of each polyplex solution was loaded in a well for electrophoresis assay on a 1%

agarose gel with Tris-acetate (TAE) running buffer at 60V for 120 min. DNA bands were visualized with ethidium bromide staining. In testing protection ability of pentablock copolymer to DNA against nuclease, DNase II (1μl of 100unit/μl) was added to preformed polyplex solutions (containing 0.25μg DNA per sample) and incubated for 20min at 37°C, followed by additional 40min incubation at 80°C to ensure enzyme deactivation. Heparin (1μl of 100μg/μl) was then added and allowed to act for 20min to release DNA packaged in the polyplexes. About 40ul of this mixture was transferred into each well of a 1% agarose gel for electrophoresis.

### 5.2.5 Cell Culture

The SKOV3, A431 and HaCat cells were grown in DMEM supplemented with 10% (v/v) FBS at 37°C under a humidified atmosphere containing 5% $CO_2$. ARPE-19 cells were grown in DMEM/F-12 containing 10% FBS under the same conditions. All cell types were sub-cultured every 2-3 days, expect for APRE-19 which was passaged once a week.

### 5.2.6 In vitro Transfection

Cells of interest were seeded into a 96-well plate or 6-well plate with an initial density of $1.2\times10^4$ or $1.5\times10^5$ cells per well and ready for transfection in one or two days after reaching 70-80% confluence. Half an hour before transfection, the old medium was replaced with fresh growth medium containing 10% FBS with or without

100μM chloroquine. Polyplexes prepared at given N/P ratios were added to each well with 0.6μg of DNA per well for 96-well plate and 3μg DNA per well for 6-well plate. Cells were allowed to incubate for 3h when the medium containing polyplexes was replaced with fresh medium with or without chloroquine (at t=3h). The chloroquine was allowed to be in contact with cells for another 21h and removed by changing the medium (at t=24h). After 45h post-transfection (at t=48h), cells in the 96-well plates were lysed and tested for luciferase activity. The luminescence was measured in arbitrary Relative Luminescence Units (RLU) on an automated Veritas™ Microplate Luminometer. Each transfection was done in triplicate. ExGen 500, a sterile solution of linear 22 kDa polyethyleneimine (PEI), was used as a positive control at N/P ratio of 6 according to the manufacturer's protocol.

### 5.2.7 Confocal Microscopy

Cells of interest were seeded onto poly-L-lysine coated coverslips and subsequently transfected with PBD containing polyplexes following the same procedures used with the 6-well plates. At specific time points during transfection or post-transfection, cells were rinsed and incubated in the medium containing 100nM LysoTracker Red for 1h. Following that, cells were fixed with fresh 4% paraformaldehyde and then treated with 300nM DAPI in PBS for 5min. The coverslip was washed thoroughly with PBS and air dried before being mounted on the glass slide with a drop of antifade reagent in between. Confocal images were collected with

the objective of 63-er Oil / N.A. 1.4 on a Leica TCS SP5 X Supercontinuum Confocal Microscope and analyzed with MetaView software (Universal Imaging Corporation). Sequential scans were used to minimize the cross-talk between different fluorochromes. The pinhole size was automatically adjusted by the software and maintained the same during imaging.

### 5.2.8 Statistics

The data is presented as mean and standard deviation was calculated over at least three independent experiments. Significant differences between two groups were evaluated by Student's t-test with $p <= 0.05$.

## 5.3 Results and Discussion

### 5.3.1 Transfection with NLS-modified Polyplexes

NLS was incorporated in the polyplex with two strategies, electrostatic coupling to DNA, and covalently conjugation to the Pluronic shield (PL-NLS). In the latter case, the NLS was expected to assist the trafficking of polyplexes toward the nucleus, and not necessarily to help the polyplexes enter the nucleus, due to the size limit of nuclear pores. However, with both types of NLS-containing polyplexes, we observed no improvement in transfection efficiency; by contrast, a dramatic decrease in transfection efficiency at higher concentration of NLS was observed, as compared to non-NLS formulations as shown in Fig. 5.1. For the condition with NLS directly

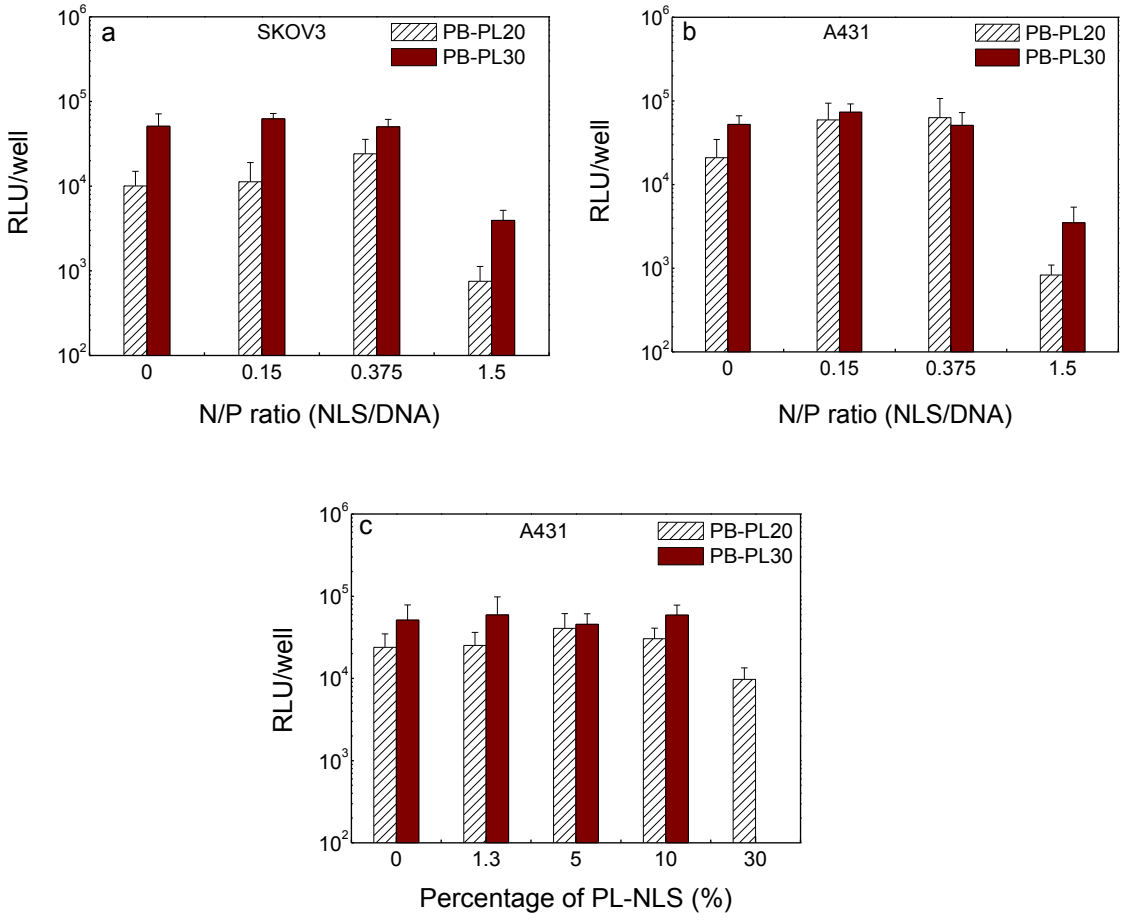


Fig. 5.1. Transfection of SKOV3 (a) and A431(b, c) cells with different types of NLS-modified polyplexes. In a and b, DNA was pre-complexed with NLS at various N/P ratios; in c, NLS was conjugated to Pluronic (PL-NLS) which was mixed with unmodified Pluronic at various amounts. PB-PL indicates that the polyplexes are composed of pentablock/DNA condensate with Pluronic F127 shield. The following number 20 or 30 denotes the N/P ratio with respect to the pentablock copolymer and DNA. Values indicate means ± standard deviations (n=3)

coupled to DNA, a large portion of DNA might stay packed in the polyplexes, thus greatly reducing the likelihood of exposing NLS to the nuclear import factors. Previous intracellular trafficking in SKOV3 cells showed that there was still a large amount of pentablock copolymer/DNA colocalization in the cytoplasm even at 21h

post-transfection(12). Once some DNA was released, the electrostatically coupled NLS could be replaced by competing proteins in the cytoplasm and not get to the nucleus. But even for vectors with NLS covalently coupled to DNA, the published results still show limited success(27-28). Since nuclear uptake could take place during cell division when cell membrane disappears, we suggest that nuclear uptake is not the bottleneck step for transfection of cancer cells using pentablock copolymer vectors. There may exist other barrier steps in the transfection process, such as endosomal escape, that block the route down to nuclear import. The significant decrease in the transfection efficiency with higher amount of NLS might be due to some of the NLS interfering with the transcription domain of the DNA(29), or the positive charges of NLS peptide weakening the stabilizing effect of Pluronic.

The same study was also conducted in normal cell lines ARPE-19 and HaCat with NLS modified vectors (some data shown in Fig. 5.2), which exhibited similar results suggesting that NLS does not improve transfection in all the different cell types studied. Thus, nuclear uptake may not be the reason for selective transfection of cancer cells over normal cells.

### 5.3.2 Effect of Chloroquine on Transfection Efficiency

Chloroquine (CLQ), a weak base that accumulates in acidic organelles such as late endosomes and lysosomes has been suggested to be able to enhance transfection efficiency of non-viral gene delivery by facilitating endosomal release and

inhibiting lysosomal enzyme activity(30). In spite of its application as a common therapeutic drug for malaria(31), CLQ is not appropriate to be applied as a transfection facilitating agent due to its toxicity at high dose levels(32). Here we used CLQ as a tool to uncover the influence of endosomal escape on the overall gene delivery with the pentablock vectors. To maintain satisfactory cell viability, CLQ was kept in growth medium only for the first 24h during transfection and post-transfection.

From the time course of gene expression, endosomal escape occurs between cellular uptake and nuclear uptake, and hence likely to compromise and even eliminate the efforts to increase gene expression through improving cellular and/or nuclear uptake. In order to test this possibility, vectors that appeared most effective in the study on EGF attachment in part I of this work(13) and NLS were included together with the unmodified formulations for transfection in the presence and absence of CLQ (Figs. 5.2a-d). The condition with CLQ showed significant transfection enhancement with the pentablock copolymer vectors in all cell types studied. In particular, the enhancement by CLQ with PB-PL based vectors was 1~2 orders of magnitude higher in non-cancerous cell lines ARPE and HaCat, as compared to cancerous cells SKOV3 and A431. For ExGen, CLQ made little difference in all cases except for HaCat in which a small 7-fold increase was observed. Similar results showing very small or negative influence of lysosomotropic agents such as CLQ on PEI mediated gene delivery were reported by others (33-35).

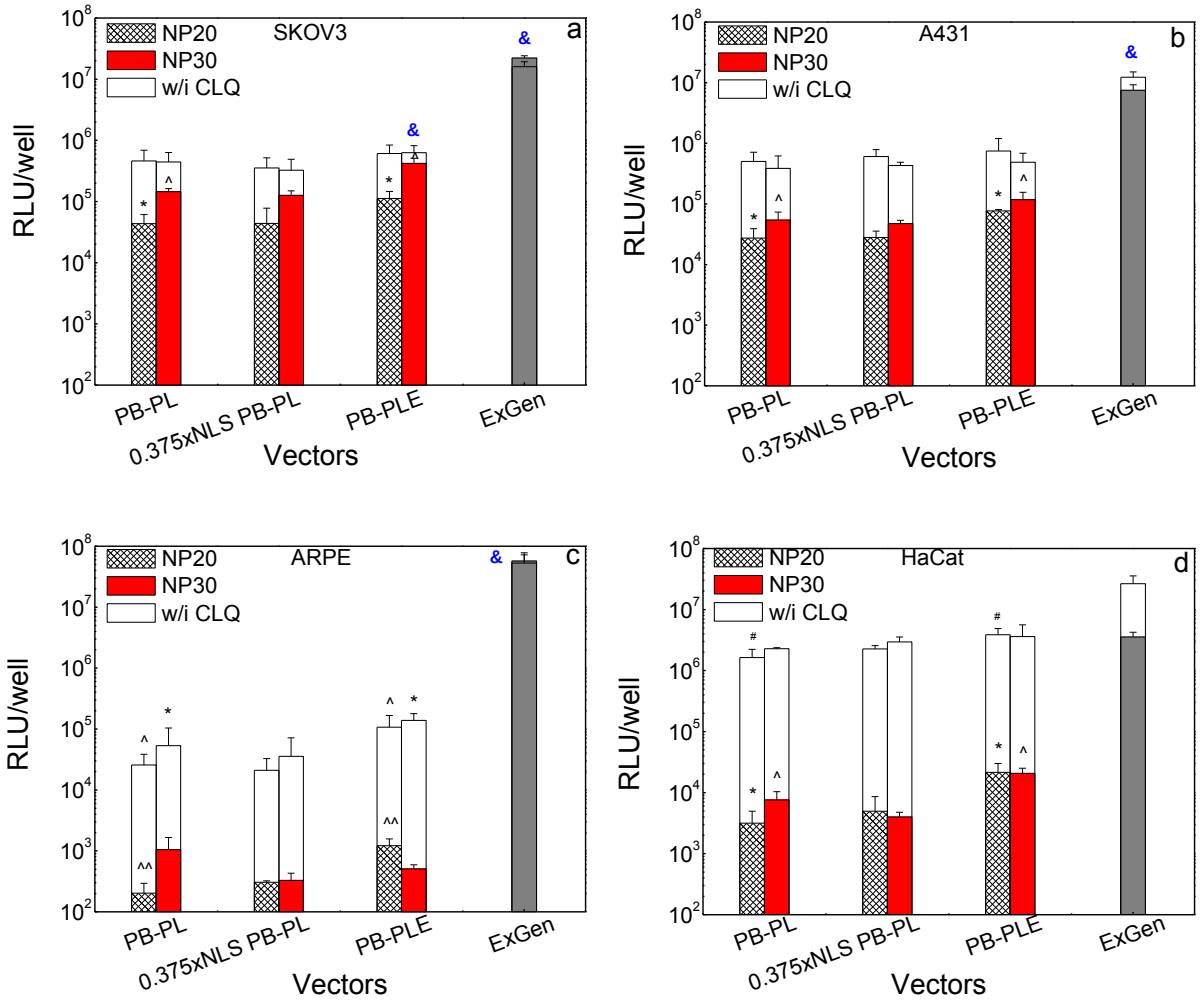


Fig. 5.2. Transfection of cancer (SKOV3, A431) (a, b) and non-cancer (ARPE, HaCat) (c, d) cell lines with unmodified polyplexes and NLS or EGF containing polyplexes in the presence (open bars) and absence (cross-hatched and filled bars) of CLQ; 0.375xNLS indicates that NLS was added at N/P ratio of 0.375 with respect to NLS and DNA. Values indicate means ± standard deviations (n=3); ^^ indicates $p<0.01$; * and ^ indicate $p<0.05$; # indicates $p<0.1$. All conditions with CLQ showed significant differences compared to conditions without CLQ except those marked with "**&**".

The evident beneficial effect from CLQ on transfection efficiency using the pentablock copolymer vectors indicates that endosomal escape and/or neutralization of lysosomal vesicles represented a significant barrier in the PB-PL based gene delivery

system, especially for non-cancerous cell lines. This result was in good agreement with our previous intracellular trafficking studies in which ARPE cells showed less nuclear uptake, as well as less pentablock copolymer and DNA colocalization, compared to SKOV3 cells(12). We hypothesized that slower proliferation rates and easier DNA degradation in ARPE cells might account for the observed difference in transfection. From the present results, failure to escape from the endolysosome, thus causing more DNA degradation could be a major issue, though inefficient nuclear uptake is still possibly related to the slower proliferation. When a large fraction of DNA is degraded in the enzyme-rich lysosomes, there would be fewer polyplexes available in the cytoplasm and even fewer that could eventually enter the nuclei. However, use of CLQ in conjunction with the NLS peptides did not lead to any enhancement in the transfection efficiency, implying that nuclear uptake is not a major intracellular barrier in this pentablock copolymer vector system. Interestingly, the use of CLQ in conjugation with EGF-attached vectors did not show any cumulative improvements in transfection compared to that achieved with either of them being used alone for SKOV3and A431 cells, but there was a slight improvement in transfection for the ARPE and HaCat cells in some of the cases. In normal cell types, ARPE and HaCat, plenty of the polyplexes internalized with the aid of EGF might have been sequestered by the endosomes, making CLQ’s effect of endosomal release more beneficial. All in all, endosomal escape seems to be the primary barrier

for both cancer and non-cancer cells, but to a much greater degree for the latter. Therefore, the selectivity we observed between the transfection of cancer and normal cells might be attributed to their diverse endo/lysosomal entrapment abilities, which in turn could result from their different intracellular pHs. As reported in literature, normal cells generally have neutral cytosolic pH around 7.2, acidic endosomal pH around 6.0 and lysosomal pH around 5.0, whereas many tumor cells have a more acidified cytosol and less acidified endo/lysosomes with both pH values being around 6.7(36). This seems to be the case for cell lines as well. Oncogene transformed 3T3 fibroblast cell lines were found to have significantly higher intralysosomal pH relative to nontransformed parental 3T3 cells(37). Although the reason for alkalinization of the lysosomal compartment has still been elusive, the elevated organelle pH in tumor cells is typically observed(38-39), which in the case of gene delivery provides a favorable environment for the transgene vector to maintain function in otherwise hostile endocytic vesicles seen in normal cells.

To verify this hypothesis, the role of pH on the ability of pentablock copolymers to protect DNA from degradation was examined with DNase II, the primary acidic endonuclease most active at pH 4.5 in lysosomal compartments. As shown in Fig. 5.3a, DNA was fully condensed and retarded by the pentablock copolymer at N/P of 20 at all three pH values investigated (lane 1, 4 and 7). The integrity of DNA released from the polyplexes showed little change with pH (lane 2, 5 and 8) as compared to

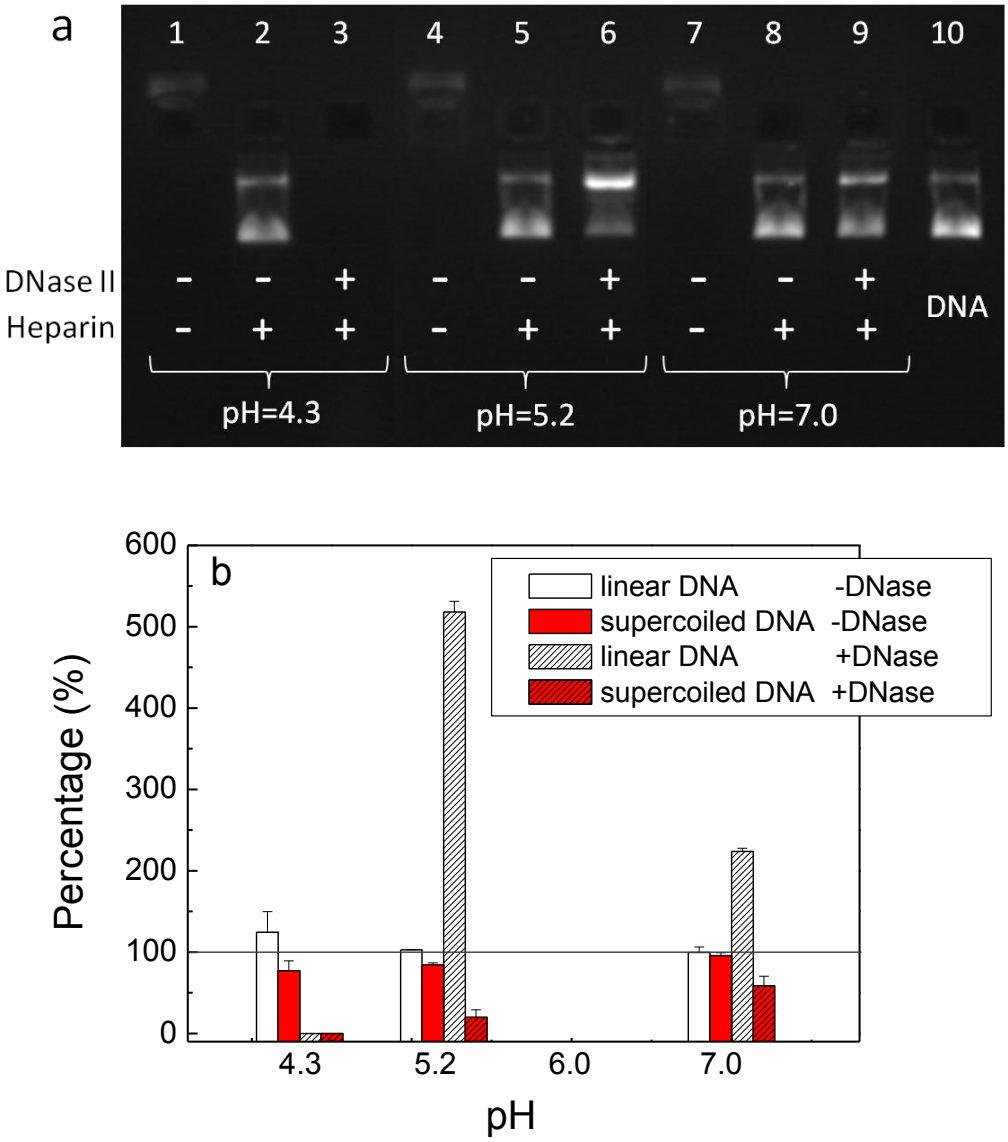


Fig. 5.3. Protection provided by pentablock copolymer to DNA against DNase II at various pH values. (a) agarose gel electrophoresis of polyplexes at N/P=20 (lane 1-9) with naked DNA (lane 10) as control; heparin was added to release DNA from the polyplex. The amount of DNA either in linear or supercoiled form released from polyplexes was quantified with respect to naked DNA and depicted in (b); results were presented as means ± SD, n=2.

naked DNA in the absence of the enzyme. However, when treated with DNase II, DNA encountered increasingly reduced protection with the pentablock copolymer as

the pH dropped from 7.0 to 4.3, with about 60% of supercoiled DNA at pH of 7.0 decreasing to 20% at pH of 5.2 and further down to zero at pH of 4.3 (Fig. 5.3b). Notably, DNase II became more detrimental to polyplexes at lower pH values, either by degrading all DNA into small fragments (lane 3) or by triggering the transformation of DNA from supercoiled structure to linear form (lane 6). The latter is known as the initial phase of the action of DNase II upon DNA substrates(40), which also occurred to some extent in the polyplex with pH of 7.0 (lane 9). Lysosomal DNase II has been identified as a significant barrier to transfection due to vector degradation upon lysosomal sequestration(41). But the barrier could be addressed by raising intralysosomal pH with lysosomotropic agents such as CLQ. On the other hand, lysosomal degradation might no longer be such a significant barrier for cells with less acidified lysosomes, such as tumor cells. That could explain the observed huge enhancements by CLQ in transfection efficiency of normal cell lines but relatively mild enhancements in cancer cell lines. In other words, the selectivity of pentablock copolymer mediated transfection between normal and cancer cells was probably due to the difference in lysosomal pH values. ExGen cannot take advantage of this pH difference to selectively transfect cell types because of its well-known proton sponge effect and other endocytosis pathways that might not involve lysosomes(42).

### 5.3.3 Visualizing the Effect of CLQ via Confocal Microscopy

CLQ penetrates and accumulates in the intracellular acidic compartments, such

as lysosomes, resulting in proton consumption and thus an increase in the flux of counterion to neutralize the membrane potential. Consequently, the intralysosomal pH may rise from 4.0~4.5 to over 6.0 as the alkalinizing action progresses(37, 43), which falls out of the pH range for most lysosomal enzymes to function(32), thereby protecting the entrapped contents. In the meantime, lysosomes might grow in volume and even end up rupturing due to the continual swelling under osmotic pressure(44). As shown in Fig. 5.4, cells transfected in the presence of CLQ showed obviously larger volume of endo/lysosomes (Fig. 5.4b, d) relative to the condition without CLQ (Fig. 5.4a, c), indicating the accumulation and disruption of CLQ in these acidic vesicles. Some vesicles achieved really impressive swelling shown by the arrows especially in SKOV3 cells. With increased osmotic pressure, these swollen vesicles might consequently rupture and lose their shapes, as seen for the most cases in HaCat cells with a lower lysosomal pH. As a result, the encapsulated polyplexes were released and became available in the cytoplasm, which can be characterized by less colocalization of pentablock copolymers and endo/lysosomes. In the absence of CLQ, we can clearly see that most of the polyplexes were separated from the endo/lysosomes of SKOV3 cells (Fig. 5.4a). By contrast, most of them were trapped in the vesicles of HaCat cells (Fig. 5.4c). With CLQ added to neutralize the acidic vesicles, a dramatically large number of polyplexes became available outside of the

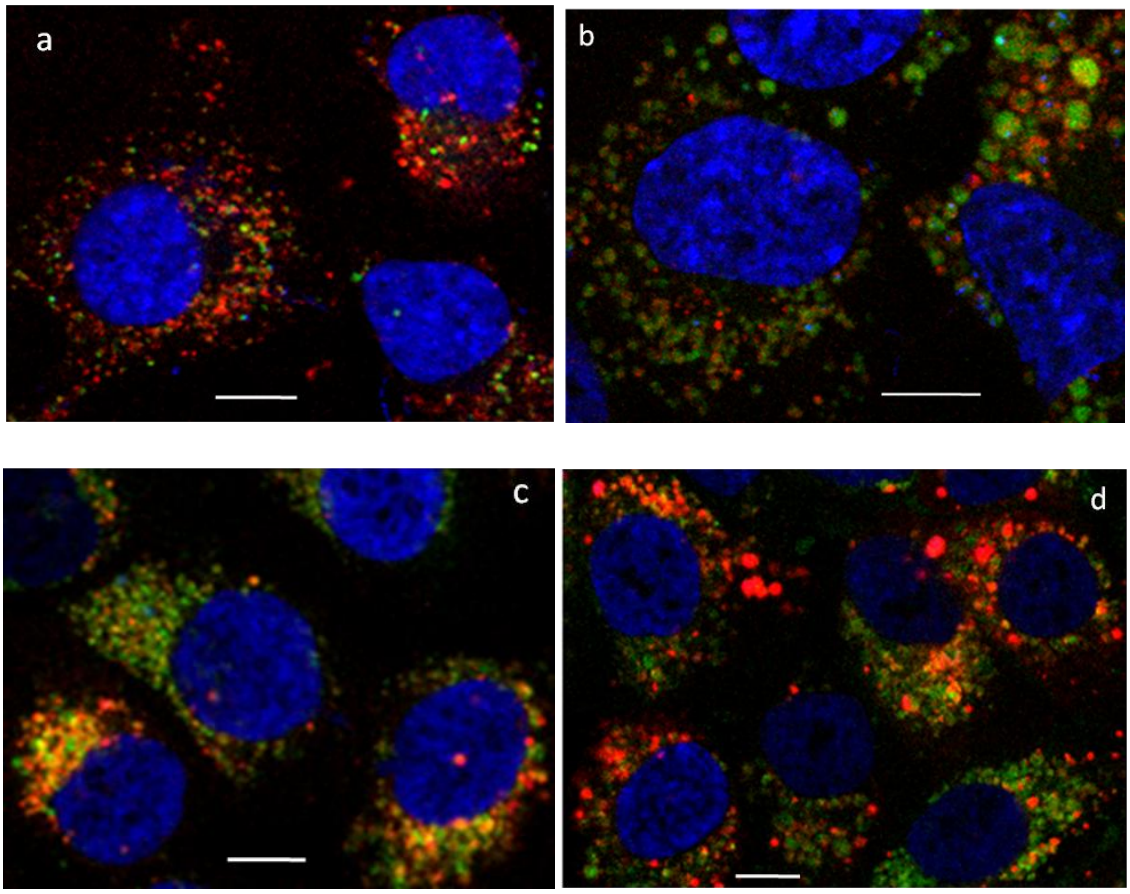


Fig. 5.4. Confocal images of SKOV3 (a, b) and HaCat (c, d) cells at 8h post-tranfection in the absence (a, c) and presence (b, d) of CLQ. Polyplexes were removed by changing media after 3h transfection. The colors green, red and blue were assigned to endo/lysosomes stained with LysoTracker Red, pentablock copolymers labeled with AF647, and nuclei stained with DAPI, respectively. Scale bar = 10μm

endo/lysosomes of HaCat cells (Fig. 5.4d). But in SKOV3 cells, the addition of CLQ did not release a huge number of additional polyplexes (Fig. 5.4b). These results align well with the differences observed in transfection efficiencies. Thus far, the differences observed due to the effect of CLQ addition in cancer and non-cancer cells suggest endosomal escape as a transfection barrier to significantly different extents

for the two cell types, which explains the selective transfection in cancer cells with pentablock copolymer vectors as seen earlier. It is difficult to obtain any information about how CLQ affected the amount or integrity of DNA from the images. Further studies will be conducted on this subject with both lysosome and DNA labeled.

### 5.3.4 Effect of Ammonium Chloride versus CLQ on Transfection Efficiency

To further confirm that the contribution of CLQ to the transfection enhancement was by removing the polyplexes from the digestive endocytic route, we replaced CLQ with ammonium chloride ($NH_4Cl$), another lysosomotropic agent (45), to examine if $NH_4Cl$ can lead to the similar enhancement as CLQ. As shown in Fig. 5.5, the addition of $NH_4Cl$ introduced certain increase in PB-PL based transfection for both cell types, especially at higher concentrations, with more intense effect in normal cell type HaCat vs. cancer cell type SKOV3, which further supports the notion that endosomal escape is the major barrier using the pentablock copolymers and is responsible for the selective transfection of cancer cells with pentablock copolymer vectors. Yet, $NH_4Cl$ addition resulted in an obviously smaller enhancement in transfection relative to CLQ even though they were expected to perform the same way in terms of disrupting endo/lysosomes. A direct reason might lie in the physiochemical properties of the two weak bases. CLQ probably has greater ability of inhibiting acidification than $NH_4Cl$; it has been reported that CLQ raised the environmental pH from 5.7 to 8.4 as compared to the neutral pH achieved with

$NH_4Cl$(46).

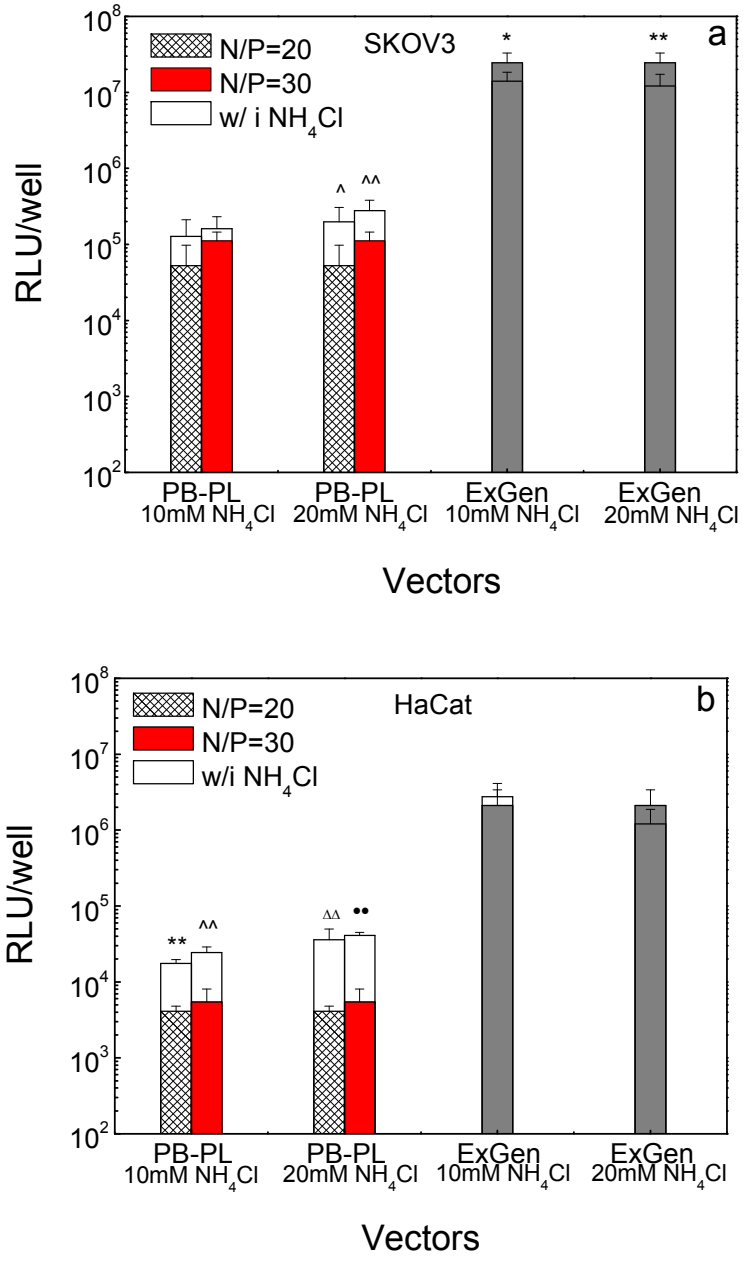


Fig. 5.5. Transfection of PB-PL based polyplexes and ExGen in the presence (open bars, indicated by w/i $NH_4Cl$) and absence (cross-hatched and filled bars) of $NH_4Cl$ on SKOV3 (a) and HaCat (b) cells at two N/P ratios. Values indicate means ± standard deviations (n=3); symbols indicate the significant differences between conditions with and without CLQ; p≤0.05 (single symbol) or ≤ 0.01(double symbols).

Besides disrupting endo/lysosomes, CLQ has been reported to be able to facilitate polyplex unpacking(46), due to its ability to bind DNA either by its intrinsic quinoleic moiety or by the positive charges after protonation. Thus, in addition to endosomal escape, CLQ triggering polyplex unpacking might be another reason for its dramatic and selective improvement in transfection. If differences in polyplex unpackaging are contributing to differences in transfection efficiencies between normal and cancer cells, the pH differences between normal and cancer cells should lead to differences in unpacking. However, agarose gel electrophoresis (Fig. 5.6) showed visible variance of DNA mobility with pH only at N/P ratios below 0.3, suggesting the polymer cannot compact DNA effectively at such low N/P ratios, leading to more unpacking at higher pH. At N/P ratios of 0.5 or higher (the

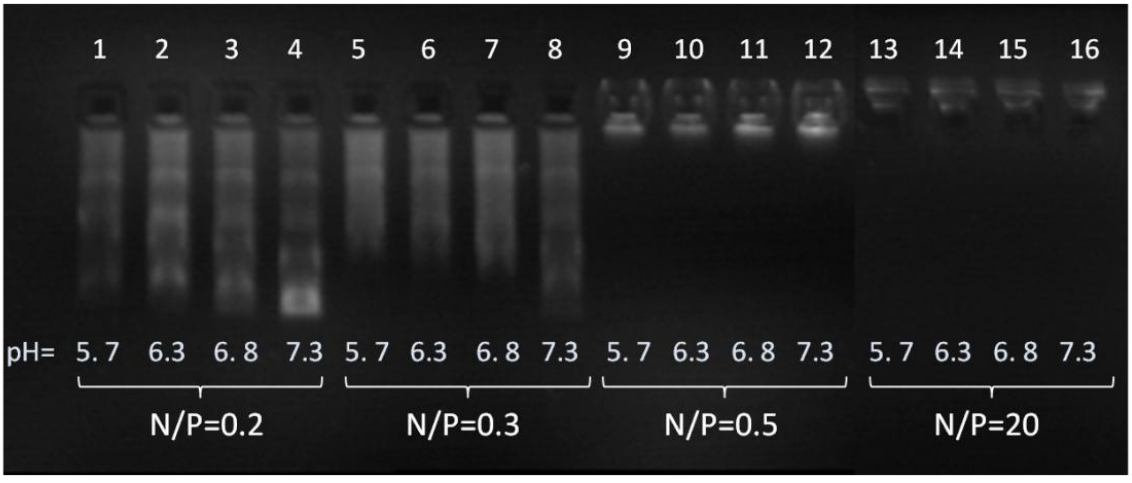


Fig. 5.6. Differences in complexation of pentablock copolymer/DNA polyplexes at different pH values and at various N/P ratios. Polyplexes were formed at 0.5x HBS buffer, pH=7 and then incubated in sodium phosphate/citric acid buffers of various pH values for 6h at 37ºC before being loaded on 1% agarose gel for electrophoresis.

transfection studies were conducted at N/P ratio of 20), pH changes did not show any effect on polyplex dissociation. Therefore, we do not expect any significant differences in unpacking of polyplexes, in normal and cancer cells due to intracellular pH differences. So even though unpacking might be a possible mechanism for CLQ enhanced transfection(47), it is probably not the reason for the selective transfection in cancer cells observed with the pentablock copolymer vectors. Therefore, we propose that the differences in pH of lysosomes played an essential role in determining transfection efficiency in pentablock copolymer mediated gene delivery in cancer cells versus normal cells. Other possible barriers such as cellular uptake and nuclear localization were found not to be as limiting as release from endocytic vesicles, when using the pentablock copolymers as vectors.

## 5.4 Conclusions

In an effort to elucidate the mechanism underlying the selective transfection between non-cancer and cancer cells mediated by the pentablock copolymer vectors but not ExGen vectors, we tested various intracellular barriers that might affect gene transfer efficiency. We conclude that escape from the endocytic pathway served as the primary intracellular barrier for pentablock copolymer-mediated transfection, whereas ExGen was not limited by this process because it facilitates endosomal escape. This, in turn, provides insights into differences in transfection efficiencies in cancer and normal cells using the pentablock copolymers because of intracellular pH

differences in the two cell types. Pentablock copolymer/DNA vectors could have been, in large part, sequestered and degraded in acidic lysosomes of non-cancer cells, but survived and maintained function in less acidic lysosomes of cancer cells. This property could be taken advantage of to design vectors selectively transfecting cells with higher lysosomal pH, such as many tumor cells. The present work highlights the importance of identifying intracellular barriers for different gene delivery systems involving vectors and cells and provides a new paradigm for designing targeting vectors based on intracellular differences between cell types, rather than through the use of targeting ligands.

## Acknowledgments

We would like to acknowledge the US Department of Energy's Ames Laboratory and the US Army (W81XWH1010806) for financial support.

## References

1. K.L. Douglas, C.A. Piccirillo, and M. Tabrizian. Cell line-dependent internalization pathways and intracellular trafficking determine transfection efficiency of nanoparticle vectors. European Journal of Pharmaceutics and Biopharmaceutics. 68:676-687 (2008).
2. S.S. Rajan, H.Y. Liu, and T.Q. Vu. Ligand-bound quantum dot probes for studying the molecular scale dynamics of receptor endocytic trafficking in live cells. ACS Nano. 2:1153-1166 (2008).
3. P. Midoux, G. Breuzard, J.P. Gomez, and C. Pichon. Polymer-Based Gene Delivery: A Current Review on the Uptake and Intracellular Trafficking of Polyplexes. Curr Gene Ther. 8:335-352 (2008).

4. R.J. Cristianoand J.A. Roth. Epidermal growth factor mediated DNA delivery into lung cancer cells via the epidermal growth factor receptor. Cancer Gene Ther. 3:4-10 (1996).
5. M. Cotten, E. Wagner, K. Zatloukal, S. Phillips, D.T. Curiel, and M.L. Birnstiel. High-efficiency receptor-mediated delivery of small and large (48 kilobase gene constructs using the endosome-disruption activity of defective or chemically inactivated adenovirus particles. Proceedings of the National Academy of Sciences of the United States of America. 89:6094-6098 (1992).
6. N.M. Moore, C.L. Sheppard, T.R. Barbour, and S.E. Sakiyama-Elbert. The effect of endosomal escape peptides on in vitro gene delivery of polyethylene glycol-based vehicles. Journal of Gene Medicine. 10:1134-1149 (2008).
7. A. El-Sayed, T. Masuda, I. Khalil, H. Akita, and H. Harashima. Enhanced gene expression by a novel stearylated INF7 peptide derivative through fusion independent endosomal escape. Journal of Controlled Release. 138:160-167 (2009).
8. K.D. Murray, C.J. Etheridge, S.I. Shah, D.A. Matthews, W. Russell, H.M.D. Gurling, and A.D. Miller. Enhanced cationic liposome-mediated transfection using the DNA-binding peptide mu (mu) from the adenovirus core. Gene Therapy. 8:453-460 (2001).
9. G.L. Lukacs, P. Haggie, O. Seksek, D. Lechardeur, N. Freedman, and A.S. Verkman. Size-dependent DNA mobility in cytoplasm and nucleus. Journal of Biological Chemistry. 275:1625-1629 (2000).
10. D.V. Schaffer, N.A. Fidelman, N. Dan, and D.A. Lauffenburger. Vector unpacking as a potential barrier for receptor-mediated polyplex gene delivery. Biotechnology and Bioengineering. 67:598-606 (2000).
11. M.E. Davis. Non-viral gene delivery systems. Current Opinion in Biotechnology. 13:128-131 (2002).
12. B. Zhang, M. Kanapathipillai, P. Bisso, and S. Mallapragada. Novel Pentablock Copolymers for Selective Gene Delivery to Cancer Cells. Pharmaceutical Research. 26:700-713 (2009).
13. B. Zhangand S. Mallapragada. The mechanism of selective transfection mediated by pentablock copolymers; Part II: nuclear entry and endosomal escape. revision submitted to Acta Biomaterialia.
14. A.V. Kabanov, E.V. Batrakova, and V.Y. Alakhov. Pluronic(R) block copolymers as novel polymer therapeutics for drug and gene delivery. Journal of Controlled Release. 82:189-212 (2002).
15. M.E. Dowty, P. Williams, G.F. Zhang, J.E. Hagstrom, and J.A. Wolff. Plasmid DNA entry into postmitotic nuclei of primary rat myotubes. Proceedings of the National Academy of Sciences

of the United States of America. 92:4572-4576 (1995).

16. Zabner J, Fasbender A J, Moninger T, et al. Cellular and molecular barriers to gene transfer by a cationic lipid. Journal of Biological Chemistry. 270:18997-19007 (1995).
17. C.W. Pouton, K.M. Wagstaff, D.M. Roth, G.W. Moseley, and D.A. Jans. Targeted delivery to the nucleus. Advanced Drug Delivery Reviews. 59:698-717 (2007).
18. D. Putnam. Polymers for gene delivery across length scales. Nat Mater. 5:439-451 (2006).
19. M. Belting, S. Sandgren, and A. Wittrup. Nuclear delivery of macromolecules: barriers and carriers. Advanced Drug Delivery Reviews. 57:505-527 (2005).
20. V. Escriou, M. Carriere, D. Scherman, and P. Wils. NLS bioconjugates for targeting therapeutic genes to the nucleus. Advanced Drug Delivery Reviews. 55:295-306 (2003).
21. D.A. Dean. Import of plasmid DNA into the nucleus is sequence specific. Exp Cell Res. 230:293-302 (1997).
22. G.L. Wilson, B.S. Dean, G. Wang, and D.A. Dean. Nuclear import of plasmid DNA in digitonin-permeabilized cells requires both cytoplasmic factors and specific DNA sequences. Journal of Biological Chemistry. 274:22025-22032 (1999).
23. A.M. Millerand D.A. Dean. Cell-specific nuclear import of plasmid DNA in smooth muscle requires tissue-specific transcription factors and DNA sequences. Gene Therapy. 15:1107-1115 (2008).
24. H. Luthmanand G. Magnusson. HIGH-EFFICIENCY POLYOMA DNA TRANSFECTION OF CHLOROQUINE TREATED-CELLS. Nucleic Acids Research. 11:1295-1308 (1983).
25. M.D. Determan, J.P. Cox, S. Seifert, P. Thiyagarajan, and S.K. Mallapragada. Synthesis and characterization of temperature and pH-responsive pentablock copolymers. Polymer. 46:6933-6946 (2005).
26. A. Agarwal, R.C. Unfer, and S.K. Mallapragada. Investigation of in vitro compatibility of novel pentablock copolymers for gene delivery. Journal of Biomedical Materials Research 81A:24-39 (2007).
27. M.A. Zanta, P. Belguise-Valladier, and J.-P. Behr. Gene delivery: A single nuclear localization signal peptide is sufficient to carry DNA to the cell nucleus. Proceedings of the National Academy of Sciences. 96:91-96 (1999).
28. M. van der Aa, G.A. Koning, C. d'Oliveira, R.S. Oosting, K.J. Wilschut, W.E. Hennink, and D.J.A. Crommelin. An NLS peptide covalently linked to linear DNA does not enhance transfection efficiency of cationic polymer based gene delivery systems. Journal of Gene Medicine. 7:208-217 (2005).
29. M. van der Aa, E. Mastrobattista, R.S. Oosting, W.E. Hennink, G.A. Koning, and D.J.A.

Crommelin. The nuclear pore complex: The gateway to successful nonviral gene delivery. Pharmaceutical Research. 23:447-459 (2006).

30. K. Ciftciand R.J. Levy. Enhanced plasmid DNA transfection with lysosomotropic agents in cultured fibroblasts. International Journal of Pharmaceutics. 218:81-92 (2001).
31. R.G. Ridley. Medical need, scientific opportunity and the drive for antimalarial drugs. Nature. 415:686-693 (2002).
32. S.P. Sundelinand A. Terman. Different effects of chloroquine and hydroxychloroquine on lysosomal function in cultured retinal pigment epithelial cells. Apmis. 110:481-489 (2002).
33. J.P. Behr. The proton sponge: A trick to enter cells the viruses did not exploit. Chimia. 51:34-36 (1997).
34. A. Akinc, M. Thomas, A.M. Klibanov, and R. Langer. Exploring polyethylenimine-mediated DNA transfection and the proton sponge hypothesis. The Journal of Gene Medicine. 7:657-663 (2005).
35. T.I. Kim, M. Ou, M. Lee, and S.W. Kim. Arginine-grafted bioreducible poly(disulfide amine) for gene delivery systems. Biomaterials. 30:658-664 (2009).
36. S.M. Simon. Role of organelle pH in tumor cell biology and drug resistance. Drug Discovery Today. 4:32-38 (1999).
37. L. Jiang, V. Maher, J. McCormick, and M. Schindler. Alkalinization of the lysosomes is correlated with ras transformation of murine and human fibroblasts. J Biol Chem. 265:4775-4777 (1990).
38. O.A. Weisz. Organelle acidification and disease. Traffic. 4:57-64 (2003).
39. M. Duvvuri, S. Konkar, K.H. Hong, B.S.J. Blagg, and J.P. Krise. A New Approach for Enhancing Differential Selectivity of Drugs to Cancer Cells. ACS Chemical Biology. 1:309-315 (2006).
40. C.J. Evansand R.J. Aguilera. DNase II: genes, enzymes and function. Gene. 322:1-15 (2003).
41. D. Pinto-Gonzalez Howell, R.J. Krieser, A. Eastman, and M.A. Barry. Deoxyribonuclease II is a Lysosomal Barrier to Transfection. Mol Ther. 8:957-963 (2003).
42. N.P. Gabrielsonand D.W. Pack. Efficient polyethylenimine-mediated gene delivery proceeds via a caveolar pathway in HeLa cells. Journal of Controlled Release. 136:54-61 (2009).
43. S. Ohkumaand B. Poole. Fluorescence probe measurement of intralysosomal pH in living cells and perturbation of pH by various agents. Proceedings of the National Academy of Sciences of the United States of America. 75:3327-3331 (1978).
44. X.H. Li, T. Wang, Z.F. Zhao, and S.A. Weinman. The ClC-3 chloride channel promotes acidification of lysosomes in CHO-K1 and Huh-7 cells. Am J Physiol-Cell Physiol.

282:C1483-C1491 (2002).

45. J. Panyam, W.Z. Zhou, S. Prabha, S.K. Sahoo, and V. Labhasetwar. Rapid endo-lysosomal escape of poly(DL-lactide-co-glycolide) nanoparticles: implications for drug and gene delivery. Faseb J. 16:10 (2002).

46. P. Erbacher, A.C. Roche, M. Monsigny, and P. Midoux. Putative role of chloroquine in gene transfer into a human hepatoma cell line by DNA lactosylated polylysine complexes. Exp Cell Res. 225:186-194 (1996).

47. J.J. Cheng, R. Zeidan, S. Mishra, A. Liu, S.H. Pun, R.P. Kulkarni, G.S. Jensen, N.C. Bellocq, and M.E. Davis. Structure - Function correlation of chloroquine and analogues as transgene expression enhancers in nonviral gene delivery. J Med Chem. 49:6522-6531 (2006).

# CHAPTER 6. SENSING POLYMER/DNA POLYPLEX DISSOCIATION USING QUANTUM DOT FLUOROPHORES

Modified from a paper published in ACS Nano, 2011, 5:129-138

Bingqi Zhang, Yanjie Zhang, Surya K. Mallapragada, and Aaron R. Clapp

## Abstract

We characterized the dissociation of polymer/DNA polyplexes designed for gene delivery using water-soluble quantum dots (QDs). A pH-responsive pentablock copolymer was designed to form stable complexes with plasmid DNA via tertiary amine segments. Dissociation of the polyplex was induced using chloroquine where the efficiency of this process was sensed through changes in QD fluorescence. We found that increasing concentrations of pentablock copolymer and DNA led to quenching of QD fluorescence while chloroquine alone had no measurable effect. The mechanism of quenching was elucidated by modeling the process as the combination of static and dynamic quenching from the pentablock copolymer and DNA, as well as self-quenching due the bridging of QDs. Tertiary amine homopolymers were also used to study the effect of chain length on quenching. Overall, these QDs were found to be highly effective at monitoring the dissociation of pentablock copolymer/DNA polyplexes in vitro and may have potential for studying the release of DNA within cells.

## 6.1 Introduction

Semiconductor quantum dots (QDs) have seen increasing use in conjunction with or as an alternative to organic fluorophores in molecular and celluar imaging for non-viral gene delivery due to their broad excitation spectra, narrow and size-tunable emission spectra, and superior brightness and photostability(1, 2). QDs can be coupled either to polymers or DNA to investigate intracellular trafficking of the target particles among stained organelles(3-8). In particular for measuring polymer-DNA interactions, the distance between polymer and DNA can be sensed by Förster resonance energy transfer (FRET) in which QDs function as fluorescence energy donors(9-11). However, regardless of method used, appropriate chemical modifications are required, either for QDs, DNA, or other DNA condensing agents, which leads to complicated processing and/or potential interference with the functionality of the biomolecules or nanocrystals. Here, we report for the first time a facile and sensitive method to examine unpacking of polymer-DNA polyplexes induced by other competing agents on the basis of QD quenching.

We have developed a promising new thermogelling cationic pentablock copolymer vector for sustained gene delivery(12, 13). In addition to favorable transfection efficiencies and low cytotoxicity, these vectors exhibited a selectivity for transfection of cancer cells versus non-cancer cells(14), however the mechanism behind this selectivity is not fully understood. There have been several studies aimed at elucidating the intracellular mechanism of gene transfection for various polymeric vectors by trafficking studies and other methods(15-17). The ability to track the

dissociation of polymer-DNA complexes intracellularly would provide answers to the key questions regarding vector unpackaging and its effect on transfection efficiency. As a common lysosomotropic agent, chloroquine (CLQ) has been found to significantly enhance transfection efficiency in many systems(18-20). Among the multiple roles CLQ may play in assisting gene delivery, facilitating dissociation of DNA from polymers has emerged as an interesting possibility as it is also helpful for evaluating intracellular gene delivery barriers(21). The main strategy currently used by researchers to measure CLQ triggered polyplex dissociation relies on intercalating DNA dyes, either by measuring the amount of released DNA following removal of intact polyplexes through membrane filtration(22, 23), or through a dye exclusion assay presuming that polyplex dissociation can be characterized by the susceptibility of DNA to dye intercalation(23). However, one essential problem in these methods is that the intercalating capacity of CLQ with DNA can compete with many of the dyes used for DNA quantification, making it extremely difficult to accurately measure the actual amount of free DNA in solution or to assess the displacing effect of CLQ. In this work, we utilize cysteine-coated CdSe-ZnS core-shell QDs in place of common DNA intercalating dyes to measure DNA released from polyplexes formed with poly(diethylaminoethylmethacrylate) (PDEAEM)/ Pluronic F127 pentablock copolymers in the presence and absence of CLQ.

## 6.2 Materials and Methods

### 6.2.1 Materials

Hexadecylamine (HDA, 90%), hexamethyldisilathiane ($TMS_2S$), trioctyl phosphine

(TOP, 90%), and diethylzinc ($Et_2Zn$) were purchased from Sigma-Aldrich (St. Louis, MO) and used as received. Cadmium acetylacetonate ($Cd(acac)_2$) and selenium shot (Se, 99.99%) were used as received from Strem Chemicals (Newburyport, MA). Trioctylphosphine oxide (TOPO, 98%) was obtained from Alfa Aesar (Ward Hill, MA) and used as received. L-cysteine (≥ 99%) was purchased from Acros Organics and used as received. Chloroquine diphosphate salt was obtained from Sigma-Aldrich. Pluronic F127 [$(PEO)_{100}$-b-$(PPO)_{65}$-b-$(PEO)_{100}$], (where PEO represents poly(ethylene oxide) and PPO represents poly(propylene oxide)) was donated by BASF (Florham Park, NJ) and used without further modification. Chloroform and carbon disulfide ($CS_2$) were used as received from Fisher Scientific (Pittsburgh, PA). 6.7kb pGWIZ-luc (GeneTherapy Systems Inc, CA) plasmid was purified with Qiagen HiSpeed Maxi Kit (Qiagen, Valencia, CA).

### 6.2.2 Preparation of Water Soluble QDs by Ligand Exchange

CdSe-ZnS core-shell QDs were synthesized using a method previously reported by Clapp *et al*.(24) and Howarth *et al*.(25) with some minor modifications. Briefly, appropriate quantities of hexadecylamine (HDA) and trioctyl phosphine oxide (TOPO, ~10-30 g) were melted in a three-neck round bottom flask at ~150 °C followed by degassing under vacuum and purging with N2 via a Schlenk line. The mixture was further heated above 300 °C where cadmium acetylacetonate ($Cd(acac)_2$) and selenium precursor (1 M trioctylphosphine coordinated selenium, TOP:Se ) were rapidly injected by syringe into the flask through a rubber septum. The temperature was then abruptly reduced to 80 °C to arrest the nanocrystal growth and ensure a

narrow size distribution of CdSe core particles. CdSe cores were subsequently overcoated with multiple ZnS layers (three or more) by dropwise addition of diethylzinc ($Et_2Zn$) and hexamethyldisilathiane ($(TMS)_2S$) at ~140 °C. The resulting core-shell QDs were allowed to stir and anneal at 80 °C overnight.

To render CdSe-ZnS QDs water soluble, a biphasic ligand reaction and exchange procedure was employed which we have reported recently(26). Briefly, CdSe-ZnS QDs, having been purified by three-fold precipitation in dry methanol, were re-suspended in chloroform ($CHCl_3$). Carbon disulfide ($CS_2$) was added to the $CHCl_3$ organic layer containing the QDs. A second aqueous phase was added to the 20 mL glass reaction vial containing dissolved cysteine (Cys). During 24 h of vigorous stirring, $CS_2$ and Cys reacted to form dithiocarbamate (DTC) ligands having high affinity for the QD surface. The newly hydrophilic Cys-capped QDs were collected from the aqueous layer and further purified using a 50k MW cutoff membrane filter (Millipore, Billerica, MA) and PD-10 chromatography column (GE Healthcare, Piscataway, NJ).

### 6.2.3 Preparation of Pentablock Copolymers and Homopolymers

Poly(diethylaminoethyl methacrylate)(PDEAEM)/Pluronic F127 pentablock copolymers and PDEAEM homopolymers were synthesized via atom transfer radical polymerization (ATRP). The detailed procedure has been described elsewhere(27).

### 6.2.4 Polyplex Formation

Appropriate amounts of pentablock copolymer in HEPES buffer and plasmid

DNA in water was mixed at N/P (nitrogen/phosphorus) ratio of 20, followed by incubation at room temperature for 30 min to ensure complete complexation.

### 6.2.5 Measurement of Fluorescence

The fluorescence spectra of QDs in the presence of pentablock copolymers, polyplexes, DNA, chloroquine, and homopolyemers were measured by a dual monochromator spectrofluorimeter (Fluoromax-4, Horiba Jobin Yvon) with excitation at 370 nm and slit widths of 3 nm (excitation and emission). To ensure an equilibrated interaction between QDs and other reagents, mixtures were allowed to incubate for 30 min following addition of QDs to each sample.

## 6.3 Results and Discussion

### 6.3.1 Polyplex Dissociation Monitored by QD Fluorescence Quenching

CdSe QDs have been reported to bind molecules having tertiary amines with high affinity(28). Though not previously demonstrated, hydrophilic Cys-capped CdSe-ZnS QDs were considered as viable binding surfaces for the pentablock copolymers (having similar blocks of tertiary amines) used in this work. Interestingly, pentablock copolymers induced significant quenching of QD fluorescence upon mixing. QDs mixed with plasmid DNA led to similar quenching effects, but to a lesser extent. In contrast, the quenching effect was completely absent when QDs were mixed with pre-formed pentablock copolymer/DNA (penta/DNA) polyplexes as shown in Fig. 6.1a (black and light blue curves). The dramatic difference in QD fluorescence intensity between bound and unbound states of pentablock copolymer

a

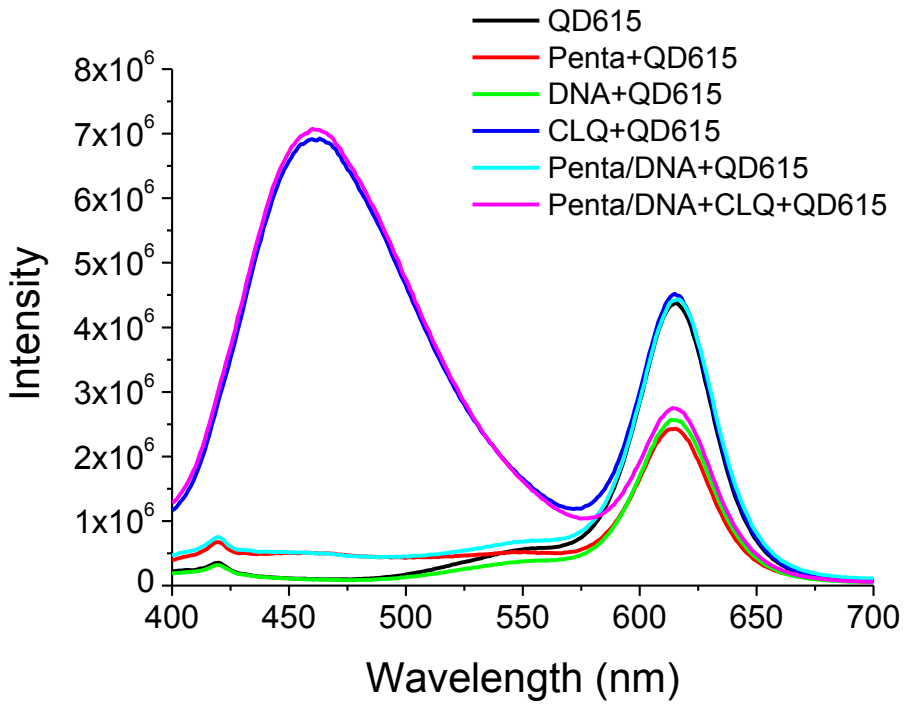
QD615
Penta+QD615
DNA+QD615
CLQ+QD615
Penta/DNA+QD615
Penta/DNA+CLQ+QD615
Intensity
8x10^6
7x10^6
6x10^6
5x10^6
4x10^6
3x10^6
2x10^6
1x10^6
0
400
450
500
550
600
650
700
Wavelength (nm)

b

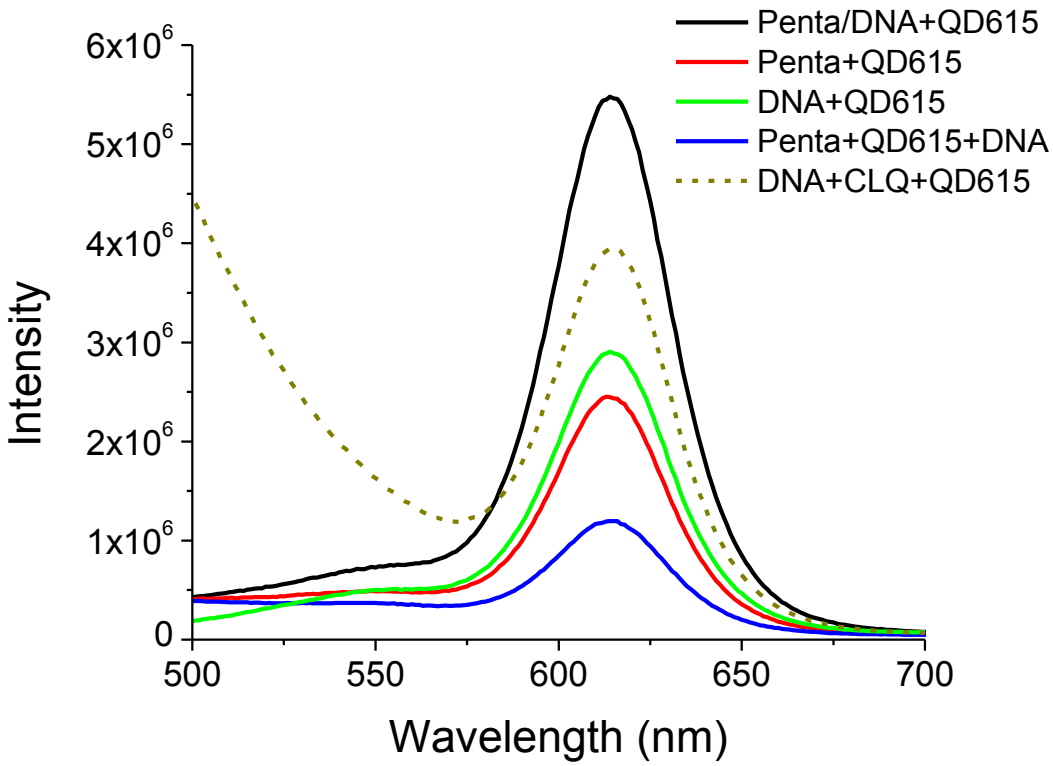
Penta/DNA+QD615
Penta+QD615
DNA+QD615
Penta+QD615+DNA
DNA+CLQ+QD615
Intensity
6x10^6
5x10^6
4x10^6
3x10^6
2x10^6
1x10^6
0
500
550
600
650
700
Wavelength (nm)

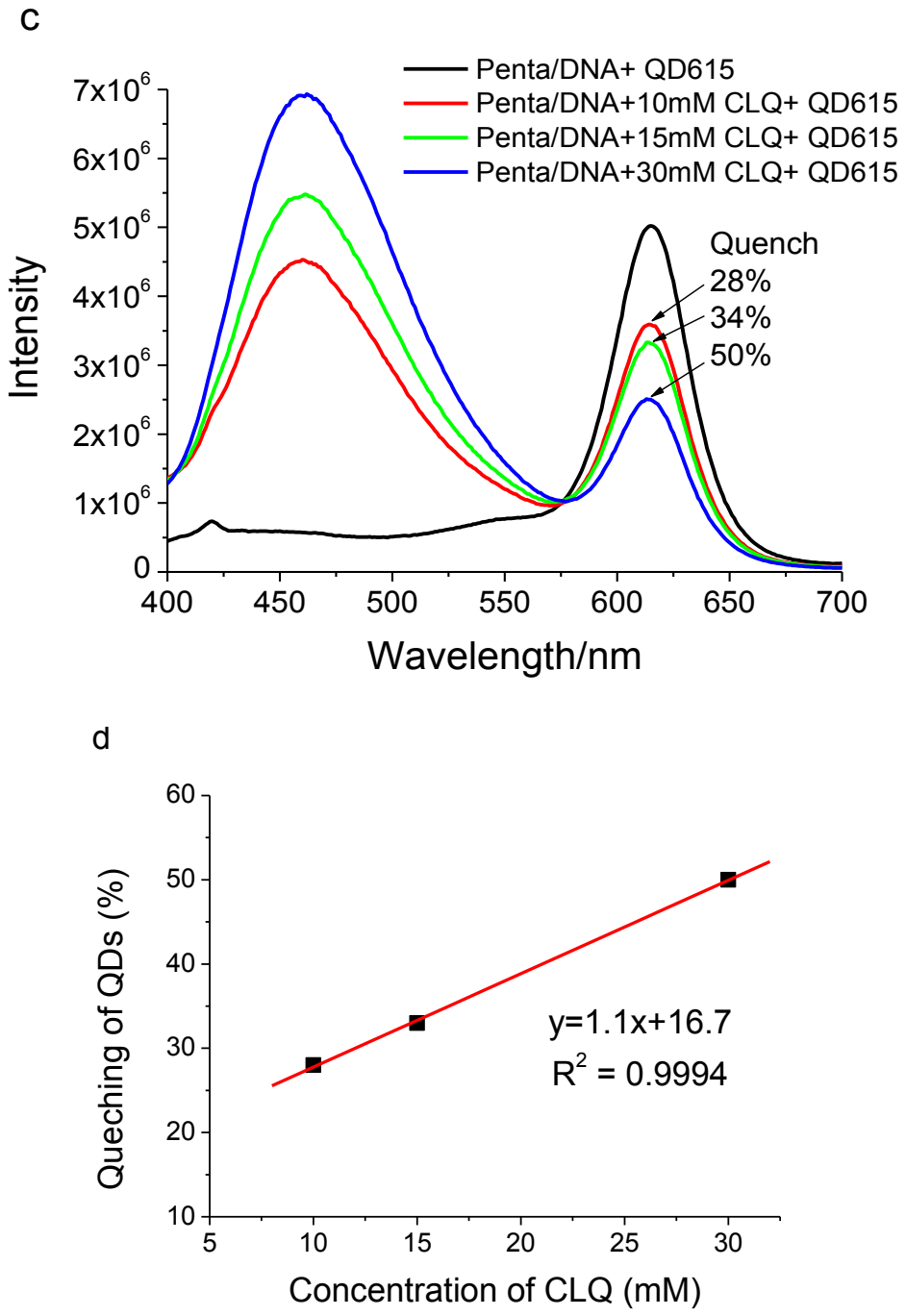


Fig. 6.1. (a) Fluorescence spectra showing the influence of pentablock copolymer (penta), DNA, CLQ, and penta/DNA polyplex on the fluorescence emission of QD615. (b) Fluorescence spectra showing the influence of penta, DNA, and polyplex on the fluorescence emission of QD615. (c) Influence of CLQ when polyplex and QD615 are mixed together. (d) Plot of QD615 quenching versus CLQ concentration generated from the data in (c).

and DNA suggested that polyplex association/dissociation might function as a potential "on/off" switch for QD fluorescence (illustrated in Fig. 6.2). CLQ alone was found not to influence the emission profile of the QDs studied (QDs having an emission maximum at 615 nm, or QD615) though CLQ itself demonstrated an intense and broad emission between 400 nm and 575 nm when excited at 370 nm (Fig 6.1a, dark blue and pink curves). Thus, we were able to investigate the stability

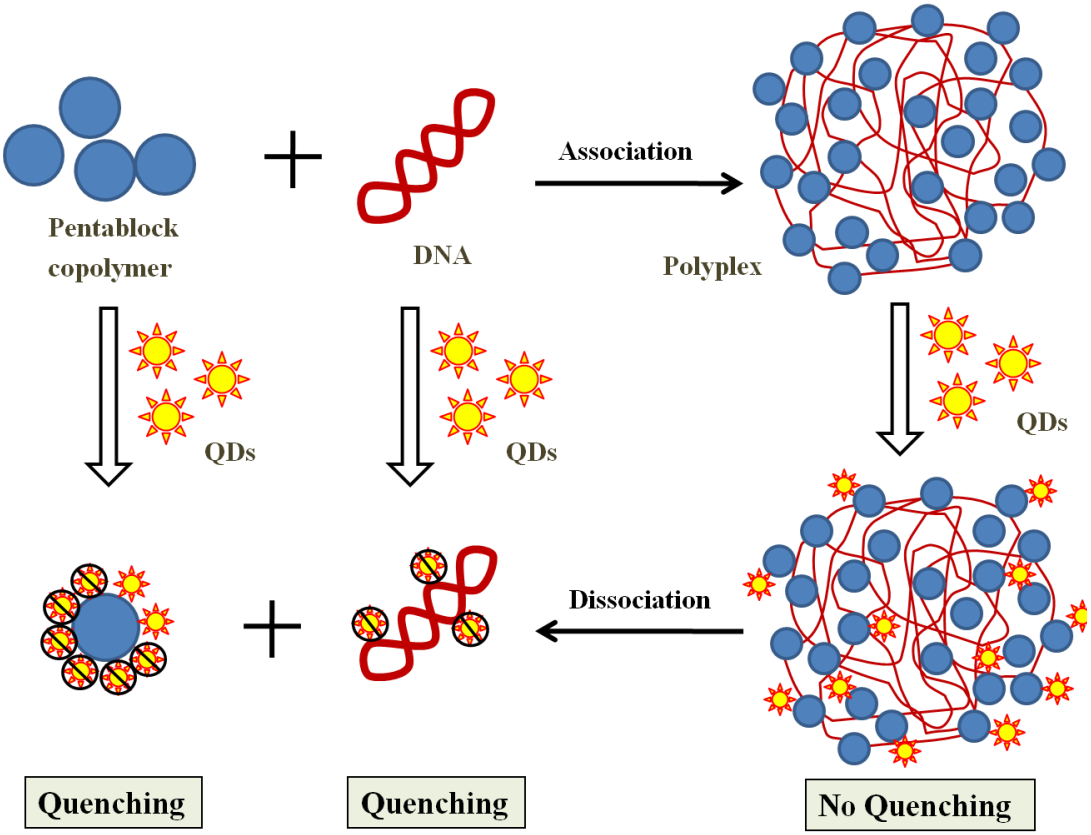


Fig. 6.2. Schematic illustration of the mechanism of sensing pentablock copolymer/DNA polyplex dissociation using QDs. QDs can be quenched by the free pentablock copolymer and/or free DNA, but not by penta/DNA polyplex. Once polyplex dissociates, the released pentablock copolymer and DNA will lead to QD quenching in such a way that polyplex dissociation can be monitored withthe decrease in QD fluorescence.

of the polyplex in the presence of CLQ by monitoring the change in QD fluorescence where any decrease in the intensity of QD emission is attributed to polyplex dissociation.

As expected, addition of CLQ to solutions containing penta/DNA polyplex and QDs resulted in significant quenching of QDs when compared with control samples lacking CLQ. This provides a strong indication that CLQ indeed facilitated polyplex dissociation. The newly released pentablock copolymers appear to quench QDs immediately once they are free in solution. Released DNA is partially complexed with CLQ and therefore exhibits relatively weaker quenching effects with QDs as compared to naked DNA mixed with QDs as shown in Fig. 6.1b. When pentablock copolymer and DNA were mixed with QDs sequentially (i.e., pentablock copolymer added to QD solution, followed by the addition of DNA), allowing time to equilibrate between additions, there was increased quenching of QDs over the effect achieved with either component alone. This indicates the pentablock copolymer and DNA did not significantly associate into polyplexes when introduced serially to a solution containing QDs. The combined quenching effects provide further evidence for association of pentablock copolymer and QDs via tertiary amines since these amine groups would otherwise interact with the phosphate groups of DNA to form polyplexes and partially restore the original fluorescence of QDs. Therefore, the quenching observed in a polyplex solution after addition of CLQ likely results from both free pentablock copolymer and CLQ-bound/free DNA. The overall quenching of QD fluorescence exhibited a linear relationship with the concentration of CLQ as

shown in Figs. 6.1c and d, further confirming the feasibility of using QDs to indicate polyplex dissociation induced by CLQ.

Although this study focused on cell-free assays, the CdSe-ZnS QDs used in this work showed no measurable acute toxicity in various cell lines due in part to a protective shell and dense coating of hydrophilic DTC-Cys ligands. The QD-based quenching method can thus be utilized to sense polyplex dissociation in cellular environments. For example, by co-incubating polyplexes and QDs with cells, dissociation of polyplexes in endosomes could be detected, which is of great importance for understanding the mechanism of gene delivery and improving transgene vectors. Furthermore, since the QDs were rendered water soluble though ligand exchange, various types of amino acids can be easily coupled to QDs as designed; for example, histidine residues can be coupled to the surface of QDs, leading them to readily escape endosomes. In this case, polyplex dissociation can be monitored by quenching of QDs throughout the cytoplasm.

### 6.3.2 Quantitative models of fluorescence quenching

Since the pentablock copolymer potentially acts as the primary quenching species, we expect the QD fluorescence to decrease (and thereby quenching to increase) with increasing polymer concentration. As shown in Fig. 6.3a, the measured QD fluorescence intensity showed an inverse dependence on the concentration of pentablock copolymer. Rather than exhibiting a linear dependence on concentration consistent with either static or dynamic quenching alone, the integrated quenching data appeared concave up (Fig. 6.3b) suggesting a

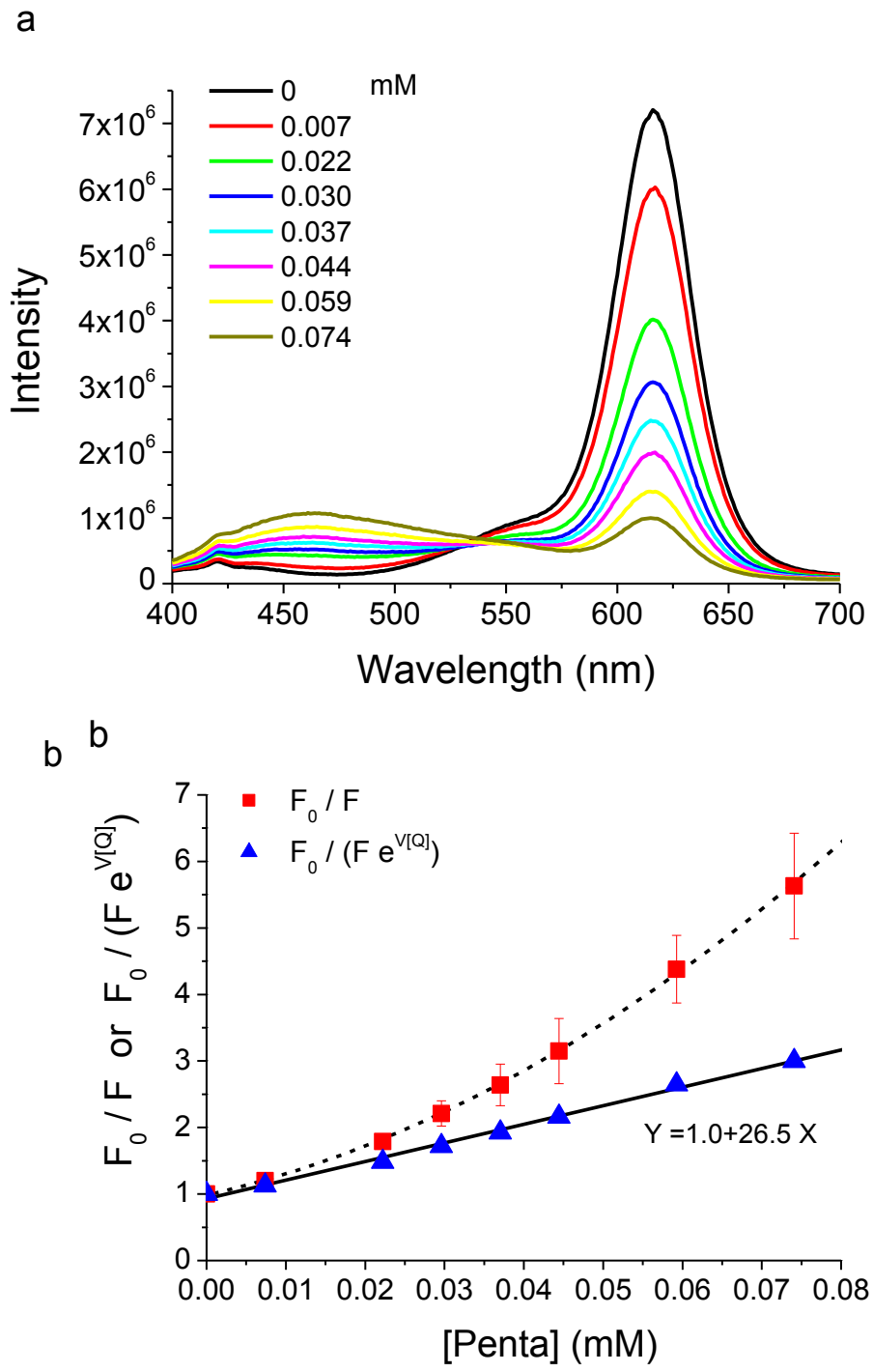


Fig. 6.3. Quenching of QD as a function of concentration of the pentablock copolymer (penta): (a) Fluorescence spectra and (b) integrated quenching using two models.

combination of quenching effects. We fit this data with a modified Stern-Volmer equation that describes combined dynamic and static quenching (Fig. 6.3b, dashed line) in which static quenching is presumed to occur when the quencher is within a characteristic radius (spherical volume) consistent with a stable complex:(29)

$$F_0/F = (1 + K_D[Q])\exp([Q]V) \qquad (1)$$

where

$$V = V_0\, N_A/1000 \qquad (2)$$

Here, $F_0$ and $F$ are the fluorescence intensities in the absence and presence of quencher, respectively; $K_D$ is the dynamic quenching constant; *[Q]* is the concentration of quencher (pentablock copolymer in this experiment); $V$ is the molar volume of the sphere within which the probability of quenching is unity; $V_0$ is the volume of the sphere in $cm^3$; and $N_A$ is the Avogadro constant. The fitted sphere volume was consistent with an interaction radius 15 nm. Alternatively, a plot of F0/($Fe^{[Q]V}$) versus [Q] yields a straight line with the slope equal to which is found to be about 26.5 $mM^{-1}$ (Fig. 6.3b, solid line).

In order to interpret this result, we measured the size distribution of QD-pentablock copolymer assemblies (micelles) in solution using dynamic light scattering. The data showed nearly monodisperse micelles having a mean diameter of 200 nm (polydispersity index, PDI = 0.062). Based on this size distribution and

the average QD diameter (~15-20 nm), there are presumably many QDs within each micelle. This physical arrangement suggests that QDs are likely to exhibit interparticle energy transfer (i.e., FRET) which would contribute to the static quenching component of the Stern-Volmer model shown in equations 1 and 2. The fitted interaction radius will then be representative of the composite effect of FRET-induced quenching as well as any direct quenching due to the pentablock copolymer alone. If FRET is a significant quenching mechanism, we expect the fitted interaction radius to be on the same order as the Förster distance for QD self-quenching ($R_0$ ~ 4-8 nm) which is considerably smaller than the average micelle size ($r_m$ ~ 100 nm). The modified Stern-Volmer model alone is insufficient to determine the relative static quenching contribution of QD self-quenching versus direct quenching from the polymer. For this, we require experiments that isolate these effects; this is the subject of the next section.

In the case of QD quenching by DNA, again there is enhanced quenching with increasing DNA concentration, yet the data is concave down (Fig. 6.4a and b) consistent with a fluorophore having accessible and inaccessible populations to the quencher and a fit to the following equation:

$$F_0/\Delta F = 1/f_a K_a [Q] + 1/f_a \qquad (3)$$

where

$$\Delta F = F_0 - F \qquad (4)$$

$$f_a = F_{0a}/F_0 \qquad (5)$$

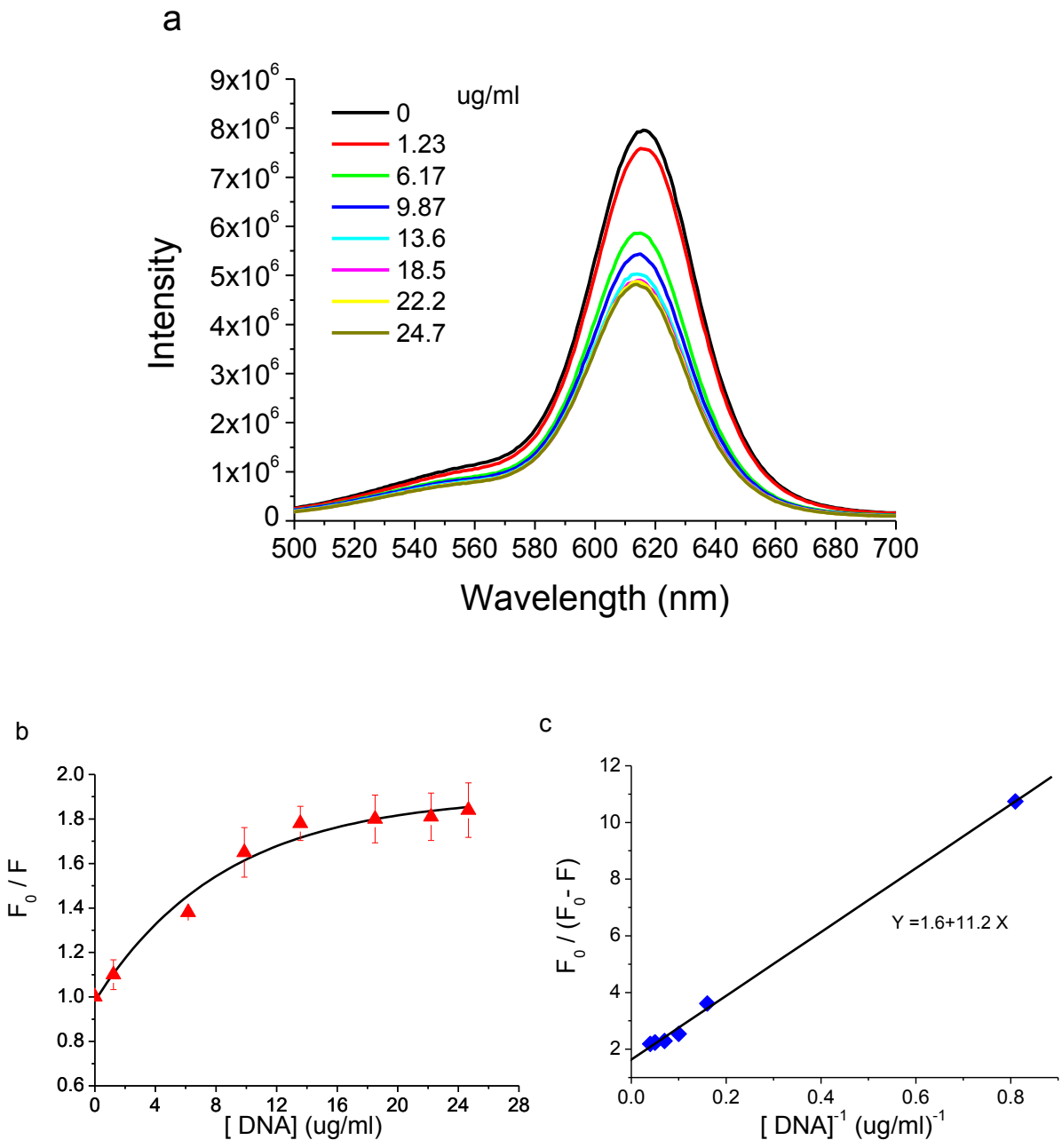


Fig. 6.4. Fluorescence emission/quenching of QD as a function of DNA: (a) measured QD emission spectra, (b) integrated QD quenching ($F_0/F$), (c) normalized quenching versus inverse DNA concentration fit with a linear quenching model.

Here, $F_0$ and $F$ again refer to the fluorescence in the absence and presence of quencher, respectively; $f_a$ is a fraction of the total fluorophore population where the subscript *a* refers to the accessible fraction that can be deactivated by the quencher species; correspondingly, $F_{0a}$ is the initial fluorescence and $K_a$ is quenching constant of the accessible fraction. For the mechanism of quenching by DNA, guanine bases are thought to be responsible as electron donors(29). Since plasmid DNA cannot maintain its circular structure but rather contorts into a supercoiled conformation in aqueous solution, the guanine bases would assume a complex distribution of accessibilities to the QD surface. As a result, it might be difficult for larger QDs to contact these quenching sites as compared to smaller QDs. Thus we assumed that only a fraction of QDs were available to be quenched by DNA. Values for and can be obtained readily from the intercept and slope by plotting $F_0 / F$ versus $[Q]^{-1}$ (Fig. 6.4c), which were found to be 0.62 and 0.14 L/μg, respectively.

### 6.3.3 Self-quenching among QDs

Considering both pentablock copolymer and DNA have the capacity to associate with QDs, they could feasibly generate a high local concentration of QDs and initiate self-quenching. The tendency of pentablock copolymer to form micelles in solution furthers the speculation that QD self-quenching is an important mechanism in these systems. In order to test this hypothesis, we examined the quenching of two distinct populations of QDs, QD519 (green emitting) and QD611 (red emitting), that can potentially form FRET donor-acceptor pairs between QDs, as reviewed by Somers *et al*.(30) If such a pair is formed in proximity sufficient for energy transfer (i.e., on

the order of the Förster distance $R_0$), we expect to see an increase in the ratio of red to green QD fluorescence (favorable quenching of the higher energy fluorophores). In order to elucidate the functional moieties responsible for the quenching behavior of the pentablock copolymer, a family of poly(dimethylaminoethyl methacrylate) (PDEAEM) homopolymers and Pluronic F127 were included in the study. These polymers comprise the end blocks and core triblock segments of the pentablock copolymer, respectively. As shown in Fig. 6.5, pentablock copolymers and PDEAEM homopolymers preferentially quenched QD519 (higher QD611/QD519 photoluminescence ratio) whereas DNA quenched each QD population about equally (ratio near 1.0). Conversely, Pluronic F127 had no measurable effect on the QD emission spectra (data not shown), indicating that the core triblock structure

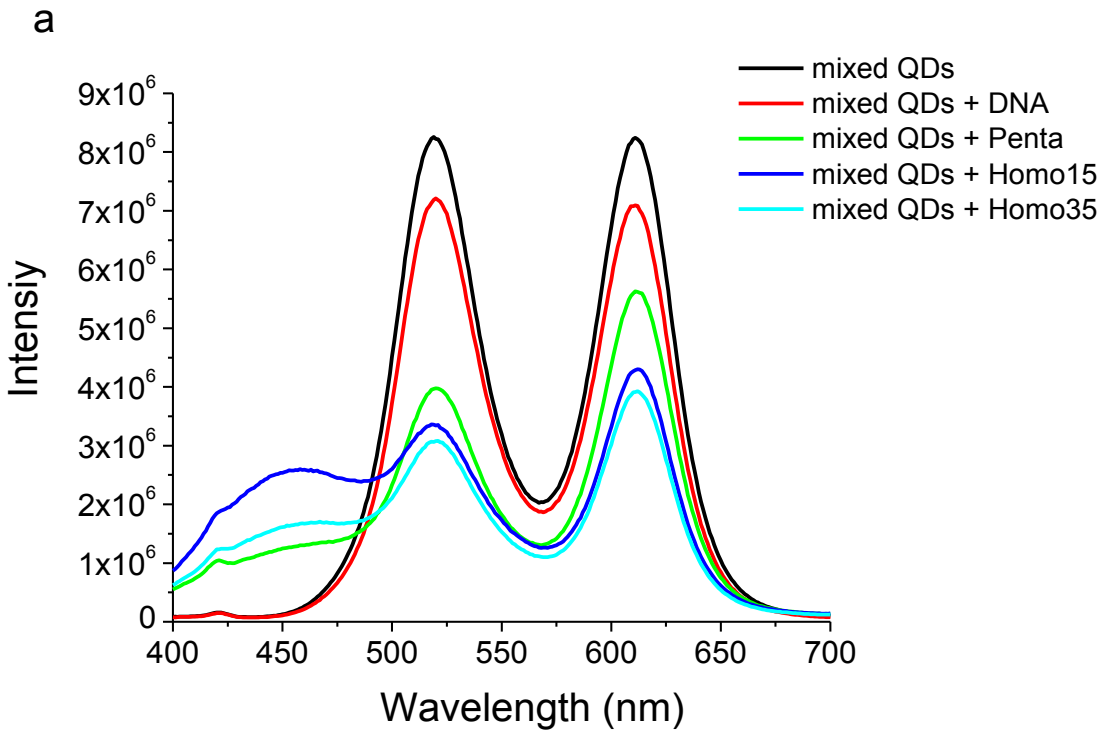

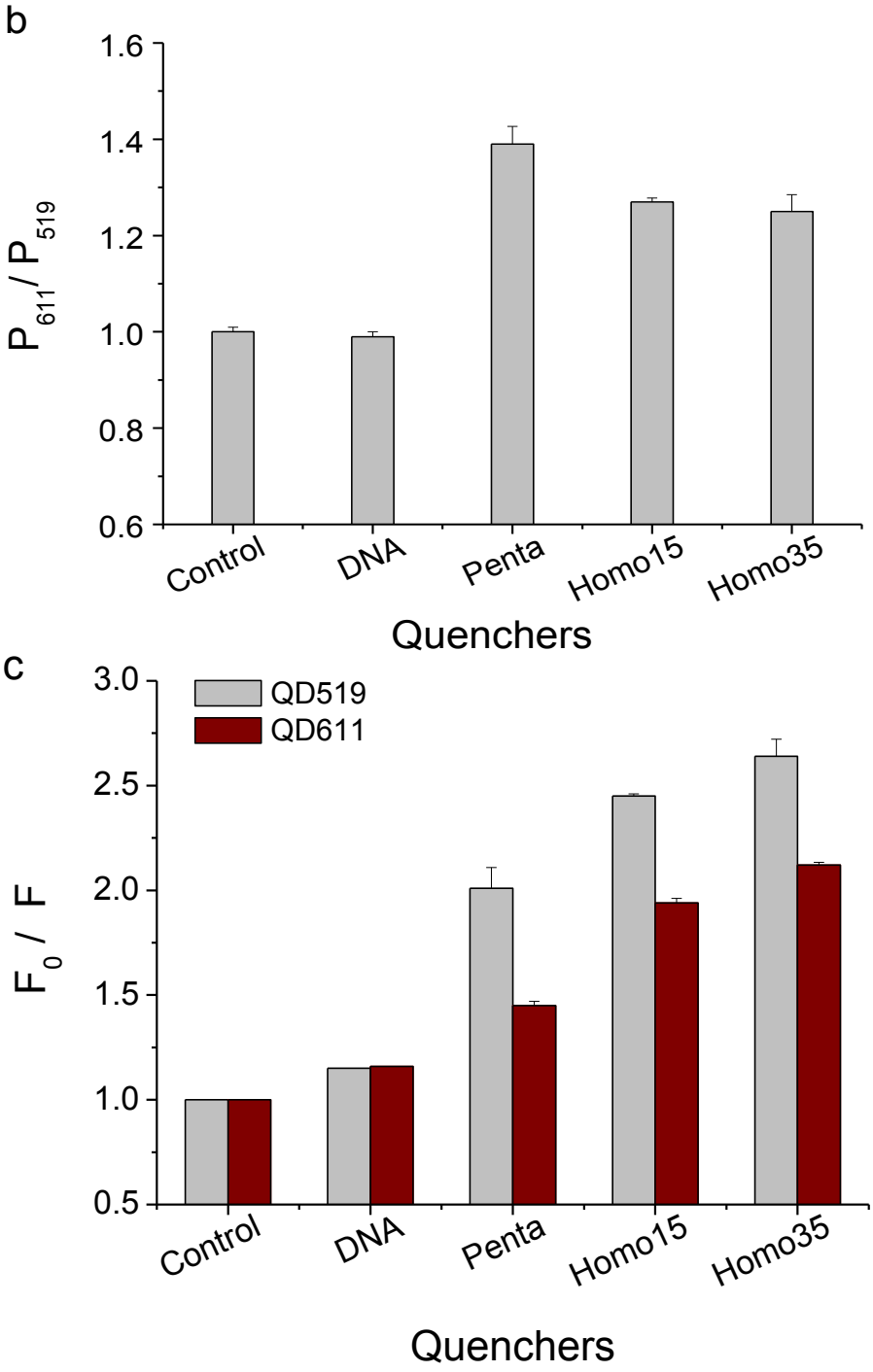


Fig. 6.5. Quenching of two populations of QDs (mixed QDs) by DNA, pentablock copolymer (penta) and poly(dimethylaminoethyl methacrylate) homopolymers with polymerization degree of 15 (Homo15) and 35 (Homo35). (a) Fluorescence spectra of QD519 and QD 611 (initially having similar intensities) mixed with various polymers. (b) Calculated ratios of the peak QD heights (QD611/QD519) shown in (a). (c) Degree of quenching for both QD519 and QD611 as a function of polymer type.

($PEO_{100}$-b-$PPO_{65}$-b-$PEO_{100}$) played no direct role in the quenching achieved with the full pentablock copolymer. The terminal PDEAEM blocks on pentablock copolymer are therefore likely to be the essential functional segments responsible for QD quenching, either by directly deactivating fluorescence relaxation pathways or aggregating QDs together. Notably, PDEAEM homopolymers exhibited variable quenching effects depending on polymerization degree (i.e., molecular weight). Although we observed greater quenching in the QD519 population as compared to QD611 for all polymers, this result alone is insufficient to demonstrate energy transfer from QD519 to QD611 unless isolated control populations of QD519 have an equal or lesser tendency to be quenched in the presence of polymer than QD611. To this end, we studied these two populations of QDs separately and found that QD611 was more readily quenched by pentablock and PDEAEM homopolymers than QD519 (Fig. 6.6), which contrasts the observations using mixed QD populations and provided compelling evidence of energy transfer from QD519 to QD611. The quenching data shown in Figs. 6.5c and 6.6c were combined into one graph to summarize the differences in polymer-induced quenching behavior between isolated and mixed QD samples. The normalized quenching ratio, $(Q611/Q519)_{mixed}$ $/(Q611/Q519)_{separate}$, was calculated and shown in Fig. 6.7 where ratios below 1.0 correspond to preferred quenching of the QD519 population in mixed QD samples, as is expected from Förster theory. From these data, we can conclude that FRET is the dominant quenching mechanism for QDs exposed to pentablock copolymers in solution. Similarly, PDEAEM homopolymers also showed capacity to facilitate self-quenching (Figs. 6.5c and 6.6c) and preferential QD519 quenching in mixed

a

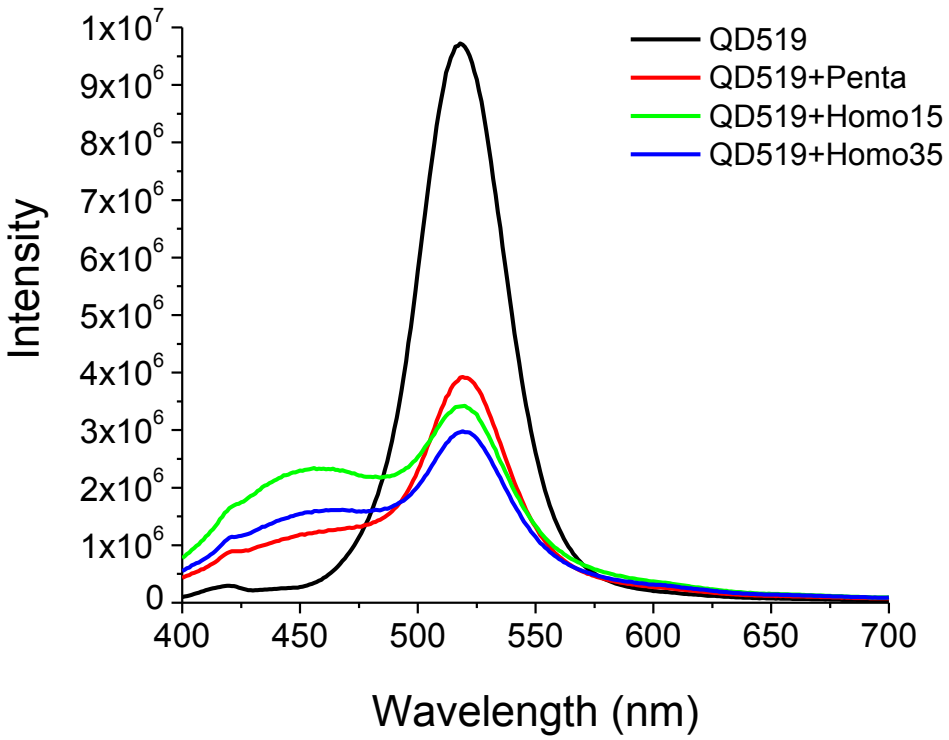
1x10^7
9x10^6
8x10^6
7x10^6
6x10^6
5x10^6
4x10^6
3x10^6
2x10^6
1x10^6
0
Intensity
400
450
500
550
600
650
700
Wavelength (nm)
QD519
QD519+Penta
QD519+Homo15
QD519+Homo35

b

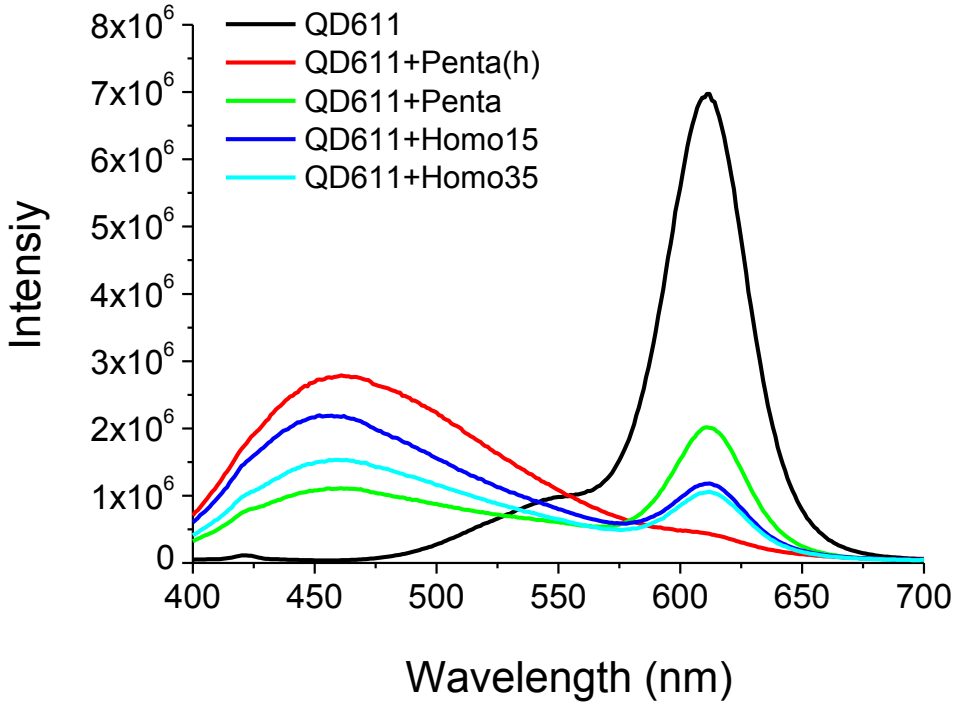
8x10^6
7x10^6
6x10^6
5x10^6
4x10^6
3x10^6
2x10^6
1x10^6
0
Intensiy
400
450
500
550
600
650
700
Wavelength (nm)
QD611
QD611+Penta(h)
QD611+Penta
QD611+Homo15
QD611+Homo35

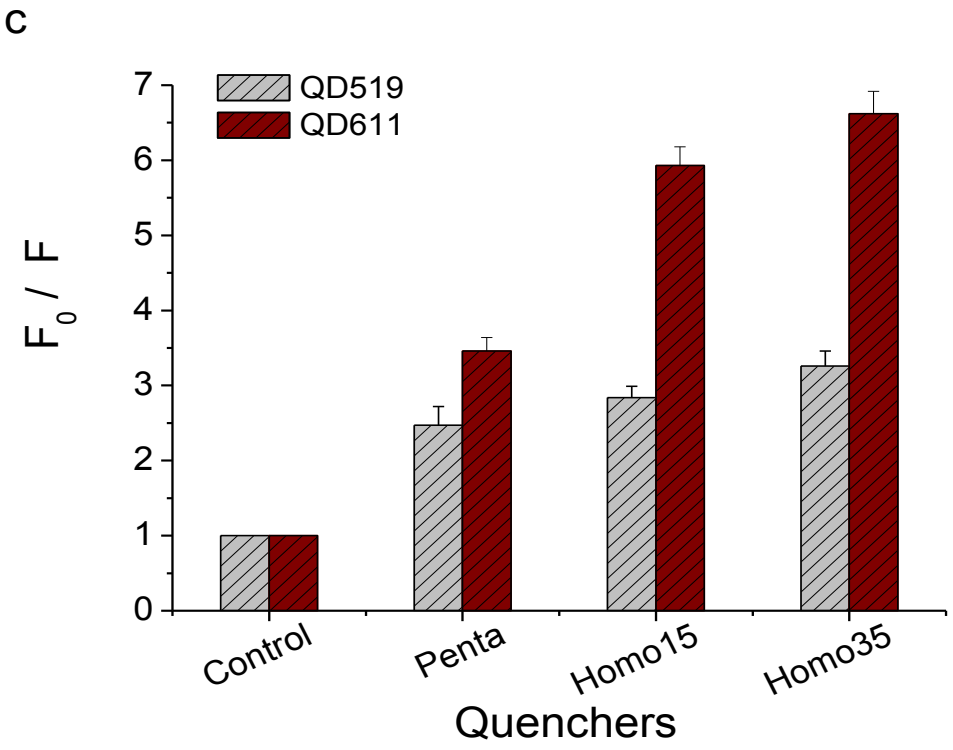


Fig. 6.6. Fluorescence emission spectra indicating quenching of (a) QD519 and (b) QD611 by pentablock copolymer (penta) and poly(dimethylaminoethyl methacrylate) homopolymers with polymerization degree of 15 (Homo15) and 35 (Homo35) at concentration of 2 mg/mL. Penta(h) in (b) refers to a high concentration of pentablock copolymer containing the same amount of PDEAEM as in other homopolymers. The quenching efficiency was given as $F_0/F$ and is depicted in (c).

samples as summarized in Fig. 6.7. As the polymerization degree of homopolymer increased from 15 to 35, the overall quenching increased slightly, and would presumably continue to increase as the molecular weight increased further.

In particular, the pentablock copolymer led to nearly complete quenching of QDs when the concentration of PDEAEM block was as high as that in other homopolymers (Fig. 6.6b), suggesting pentablock copolymers are more efficient at quenching QDs compared to homopolymers when holding the total mass of

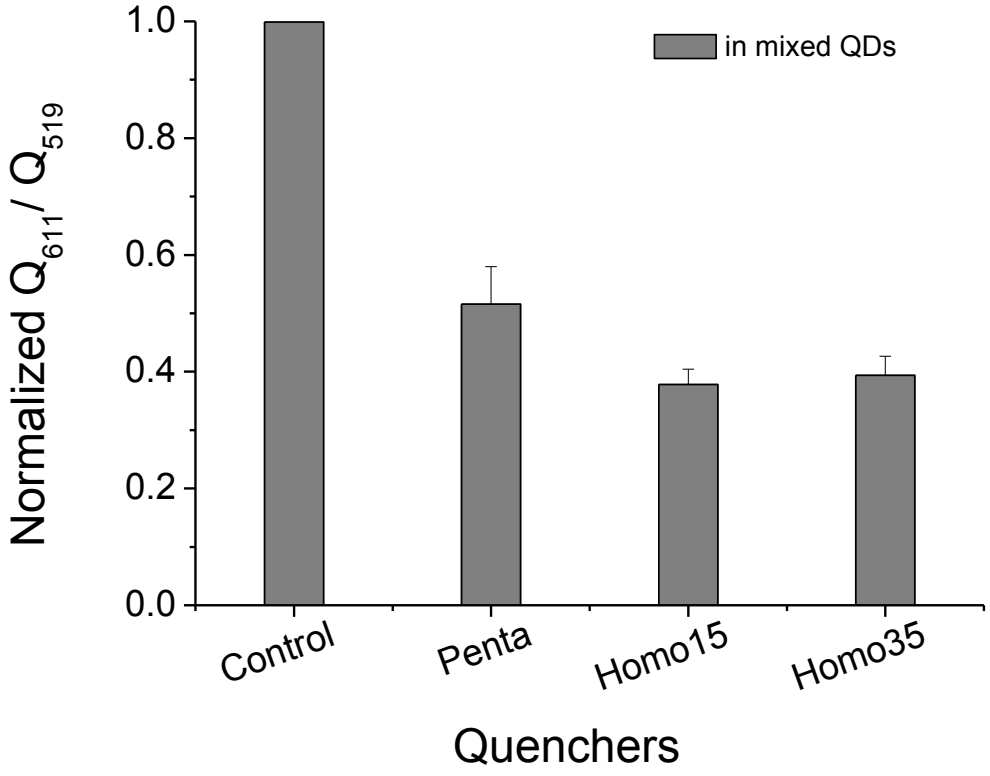


Fig. 6.7. The normalized ratio of quenching of QD611 ($Q_{611}$) to quenching of QD519 ($Q_{519}$) in mixed samples. $Q$ denotes quenching extent, defined as $F_0/F$; normalization was achieved by dividing the ratio of $Q_{611}/Q_{519}$ for mixed QDs by the ratio for separate QDs. The normalized ratio indicates quenching by energy transfer between QD611 and QD519 in mixed QD samples where a value<1.0 is consistent with preferential quenching of the QD519 population (which was true for all three polymer tested).

available PDEAEM constant. This is notable because the core triblock Pluronic F127 alone showed no quenching effect with QDs whatsoever. In an effort to elucidate the mechanism of quenching initiated by different polymers, varying amounts of PDEAEM homopolymers having degrees of polymerization of 15 (Homo15) and 35 (Homo35) were mixed with QDs to study quenching as a function

of concentration. As shown in Fig. 6.8, the relationship between quenching extent and homopolymer concentration was well-described by the same Stern-Volmer model (equations 1 and 2) used to characterize pentablock copolymer-induced quenching, indicating that homo- and pentablock polymers share a similar mechanism of QD quenching. However, the fitted quenching constants, $K_D$, for Homo15 and Homo35 were found to be 0.85 $mM^{-1}$ and 4.7 $mM^{-1}$, respectively, far lower than the 26.5 $mM^{-1}$ value measured using pentablock copolymer. The unique

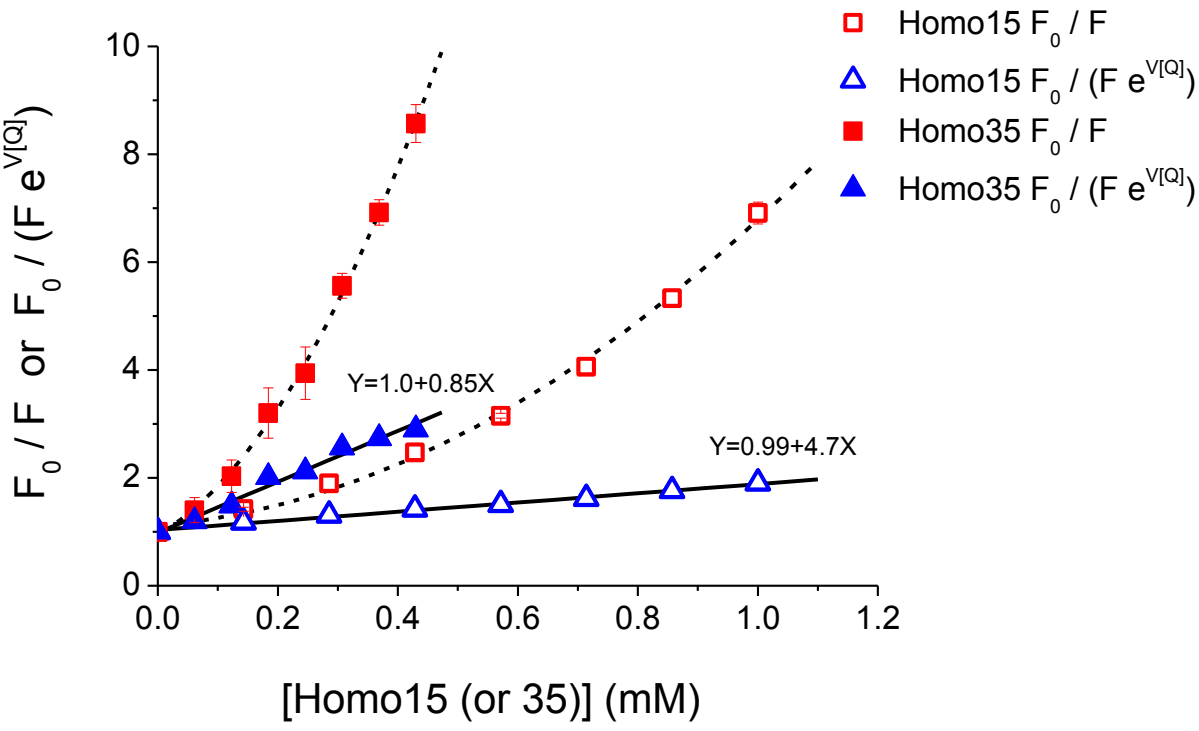


Fig. 6.8. Quenching of QDs as a function of concentration of homopolymers (Homo15, Homo35). Squares show plots of quenching using the standard definition of $F_0/F$. Triangles show a rescaled version of quenching consistent with a Stern-Volmer model of static and dynamic quenching. The latter definition provides a linear fit to the data.

micellar structure of pentablock copolymers in solution likely accounts for this discrepancy where several QDs can bind each micelle thus facilitating and enhancing self-quenching.

FRET-induced fluorescence quenching is expected to show strong wavelength dependence due to variations donor-acceptor spectral overlap. In our study, all PDEAEM-containing polymers showed obvious wavelength-dependent quenching behavior when mixed with QDs. Quenching measured as a function of wavelength (Fig. 6.9) appeared similar in shape to a plot of the spectral overlap function from Förster theory, J(λ), (not shown) which considers the QD emission and absorption spectral overlap; this further implicates a QD-to-QD self-quenching mechanism.

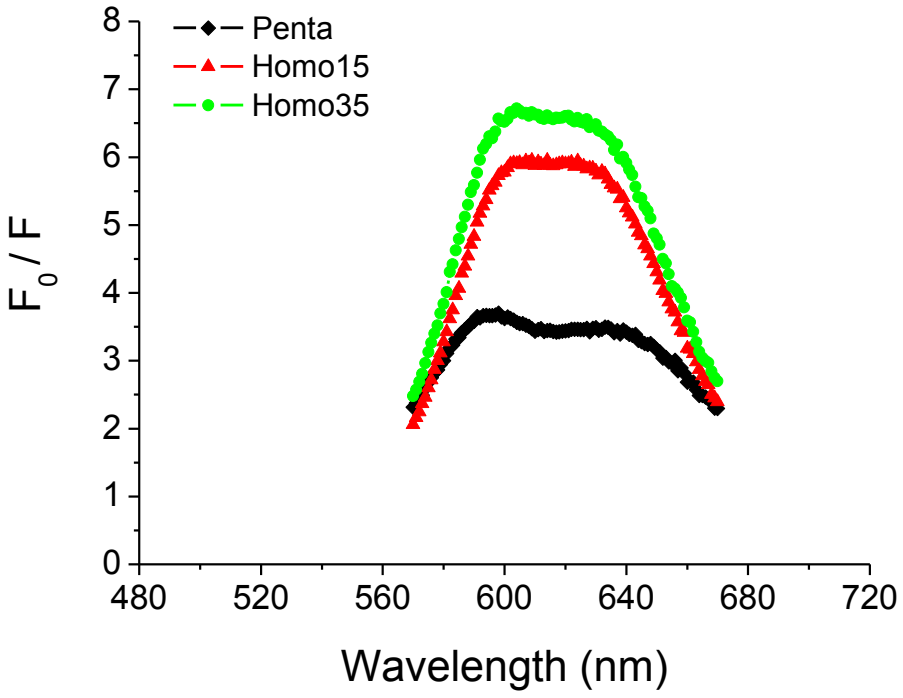


Fig. 6.9. Wavelength dependent quenching of QDs in the presence of various polymer quenchers.

Static quenching could also occur through complexation between the pentablock copolymer and QDs, although this type of quenching typically shows little dependence on wavelength, as in a recent example of static quenching of QDs by Medintz et al.(31), and is inconsistent with the wavelength dependence shown in Fig. 6.9. Although substantial quenching of QDs takes place immediately in the presence of PDEAEM homopolymer, maximum quenching occurs several minutes after the initial mixing as shown in Fig. 6.10. The measured quenching dynamics are consistent with multiple time scales associated with static and dynamic processes,

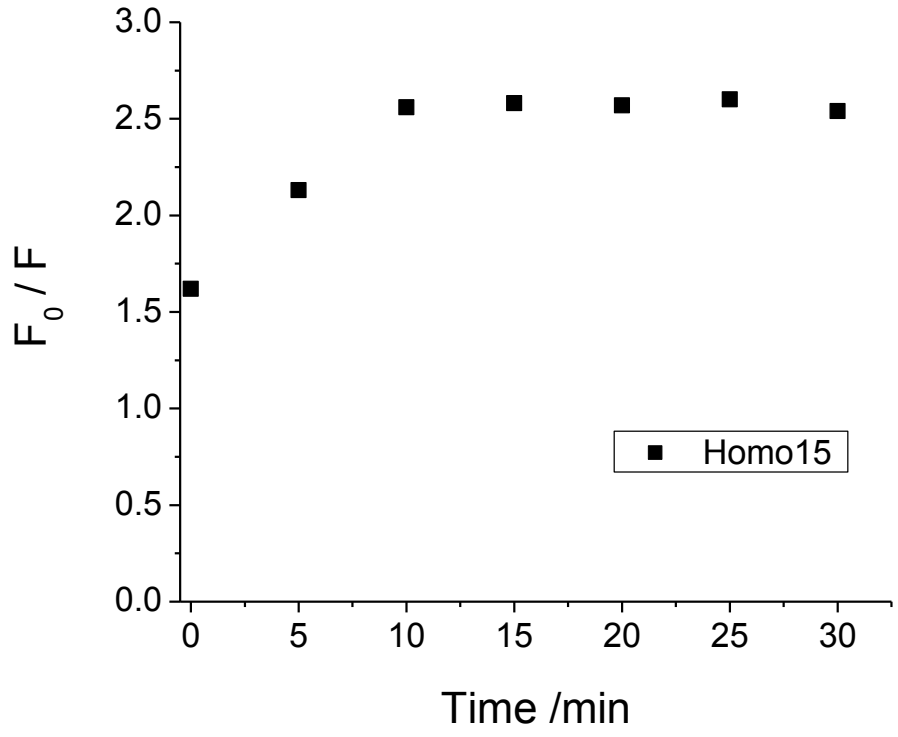


Fig. 6.10. Homo15 induced quenching of QD with time. Fluorescence of QDs in the absence of quencher (Homo15), $F_0$, was measured at different time points to provide accurate control for corresponding measure of sample quenching. Equilibrium was reached in about 10 minutes.

but also reflect the unique aspects of the QD-polymer system. In this case, we infer that immediate quenching results from collisions among QDs and polymer molecules, but that static complexation of QDs and polymers requires additional time to reach equilibrium resulting in saturated quenching after several minutes. The concept of static quenching in this system is unusual as it is dominated by QD self-quenching interactions which are mediated by associations with polymer.

## 6.4 Conclusions

We have shown that water-soluble Cys-capped CdSe-ZnS QDs are capable of sensing the dissociation of DNA/polymer polyplexes following exposure to chloroquine. Upon exposure to free pentablock copolymer and/or DNA, the QD fluorescence is quenched increasingly with concentration. The mechanism of fluorescence quenching was determined by exposing QDs to polymers and DNA individually and in various combinations. Studies with PDEAEM homopolymers suggested that tertiary amines were the functional groups responsible for quenching during exposure to the pentablock copolymer. However, the greatest quenching effect was observed when using pentablock copolymer, presumably due to its unique micellar conformation. QD fluorescence quenching was modeled using modified Stern-Volmer equations that account for static and dynamic quenching subject to modifications specific to DNA and PDEAEM. Studies with mixed populations of QDs showed that energy transfer plays a significant role in the overall quenching effect using PDEAEM and pentablock copolymer. These results

collectively suggest that these QDs have the potential to sense the dissociation of DNA cargo from polyplexes both in vitro and within living cells.

## Acknowledgments

We would like to thank Dr. Mathumai Kanapathipillai for help with polymer synthesis. ARC thanks Iowa State University startup funds for supporting this work.

## References

1. A.P. Alivisatos, W.W. Gu, and C. Larabell. Quantum dots as cellular probes. Annual Review of Biomedical Engineering. 7:55-76 (2005).
2. I.L. Medintz, H.T. Uyeda, E.R. Goldman, and H. Mattoussi. Quantum dot bioconjugates for imaging, labelling and sensing. Nature Materials. 4:435-446 (2005).
3. H. Duanand S. Nie. Cell-Penetrating Quantum Dots Based on Multivalent and Endosome-Disrupting Surface Coatings. Journal of the American Chemical Society. 129:3333-3338 (2007).
4. S.S. Rajan, H.Y. Liu, and T.Q. Vu. Ligand-bound quantum dot probes for studying the molecular scale dynamics of receptor endocytic trafficking in live cells. Acs Nano. 2:1153-1166 (2008).
5. V. Biju, D. Muraleedharan, K. Nakayama, Y. Shinohara, T. Itoh, Y. Baba, and M. Ishikawa. Quantum dot-insect neuropeptide conjugates for fluorescence imaging, transfection, and nucleus targeting of living cells. Langmuir. 23:10254-10261 (2007).
6. X.H. Gao, Y.Y. Cui, R.M. Levenson, L.W.K. Chung, and S.M. Nie. In vivo cancer targeting and imaging with semiconductor quantum dots. Nature Biotechnology. 22:969-976 (2004).
7. J.K. Jaiswal, H. Mattoussi, J.M. Mauro, and S.M. Simon. Long-term multiple color imaging of live cells using quantum dot bioconjugates. Nature Biotechnology. 21:47-51 (2003).
8. C. Walther, K. Meyer, R. Rennert, and I. Neundorf. Quantum Dot−Carrier Peptide Conjugates Suitable for Imaging and Delivery Applications. Bioconjugate Chemistry. 19:2346-2356 (2008).
9. H.H. Chen, Y.P. Ho, X. Jiang, H.Q. Mao, T.H. Wang, and K.W. Leong. Simultaneous non-invasive analysis of DNA condensation and stability by two-step QD-FRET. Nano Today. 4:125-134 (2009).

10. M. Bruchez, M. Moronne, P. Gin, S. Weiss, and A.P. Alivisatos. Semiconductor nanocrystals as fluorescent biological labels. Science. 281:2013-2016 (1998).
11. W.C.W. Chanand S.M. Nie. Quantum dot bioconjugates for ultrasensitive nonisotopic detection. Science. 281:2016-2018 (1998).
12. A. Agarwal, R. Vilensky, A. Stockdale, Y. Talmon, R.C. Unfer, and S.K. Mallapragada. Colloidally stable novel copolymeric system for gene delivery in complete growth media. Journal of Controlled Release. 121:28-37 (2007).
13. A. Agarwal, R.C. Unfer, and S.K. Mallapragada. Dual-role self-assembling nanoplexes for efficient gene transfection and sustained gene delivery. Biomaterials. 29:607-617 (2008).
14. B. Zhang, M. Kanapathipillai, P. Bisso, and S. Mallapragada. Novel Pentablock Copolymers for Selective Gene Delivery to Cancer Cells. Pharmaceutical Research. 26:700-713 (2009).
15. A. Remy-Kristensen, J.-P. Clamme, C. Vuilleumier, J.-G. Kuhry, and Y. Mely. Role of endocytosis in the transfection of L929 fibroblasts by polyethylenimine/DNA complexes. Biochimica et Biophysica Acta (BBA) - Biomembranes. 1514:21-32 (2001).
16. U.S. Huth, R. Schubert, and R. Peschka-Süss. Investigating the uptake and intracellular fate of pH-sensitive liposomes by flow cytometry and spectral bio-imaging. Journal of Controlled Release. 110:490-504 (2006).
17. G. Breuzard, M. Tertil, C. Goncalves, H. Cheradame, P. Geguan, C. Pichon, and P. Midoux. Nuclear delivery of N kappa B-assisted DNA/polymer complexes: plasmid DNA quantitation by confocal laser scanning microscopy and evidence of nuclear polyplexes by FRET imaging. Nucleic Acids Research. 36:12 (2008).
18. J. Xavier, S. Singh, D.A. Dean, N.M. Rao, and V. Gopal. Designed multi-domain protein as a carrier of nucleic acids into cells. Journal of Controlled Release. 133:154-160 (2009).
19. N.M. Moore, C.L. Sheppard, and S.E. Sakiyama-Elbert. Characterization of a multifunctional PEG-based gene delivery system containing nuclear localization signals and endosomal escape peptides. Acta Biomaterialia. 5:854-864 (2009).
20. G. Shen, H.F. Fang, Y.Y. Song, A.A. Bielska, Z.H. Wang, and J.S.A. Taylor. Phospholipid Conjugate for Intracellular Delivery of Peptide Nucleic Acids. Bioconjugate Chemistry. 20:1729-1736 (2009).
21. S. Yang, D.J. Coles, A. Esposito, D.J. Mitchell, I. Toth, and R.F. Minchin. Cellular uptake of self-assembled cationic peptide-DNA complexes: Multifunctional role of the enhancer chloroquine. Journal of Controlled Release. 135:159-165 (2009).
22. P. Erbacher, A.C. Roche, M. Monsigny, and P. Midoux. Putative role of chloroquine in gene transfer into a human hepatoma cell line by DNA lactosylated polylysine complexes. Experimental Cell Research. 225:186-194 (1996).

23. J.J. Cheng, R. Zeidan, S. Mishra, A. Liu, S.H. Pun, R.P. Kulkarni, G.S. Jensen, N.C. Bellocq, and M.E. Davis. Structure - Function correlation of chloroquine and analogues as transgene expression enhancers in nonviral gene delivery. Journal of Medicinal Chemistry. 49:6522-6531 (2006).

24. A.R. Clapp, E.R. Goldman, and H. Mattoussi. Capping of CdSe-ZnS quantum dots with DHLA and subsequent conjugation with proteins. Nature Protocols. 1:1258-1266 (2006).

25. M. Howarth, W.H. Liu, S. Puthenveetil, Y. Zheng, L.F. Marshall, M.M. Schmidt, K.D. Wittrup, M.G. Bawendi, and A.Y. Ting. Monovalent, reduced-size quantum dots for imaging receptors on living cells. Nature Methods. 5:397-399 (2008).

26. Y. Zhang, A.M. Schnoes, and A.R. Clapp. Dithiocarbamates as Capping Ligands for Water-Soluble Quantum Dots. ACS Applied Materials & Interfaces. 2: 3384-3395 (2010).

27. M.D. Determan, J.P. Cox, S. Seifert, P. Thiyagarajan, and S.K. Mallapragada. Synthesis and characterization of temperature and pH-responsive pentablock copolymers. Polymer. 46:6933-6946 (2005).

28. M.F. Wang, T.E. Dykstra, X.D. Lou, M.R. Salvador, G.D. Scholes, and M.A. Winnik. Colloidal CdSe nanocrystals passivated by a dye-labeled multidentate polymer: Quantitative analysis by size-exclusion chromatography. Angewandte Chemie-International Edition. 45:2221-2224 (2006).

29. J.R. Lakowicz. Principles of Fluorescence Spectroscopy, Springer, 2006.

30. R.C. Somers, M.G. Bawendi, and D.G. Nocera. CdSe nanocrystal based chem-/bio-sensors. Chemical Society Reviews. 36:579-591 (2007).

31. I.L. Medintz, T. Pons, S.A. Trammell, A.F. Grimes, D.S. English, J.B. Blanco-Canosa, P.E. Dawson, and H. Mattoussi. Interactions between Redox Complexes and Semiconductor Quantum Dots Coupled via a Peptide Bridge. Journal of the American Chemical Society. 130:16745-16756 (2008).

# CHAPTER 7. INVESTIGATION OF SUSTAINED CO-DELIVERY OF GENE AND DRUG IN VITRO USING INJECTABLE SELF-ASSEMBLED BLOCK COPOLYMERS

## 7.1 Introduction

Sustained gene delivery has attracted much attention over the past decade by its ability to maintain long term transfection in the target tissue and achieve a sustained therapeutic effect that otherwise must rely on repeated injections(1). In the development of such a system, investigating the *in vitro* release of the vector is usually necessary to acquire a reasonably high and steady release profile by optimizing formulation. More importantly, the released gene vector should maintain its function and possess a satisfactory ability to transfect cells. Traditionally, such studies have involved collecting the vector released within a certain time course in an acellular environment and comparing its transfection efficacy with the control vectors without simulating the release process(2-4). This comparison is convincing in terms of vector function preservation; however, it cannot reflect the real transfection ability of the sustained release system, with the sustained release and transfection being treated as two separate processes. Thus, a more practical testing method is needed to investigate the transfection efficacy of a specific sustained release system. In this study, we reported a device that allows the vector to be directly released to cells, by using a polyethylene glycol diacrylate (PEG-DA) barrier gel to mimic the role of tumor extracellular matrix in providing a diffusion barrier for

the therapeutic agents to reach tumor cells. The released vector can then directly transfect cells using the injectable poly(diethylaminoethyl methacrylate) (PDEAEM)-Pluronic F127-PDEAEM pentablock copolymer (PB) vector system.

The self-assembled PB was previously synthesized via atom transfer radical polymerization (ATRP)(5), with Pluronic F127 macroinitiator to exhibit thermosensitive gelation. The PDEAEM blocks facilitate DNA condensation. This novel vector can be injected intratumorally and can undergo sol-gel transition at physiological temperatures, providing vector release in a sustained manner. Upon copolymerization, the PB exhibits enhanced mechanical property as compared to the Pluronic F127 (PL) alone(4), which is favorable for *in vivo* sustained release, because stronger gels can provide longer sustained delivery and can maintain mechanical integrity longer. Self-assembled injectable hydrogels eventually dissolve and are clinically superior to other chemically cross-linked hydrogels that involve harsh crosslinking environments(6), or scaffolds(7) that need to be surgically implanted. In order to improve the stability of PB vectors in a physiological environment, free PL was subsequently added to PB/DNA complex to form a shield on the access charges by self-assembly, thus preventing aggregation with serum proteins(8). Along with the benefit, PL shield also provides the possibility of encapsulating hydrophobic anti-cancer drugs due to its amphiphilic nature(9), enabling the whole vector to deliver gene and drug simultaneously. Moreover, PL alone has been reported to have a chemosensitizing effect in multidrug-resistant (MDR) cells by inhibiting the P-glycoprotein related drug efflux(10).

The advantage of co-delivery of gene and drug has been shown to be that expression of specific genes can help render drug-resistant cells sensitized back to the drug(11-12), and uptake of drug into cells can enhance the level of gene expression(12-14). Thus, a synergistic effect can be expected with a combination of gene therapy and drug treatment. Regarding this combination, it could be achieved by combining two separate treatments (gene and drug) physically(11), or by combining gene and drug in the same carrier and using it as a single treatment(12, 15). The latter is more advantageous, for it can ensure delivery of gene and drug into the same cell, thus maximizing the synergistic effect. Yet it is also more complicated, for it involves synthesis of a new carrier and dealing with all possible interferences between the two payloads. Here we report an easily-implemented method for combinational delivery of gene and drug with PB-PL type of carriers. The anticancer drug paclitaxel (PTX) was incorporated in the PL shield and self-assembled into the PB/DNA complex later. By loading PTX and DNA separately, the potential interference can be reduced dramatically. More importantly, the two anti-cancer agents will be delivered in a simultaneous and sustained manner.

## 7.2 Experimental

### 7.2.1 Materials

Poly(ethylene glycol) diacrylate (PEG-DA) MW=4,000 was purchased from Polysciences Inc. (Warrington, PA). Pluronic F127 [$(PEO)_{100}$-b-$(PPO)_{65}$-b-$(PEO)_{100}$], (where PEO represents poly(ethylene oxide) and PPO represents poly(propylene oxide)) and photoinitiator 4-(2-hydroxyethoxy)phenyl-(2-hydroxy-2-propyl)ketone

(Irgacure 2959) was obtained from BASF (Florham Park, NJ) and used without further modification. Lactate dehydrogenase (LDH) assay kit and heparin sodium salt was obtained from Sigma-Aldrich (St Louis, MO). Luciferase assay system and passive lysis buffer were purchased from Promega (Madison, WI). Cell culture reagents: Dulbecco's Modified Eagle Medium (DMEM), heat inactivated fetal bovine serum (FBS), 0.25% trypsin-EDTA and Hank's buffered salt saline (HBSS) were purchased from Invitrogen (Carlsbad, CA), Dulbecco's MEM: Ham's Nutrient Mixture F-12, 1:1 Mix (DMEM/F-12) was purchased from ATCC (Manassas, VA). ExGen 500 was purchased from Fermentas Life Sciences (Hanover, MD). HiSpeed Plasmid Maxi Kit was obtained from Qiagen (Valencia, CA). 6.7kb pGWIZ-luc (GeneTherapy Systems Inc, CA) plasmid encoding the luciferase reporter gene and 4.7kb EGFP-N1 (ClonTech, CA) plasmid encoding GFP reporter gene were purified with Qiagen HiSpeed Maxi Kit. Polyester membrane with diameter of 24mm and pore size of 3.0μm were purchased from Corning (Lowell, MA). PicoGreen *ds*DNA Reagent was purchased from Invitrogen.

### 7.2.2 Cell Culture

The human ovarian carcinoma cell line SKOV3 and human retinal cell line ARPE-19 were obtained from ATCC™ (Manassas, VA). SKOV3 Cells were grown in DMEM supplemented with 10% (v/v) heat-inactivated FBS at 37°C under a humidified atmosphere containing 5% $CO_2$. ARPE-19 cells were cultured the same way but with DMEM/F-12 media. Subculture was carried out every 2~3 days.

### 7.2.3 Barrier Gel Formation

To simulate extracellular matrix environment for the *in vitro* studies, a hydrogel system was created. To a well of 24-well plate, 75mg of PEG-DA, 100µl of photo initiator (0.2 wt.% solution in water), 200µl of deionized water and appropriate amount of Pluronic F127 were added with the final F127concentration of 0, 7, 12, 15 and 17 % by weight. The plate was then placed in a refrigerator overnight and gently vortexed before exposure to UV light. The solution was photo crosslinked under UV beam with 50Mw/cm$^2$ for 2min. To avoid interference among nearby wells, a copper tube that fits into the well of interest was used along with a thick black paper covering other wells. After gel formation, they were carefully scraped out with a spatula and soaked in 50ml of DI water for three days at -4°C with water changed every day. To calculate the mass loss and swelling ratio, gels were dehydrated in an oven at 37°C and rehydrated thereafter. By comparing the weight of dehydrated gel with the weight of all feed chemicals, we found that F127 was completely removed by the third day of dissolution. After rehydration, the swelling ratio was determined by the ratio of the weight of rehydrated gel to that of dehydrated gel, which was found to be about 1200-1300% for a PEG-DA gel with 15% F127 dissolved away. When referring to PEG-DA gel throughout the manuscript, we mean a PEG-DA gel with F127 removed by dissolution in water. Gels formed in this way contain a concave top surface which allows sample loading.

For making gels with an indentation, the plate lid was molded with a glass tube (d=10mm). Instead of shining UV from above, the incident UV light was made to shine from below. After formation of gel, the mold was removed from the gel with great care to avoid any damage to the boundary of indentation. The capacity of

indentation depends on the length of mold (glass tube) and volume of gel solution. The complete process of making a molded PEG-DA gel for investigating sustained release is depicted in Fig. 7.1.

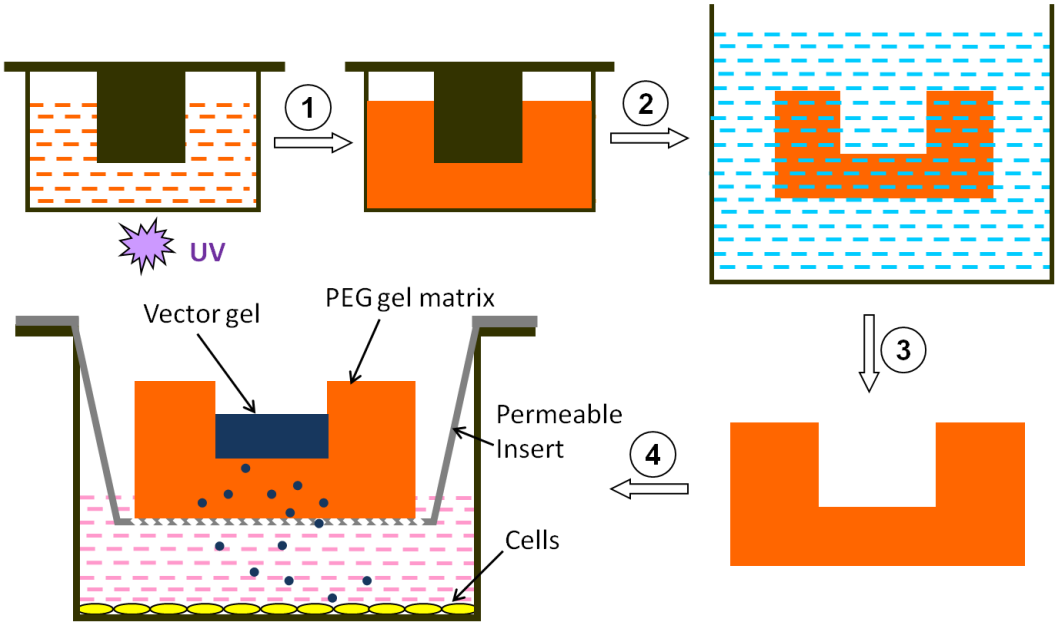


Fig. 7.1. Process of making PEG-DA gel matrix with an indentation for sustained gene delivery; (1) gel solution containing PEG-DA, Pluronic F127 and photo initiator was UV crosslinked in a well mold; (2) solid gel was removed from the mold and soaked in deionized water to dissolve away Pluronic F127; (3) PEG-DA gel matrix was obtained and disinfected; (4) PEG-DA gel was set in a cell-culture well with a supporting permeable insert; vector gel solution was injected to the indentation and solidified in response to change of temperature, releasing vector to cells in a sustained fashion. Mold shown here was flat-bottomed, but a round-bottomed mold was also available depending on need.

### 7.2.4 Polyplex Formation

Pentablock copolymers (PB) used in this study were synthesized by ATRP as reported previously. All polymer solutions were prepared in 0.5× HBS buffer, pH 7.0 unless stated otherwise. To form the polyplex with desired N/P (nitrogen/phosphate)

ratios, various amounts of pentablock copolymer (2mg/ml) was added to the fixed amount of DNA at equal volume. The mixture was then gently vortexed and allowed to stand at room temperature for 20min. In an effort to improve the stability of polyplex with serum, free Pluronic F127 (PL) (10 mg/ml) was further added at the same volume to give a weight ratio of 5:1 with regard to the corresponding PB. Upon this, PL will self-assemble with PB on the surface of PB/DNA polyplexes and form a shield layer through the hydrophobic interaction. The cytotoxicity and stability of resultant PB-PL/DNA polyplex has been thoroughly investigated in previous papers(8, 16).

### 7.2.5 In vitro Polyplex Release

Appropriate amount of Pluronic F127 was added to the polyplex solution at low temperatures (e.g. 4°C), to make the final F127 concentration around 20 wt%. With this concentration, the vector solution can be injected as liquid and form a solid gel in response to the change in surrounding temperature. The pre-warmed PEG-DA gels (soaked in warmed PBS buffer or cell growth medium) were placed in the Transwell inserts equipped on the 6-well plate containing 1.5ml of PBS or growth medium in each well. The prepared vector solution was injected into the concave surface of non-molded gels or the indentation of molded gels. Gelation occurred instantly due to temperature change. The plate was then placed on an incubator shaker and shaken with 100 rpm at 37°C for a week. All buffer in the well was collected every day and replaced with 1.5ml of fresh PBS. 150μl of each collected sample was treated with 2μl of heparin (200μg/μl) for 40min to separate DNA from

pentablock copolymer. The concentration of DNA was then measured with Picogreen assay on a dual monochromator spectrofluorimeter (Fluoromax-4, Horiba Jobin Yvon) with excitation at 480 nm and slit widths of 3 nm (excitation and emission). Data were recorded at the emission peak (520nm) for DNA-bound picogreen and analyzed using a standard curve.

### 7.2.6 In vitro Transfection

Cells were seeded into 96-well or 6-well plates one day prior to transfection with initial numbers of ~$1.2\times10^4$ or ~$1.0\times10^5$ cells per well, respectively. After 24h growth, cells reached a 70~80% confluence when the old medium was replaced with fresh growth medium containing 10% FBS. Transfection was then carried out by adding polyplexes of various formulations to the medium with 0.6μg pGIZ-luc or 3μg EGFP-N1 DNA per well for 96-well or 6-well plate, respectively. Cells were allowed to incubate with polyplexes for 3h, followed by changing the old medium to remove the polyplexes. After an additional 45h post-transfection, cells in the 96-well plates were lysed and analyzed for luciferase activity with luciferase assay kit on an automated Veritas™ Microplate Luminometer. The luminescence was measured in arbitrary Relative Luminescence Units (RLU). Cells in 6-well plate were examined for GFP expression with fluorescence microscope (Nikon, Eclipse-Ti). Each transfection was done in triplicate. ExGen 500, a sterile solution of linear 22kDa polyethylenimine (PEI), was used as positive control at an N/P ratio of 6 according to the manufacturer's protocol.

### 7.2.7 Cytotoxicity

The cytotoxicity of polyplexes was examined with LDH assay kit, based on the amount of cytoplasmic LDH released into the medium following cell membrane rupture. Samples were collected at the end of 45h post-transfection. Blank cells were used as a negative control to provide 0% cytotoxicity and Triton-X was used as a positive control to provide 100% cytotoxicity. Cell viability was determined as follows:

$$\text{Cell viability \%} = 100 - \frac{\text{Abs (sample)} - \text{Abs (blank cells)}}{\text{Abs (Triton-x)} - \text{Abs (blank cells)}} \times 100$$

### 7.2.8 Drug Encapsulation

The paclitaxel (PTX) was encapsulated in Pluronic F127 micelles by solvent evaporation method. Briefly, 2mg of PTX and 100mg of F127 were dissolved in 10ml of acetonitrile in a 50ml flask. The solvent was then removed using a rotary evaporator under reduced pressure at 50°C. A solid layer formed around the flask which was then placed in a vacuum oven at room temperature overnight to remove the residual solvent. The flask was reheated in a water bath at 60°C, followed by addition of 10ml warmed water (60°C) with medium stirring. The resultant PTX loaded F127 micelle solution was filtered into a 0.22μm filter to remove the undissolved PTX and other impurities. The filtrate was then lyophilized and stored at 4°C for later use. The content of PTX was determined using a standard curve of absorbance at 227 nm, which was found to be about 1.4 wt%. The drug loading efficiency was found to be about 73% by dividing the weight of feed drug by the weight of encapsulated drug.

### 7.2.9 Gene and Drug Co-delivery

Polyplexes were formed in a similar way as described above, but instead of using free Pluronic F127 alone to provide an additional shield, desired amount of PTX-loaded F127 was mixed in at this step. In such a way, PTX and DNA could be delivered with a single carrier at the same time. Transfection followed the procedure stated above.

## 7.3 Results and Discussion

### 7.3.1 Effect of F127 on the Property of PEG-DA Gels

In the development of a barrier gel that can mimic tumor extracellular matrix to hinder delivery of macromolecules such as DNA vectors, we were hoping a reasonable diffusion rate that can be readily adjusted. Co-dissolving Pluronic F127 with the PEG-DA provides a simple and inexpensive method. After gel formation by crosslinking in the presence of various amounts of F127, all gels looked identically clear(data not shown). However, after rinsing off F127, gels appeared quite different in transparency though they were of the same composition(Fig. 7.2A). Compared to the plain PEG-DA gel that maintained the transparent appearance in the whole process, gels with addition of F127 experienced a change from transparent to opaque at different extents. The development of opaqueness, which should result from phase separation and/or increased number of pores/channels(17), showed a positive correlation with the amount of F127, indicating addition and removal of F127 can bring a more loosely network morphology and in turn may increase the diffusional transport of macromolecules through the gel. Indeed, PB-PL/DNA

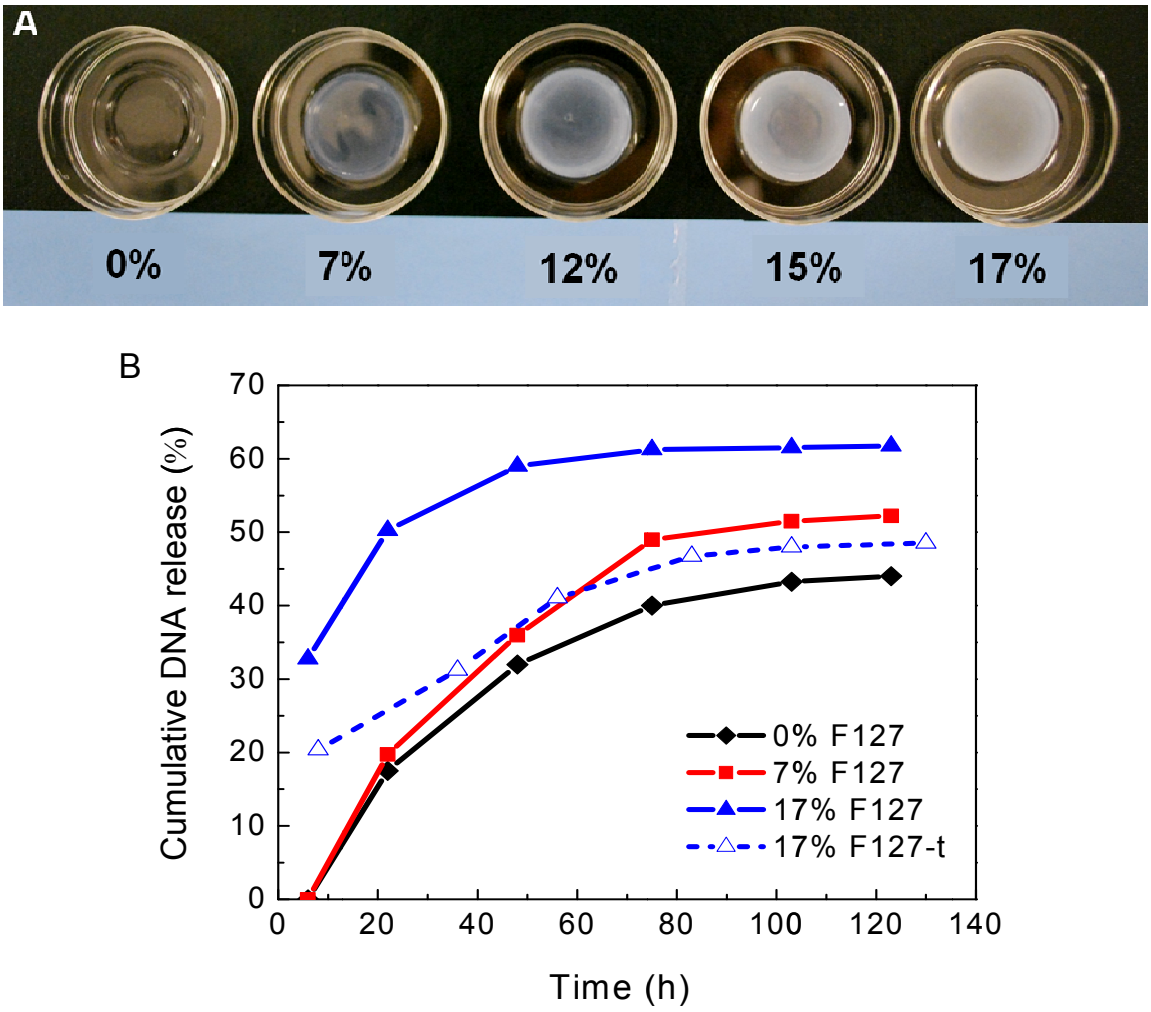


Fig. 7.2. (A) Appearance of PEG-DA gels after washing away all Pluronic F127 that was added to the gel solution at various concentrations before crosslinking. All gels were crosslinked by 2min exposure to UV light and appeared identically transparent before F127 was washed away; (B) release of DNA from PEG-DA gels that were made out of 300µl gel solution except 17% F127-t where 600 µl was used. Vector gel solution containing 4µg DNA was loaded into the indentation of each PEG-DA gel where it solidified as a vector gel at 37 C.

polyplexes were found to be released faster through a F127 treated gel (Fig. 7.2B), with eventually 62% of DNA payload released from 17% F127 gel and 52% from 7% F127 gel, as compared to 44% from the plain gel where there was considerable fraction of DNA being sequestered in the gel matrix. When the thickness of the gel

Table 7.1. Average dye exclusion of polyplexes released by various samples within first 4 days

| | Polyplex in buffer | Polyplex in released samples (first 4 days) | | |
|---|---|---|---|---|
| | | 0% F127 | 7% F127 | 17% F127 |
| Dye exclusion (%) | 87±2 | 76±5 | 79±5 | 84±4 |

was doubled (refer to 17% F127-t), the release of DNA showed a dramatic decrease with more DNA entrapped in the gel, probably due to the increased volume of small and/or non-interconnected pores. It has been reported that the mesh size of PEG-DA gel fluctuated with the thickness of the gel as well as the depth of cross-section, and the center plane exhibited significantly smaller pores than top and bottom planes(18). However, the initial burst release only occurred with the two 17% F127 gels as recorded at t = 6h, implying removal of F127 at this concentration might generate similar micro-channels to allow fast transport across the gel. In addition to a desired release rate, DNA also needs to be safely packaged in the released sample to allow an effective transfection. The integrity of released polyplex was examined by dye exclusion assay using Picogreen, an ultrasensitive double-stranded DNA dye that exhibits significant fluorescence enhancement upon intercalating DNA. The inaccessibility of DNA characterized by dye exclusion will indicate the affinity between DNA and the pentablock copolymers. As shown in Table 1, all released polyplexes showed an average dye exclusion of about 80%, similar to the case of polyplex formulated in solution. Therefore, the PB-PL/DNA polyplex maintained the complexed structure during transport across the gel even after four day release and is thus expected to have the similar transfection ability as that seen with the control polyplex.

### 7.3.2 Release of DNA from Molded PEG-DA Gels

To make a PEG-DA gel with greater capacity for vector gel loading, we developed a well mold that can produce an indentation of desired shape and size on the top of gel (Fig. 7.1). Two factors were investigated for their influence on DNA release, the volume of gel solution (thickness of gel) and UV exposure time. Fig. 7.3 shows release profiles of DNA from three 17% F127 gels. The duration of UV exposure plays an important role in gel permeability, as demonstrated by 100% DNA released from UV-1.5 gel (red-square curve) versus 65% released from UV-2 gel (black-circle curve). Again, thicker gels showed greater resistance to the vector diffusion, and this effect seemed to be remarkably intensive in the molded gel. With all the other conditions being the same, V-850 gel (blue-triangle curve) lead to only about 35% release of DNA as compared to 100% release from V-700 gel (red-

A

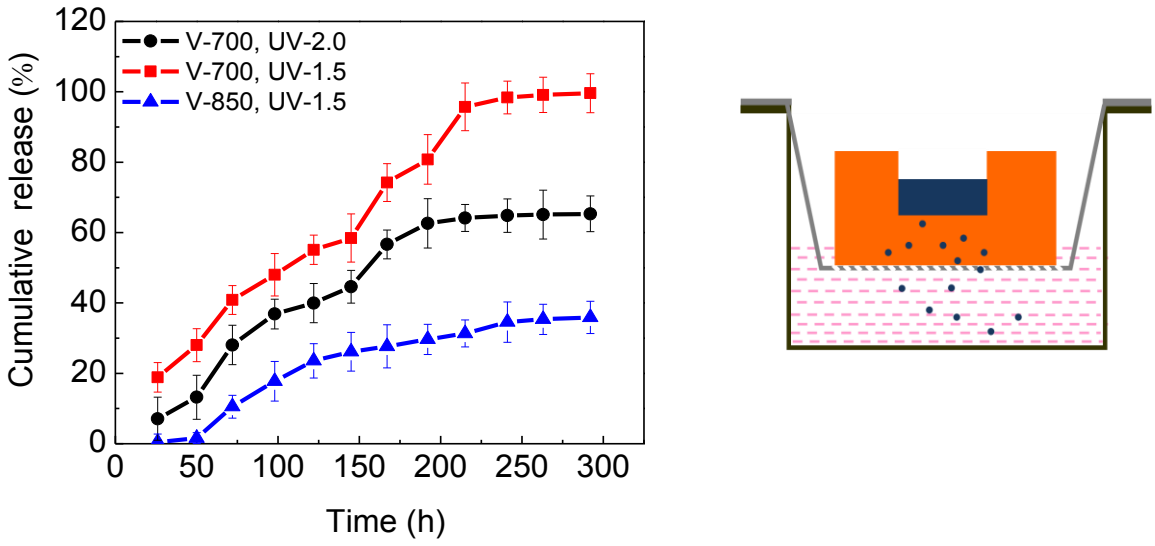


Fig. 7.3. DNA release from the PB-PL vectors through PEG-DA gels (17% F127) in various conditions specified by: V – volume of PEG-DA gel solution in μl and UV – UV exposure time in min. All samples were released in PBS buffer. The amount of DNA initially added to the vector solution was 8ug for all samples.

-square curve). One possible reason for the thickness effect lies in the additional sequestration of vector molecules by the side wall around the indentation. Besides diffusing straight down through the gel, the vector may also diffuse outward to the side wall and probably get entrapped somewhere during the subsequent transport. When loading twice the amount of vector on V-850 gel, the total amount of released DNA was found to be higher (data not shown), suggesting the entrapped vectors did not block the effective pores to allow additional vectors passing through. In addition to release into buffer, samples were also allowed to release into cell growth medium containing serum through medium-soaked PEG-DA gels. Similar release profiles were obtained as seen with the release into buffer (data not shown).

Thus far, we have examined the influence of various factors on the release of vector from PEG-DA gels and found that the V-700, UV-1.5 gels can provide a relatively fast and steady release within nine days, which make it appropriate for *in vitro* gene release study. The extracellular matrix (ECM) of the tumor acts as a potent barrier against the transport of biopharmaceuticals such as gene vectors and therapeutic proteins. There are numerous influencing factors limiting the diffusion of macromolecules through ECM, such as the tumor type, the content of collagen(19), and the amount of glycosaminoglycan (GAG)(20-21). Additionally, the dynamic nature of ECM and vasculature(22) make it extremely difficult to predict or mimic the real transport in the tumor matrix using synthetic gels. What we have presented here is an attempt to render a more practical experimental set-up for *in vitro* sustained gene release with an inexpensive and easily implemented barrier gel.

### 7.3.3 In vitro Co-delivery of DNA and Paclitaxel

Besides gene delivery, we have also incorporated anti-cancer drug paclitaxel (PTX) in the vector to make it able to deliver gene and drug simultaneously. Since PTX was encapsulated in the Pluronic F127 (PL) shield rather than the DNA condensing pentablock copolymers (PB), the drug loading was assumed not to induce any change to the interaction between DNA and PB. This assumption will be tested by gel electrophoresis later. One of the advantages by combined delivery of gene and drug lies in the positive synergistic influence of drug on gene expression, as it has been reported by others(12-13). Fig. 7.4 shows the influence of PTX on luciferase gene expression in cancerous SKOV3 and non-cancerous ARPE cells. As expected, the presence of PTX lead to enhancement of transfection efficiency, but to a different degree for each cell type with little dependence on the concentration of PTX studied. SKOV3 showed an up to 12-fold increase in luciferase level as opposed to the moderate 3-fold increase seen in APRE-19 cells at N/P of 20 with 50% of F127 shield having PTX payload. Considering the overall low level of gene expression in ARPE-19, especially for the control vector at N/P of 20 which only one order of magnitude higher than blank cells (data now shown), the effect of PTX in enhancing transfection was very limited in this cell type. We have previously reported that the PB-PL/DNA vector presents a selective transfection in cancerous over non-cancerous cells due to greater lysosomal sequestration of DNA in the latter case(23-25). Addition of chloroquine (CLQ), a transfection enhancer, resulted in significant higher fold-increase in APRE-19 cells when compared to SKOV3 cells(25), which is contrary to what was seen here with PTX. CLQ restored the gene

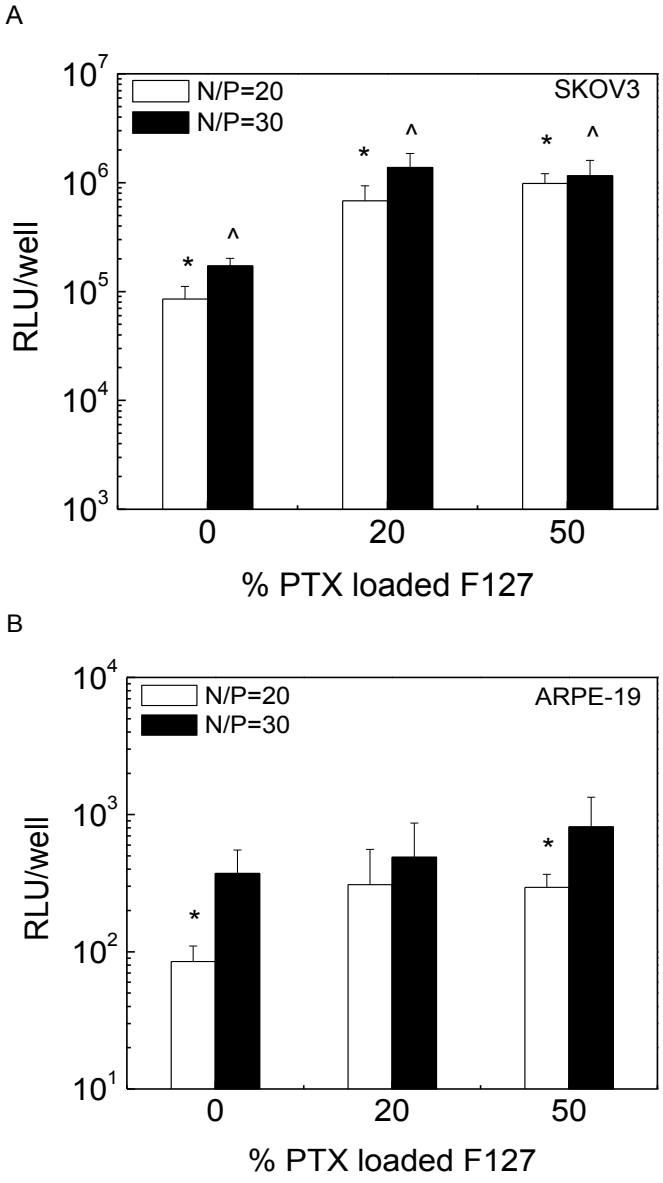


Fig. 7.4. Effect of PTX on luciferase based transfection efficiency of SKOV3 (A) and ARPE (B) cells mediated by PB-PL/DNA polyplex containing various percent of PTX loaded F127 in the free Pluronic F127 (PL) shield. $P<0.01$

expression in ARPE-19 cells probably by overcoming the lysosomal barrier that served as a primary cause of low transfection, whereas PTX failed to so. The most direct reason should be the fact that PTX used a different mechanism to improve

gene expression, which is possibly related to its anti-mitotic function(13). Since PTX must get to microtubules in the cytosol to function through binding to the tubulin, entrapping in the endo/lysosomal vesicles would completely inhibit the function of PTX. Previous intracellular trafficking results indicate that there were a lot more polyplexes getting entrapped in the more acidic vesicles in non-cancerous cells relative to in the less acidic vesicles in cancerous cells(25). Therefore, lack of enhanced gene expression in PTX treated APRE-19 cells might result from the endo/lysosomal entrapment. The entrapped particles could then be exported out of the cell by exocytosis as what has been reported about colloidal silica nanoparaticles(26). Besides, the non-cancerous ARPE-19 cells could be more resistant to PTX compared to cancerous cells. A study on K858, an anti-mitotic agent that can induce similar mitotic arrest as PTX, showed that ARPE-19 cells were slightly affected by this agent relative to other cancerous cells(27). In this sense, even if PTX could be released to the cytoplasm of ARPE-19 cells, its ability to enhance gene expression by arresting mitosis might be quite weak. In contrast, the SKOV3 cells, which have been found PTX sensitive(28), could benefit from PTX easily to gain an enhancement in gene expression. The similar effect of PTX on

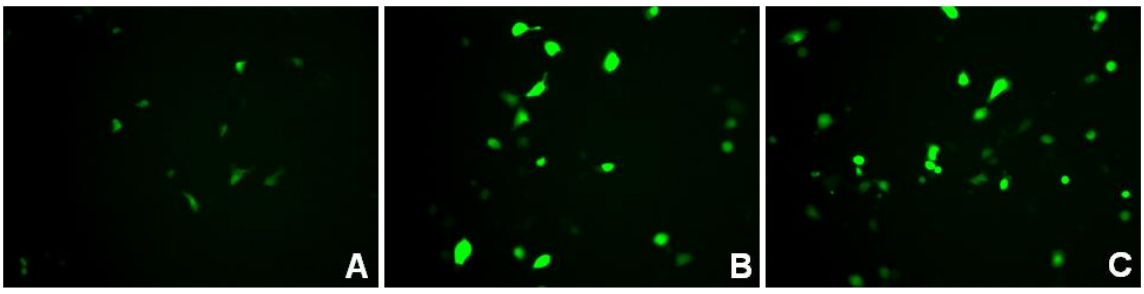


Fig. 7.5. EGFP expression in SKOV3 cells transfected with PB-PL/DNA at N/P=20, with free Pluronic F127 shield composed of 0% (A), 20% (B), 50% (C) PTX-loaded F127.

SKOV3 cells was also observed with transfection by DNA encoding EGFP reporter gene as shown in Fig. 7.5.

Cytotoxicity measurement further confirmed the above analysis about the selective enhancement of gene expression by PTX in SKOV3 and ARPE-19 cells. As shown in Fig. 7.6, PTX brought about additional ~20% cell death compared to the

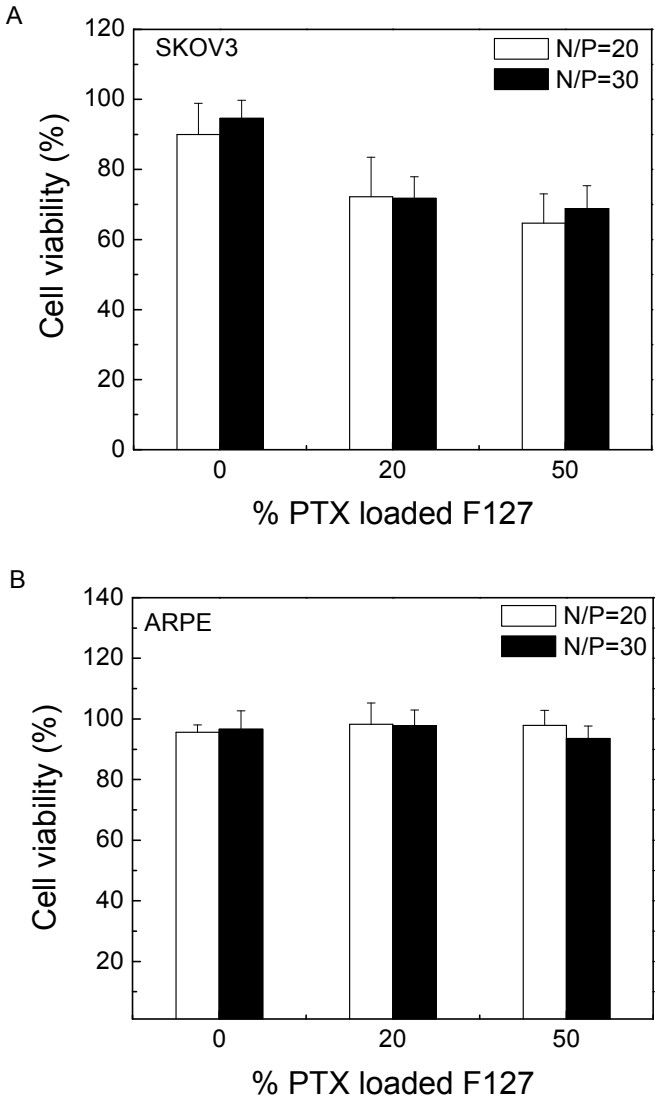


Fig. 7.6. LDH based cell viability of PB-PL/DNA polyplex formulated with various percent of PTX loaded F127 in the free Pluronic F127 shield on SKOV3 (A) and ARPE-19 (B) cells.

condition without PTX in SKOV3 cells, whereas it barely affect the viability of APRE-19 cells. Since the cytotoxicity was determined based on Lactate dehydrogenase (LDH) level, which measures the cell death following loss of cell membrane integrity, it may not reflect all kinds of cytotoxicity induced by PTX. Other measurement methods will be used to in future. Taken together, co-delivery of DNA with PTX clearly generated a synergistic effect demonstrated by the increased gene expression, and the original selective transfection presented in the PB-PL type of vector was retained in the co-delivery method.

### 7.3.4 In vitro sustained delivery of DNA and PTX to cells

With the above discussion about release of vector through PEG-DA barrier gel and enhancing effect of PTX on gene expression, sustained delivery and DNA and PTX will be conducted with cultured cells in future.

## 7. 4 Conclusions

F127-treated PEG-DA gels were developed as a diffusion barrier to simulate the tumor matrix in an in vitro release study on injectable PB vectors. Various influencing factors of vector release rate were investigated and optimized. It was found that nearly 100% of vector could be released through the optimal PEG-DA gel, with a well-maintained polyplex structure. Paclitaxel (PTX) was co-packaged in the PB-PL type of vectors together with DNA, leading to a synergistic effect demonstrated by significant enhancement in gene expression in cultured human ovarian cancer

SKOV3 cells. The co-delivery of drug and gene with PB based vectors will be further investigated for *in vitro* sustained release in future.

**Acknowledgments**

We would like to thank Dr. Bob Lipert from Ames Laboratory for the helpful discussion on making PEG-DA gels. We also like to thank Michael Fleming from the REU program for help with collecting and measuring released samples.

## References

1. A. Agarwaland S.K. Mallapragada. Synthetic sustained gene delivery systems. Curr Top Med Chem. 8:311-330 (2008).
2. K.W. Chun, J.B. Lee, S.H. Kim, and T.G. Park. Controlled release of plasmid DNA from photo-cross-linked pluronic hydrogels. Biomaterials. 26:3319-3326 (2005).
3. D.J. Quickand K.S. Anseth. DNA delivery from photocrosslinked PEG hydrogels: encapsulation efficiency, release profiles, and DNA quality. Journal of Controlled Release. 96:341-351 (2004).
4. A. Agarwal, R.C. Unfer, and S.K. Mallapragada. Dual-role self-assembling nanoplexes for efficient gene transfection and sustained gene delivery. Biomaterials. 29:607-617 (2008).
5. M.D. Determan, J.P. Cox, S. Seifert, P. Thiyagarajan, and S.K. Mallapragada. Synthesis and characterization of temperature and pH-responsive pentablock copolymers. Polymer. 46:6933-6946 (2005).
6. D. Lee, W. Zhang, S. Shirley, X. Kong, G. Hellermann, R. Lockey, and S. Mohapatra. Thiolated Chitosan/DNA Nanocomplexes Exhibit Enhanced and Sustained Gene Delivery. Pharmaceutical Research. 24:157-167 (2007).
7. H. Cohen-Sacks, V. Elazar, J. Gao, A. Golomb, H. Adwan, N. Korchov, R.J. Levy, M.R. Berger, and G. Golomb. Delivery and expression of pDNA embedded in collagen matrices. Journal of Controlled Release. 95:309-320 (2004).
8. A. Agarwal, R. Vilensky, A. Stockdale, Y. Talmon, R.C. Unfer, and S.K. Mallapragada. Colloidally stable novel copolymeric system for gene delivery in complete growth media. Journal of Controlled Release. 121:28-37 (2007).

9. A.V. Kabanov, E.V. Batrakova, and V.Y. Alakhov. Pluronic(R) block copolymers as novel polymer therapeutics for drug and gene delivery. Journal of Controlled Release. 82:189-212 (2002).
10. A.V. Kabanov, E.V. Batrakova, and D.W. Miller. Pluronic((R)) block copolymers as modulators of drug efflux transporter activity in the blood-brain barrier. Advanced Drug Delivery Reviews. 55:151-164 (2003).
11. M.M. Janat-Amsbury, J.W. Yockman, M. Lee, S. Kern, D.Y. Furgeson, M. Bikram, and S.W. Kim. Combination of local, nonviral IL12 gene therapy and systemic paclitaxel treatment in a metastatic breast cancer model. Molecular Therapy. 9:829-836 (2004).
12. Y. Wang, S. Gao, W.-H. Ye, H.S. Yoon, and Y.-Y. Yang. Co-delivery of drugs and DNA from cationic core-shell nanoparticles self-assembled from a biodegradable copolymer. Nat Mater. 5:791-796 (2006).
13. R.R. Nair, J.R. Rodgers, and L.A. Schwarz. Enhancement of transgene expression by combining glucocorticoids and anti-mitotic agents during transient transfection using DNA-cationic liposomes. Molecular Therapy. 5:455-462 (2002).
14. N. Wiradharma, Y.W. Tong, and Y.Y. Yang. Design and Evaluation of Peptide Amphiphiles with Different Hydrophobic Blocks for Simultaneous Delivery of Drugs and Genes. Macromolecular Rapid Communications. 31:1212-1217 (2010).
15. L.Y. Qiuand Y.H. Bae. Self-assembled polyethylenimine-graft-poly(epsilon-caprolactone) micelles as potential dual carriers of genes and anticancer drugs. Biomaterials. 28:4132-4142 (2007).
16. A. Agarwal, R. Unfer, and S.K. Mallapragada. Investigation of in vitro biocompatibility of novel pentablock copolymers for gene delivery. Journal of Biomedical Materials Research Part A. 81A:24-39 (2007).
17. S.A. Zawkoand C.E. Schmidt. Crystal templating dendritic pore networks and fibrillar microstructure into hydrogels. Acta Biomater. 6:2415-2421 (2010).
18. Y.H. Wu, H.B. Park, T. Kai, B.D. Freeman, and D.S. Kalika. Water uptake, transport and structure characterization in poly(ethylene glycol) diacrylate hydrogels. J Membr Sci. 347:197-208 (2010).
19. A. Pluen, Y. Boucher, S. Ramanujan, T.D. McKee, T. Gohongi, E. di Tomaso, E.B. Brown, Y. Izumi, R.B. Campbell, D.A. Berk, and R.K. Jain. Role of tumor-host interactions in interstitial diffusion of macromolecules: Cranial vs. subcutaneous tumors. Proceedings of the National Academy of Sciences of the United States of America. 98:4628-4633 (2001).
20. P.A. Netti, D.A. Berk, M.A. Swartz, A.J. Grodzinsky, and R.K. Jain. Role of extracellular matrix assembly in interstitial transport in solid tumors. Cancer Research. 60:2497-2503 (2000).

21. C.d.L. Davies, D.A. Berk, A. Pluen, and R.K. Jain. Comparison of IgG diffusion and extracellular matrix composition in rhabdomyosarcomas grown in mice versus in vitro as spheroids reveals the role of host stromal cells. Br J Cancer. 86:1639-1644 (2002).

22. W.L. Monsky, D. Fukumura, T. Gohongi, M. Ancukiewcz, H.A. Weich, V.P. Torchilin, F. Yuan, and R.K. Jain. Augmentation of transvascular transport of macromolecules and nanoparticles in tumors using vascular endothelial growth factor. Cancer Research. 59:4129-4135 (1999).

23. B. Zhang, M. Kanapathipillai, P. Bisso, and S. Mallapragada. Novel Pentablock Copolymers for Selective Gene Delivery to Cancer Cells. Pharmaceutical Research. 26:700-713 (2009).

24. B. Zhang and S. Mallapragada. The mechanism of selective transfection mediated by pentablock copolymers; Part I: investigation of cellular uptake. revision submitted to Acta Biomaterialia.

25. B. Zhang and S. Mallapragada. The mechanism of selective transfection mediated by pentablock copolymers; Part II: nuclear entry and endosomal escape. revision submitted to Acta Biomaterialia.

26. J.S. Park, T.H. Han, K.Y. Lee, S.S. Han, J.J. Hwang, D.H. Moon, S.Y. Kim, and Y.W. Cho. N-acetyl histidine-conjugated glycol chitosan self-assembled nanoparticles for intracytoplasmic delivery of drugs: Endocytosis, exocytosis and drug release. Journal of Controlled Release. 115:37-45 (2006).

27. R. Nakai, S. Iida, T. Takahashi, T. Tsujita, S. Okamoto, C. Takada, K. Akasaka, S. Ichikawa, H. Ishida, H. Kusaka, S. Akinaga, C. Murakata, S. Honda, M. Nitta, H. Saya, and Y. Yamashita. K858, a Novel Inhibitor of Mitotic Kinesin Eg5 and Antitumor Agent, Induces Cell Death in Cancer Cells. Cancer Research. 69:3901-3909 (2009).

28. Z.F. Duan, A.J. Feller, R.T. Penson, B.A. Chabner, and M.V. Seiden. Discovery of differentially expressed genes associated with paclitaxel resistance using cDNA array technology: Analysis of interleukin (IL) 6, IL-8, and monocyte chemotactic protein 1 in the paclitaxel-resistant phenotype. Clinical Cancer Research. 5:3445-3453 (1999).

# CHAPTER 8. GENERAL CONCLUSIONS

## 8.1 General Discussion

In recent years, more and more attention has been given to how transgene vectors should be designed to make the therapeutic efficacy higher while reducing side effects. Although low transfection efficiency has been widely known as the bottleneck for non-viral vectors, numerous strategies have been employed to overcome this hurdle, some of which showed exciting results in achieving a high gene expression, such as synthetic viruses that incorporate an active domain of a specific virus (1-4) and multifunctional polymers which can overcome multiple intracellular barriers (5-7). Besides high efficiency, the ideal transgene vectors should also provide a targeted transfection with low toxicity in the long term. The novel pentablock copolymer reported here holds the promise for such a versatile vector with the most attractive feature being injectable for sustained release. Moreover, we have recently found that the pentablock copolymer vectors posses an ability to selectively transfect cancer cells over non-cancer cells in *in vitro* cultures. This is an interesting finding since this selectivity does not arise from any targeting ligands attached to the vector. Understanding the mechanism of this selectivity will enable us to better design polymeric vectors with *inherent selectivity for specific cell types based on intracellular differences* and not on the use of targeting ligands that have shown variable success.

According to the results from intracellular trafficking of PB vector in cancer and non-cancer cells, we assumed that the selectivity was due to different intracellular barriers to transfection in the different cell types. Cellular uptake, endosomal escape and nuclear entry are commonly identified intracellular barriers that have been investigated for their influence on transfection efficiency. Thus, our approach focused on identifying the intracellular transfection barriers for this PB vector system and then investigating the differences in these barriers between cancer cell lines and non-cancer cell lines. For each barrier, a corresponding approach was employed to overcome that barrier; epidermal growth factor (EGF) for cellular uptake, chloroquine (CLQ) for endosomal escape and nuclear localization signal (NLS) for nuclear entry. After examining these three possible barriers, we concluded that escape from the endocytic pathway served as the primary intracellular barrier for PB-mediated transfection. This, in turn, provides insights into intracellular pH differences. PB/DNA vectors could have been, in large part, sequestered and degraded in acidic lysosomes of non-cancer cells, but survived and maintained function in less acidic lysosomes of cancer cells. This property could be taken advantage of to design vectors selectively transfecting cells with higher lysosomal pH, such as many tumor cells. The work highlights the importance of identifying intracellular barriers for different gene delivery systems involving vectors and cells, and provides a new paradigm for designing targeting vectors based on intracellular differences between cell types, rather than through the use of targeting ligands.

As a common lysosomotropic agent, chloroquine (CLQ) has been found to significantly enhance transfection efficiency in many systems(6, 8-9). Especially in

our study, CLQ was the only agent that increased the transfection efficiency both in cancer and normal cells. To understand the function of CLQ may be helpful for designing high efficient vectors. Among the multiple roles CLQ may play in assisting gene delivery, facilitating endosomal escape is of most importance, but recently facilitating dissociation of DNA from polymers has emerged as an another interesting possibility(10). Current methods involving DNA dyes cannot accurately assess the displacing effect of CLQ. In this work, we utilized cysteine-coated CdSe-ZnS core-shell QDs in place of common DNA intercalating dyes to measure DNA released from PB/DNA polyplexes in the presence and absence of CLQ. We found that increasing concentrations of PB and DNA led to quenching of QD fluorescence while CLQ alone had no measurable effect. Thus, CLQ induced dissociation of the polyplex was sensed through changes in QD fluorescence. As expected, addition of CLQ to solutions containing PB/DNA polyplex and QDs resulted in significant quenching of QDs when compared with control samples lacking CLQ. This provides a strong indication that CLQ indeed facilitated polyplex dissociation. The mechanism of quenching was elucidated by modeling the process as the combination of static and dynamic quenching from the PB and DNA, as well as self-quenching due the bridging of QDs.

With the inherent transfection selectivity, PB vectors were developed further to deliver drug and gene simultaneously. The hydrophobic anti-cancer drug paclitaxel (PTX) was encapsulated in the Pluronic F127 (PL), which could self-assemble into the PB/DNA complexes to form a shield layer against aggregation in the presence of serum proteins. Separate loading of drug and DNA was believed to be able to

minimize the interference that may happen to the integral loading. Co-delivery of PTX and DNA with PB-PL/DNA vector led to enhanced gene expression and reduced cell viability when compared to DNA delivery. But the synergistic effect was only found significant in cancer cells (SKOV3) but not in non-cancer cells (ARPE-19). One reason may correlate with the selective transfection discussed above. Greater endo/lysosomal sequestration in non-cancer cells might inhibit the interaction of PTX with microtubules to facilitate gene expression. Besides, the different degree of drug resistance or drug sensitivity between SKOV3 and APRE-19 cells could be another reason.

As the PB vector system holds a promise for sustained delivery, a convenient and practical method is necessary to examine the release of vector *in vitro*. Although we have studied the release in a test tube before, it cannot reflect the real transfecting ability of the sustained release system by making the release and transfection as two separate processes. Here, we reported a device that allows the vector to be directly released to cells, by using a poly(ethylene glycol) diacrylate (PEG-DA) barrier gel to mimic the role of tumor extracellular matrix in resisting therapeutic agents to reach tumor cells. Various factors that influence the permeability of PEG-DA gels were investigated and optimized. It was found that the released vectors maintained the integrity as a polyplex even after four day release. Thus we can expect the released polyplexes to have the similar transfection ability as regular polyplexes administered in solution. By loading DNA and PTX together in the PB-PL type of vector, an instant sustained co-delivery of gene and drug to cultured cells could be accomplished *in vitro* by using PEG-DA barrier gel.

## 8.2 Recommendations for Future Research

With all *in vitro* investigations of PB based vectors, the next logical step is to conduct *in vivo* experiments to assess the performance of the vectors in animal models. Preliminary results have proved the effectiveness of PB vectors in delivering luciferase reporter gene to mice tumor by direct subcutaneous injections. Based on the optimized formulations and preparation protocol, a real therapeutic gene, such as iterleukin-12 (IL-12) a highly potent anti-tumor cytokine, should be used in place of the luciferase reporter gene to assess the inhibition of tumor progression by PB vector treatment. Moreover, co-delivery of PTX and IL-12 could be also undertaken to gain a synergistic effect, with PTX delivery alone and IL-12 delivery alone as negative controls. However, the synergistic effect may not be accessible in cancer cells developing the multiple drug resistance (MDR) phenotype. MDR is known as one major limitation for current chemotherapy. Recent research results suggested that MDR is related to gene malfunction caused by chromosomal alterations in cancer cells(11-12). Correction of malfunctioned genes through gene delivery would be a promising method to solve MDR or in some extent to sensitize drug resistant cells towards to anticancer drugs again. Besides, small interfering RNA (siRNA) technology could be a promising alternative, for siRNA is chemically synthesizable and easy to be tailored for a special need. It has been reported that co-delivery of PTX and Bcl-2 targeted siRNA effectively sensitized PTX resistant MDA-M8-231 human breast cancer cells to PTX(13). But before use of siRNA as payload, a detailed characterization of PB/siRNA complexes is recommended. Instead of using

PB vectors as a dilute solution, concentrated solution could be administered intratumorally as to benefit from the sustained release following body temperature triggered gelation. With a single injection, the therapeutic effect is expected to maintain at an appropriate level for a long period of time.

Regarding the technique using QDs to sense the dissociation of polyplexes, we can further its application in intracellular environments. To explore the change in polyplex formation in cytoplasm as well as in acidic vesicles (e.g. endosomes) would surely help researchers design vectors that can effectively condense and protect DNA payloads. We have found that QDs are capable of distributing evenly within the cytoplasm in large numbers. Thus, it is likely for these dispersed dots to sense dissociation of polyplexes as they do in solution. Furthermore, since the QDs were rendered water soluble though ligand exchange, various types of amino acids can be easily coupled to QDs as designed; for example, histidine residues can be coupled to the surface of QDs, leading them to readily escape endosomes. In this case, there could be many more QDs available in the cytoplasm.

## References

1. E. Wagner, C. Plank, K. Zatloukal, M. Cotten, and M.L. Birnstiel. Influenza-virus hemagglutinin-HA-2 N-terminal fusogenic peptides augment gene-transfer by transferrin polylysine DNA complexes - toward a synthetic virus-like gene-transfer vehicle. Proceedings of the National Academy of Sciences of the United States of America. 89:7934-7938 (1992).
2. E. Wagner, K. Zatloukal, M. Cotten, H. Kirlappos, K. Mechtler, D.T. Curiel, and M.L. Birnstiel. Coupling of adenovirus to transferrin polylysine DNA complexes greatly enhances receptor-mediated gene delivery and expression of transfected genes. Proceedings of the National Academy of Sciences of the United States of America. 89:6099-6103 (1992).

3. A. El-Sayed, T. Masuda, I. Khalil, H. Akita, and H. Harashima. Enhanced gene expression by a novel stearylated INF7 peptide derivative through fusion independent endosomal escape. Journal of Controlled Release. 138:160-167 (2009).
4. N. Ferrer-Miralles, E. Vázquez, and A. Villaverde. Membrane-active peptides for non-viral gene therapy: making the safest easier. Trends in Biotechnology. 26:267-275 (2008).
5. Kogure K, Moriguchi M, Sasaki K, et al. . Development of a non-viral multifunctionl envelope-type nano device by a novel lipid film hydration method. Journal of Controlled Release. 98:317-323 (2004).
6. N.M. Moore, C.L. Sheppard, and S.E. Sakiyama-Elbert. Characterization of a multifunctional PEG-based gene delivery system containing nuclear localization signals and endosomal escape peptides. Acta Biomater. 5:854-864 (2009).
7. H. Akitaand H. Harashima. Advances in non-viral gene delivery: using multifunctional envelope-type nano-device. Expert Opin Drug Deliv. 5:847-859 (2008).
8. J. Xavier, S. Singh, D.A. Dean, N.M. Rao, and V. Gopal. Designed multi-domain protein as a carrier of nucleic acids into cells. Journal of Controlled Release. 133:154-160 (2009).
9. G. Shen, H.F. Fang, Y.Y. Song, A.A. Bielska, Z.H. Wang, and J.S.A. Taylor. Phospholipid Conjugate for Intracellular Delivery of Peptide Nucleic Acids. Bioconjugate Chemistry. 20:1729-1736 (2009).
10. S. Yang, D.J. Coles, A. Esposito, D.J. Mitchell, I. Toth, and R.F. Minchin. Cellular uptake of self-assembled cationic peptide-DNA complexes: Multifunctional role of the enhancer chloroquine. Journal of Controlled Release. 135:159-165 (2009).
11. R.H. Li, R. Hehlman, R. Sachs, and P. Duesberg. Chromosomal alterations cause the high rates and wide ranges of drug resistance in cancer cells. Cancer Genetics and Cytogenetics. 163:44-56 (2005).
12. P. Duesberg, R.H. Li, R. Sachs, A. Fabarius, M.B. Upender, and R. Hehlmann. Cancer drug resistance: The central role of the karyotype. Drug Resistance Updates. 10:51-58 (2007).
13. Y. Wang, S. Gao, W.-H. Ye, H.S. Yoon, and Y.-Y. Yang. Co-delivery of drugs and DNA from cationic core-shell nanoparticles self-assembled from a biodegradable copolymer. Nat Mater. 5:791-796 (2006).